Process Characterisation of a Manufactured Living Dermal Equivalent (ICX-SKN) and use of Ultrasound for Product Improvement

By

Jasmin Kee

A Doctoral Thesis

Submitted in partial fulfilment of the requirements
for the award of

Doctor of Philosophy of Loughborough University

July 2009

Abstract

The routine use of regenerative medicine products in patients requires cost-effective manufacturing processes and products that meet business and customer needs. The dermal skin substitute ICX-SKN, produced by Intercytex for the treatment of acute wounds, completed Phase I clinical trials in 2007. ICX-SKN is manufactured by seeding neonatal human dermal fibroblasts in a fibrin matrix and culturing for 49 days to form a collagen matrix synthesised by the cells.

The results captured by this thesis demonstrate an integrated engineering and biological science approach to improve the current ICX-SKN process model and identify methods for process and product improvement. Measurement of the changes in the biochemical, mechanical and physical properties of ICX-SKN during the 49 day manufacturing period produced an improved four-phase process model describing cell proliferation, matrix compaction, fibrin degradation, collagen synthesis and matrix remodelling.

Ultrasound was identified as a scalable form of mechanical stimulation for product improvement particularly as it does not require physical coupling to the constructs. A custom-built ultrasound device was used to investigate the effect of ultrasound on collagen synthesis and mechanical properties. A design of experiments showed that different combinations of ultrasound intensity (0.5-2.5W/cm^2), duty cycle (5-80%) and duration (5–30minutes) affected the shear storage modulus (G') and collagen content. However, a significant effect on G' only resulted from combinations of duty cycle and duration. Further experiments to improve the properties of the construct, using 0.5W/cm^2 intensity, 50% duty cycle and 14 minute duration resulted in a 73% increase in G' primarily through increased collagen deposition.

The results showed that further work is required to minimise process variation through control of the input raw materials. Optimisation of the fibrin matrix and diffusion of the culture media were identified as key areas to improve manufacturing cost-effectiveness. Enhanced understanding of the physical and molecular mechanisms by which ultrasound elicits cell responses will enable further optimisation of the ultrasound process for product improvement.

Table of Contents

List of Figures

List of Tables

Abbreviations

BSC	Biological Safety Cabinet
CLFM	Confocal Laser Fluorescent Scanning Microscopy
DMA	Dynamic Mechanical Analysis
DOE	Design of Experiments
D-2	Day -2 referring to day the SKN constructs were cast
D0	Day 0 referring to day the SKN constructs were first fed with Total Media
E	Young's Modulus
ECM	Extracellular Matrix
EGF	Epidermal Growth Factor
ELISA	Enzyme-linked Imunosorbent Assay
ESEM	Environmental Scanning Electron Microscopy
EVG	Elastic Van Gieson
FTSG	Full Thickness Skin Graft
GAG	Glycosoaminoglycans
GMP	Good Manufacturing Practice
G'	Shear Storage Modulus
G"	Shear Loss Modulus
HDF	Human Dermal Fibroblasts
ICX-SKN	Dermal skin substitute constructs produced using human fibrinogen and used in Phase I Clinical trials
IHC	Immunohistochemistry
MMP	Matrix metalloproteinases
MT	Masson's Trichrome
NHS	National Health Service
PG	Proteoglycans
PGA	Polyglycolic acid
PLLA	Poly (L-lactic acid)
SEM	Scanning Electron Microscopy
SKN	Dermal skin substitute constructs produced using bovine fibrinogen and used for the experiments in this thesis
SMC	Smooth Muscle Cells
STSG	Split Thickness Skin Graft
TEM	Transmission Electron Microscopy
TGF-β	Transforming Growth Factor β
UTS	Ultimate Tensile Strength

Acknowledgements

There are many people that have made this thesis possible. My thanks go to:

My supervisor Professor D.J.Williams for his unwavering support and belief in my research and inspiring vision and ambition for the growth of the regenerative medicine industry.

My industrial supervisor Dr P.Johnson, Research Director, Intercytex for her invaluable guidance and advice during this project. Dr M.Flasza-Baron and the research team at Intercytex for their time and patience when teaching me about the biological aspects of ICX-SKN. Dr P.Kemp, CSO, Intercytex for his high level guidance and insight into the regenerative medicine industry and funding of this project.

Dr M.Mather, Electrical and Electronic Engineering, Nottingham University, for her significant contribution and advice on the design of the ultrasound stimulation device, development of the ultrasound stimulation protocols, and calibration of the SonoPlus490 ultrasound unit.

Mr S.Hall and Mr B.Morris, Medical Engineering Workshop, Nottingham University, for their advice on and manufacture of the ultrasound stimulation device.

Dr S.Anderson, Ms M.Smith and Ms D.Christie, Advance Microscopy Unit, Nottingham University for development of the methodologies for preparation and imaging of the SKN constructs by light microscopy and TEM.

Dr A.Brain, Centre for Ultrastructural Imaging, King's College London, for development of the methodology for preparation and imaging of the SKN constructs by SEM.

Dr I.Notingher and Miss A. Żołądek, Nanoscience Group, Nottingham University for their advice and use of the Raman Spectroscopy system.

Mr J.Singh, Metrology Workshop, Loughborough University for his advice in the development of the Precision Surface Profiling measurement method.

Mr S.Goodyear, Anton Paar and Dr L.Hamilton, Nottingham University for their advice on rheological testing and the use of the rheometer.

Professor J.M.Kearney and Dr P.Rooney, NHS Blood and Transplant Tissue Services, Liverpool, for their time discussing the clinical aspects surrounding skin allografts and for the donation of human cadaver skin samples.

Mr L.Cheng, Consultant Maxillofacial Surgeon, St. Bartholomew's and The London Hospitals, for his time discussing the clinical aspects of skin grafting and skin substitutes.

The Engineering and Physical Sciences Research Council for the funding of the studentship.

Chapter 1 Introduction

1.0. Regenerative Medicine

The vision of regenerative medicine or tissue engineering to provide therapies for the regeneration, repair and replacement of failing tissues and organs led to investment and rapid growth of the industry between the early 1990s and 2000. Large investment in the industry resulted in a number of commercially available tissue-engineered products such as those for skin and cartilage regeneration. However, the limited efficacy of the products over existing gold standard treatments and the high cost of production contributed to a downturn in the industry between 2000 and 2002. During this period, there was a reduction in the availability of funding and a number of the leading companies filed for bankruptcy. The need to address both scientific and commercial challenges to provide commercially viable products and further growth of the industry was apparent. Since 2002, the focus of regenerative medicine companies has been redirected from scientific research to commercialisation of products. Particular emphasis has been placed on addressing the challenges posed by reimbursement, regulation, manufacturing, marketing and distribution to realise the routine use of regenerative medicine products in patients.

The manufacturing challenges facing regenerative medicine products is the focus of this thesis and are described in the next section. The skin graft replacement product, ICX-SKN produced by Intercytex will be used in this thesis as a demonstrator regenerative medicine product for addressing the manufacturing challenges.

1.1. Problem Statement

The current manufacturing challenges for regenerative medicine products include firstly, the development of cost-effective processes that allow for profitable reimbursement. Secondly, the repeatable manufacture of product to pre-determined specifications according to Good Manufacturing Practice (GMP) as required by regulation. Finally, the development of systems for repeatable and reproducible measurement of product properties and processing parameters is required for compliance with GMP.

The use of cells in the production of regenerative medicine products presents additional challenges as the processing conditions required to elicit the desired cell responses are not fully understood. The development of product specification presents financial challenges as testing of the efficacy of the products in human clinical trials is very costly. The successful development of manufacturing processes to produce products which meet business and customer needs requires an integrated approach which combines manufacturing engineering and life science skills.

Intercytex is an emerging healthcare company based in the UK and North America using proprietary cell therapy to develop products to restore and regenerate skin (www.intercytex.com). A current product in development is ICX-SKN, a skin graft replacement for burns and acute wounds. ICX-SKN comprises of allogeneic neonatal human dermal fibroblasts in a human collagen matrix and completed Phase I clinical trials in 2007. ICX-SKN is manufactured by seeding fibroblast cells in a fibrin matrix. During the 49 day manufacturing process, the cells breakdown the fibrin matrix and synthesise a collagen matrix which forms the basis of the final product.

The processes that occur during the remodelling of fibrin matrices and secretion of a collagen matrix by cells has been widely reported by researchers developing in-vitro wound healing models and tissue-engineered constructs for dermal, arterial and valve replacements. However, these studies have typically been carried out over a 21 day period and there is limited data about the changes in physical, biochemical and mechanical properties over a 49 day period as used for the manufacture of ICX-SKN. An improved understanding of the 49 day ICX-SKN manufacturing process would enable identification of areas for process and product improvement and provide a benchmark for the assessment of process changes. In addition, the ICX-SKN construct has gel-like properties which present difficulties when handling as they are prone to tearing and difficulties with characterisation of their properties due to the high volume fraction of water. Developments of repeatable and reproducible measurement techniques suitable for testing ICX-SKN are required.

Identification of methods to increase collagen deposited in the matrix and improve the mechanical properties is also required for product improvement. Biochemical and mechanical stimulation has been used to increase collagen synthesis and mechanical properties of tissue-engineered constructs formed from cell seeded fibrin matrices. The current manufacturing process for ICX-SKN uses a culture media supplemented with growth factors to stimulate collagen synthesis from the cells. However, the use of mechanical stimulation to improve the properties of ICX-SKN has not been investigated. Application of tensile, compressive and shear forces to tissue-engineered construct has been shown to improve the properties of a number of tissue-engineered constructs. However, these methods typically required physical coupling to the constructs which would be problematic for ICX-SKN constructs which are prone to tearing due to their gel-like properties.

Ultrasound stimulation provides a form of mechanical stimulation which can be coupled to the constructs through a liquid path such as the culture media. Ultrasound stimulation in the therapeutic range has been used in-vivo to accelerate wound healing in bone and soft tissue. Ultrasound has been used in-vitro to increase collagen synthesis in tissue-engineered constructs for cartilage and intervertebral disc regeneration. However, the effect of ultrasound on dermal fibroblast seeded fibrin matrices has not been reported in the public domain. In addition, there are many combinations of ultrasound parameters such as the frequency, magnitude and duration that can be used to stimulate cell seeded constructs. The optimum combination of ultrasound parameters to stimulate collagen synthesis has not yet been determined.

In summary, an integrated biological, manufacturing and process engineering approach is used in this thesis to develop the early-stage ICX-SKN product. This thesis focuses on firstly, the repeatable and reproducible measurement of the changes in physical, biochemical and mechanical properties of the ICX-SKN construct during the 49 day manufacturing process to provide an improved process model and identify areas for process improvement. Secondly, the identification of the range and combinations of ultrasound intensity, duty cycle and duration for increasing collagen synthesis and improvement of mechanical properties of the ICX-SKN construct.

1.2. Thesis Structure

The literature review in Chapter 2 describes firstly, the current gold standard of skin grafting for the treatment of acute wounds and the need for skin substitutes. Secondly, the processes that occur when cells remodel a fibrin matrix and secrete a collagen matrix in-vivo during wound healing and in-vitro. Thirdly, current characterisation techniques to qualify and quantify the physical, biochemical and mechanical properties of cell seeded matrices. Finally, the effect of ultrasound on cell seeded matrices and the mechanisms by which ultrasound elicits cell responses is described.

Chapter 3 describes the materials and methods used to characterise the physical, structural, biochemical and mechanical properties of SKN constructs during manufacturing. Characterisation techniques suitable for measurement of cell-seeded matrices with gel-like properties developed from established techniques and novel application of non-destructive testing techniques are described. This approach provided an increased understanding of the processes that occurred during the manufacturing of ICX-SKN and identified four key phases in the manufacturing process.

Chapter 4 describes the experimental arrangement of the custom-built ultrasound stimulation device for the reproducible and repeatable stimulation of the ICX-SKN constructs. The design of experiments (DOE) study to investigate the effect of different combinations of ultrasound parameters on the structural, biochemical and mechanical properties of ICX-SKN constructs is also described. Chapter 5 describes the use of ultrasound stimulation for the improvement of the properties of the ICX-SKN constructs based on suitable ultrasound parameters identified in the DOE.

The conclusions in Chapter 6 integrate and expand on the conclusions of the characterisation and ultrasound studies. Areas of further work to improve the efficiency of the manufacturing process and reduce batch-to-batch variation are described in Chapter 7. Further work to improve the effect of ultrasound on the properties of the ICX-SKN constructs, and to improve understanding of the mechanisms by which ultrasound stimulates cell responses are also described.

1.3. Thesis Contributions

- Identification of four key phases in the 49 day ICX-SKN manufacturing process which increased the understanding of processes that occur in cell-seeded fibrin matrices in-vitro.

- Demonstration of methodologies for repeatable quantification and qualification of the biochemical and mechanical properties of the ICX-SKN constructs and tissue-engineered constructs with gel-like properties.

- Demonstration of the novel application of non-destructive 3D Surface profiling and Raman spectroscopy for the characterisation of the changes in physical and biochemical properties of the ICX-SKN constructs.

- Design and build of a novel ultrasound device for repeatable and reproducible delivery of ultrasound to tissue-engineered constructs.

- Application of a design of experiments methodology to efficiently assess the effects of ultrasound in the therapeutic range on the collagen synthesis and mechanical properties of ICX-SKN.

- Evidence to show that the combination of ultrasound duty cycle and duration have a significant effect on the mechanical properties of ICX-SKN constructs in comparison to other combinations of ultrasound intensity, duty cycle and duration which had no significant effect.

- Demonstration of the use of ultrasound stimulation to achieve a step change in mechanical properties of ICX-SKN for product improvement.

Chapter 2 Literature Review

2.0. Introduction

This chapter reviews the clinical, commercial and scientific issues associated with the development of an early stage tissue-engineered constructs for treatment of acute wounds. The composition, structure and function of skin and wound healing events that occur when the skin suffers injury or insult are described in sections 2.1 and 2.2. The advantages and disadvantages of the current gold standard skin grafting treatment for secondary intention acute wounds and benefits of development of skin substitutes are discussed in section 2.3.

ICX-SKN, a dermal skin substitute currently being developed by healthcare company Intercytex will be used in this thesis as a demonstrator product for improvement of the manufacturing process and product properties. The production of ICX-SKN is described in detail in section 2.4 together with the current understanding of the processes that occur during the manufacturing period to produce the collagen matrix which forms the ICX-SKN product.

Cell seeded fibrin gels have been investigated in-vitro by researchers investigating the wound healing remodelling process and developing tissue-engineered constructs. The processes that occur in-vitro to convert the fibrin matrix into a collagen matrix are reviewed in section 2.5. The current characterisation techniques used to measure the changes that occur during the remodelling process are reviewed in section 2.6. The use of biochemical and mechanical stimulation to increase collagen synthesis and mechanical properties of the matrices, are reviewed in section 2.7. In addition, the mechanotransduction process by which mechanical stimulation is transmitted from the extracellular matrix to the cells on a molecular level is described. Finally, the use of ultrasound as a form of mechanical stimulation and its suitability of scale-up is reviewed in section 2.8.

2.1. Composition, Structure and Function of the Skin

The skin is one of the largest organs of the human body. It functions to protect the body from injury and dehydration, provide defence against bacterial infection and regulate temperature (Barbucci 2002). It is composed of approximately 70% water, 25% protein, 2% lipids, and the remaining 3% is comprised of glycosaminoglycans (GAGs), proteoglycans (PGs), trace minerals and other chemicals (Barbucci 2002). The skin is composed of two principle layers (Figure 1), the outer epidermis which provides the protective, semi-permeable layer (Madison 2003) and the underlying dermis which provides the majority of the mechanical properties of the skin (Lai-Cheong, McGrath 2009).

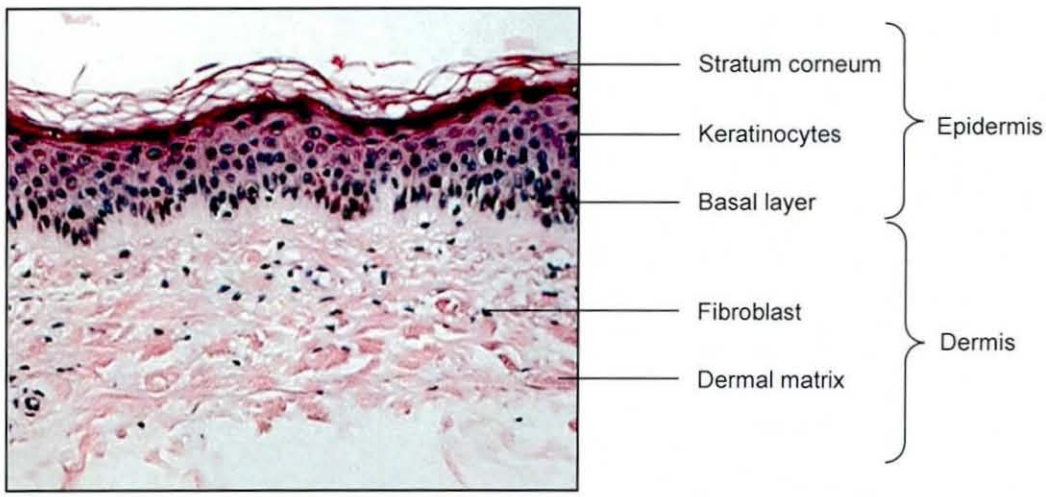

Figure 1 Cross-section of normal human skin. (Reprinted with permission from Organogenesis Inc.)

The avascular epidermis comprises of up to four layers of keratinocytes cells which continually differentiate and move from the inner basal layer to the outer stratum corneum layer where they are sloughed off every 2 - 3 weeks (Madison 2003). The dermis is 2-4mm thick and is predominately comprised of extracellular matrix (ECM) inter-dispersed between skin appendages, nerves, blood vessels and dermal fibroblast cells (Seeley, Stephens et al. 2006, Tobin 2006). The ECM comprises of fibrillar proteins such as collagen and elastin, embedded in a viscous ground substance comprising of water, proteoglycans and glycosaminoglycans. Collagen forms the majority of the dermis accounting for approximately 70% of the dry weight (Table 1).

The viscous ground substance and elastic collagen and elastin fibres give the dermis its viscoelastic properties which allow deformation and recovery of the skin (Ventre, Mollica et al. 2009, Silver, Seehra et al. 2002). The glycosaminoglycans (GAGs) and proteoglycans are attached to the collagen fibres and they function to bind the water in the ground substance to the collagen fibres. The GAGs and proteoglycans have also been shown to play an important role in extracellular assembly of collagen by binding collagen type I fibres and controlling the inter-fibrillar spaces (Carrino, Sorrell et al. 2000, Danielson, Baribault et al. 1997, Reed, Iozzo 2002, Kuwaba, Kobayashi et al. 2001, Longas, Fleischmajer 1985).

The dermal fibroblasts cells are responsible for maintaining and remodelling the ECM in response to biochemical and mechanical stimuli (Boyce 2001). The fibroblasts remodel the ECM by a number of mechanisms such as secretion of matrix metalloproteinase (MMP) enzymes which breakdown the ECM and secretion of new fibrillar proteins (Stamenkovic 2003). The results of this remodelling are apparent in different areas of the body. For instance, the attachment of the skin to the body is loose over joint flexures to allow for a range of movements but is relatively tighter and thicker on the soles of the feet to provide protection from the frequent pressures to which they are subjected (Forslind 1995, Jarrett 1978, Seeley, Stephens et al. 2006).

Component	**%**
Collagen fibres	66 - 69
Non-fibre forming collagens	2-4
Elastin	2-4
Hyaluronic Acid (GAG)	0.03 - 0.09

Table 1 Composition of the dry weight of the main components in the dermis (Silver, Siperko et al. 2003)

2.1.1. Dermal Response to Mechanical Deformation

Mechanical testing of the dermis has shown that different components of the ECM respond at increasing levels of strain (Forslind 1995, Silver, Siperko et al. 2003, Waller, Maibach 2006, Pins, Christiansen et al. 1997, Silver, Christiansen et al. 2001). At low strains of 0%-30%, skin responds elastically due to the stretching of the elastin fibres. At 30%-60% strain skin demonstrates viscoelastic behaviour due to the gradual straightening of the collagen fibres and displacement of the viscous ground substance and water molecules bound to proteoglycans and GAGs. At high strains, 60%–70%, internal disruption and sliding between the collagen fibres and fibrils occurs. The ultimate tensile strength of skin, including the epidermal layer, has been reported to be 21–34MPa (Bhat 2005, Edwards, Marks 1995) and in the elastic region the Young's modulus as 0.4-0.8MPa (Clark, Cheng et al. 1996, Manschot, Brakee 1987).

2.1.2. Structure and Function of Collagen in the Dermis

Many types of collagen have been identified in the dermis and provide a variety of functions. The collagen fibres are composed of collagen type I (80-90%), collagen type III (8-11%) and collagen type V (2-4%) and provide the majority of the elastic properties and tensile strength of the dermis (Tobin 2006, Silver, Siperko et al. 2003). Non-fibril forming fibres such as collagen type XII and XIV are present on the surface of these fibres although their function is not fully understood (Lavker, Zheng et al. 1987, Keene, Marinkovich et al. 1997). Other types of collagen such as type IV and VI and VII (1-5%) also form fibrillar networks that contribute towards the organisation and mechanical properties of the dermis (Keene, Marinkovich et al. 1997) and function to anchor the dermal ECM to the basement membrane between the dermis and epidermis (Silver, Siperko et al. 2003).

There has been much research into the mechanisms by which collagen is produced by the fibroblast cells in the dermis (Kadler, Holmes et al. 1996, Ghosh 2002) and is summarised below. In response to biochemical and mechanical stimuli, procollagen amino acid chains with the repeating structure of Gly-Xaa-Yaa are produced in the cell nucleus. Three procollagen molecules, approximately 300nm in length and 1.5nm in diameter, are processed into a triple helical structure in the endoplasmic reticulum by hydroxylation and hydrogen bonding of the chains. These procollagen assemblies are then packaged in secretory vesicles in the Golgi apparatus which move to the cell membrane and are secreted into the extracellular space.

The procollagen molecules form larger collagen fibrils by bonding longitudinally through specific cleavage of their end N and C-terminal propeptides, and laterally through lysyl oxidase cross-linking. The fibrils (56–62nm in diameter) cross-link to one another form collagen fibres of between 0.3- 40μm giving the skin its tensile strength and elasticity (Ghosh 2002, Ushiki 2002, Bhogal, Stoica et al. 2005, Barton, Marks 1984).

2.2. Primary Intention Wound Healing

When the body suffers an insult or injury such as a breakage in the skin, a cascade of events occurs to heal the wounded area. For acute wounds which heal by primary intention that is, without human intervention, there are four stages to wound healing - haemostasis, inflammation, proliferation and remodelling (Clark 1996, Li, Chen et al. 2007, Broughton, Janis et al. 2006) and are summarised below.

During haemostasis platelets from the blood release fibrinogen in the wound site which is then cleaved by thrombin to form a fibrin clot or provisional matrix within minutes of the injury. The provisional matrix controls the blood flow and provides a temporary protective barrier for the body. The platelets release cytokines and growth factors which stimulate migration and proliferation of cells that are required in subsequent stages of wound healing. The inflammation stage occurs after a few hours when inflammatory cells such as macrophages and monocytes migrate to the wound site and remove foreign particles and dead or injured cells. Macrophages and platelets secrete growth factors and cytokines that promote angiogenesis and stimulate migration and proliferation of surrounding fibroblasts into the provisional matrix. Re-epithelialisation of the wound by migrating keratinocytes also begins during this time.

During the proliferation stage, the provisional matrix is broken down by digestive enzymes secreted by the macrophages and proliferating fibroblasts after 3-5 days. New blood vessels form an interconnecting network which provides oxygen and nutrients required by fibroblasts for the active synthesis of proteins such as collagen. After 4-5 days, the fibroblasts synthesise and deposit a loose extracellular matrix including, collagen types I, III and V, glycosaminoglycans and proteoglycans. The collagen molecules polymerise into randomly organised fibrils over a period of about 2 weeks and this matrix is known as granulation tissue. The contractile fibroblast phenotype, the myofibroblast, acts to pull the wound margins together, causing the wound to shrink and reducing the surface area that the keratinocytes need to cover for complete re-epithelialisation.

Finally, remodelling of the granulation tissue occurs through the breakdown of collagen type III and further secretion of collagen type I by fibroblasts. The higher tensile strength of collagen type I compared to collagen type III and the reorganisation of ECM molecules by the fibroblasts result in the wound regaining approximately 20% of its tensile strength after 21 days (Oxlund 1986). Further remodelling in response to local stimuli, such as mechanical stimulation from moving joints, occurs over a period of years through the development of collagen fibrils and fibre bundles (Clark 1996, Li, Chen et al. 2007, Broughton, Janis et al. 2006). The change in composition of proteoglycans provides additional stability by binding to the collagen fibrils and filling the interstitial spaces (Chiquet-Ehrismann, Tucker 2004). The healed wound is reported to regain only 70-80% of the tensile strength of unwounded skin (Oxlund 1986) and often results in scarring caused by formation of dense collagen bundles.

The wound healing process which remodels the fibrin clot to a functional collagen matrix forms the basis of the ICX-SKN manufacturing process discussed in section 2.4.1. However, the processes that occur in-vivo differ from that in-vitro and are discussed in section 2.5.

2.3. Secondary Intention Wound Healing

Secondary intention acute wounds, such as burns and those caused by accidents or surgical procedures, require human intervention for healing in comparison to the primary intention wounds described previously. The current gold standard for healing these wounds is skin grafting where the patient's own skin is transplanted from a healthy donor site to the wound site (Horch 2006). These procedures have high success rates of more than 90% (Molnar, DeFranzo et al. 2004) and produce generally good cosmetic results. Skin grafts are autologous (from the patient) which reduces the risk of rejection, and retain structures such as blood capillaries which aid integration in the wound site by readily allowing vascularisation (Cheng 2006). The failure of skin grafts to take to a wound are generally caused by poor vascularisation of the skin graft which then results in a deficiency of nutrients and oxygen, and the movement of the graft in the wound site which can lead to haematomas at the graft-wound interface (Cheng 2006).

Despite the high success rate, skin grafting has a number of disadvantages. These include firstly, the need for sufficient, suitable donor sites which may be problematic in elderly or weak patients or patients with burns covering large areas of the body. Secondly, skin grafting creates a second wound at the donor site. This forms another source at risk of infection and is reported to be slow and painful when healing (Cheng 2006, Damodaran, Syed et al. 2008). Thirdly, the clinicians are required to make a choice between using a full-thickness skin graft (dermis and epidermis) or split-thickness skin graft (epidermis and thin layer of dermis). Full-thickness skin grafts (FTSG) prevent contraction of the wound and subsequent scarring but the donor site takes longer to heal compared to split-thickness skin grafts (STSG). In contrast, STSGs are superior when matching the pigmentation, texture and structure of the graft to the skin surrounding the wound but are more prone to scarring and contraction at the wound site (Cheng 2006).

Finally, the increasing incidence of skin carcinomas (Bath-Hextall, Leonardi-Bee et al. 2007, Welch, Woloshin et al. 2005) especially those in highly visible regions of the body presents an additional dilemma for clinicians (Cheng 2006). The size and depth excised around the carcinoma needs to be sufficient to minimise the risk of recurrence but improved cosmetic results are achieved through smaller excisions and the associated social and psychological impact on the patient needs to be considered (Cheng 2006).

2.3.1. Allografts

When rapid closure of the wound is necessary to prevent morbidity but insufficient patient donor skin is available, donor, cadaver skin allografts from national tissue banks are conventionally used. The allograft provides time for the patient's skin to grow so that it is suitable for skin grafting and the structure of the allograft reduces contraction of the wound. The cost of a split thickness allograft is relatively cheap, at £1.73/cm^2 (UK NHS price 2009, http://tissue.blood.co.uk). However, allografts are only a temporary wound cover as they are required to be surgically removed before rejection by the body for immunological reasons (Kearney 2007).

The limitations of skin grafts and allografts have led to the research and development of skin substitutes. In 1987, at the National Science Foundation Meeting, a goal was set "to create a readily available tissue replacement with the biologic and pharmacologic properties of human skin" and to provide alternatives for clinicians (Bello, Phillips 2000). Since then, numerous products have been developed for treatment of both chronic wounds such as diabetic foot ulcers and chronic leg ulcers, and acute wounds such as burns and surgical excisions. These products have been recently reviewed by Damodaran, Syed et al. 2008, Auger, Lacroix et al. 2009, Clark, Ghosh et al. 2007, MacNeil 2007. Skin substitutes can be split into three categories – epidermal only, dermal only and combined epidermal and dermal. Skin substitutes for treatment of acute wounds are reviewed below.

2.3.2. Epidermal Skin Substitutes

Epidermal skin substitutes comprise of approximately 2-8 layers of autologous (from the patient) cells, such as keratinocytes. These are usually housed on a synthetic membrane for ease of application to the wound. They are produced by expanding patient cells, taken from a small skin biopsy, in a laboratory and are then delivered back to the patient for application. This process was first demonstrated by Rheinwald and Green in the 1970s when it was shown that in 3 weeks, cells from a small skin biopsy of $1cm^2$ could be expanded in-vitro to produce enough cells for an epidermal layer that could cover the whole body. Currently, epidermal skin substitute Epicel® (Genzyme Tissue Repair Cambridge, MA) is commercially available for the treatment of burns (Table 2). MySkin™ (CellTran, Sheffield, UK) also for the treatment of burns was commercially available in the UK. However, CellTran is currently under administration (http://www.celltran.com, 2009).

Clinical studies reported that MySkin™ accelerated re-epithelialisation (Zhu, Warner et al. 2005) and Epicel® aided rapid vascularisation of the dermis in burns patients compared to using a STSG (Balasubramani, Kumar et al. 2001, Carsin, Ainaud et al. 2000). However, several disadvantages were also reported. These included the fragility of the Epicel® product (Lobmann, Pittasch et al. 2003), susceptibility to infection and contractures (Clark, Ghosh et al. 2007, Rue, Cioffi et al. 1993, Williamson, Snelling et al. 1995), and the high costs estimated at US$13 000 for coverage of 1% total body surface area (TBSA) for Epicel® (Clark, Ghosh et al. 2007).

In addition, the short shelf life of less than 48 hours, presented logistical challenges of co-ordinating the culture of the epidermal skin substitutes in the laboratory with delivery at the place of use when required by the clinicians (Ehrenreich, Ruszczak 2006, Gobet, Raghunath et al. 1997, Supp, Boyce 2005). MySkin™ was reported to be robust to handle. However, the impact of a short shelf life on the commercial viability of such products was highlighted in a report that approximately 50% of MySkin™ manufactured was disposed of due to rescheduling of operation times or deterioration of the patient's condition before the scheduled operations (MacNeil 2006).

2.3.3. Dermal Skin Substitutes

Dermal skin substitutes are composed of a matrix which provides structural support within the wound, similar to a FTSG, and a template for adhesion and migration of patient cells from the surrounding tissue. In comparison to epidermal skin substitutes, dermal substitutes generally have a longer shelf life of more than 9 months which reduces the logistical challenges and provides potential for an off-the shelf product (Table 2). There are a wide range of commercially available dermal substitutes such as Alloderm (Life Cell Corporation NJ), TransCyte® (Smith and Nephew, UK) and Integra (Integra Life Sciences, NJ). The matrices of the dermal substitutes are typically collagen based but are manufactured using different approaches as summarised below.

2.3.3.1. Alloderm

Alloderm (Life Cell Corporation, NJ), was developed to incorporate the structural benefits of allografts but eliminate the need for surgical removal. Alloderm is produced by removing the epidermis and cells that could lead to graft rejection from donated human skin tissue from tissue banks. It is intended to be used in full-thickness burns with a split-thickness skin graft (http://www.lifecell.com, downloaded 2009). Clinical studies reported that subjective assessment of cosmetic results favoured the Alloderm group in burns patients compared to STSGs (Lattari, Jones et al. 1997, Sheridan, Morgan et al. 2001, Wainwright, Madden et al. 1996). In addition, the vascular structures retained in Alloderm were reported to aid rapid revascularisation (Butler, Langstein et al. 2005, Diaz, Guy et al. 2006, Kim, Bruen et al. 2006, Menon, Rodriguez et al. 2003) and reduce the length of hospital stay and associated medical costs (Butler, Langstein et al. 2005, Buinewicz, Rosen 2004, Kaleya, Thomas 2005). Alloderm is one of the most commercially successful skin substitutes and has been used to treat over 1 million patients since its launch in 1994 (http://www.lifecell.com, 2009). However, successful grafting of Alloderm was shown to be highly dependent on the dressing technique used by the clinician as it was more sensitive to shear stresses and prone to desiccation than STSGs (Kearney 2001).

2.3.3.2. Transcyte®

TransCyte® (Smith and Nephew, UK) is temporary skin substitute produced in-vitro using newborn human fibroblast cells in a nylon mesh coated with porcine collagen. The cells enhance the matrix with structural and provisional matrix proteins, glycosaminoglycans and growth factors with the aim of producing a template that facilitates wound healing (http://wound.smith-nephew.com/za/Product). At the end of the manufacturing process, the cells are destroyed by freezing before grafting. TransCyte® is similar to allografts, as it has to be surgically removed to avoid immunological rejection and allergic reactions to the polymer membrane and nylon mesh coated with porcine collagen (http://wound.smith-nephew.com). Clinical studies reported that TransCyte® was easier to remove than the allografts and required a lower percentage of STSG when treating paediatric burns of greater than 7% TBSA (Purdue, Hunt et al. 1997, Kumar, Kimble et al. 2004, Lukish, Eichelberger et al. 2001).

2.3.3.3. Integra

Integra (Integra Life Sciences, NJ) was developed in the 1970s (Yannas, Burke 1980) and became the first marketed tissue-engineered skin with FDA approval in 1996. Integra consists of a porous, cross-linked, bovine collagen and chondroitin-6-sulphate dermal template and a silicone epidermal analogue layer intended for use on deep partial-thickness or full-thickness wounds (http://www.integra-ls.com). The pore size was designed to encourage adhesion, migration and proliferation of the patient's cells into the template when implanted in the wound bed (Dagalakis, Flink et al. 1980). Once inside the template the host cells synthesise a new collagen matrix and the dermal template degrades. The silicone epidermal layer is removed and replaced with a thin STSG after the new collagen matrix is vascularised (Balasubramani, Kumar et al. 2001, Jones, Currie et al. 2002).

Clinical studies reported subjective improvements in cosmetic results and faster healing of the donor sites with less hypertrophic scarring when treated with Integra (Heimbach, Luterman et al. 1988, Heimbach, Warden et al. 2003, Moiemen, Vlachou et al. 2006). However, it was also shown that Integra had poorer take rates of 80-85% compared to 93-95% for STSGs and was susceptible to infection.

2.3.4. Epidermal and Dermal Skin Substitutes

Currently, Apligraf (Organogenesis, MA) is the only commercially available bi-layered skin substitute but is intended for the treatment of chronic wounds. The most promising bi-layered skin substitute currently in development for the treatment of burns is Permaderm (Lonza, Switzerland). Permaderm comprises of autologous keratinocytes and fibroblasts in a bovine collagen matrix (Boyce 2001). Initial studies have shown that Permaderm can be used to reduce the area of donor skin required when treating patients with full thickness burns of greater than 50% TBSA and has comparable cosmetic results to treatment with conventional skin grafts (Boyce, Kagan et al. 2002, Boyce, Kagan et al. 2006). However, there is no indication of clinical trials or commercial availability in the near future (Auger, Lacroix et al. 2009). In addition, the use of autologous cells presents logistical difficulties and delays in treatment of the patient, similar to those discussed for epidermal skin substitutes and the commercial viability needs to be proven.

In conclusion, there remains an opportunity for development of a skin substitute for routine treatment of acute wounds. There are both scientific and commercial challenges that still need to be overcome for the routine use of skin substitutes in patients. The key challenges are development of a skin substitute that is easy to handle, has a suitable shelf life that minimises logistical and supply chain difficulties and demonstrates significant benefit over current gold standard (MacNeil 2007). The cost of production of skin substitutes also needs to allow for profitable reimbursement (MacNeil 2007).

Co./Product	Description	Indication	Shelf Life	Cost**	Pros	Cons
Epidermal Only						
Genzyme/ Epicel®	2-8 layers co-culture of autologous keratinocytes and murine cells on surgical dressing material	Burns > 30% TBSA	24hrs	*$13 000/ 1%TBSA	Accelerated dermal vascularisation	Fragility Cost Culture time Logistical difficulties
CellTran/ MySkin™	Co-culturing autologous keratinocytes and murine cells on a medical grade polymer	Burns, ulcers	Data unavailable	Data unavailable	Robust to handle	Logistical difficulties
Dermal Only						
National Tissue Banks/ Allograft	Donor, cadaver skin	Burn	>2 years Stored in LN_2	£1.73/cm^2	Immediate wound coverage	Requires surgical removal
Smith and Nephew/ Transcyte®	Porcine collagen dermal matrix enhanced with HDF secreted proteins and growth factors with removable epidermal silicone membrane	Burns	9 months	£921/unit (7.87/cm^2)	Improved efficacy compared to donor skin allografts	Requires surgical removal
LifeCell Corp./ Alloderm	Donor, cadaver skin with removed epidermis and cells that could lead to graft rejection	Burns Soft tissue defect	2 years	£238/unit (£5.90/cm^2)	Mechanical properties. Rapid vascularisation through vascular structures	Efficacy dependent on dressing technique
Intregra Life Sciences Corp/ Integra DRT	Cross-linked bovine collagen-chondroitin-6-sulfate dermal matrix with removable silicone epidermis	Burns Scar contractures Surgical/trauma wounds	2 years	£830/unit (£3.13.cm^2)	Improved cosmetic results vs. STSG	Increased graft rejection vs. STSG Susceptible to infection
Epidermal and Dermal						
Lonza/ Permaderm	Autologous keratinocytes and fibroblasts in bovine collagen matrix	Burns	Data unavailable	N/A	Reduces skin grafting required	Logistical difficulties Not commercially available

Table 2 Commercially available skin substitute products for treatment of acute wounds *Clark, Ghosh et al. 2007 **Jones, Currie et al. 2002

2.4. Intercytex and ICX-SKN – A Manufactured Living Dermal Skin Equivalent

Intercytex is an emerging healthcare company based in the UK and North America using a proprietary cell therapy to develop products to restore and regenerate skin (www.intercytex.com). Intercytex's ICX-SKN product aims to be a skin graft replacement for burns and acute wounds. ICX-SKN comprises of living allogeneic neonatal human dermal fibroblasts (HDF) in a human collagen matrix synthesised by the cells and successfully completed Phase I clinical trials in 2007 (Boyd, Flasza et al. 2007). The manufacturing process, current understanding of the events that occur during manufacturing to produce ICX-SKN, and the proposed mechanism of action in-vivo are described below.

2.4.1. Manufacturing Process

The manufacture of ICX-SKN is described in detail by (Flasza, Kemp et al. 2007) and summarised in Figure 2. The ICX-SKN construct is manufactured by embedding allogeneic neonatal human dermal fibroblasts (HDF) in a fibrin matrix and culturing the constructs using a specific media formulation for 49 days. During the manufacturing period the cells proliferate, breakdown the fibrin matrix and secrete a new collagen matrix in a similar sequence of events to those found during in-vivo wound healing (section 2.2). After 49 days, the ICX-SKN constructs are freeze dried for storage and sterilised by gamma-irradiation. Prior to packaging and shipping, the constructs are rehydrated and repopulated with HDF cells which secrete structural and provisional matrix proteins, glycosaminoglycans and growth factors before application in the wound.

During manufacturing, it is hypothesised that the rate of fibrin degradation and collagen synthesis by the HDF cells is critical to the successful production of ICX-SKN (Personal communication with Dr.P.Kemp, CSO, Intercytex, 2007). A high fibrin degradation rate may result in no matrix to support the cells which would lead to the cells growing in monolayers and secreting collagen on the surface of the tissue culture plastic. A low fibrin degradation rates may result in long manufacturing times which will impact the cost of manufacture and commercial viability (Figure 3). A balance

between the fibrin degradation rate, collagen secretion rate and cost of manufacture is necessary for the commercial success of ICX-SKN.

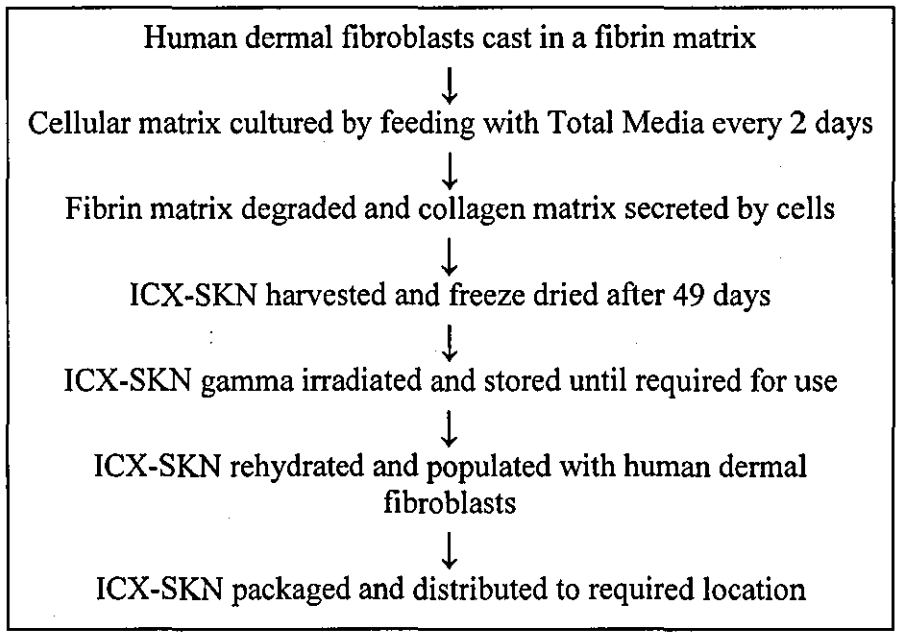

Figure 2 Summary of the ICX-SKN manufacturing process

2.4.2. Phase I Clinical Trial Results

The Phase I Clinical trial results are described in detail by Boyd, Flasza et al. 2007 and are summarised below. ICX-SKN constructs were applied to full thickness excisions (5mm x 15mm), made in six healthy volunteers, for 28 days. No adverse responses in the volunteers were observed and there was minimal scarring after 28 days. Histopathology of the excised wound after 28 days showed that in 5 out of the 6 patients a complete epidermis of keratinocytes with all components including the stratum corneum and spinous layer was formed as well as rete ridges at the epidermal and dermal interface. Migration and proliferation of host fibroblasts was observed in the graft and there was excellent integration between the graft and surrounding tissue. Furthermore, the formation of small blood vessels were observed providing evidence that the structure of the matrix allowed vascularisation. The presence of allogeneic HDF cells did not cause any adverse immune reactions towards ICX-SKN and there was only a small presence of non-specific inflammatory cells in the graft.

2.4.3. Proposed Healing Mechanism

The processes that occur to integrate ICX-SKN with the surrounding skin and encourage tissue regeneration in-vivo are not known. It is hypothesised that the allogeneic and patient HDF cells detected in the ICX-SKN construct during the Phase I clinical trials secreted growth factors, cytokines, collagen and other extracellular matrix components to breakdown the ICX-SKN matrix and form a new collagen matrix secreted from the patient's cells (Boyd, Flasza et al. 2007). In addition, the mechanical properties of the matrix were hypothesised to provide structural support for the cells in the wound.

The rate at which the ICX-SKN matrix is broken down and the new dermal matrix secreted is hypothesised to be critical for the success of ICX-SKN in-vivo (Personal communication with Dr.P.Kemp, CSO, Intercytex, 2007). If the breakdown of the ICX-SKN matrix is too rapid, the wound will reopen. If the breakdown of the ICX-SKN matrix is too slow, there is a risk that it will be encapsulated by the new dermal matrix rather than integrated with it which may impact cosmetic results (Figure 3).

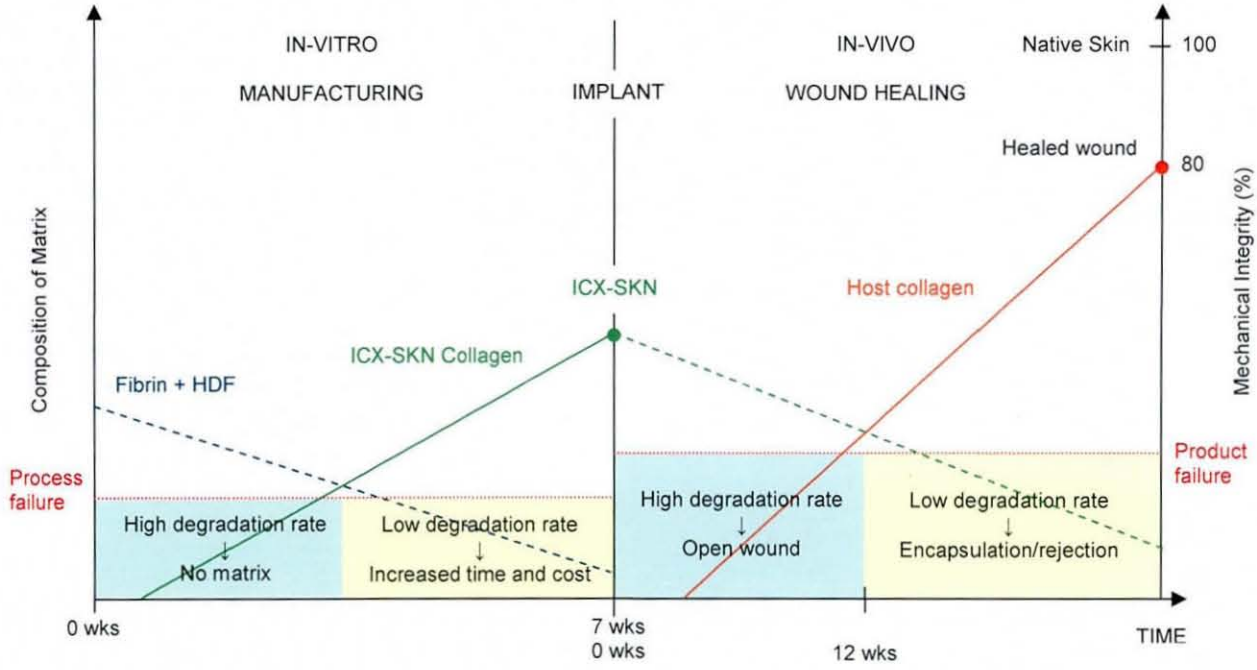

Figure 3 Proposed ICX-SKN manufacturing process model and mechanism of action in-vivo (Personal communication with Dr.P.Kemp, CSO, Intercytex)

Further understanding of the processes that occur during manufacturing are required to identify areas for process improvement for cost-effective manufacture and to provide a benchmark for the assessment of process changes. Identification of methods to improve the product is also required. The key areas for product improvement are to increase the collagen content to improve persistence of the construct in the wound and to increase the mechanical properties to improve the ease of handling of the construct. However, improvement of the ICX-SKN construct must also provide a matrix structure that facilitates vascularisation and cell adhesion, migration and proliferation in-vivo to allow for integration of the construct into the wound site.

In addition, further development of repeatable and reproducible characterisation techniques to measure key processing parameters and final product properties is required. This will improve the understanding of the process variation and aid development of a product specification. This is important for commercialisation of ICX-SKN and tissue-engineered products as repeatable manufacture of product to pre-determined specifications is required by regulation under Good Manufacturing Practice (GMP).

2.5. Cell Seeded Fibrin Matrices

2.5.1. Introduction

Cell-seeded fibrin matrices have been studied in-vitro as wound healing models and for the development of tissue-engineered constructs (Grinnell 2003). Collagen matrices synthesised from cells in fibrin matrices have been investigated for dermal, valve and arterial replacements (Neidert, Lee et al. 2002, Grouf, Throm et al. 2007, Ahlfors, Billiar 2007, Balestrini, Billiar 2006) and for cardiovascular applications using smooth muscle cells (Grassl, Oegema et al. 2002, Ross, Tranquillo 2003). The processes that occur in cell seeded fibrin matrices and methods for improving collagen content and mechanical properties of the constructs are described below.

2.5.2. Cell Proliferation

A wide range of cell densities, between $1x10^5$ and $2x10^6$, have been used to seed fibrin matrices. Cell proliferation resulting in a more than 2-fold increase in the total cell number has been reported for human dermal fibroblast (HDF) and smooth muscle cells (Ahlfors, Billiar 2007, Ross, Tranquillo 2003). A study of HDF cell proliferation in fibrin matrices over 9 days showed that the number of cells did not increase for the first 3 days but subsequently doubled every 3 days until day 9 (Tuan, Song et al. 1996). The degree of cell proliferation has been shown to be dependent on the formulation of fibrinogen and thrombin used to produce the fibrin matrix (Dickneite, Metzner et al. 2004). HDF cells were shown to proliferate poorly in formulations that consisted of a high fibrinogen concentration (34–50mg/mL) and a low thrombin concentration (1U/mL) in comparison to formulations with a lower fibrinogen concentration (5mg/mL-17 mg/mL) and low to medium thrombin concentration (1U/mL and 167 U/mL) (Cox, Cole et al. 2004).

The reasons for the differences in cell proliferation are not fully understood. However, it was suggested that spreading and rounding of the fibroblasts as they adhere and detach from the fibrin matrix during the normal 16-18 hour cell proliferation cycle was affected by the fibrin formulation (Cox, Cole et al. 2004). This is supported by studies of the structure of fibrin matrices which have shown that higher thrombin concentrations produce denser matrices with thinner fibrin fibrils (Wolberg 2007). In

addition, the mechanical properties of the fibrin matrix have been shown to increase with increasing fibrinogen concentrations (Benkherourou, Gumery et al. 2000, Mooney, Costales et al. 2008, Mooney, Costales et al. 2006) and may also provide mechanical signalling to the cells which affect cell proliferation. (Duong, Wu et al. 2009).

The ability for the cells to proliferate and the number of cells in the fibrin matrices may be an important factor to consider when manufacturing tissue-engineered constructs from cell seeded fibrin matrices. This is because the cells are responsible for the remodelling of the fibrin matrix as they degrade the fibrin matrix and secrete collagen which forms the final product. The number of cells present in the matrix may therefore affect the efficiency of the manufacturing process.

2.5.3. Matrix Compaction

Cells seeded in matrices restrained around the edges (usually by the culture dish) compact the matrix causing a decrease in the thickness (Grinnell 2003, Neidert, Lee et al. 2002, Ahlfors, Billiar 2007, Ross, Tranquillo 2003). It has been shown that HDF cells seeded in a restrained fibrin matrix reorganise the fibrin fibrils which causes the compaction and generate tension in the matrix (Tuan, Song et al. 1996). Studies of HDF cells seeded in a collagen matrix have shown that the cells establish a level of "tensional homeostasis" within the matrix at which this level is maintained against opposing influences of external loading and unloading (Brown, Prajapati et al. 1998). It was suggested that this was achieved through rapid contraction and relaxation of the HDF cells through reorganisation of the cell cytoskeleton (Brown, Prajapati et al. 1998).

The thickness of cell seeded fibrin matrices has been shown to decrease over a period of 4 to 28 days (Neidert, Lee et al. 2002, Grouf, Throm et al. 2007, Ahlfors, Billiar 2007, Grassl, Oegema et al. 2002, Ross, Tranquillo 2003, Sander, Johnson et al. 2008). The differences in the period of compaction may have been due to the differences in cell seeding density and fibrin formulation used in each of the studies. This may have affected the rate at which the fibrin fibrils were reorganised by the cells to achieve tensional homeostasis. The degree of compaction by the cells was typically more than 70% resulting in decreases in the thickness of the matrices from approximately 2mm to

200μm. In addition, release of these constructs from the restraints resulted in retraction of the matrices showing that the matrices are under tension (Grinnell 2003, Feng, Yamato et al. 2003). Dermal skin substitutes such as ICX-SKN aim to provide structural support in the wound. Control of the compaction and retraction is necessary for control of the physical and structural properties of the final construct.

2.5.4. Fibrin Degradation

The rate of degradation of the fibrin matrix has not been widely reported. One study of SMCs seeded in a fibrin matrix showed that fibrin degradation occurred over approximately 18 days by measuring the levels of fluorescently labelled fibrinogen (Grassl, Oegema et al. 2002). This was supported by another study which showed by histological analysis that a fibrin matrix seeded with smooth muscle cells was predominantly composed of collagen after 3 weeks (Ross, Tranquillo 2003). In comparison, histological analysis of a HDF seeded fibrin matrix showed that fibrin was present in the matrix after 51 days (Neidert, Lee et al. 2002, Neidert, Tranquillo 2006).

Studies have also monitored the gene expression of matrix metalloproteinase (MMP) enzymes as an indication of the degree of matrix remodelling that occurs in cell seeded fibrin matrices. In a 5 week study of an SMC seeded fibrin matrix, it was shown that expression of MMP1 and MMP2, associated with degradation of collagen and fibrin (Kato, Yasukawa et al. 2000, Page-McCaw, Ewald et al. 2007, Green, Almholt et al. 2008), peaked after 3 weeks (Ross, Tranquillo 2003). It is likely that the initial increase in the MMPs in the first 3 weeks was associated with degradation of fibrin. However, measurements of the levels of MMPs are only an indication of the degree of remodelling that is occurring and not the specific proteins that are being remodelled. Further understanding of the rate of fibrin degradation would be beneficial as it has been reported that the presence of fibrin stimulates collagen secretion from the cells (Grassl, Oegema et al. 2002).

2.5.5. Synthesis of Collagen and other ECM Proteins

Collagen synthesis has been shown to begin 2 to 7 days after seeding the cells in fibrin matrices (Ross, Tranquillo 2003, Tuan, Song et al. 1996). Independent studies of HDF seeded fibrin matrices showed that 32% (Ahlfors, Billiar 2007) and 33% (Neidert, Lee et al. 2002) of the dry weight of the matrix was composed of collagen after 21 days. However, the absolute collagen content differed significantly between these studies which reported the total collagen content as 510μg and 50μg respectively. The differences were suggested to be due to the different media formulation and lower number of cells initially seeded in the latter study (Ahlfors, Billiar 2007). The latter study also showed that the collagen content increased by 130% when culturing constructs for a further 30 days (Neidert, Lee et al. 2002).

In addition, a 5 week study of SMC seeded fibrin gels showed that the amount of collagen deposited in the matrix increased over the whole 5 week period although expression of the collagen type I and type III genes peaked after 3 weeks (Ross, Tranquillo 2003). The gene expression of collagen type I was also shown to be 8 to 10 times greater that the expression of collagen type III. Finally other ECM components have also been shown to be synthesised in cell seeded fibrin matrices. Proteoglycans were shown to account for 2% of the dry weight of HDF seeded fibrin gels after 21 days (Ahlfors, Billiar 2007) and elastin was detected in SMC seeded fibrin gels after 28 days (Ross, Tranquillo 2003).

2.5.6. Mechanical Properties

A number of studies have shown that the increase in collagen content in the fibrin gels correlates with an increase in mechanical properties (Neidert, Lee et al. 2002, Ahlfors, Billiar 2007, Grassl, Oegema et al. 2002). Studies of SMC and HDF seeded fibrin matrices showed a 51% increase in ultimate tensile strength (UTS) after 35 days (Ross, Tranquillo 2003) and a 150% increase in UTS after 51 days (Neidert, Lee et al. 2002) compared to the UTS after 21 days respectively. The increase in UTS was associated with lysyl-oxidase cross-linking of the collagen fibrils (Neidert, Lee et al. 2002, Ross, Tranquillo 2003) and formation of collagen fibril bundles (Ahlfors, Billiar 2007).

The increase in UTS also correlated with the increase in collagen content. The UTS of the matrix with 510μg of collagen discussed previously was 133KPa (Ahlfors, Billiar 2007) compared to 2.4KPa for the matrix containing 50μg collagen (Neidert, Lee et al. 2002). These findings were supported by studies of collagen gels which showed that the viscoelastic properties of the matrices increase with increasing collagen cross-linking and collagen concentration (Bron, Koenderink et al. 2008, Battista, Guarnieri et al. 2005, Raub, Suresh et al. 2007, Raeber, Lutolf et al. 2005). The in-vitro fibrin remodelling processes are summarised in Figure 4.

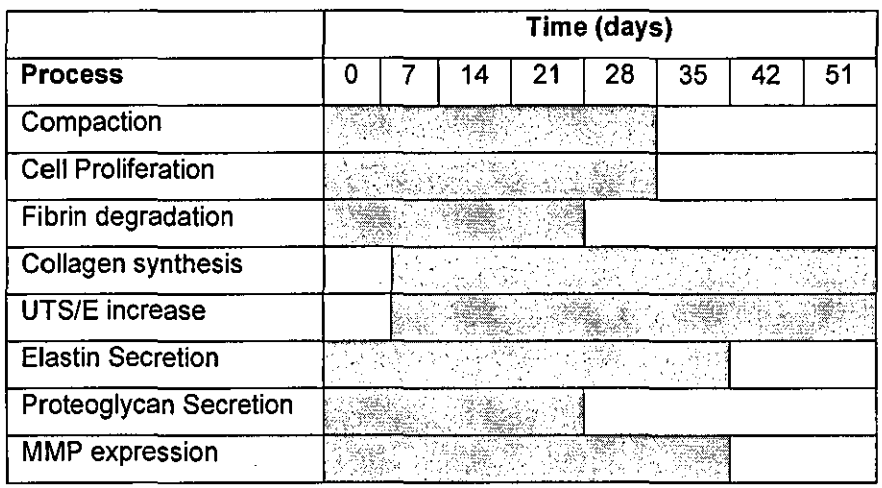

Figure 4 Main processes that occur over time in SMC and HDF seeded fibrin matrices

2.6. Characterisation Techniques

A number of techniques have been used to measure the changes in physical biochemical and mechanical properties of cell seeded matrices. Light and electron microscopy techniques are widely used to qualitatively assess the changes in structure and biochemical composition. Quantitative tests to measure the collagen content and mechanical properties have also been established. However, cell seeded fibrin matrices are initially difficult to handle due to their gel-like consistency and repeatable measurement of their properties can be problematic. The repeatability and reproducibility of these techniques for use on cell seeded fibrin matrices with gel-like properties are reviewed below.

2.6.1. Structural Characterisation

Established light microscopy techniques such as histology and immunohistochemistry for observing the structure of tissues have been applied to tissue-engineered constructs. Histological stains such as Masson's Trichrome, Verhoeff's Van-Gieson's and Alcian Blue are used for detection of fibrillar proteins such as collagen, fibrin and elastin, and other ECM components such as proteoglycans and GAGs in connective tissue (Clark 1973). These stains have also been applied to tissue-engineered constructs (Robinson, Johnson et al. 2008, Hoerstrup, Kadner et al. 2002, Mol, van Lieshout et al. 2005). Similarly, immunohistochemistry (IHC) has been used to identify specific fibrillar proteins and ECM components such as human collagen type I and the proteoglycans decorin and versican in tissue-engineered constructs (Cuttle, Nataatmadja et al. 2005, Fathke, Wilson et al. 2006, Junge, Klinge et al. 2004, Sullivan, Puolakkainen et al. 2008, Hayes, Hughes et al. 2008, Heydarkhan-Hagvall, Esguerra et al. 2006).

Electron microscopy is an established technique for analysing the structure of the extracellular matrix in tissues at higher magnifications. Tissue samples for electron microscopy are generally prepared by fixation followed by chemical dehydration to preserve the native structure and remove any liquid from the sample which would damage the electron microscopy equipment when imaging (Bozzola, Russell 1999). However, preparation of tissue-engineered samples for electron microscopy is problematic as the samples typically have high water contents of over 50%.

Conventional methods to prepare the samples often lead to disruption of the native structure and introduction of artefacts (Al-Amoudi, Norlen et al. 2004, Muscariello, Rosso et al. 2005). Recent advances in this field to facilitate the preparation and imaging of such samples have been reviewed by (Starborg, Lu et al. 2008) and are summarised below.

Firstly, for scanning electron microscopy (SEM) which provides images of sample surfaces, freezing of the samples to preserve the native structure has been investigated. Low temperature freezing of samples using slush liquid nitrogen at -196°C followed by freeze fracturing and then freeze-etching at -90°C to remove the water has been used for tissue-engineered constructs (Köse, Kenar et al. 2003, Wright, Conticello et al. 2003). However, this technique is prone to ice crystal formation when freezing and can damage the structure of the matrix.

High pressure freezing has been developed to minimise the formation of ice crystals in samples and many authors have reported successful use of this technique for the imaging of cells and hydrogels (Al-Amoudi, Norlen et al. 2004, McDonald, Morphew et al. 2007, Serp, Mueller et al. 2002). However, high pressure freezing equipment is expensive and small samples of less than $3mm^3$ are required which are often difficult to prepare and handle without damaging (McDonald, Morphew et al. 2007). The use of cryoprotectants such as dimethyl sulfoxide, in the samples before freezing has proved successful in larger biological samples to prevent ice crystal formation (Dahl, Chen et al. 2006). However, cryoprotectants can be toxic to cells so the concentration and duration of the cryoprotectants on the samples must be carefully monitored.

Secondly, environmental scanning electron microscopy (ESEM) has been developed to image samples in the wet state without the need for any sample preparation (Muscariello, Rosso et al. 2005). Many successful studies of interactions between mammalian cells and biomaterials have been reported (Muscariello, Rosso et al. 2005, Motta, Migliaresi et al. 2004). However, there are also difficulties associated with using wet samples. The low vacuum used in the ESEM can cause the samples to change shape during imaging which can result in blurring. Also, the wet samples can produce different charge status across the surface which results in dark and light areas observed

in the images. The resulting images may provide misleading information of the surface topography (Muscariello, Rosso et al. 2005).

Thirdly, observation of the cross-sections of samples has been demonstrated using transmission electron microscopy (TEM). The most effective technique for minimal artefacts formation and good structural preservation of samples has been reported to be through use of resin embedded samples. Resin is slowly infiltrated into the samples replacing the liquid with minimal damage to the constructs (Edelmann 2002). Detail of internal cellular organelles and interactions between cells and fibrillar molecules can be observed however, the preparation is labour intensive and TEM is restricted to a single slice in a three dimensional structure (Starborg, Lu et al. 2008).

More recently, automated electron tomography techniques are being developed which take multiple thin, serial TEM sections which are then recreated into three dimensional images (Starborg, Lu et al. 2008). This method is advantageous as it can provide information about changes in structure through the whole sample. However, automated electron tomography is in its infancy and a single three dimensional compilation takes several days and much computing power.

2.6.2. Fibrin Degradation and Collagen Synthesis

Quantification of the rate of fibrin degradation in cell seeded fibrin gels is not widely reported. One study measured the fluorescence intensity from fluorescently labelled fibrinogen used to produce the fibrin matrix (Grassl, Oegema et al. 2002). Other studies have used Masson Trichrome staining for histological detection of fibrin (Neidert, Lee et al. 2002, Ross, Tranquillo 2003, Grassl, Oegema et al. 2003).

Techniques to quantify the collagen content in tissue-engineered constructs are more widely reported. Assays that measure the content of hydroxyproline as an indication of total collagen content (Stegemann, Stalder 1967) and dye-based assays that bind to amino acid side chains present in collagen (Junqueira, Bignolas et al. 1979) are commonly used. Measurement of hydroxyproline has been used to determine the collagen content in several cell-seeded fibrin matrices (Neidert, Lee et al. 2002, Ross, Tranquillo 2003, Grassl, Oegema et al. 2003). Similarly, the Sircol™ assay which uses

Sirius red dye to bind to acid soluble collagen type I to IV and has been used by several authors (Mol, van Lieshout et al. 2005, Hansen, Schünke et al. 2001, Ibusuki, Fujii et al. 2003).

However, studies conducted by Intercytex showed that both the hydroxyproline and Sircol™ assays produced positive readings when applied to control fibrin gels (Marshall 2005). In addition, for the hydroxyproline assay, collagen gels mixed with the fibrin gel resulted in higher absorbance readings compared to collagen only samples. In comparison, use of an enzyme-linked immunosorbent assay (ELISA) for collagen type I has been shown to not produce a positive reading from the control fibrin matrices. Increasing collagen concentrations were also shown in ICX-SKN samples over the manufacturing period using ELISA (Marshall 2005). The use of ELISA for detection of collagen in several tissue-engineered constructs has been reported (Chen, Altman et al. 2003, Blunk, Sieminski et al. 2002, Hsu, Whu et al. 2004). However, detection of collagen type I synthesised by cells seeded in fibrin matrices has not been reported.

Finally, other studies have used real-time PCR to quantify the gene expression of collagen, lysyl oxidase required for collagen cross-linking, MMPs which aid remodelling of the ECM and elastin (Ross, Tranquillo 2003, Thampatty, Li et al. 2007). Although gene expression provides valuable understanding of intercellular responses it does not necessarily correlate with secretion of the proteins or enzymes by the cells in the matrix.

2.6.3. Mechanical Properties

Mechanical testing of tissue-engineered constructs can provide supporting data for the qualitative structural observations and valuable understanding of the possible functionality of the constructs in–vivo (Billiar, Throm et al. 2005). Changes in mechanical properties can show important developmental processes such as deposition of structural proteins, remodelling of the proteins into a hierarchical arrangement such as collagen bundles, and physical and chemical bonding between the proteins (Sheu, Huang et al. 2001, Huang, McWilliams et al. 2003). Mechanical characterisation can therefore be potentially be used for process optimisation and quality control during manufacturing (Billiar, Throm et al. 2005). A number of techniques have been used to

determine the mechanical properties of tissue-engineered constructs and are reviewed below.

Tensile testing has been widely used to measure the ultimate tensile strength (UTS) and Young's Modulus (E) of tissue-engineered cartilage, tendon, heart valves and ligaments (Screen, Shelton et al. 2005, Screen, Lee et al. 2004, Moffat, Sun et al. 2008, Fratzl, Misof et al. 1998). The constructs are typically secured in uniaxial or biaxial testing machines using serrated grips or via sutures (Screen, Lee et al. 2004, Lu, Sacks et al. 2005). However, repeatability of the results is problematic for tissue-engineered construct with gel-like properties as they are difficult to handle and load into the machines without damage.

It has been reported that such constructs are prone to failure at the grips due to stress concentrations. Also, the established "dog-bone" shape used to improve repeatability and accuracy of the test is difficult to cut in soft materials without introducing defects and premature failure of the samples propagating from these defects can occur (Billiar, Throm et al. 2005). In addition, it has been suggested that the strength and extensibility of uniaxially tested soft tissue samples is overestimated due to unrestrained reorientation of the structural fibres in the direction of stretch (Feng, Yamato et al. 2003).

Inflation techniques to determine mechanical properties of planar tissue-engineered constructs have been used to address the issues with tensile testing described above. The construct is typically secured between two plates. The lower plate has a circular opening through which the constructs is inflated with a fluid or compressed air (Billiar, Throm et al. 2005). The UTS and extensibility of a HDF seeded fibrin gels was reported to be approximately 28KPa after 25 days in culture (Billiar, Throm et al. 2005) using this method. The advantages of this method include the minimal handling and cutting of the samples required prior to testing and reduction of stress concentrations around the grips (Billiar, Throm et al. 2005). The disadvantages of this type of test are firstly, the need for the samples to isotropic and produce a perfect spherical cap. Secondly, the porous nature of the constructs may allow for perfusion of the inflation fluid through the sample which can interfere with optical measurement systems (Billiar, Throm et al. 2005).

Finally, rheology and dynamic mechanical analysis (DMA) have been used to measure the viscoelastic properties of soft tissue-engineered constructs for applications such as bladder reconstruction (Freytes, Martin et al. 2008), intervertebral disc regeneration (Bron, Koenderink et al. 2008) and wound healing (Holt, Tripathi et al. 2008). The serrated parallel plate set-up is typically used for rheological testing. The construct is placed between a stationary base plate and top plate which oscillates at a specified frequency or strain. The elastic properties of the constructs are represented by the shear storage modulus (G') and the viscous properties by the shear loss modulus (G"). Studies have shown that G' and G" are related to the microstructure and composition of the constructs. G' and G" have been shown to increase with decreasing pore sizes (Borzacchiello, Mayol et al. 2007), increasing degrees of chemical cross-linking (Sheu, Huang et al. 2001, Sosnik, Sefton 2005, Vanderhooft, Alcoutlabi et al. 2008) and increasing concentrations of solid microbeads (Zhao, Ma et al. 2008).

Rheological testing of pig skin showed that at low frequencies the gradual increase of G' and G" was observed. This was attributed to the elastic straightening and relaxation of the collagen and elastin fibres (G') and viscous movement of the ground substance between the fibres (G"). At higher frequencies a pronounced increase in G' and G" was observed and attributed to the inability of the viscous components of the dermis to adapt to the rate of load application causing compaction of the fibres (Holt, Tripathi et al. 2008). Furthermore, the strain rate dependency of the shear modulus in pig skin has also been reported when testing using uniaxial compression testing and was attributed to the viscous losses within the ground substance between the collagen fibres and viscoelastic losses within the collagen fibrils (Shergold, Fleck et al. 2006).

These results are supported by dynamic mechanical analysis (DMA) of collagen gels which showed increasing G' and G" with increasing cross-linking by glutaraldehyde additions (Sheu, Huang et al. 2001). Shearing DMA uses similar principles to rheology but linear rather than oscillatory shear is used. However, DMA can usually only tests small samples, approximately $10mm^2$, and many studies have reported difficulties with slippage between the DMA plates (Sheu, Huang et al. 2001). Studies of fibrin gels have shown that increasing the fibrinogen concentration causes increases in G' due to structural changes in the fibrin matrices (Eyrich, Brandl et al. 2007).

2.7. Factors that Affect the Fibrin Remodelling Process

A number of factors that affect the degree of compaction, cell proliferation and collagen synthesis in cell seeded fibrin gels have been reported. The effect of the fibrin matrix formulation on cell proliferation and the potential benefits of increasing the number of cells in fibrin based tissue-engineered constructs has been described previously in section 2.5.2. Other studies have shown that the number of cells in the construct can also be increased by supplementing the culture media with TGF- β1 (Ross, Tranquillo 2003), increasing the frequency of the media change from once per week to three times per week (Neidert, Lee et al. 2002) and by application of external mechanical stimulation (Prajapati, Eastwood et al. 2000b, Eastwood, Mudera et al. 1998). The initial cell seeding density has also been shown to increase the rate of collagen synthesis from SMCs seeded in fibrin matrices but did not affect the total amount of collagen in the matrix after 5 weeks in culture (Ross, Tranquillo 2003). An increase in the rate of collagen synthesis would be beneficial when manufacturing fibrin based tissue-engineered constructs as it may lead to a decrease in manufacturing time and associated costs.

In addition, a current challenge for tissue-engineered constructs is to improve the properties of the final matrix to achieve biological functionality and the mechanical properties for application in vivo. A number of approaches have (Neidert, Lee et al. 2002) been investigated to improve the properties of tissue-engineered constructs and have been focused on increasing the collagen synthesis in the constructs. Biochemical stimulation through the addition of growth factors to the media has been shown to be a practical method of increasing collagen synthesis. Application of external mechanical stimulation has been shown to further improve the properties of the constructs and both of these areas are reviewed below.

2.7.1. Biochemical Stimulation

The growth factor TGF-β1 has been widely reported to increase ECM and collagen deposition in-vivo during wound healing and in-vitro when used to supplement culture media used for cellular fibrin gels. A 0.66 fold to 4-fold increase in collagen synthesis from cells in fibrin gels have been reported (Table 3) as well as an increase in lysyl oxidase synthesis which is required for cross linking of collagen fibrils (Colwell, Faudoa et al. 2007, Sales, Engelmayr Jr et al. 2006, Grande 1997, Hong, Uzel et al. 1999, Rodriguez, Martinez-Gonzalez et al. 2008). In addition, the use of combinations of TGF-β1, plasmin and insulin have been shown to further increase collagen synthesis (Neidert, Lee et al. 2002, Grassl, Oegema et al. 2002). The addition of insulin alone was shown to cause a similar 4-fold increase in collagen synthesis to the addition of TGF-β1 alone. However the addition of plasmin in the absence of TGF-β1 and insulin did not cause and increase in collagen synthesis or UTS. This suggested that combinations of growth factors can have a synergistic effect on collagen synthesis.

However, TGF-β1 is a relatively expensive growth factor and has a half life of less than 30 minutes in-vivo (Neidert, Lee et al. 2002). The use of TGF-β1 on a commercial scale may cause manufacturing complications and impact cost effectiveness. Other authors have investigated the use of alternative growth factors such as epidermal growth factor (EGF) to address these issues (Grouf, Throm et al. 2007). In a comparative study of EGF and TGF-β1, EGF was shown to increase collagen synthesis by 15% more than TGF-β1 and increase the UTS 10 fold (Grouf, Throm et al. 2007). Finally, the addition of ascorbic acid to the media has also been shown to affect collagen synthesis by human dermal fibroblasts in a fibrin matrix in a dose-dependent manner. Additions of 10μg/ml of ascorbic acid were shown to increase collagen synthesis but addition of 50μg/ml decreased collagen synthesis compared to the control not supplemented with ascorbic acid.

TGF-β1 was also shown to suppress cell proliferation but contrasting results of increased cell proliferation have also been reported (Grouf, Throm et al. 2007, Ross, Tranquillo 2003). In the latter study, the media used was supplemented with both TGF-β1 and insulin which may explain the different results observed in these studies.

Medium Additions		Collagen content	UTS	Cell Number	Reference
5ng/ml	TGF-β1	↑ x4	↑ 4.1	-	(Neidert, Lee et al. 2002)
5ng/ml 2µg/ml	TGF-β1 Insulin	↑ x7	↑ 6.1	-	
5ng/ml 0.01U/ml 2µg/ml	TGF-β1 Plasmin Insulin	↑ x9	↑ 8.4	-	
2µg/ml	Insulin	↑ x4	↑ 3.5	-	
2.5ng/ml 2µg/ml	TGF-β1 Insulin	↑ x3.5	↑ x3	↑ x2.5	(Ross, Tranquillo 2003)
5ng/ml	TGF-β1	↑ x4	↑ x10	-	(Grassl, Oegema et al. 2002)
5ng/ml 2µg/ml	TGF-β1 Insulin	↑ x5.8	↑ x18	-	
5ng/ml	EGF	↑ x0.96	↑ x2		(Grouf, Throm et al. 2007)
5ng/ml	TGF-β1	↑ x0.66	↑ x0.2	↓ x2.6	
10µg/ml	Ascorbic Acid	↑ x2	-	-	(Gillery, Bellon et al. 1989)
50µg/ml	Ascorbic Acid	↓	-	-	

Table 3 The effect of media supplements on collagen synthesis, UTS and cell number in cell-seeded fibrin scaffolds. Numbers represent fold increase compared to control

2.7.2. Mechanical Stimulation

2.7.2.1. Cellular Responses

Application of mechanical stimulation has been widely reported to improve the properties of tissue-engineered constructs for a range of applications. Application of tensile, compressive and shear forces to tissue-engineered constructs for vascular, ligament, tendon and intervertebral discs regeneration (Isenberg, Williams et al. 2006, Henshaw, Attia et al. 2006, Screen, Shelton et al. 2005, MacKenna, Summerour et al. 2000, Neidlinger-Wilke, Wurtz et al. 2005) has been shown to increase collagen synthesis and the mechanical properties of the constructs (Table 4). A particular study of interest applied 16% equibiaxial strain at 0.2Hz to a HDF seeded fibrin gel for 8 days and showed that collagen synthesis increased by 15% and mechanical properties by 10% (Balestrini, Billiar 2006). A follow up study by the same research group investigated the effects of the magnitude of strain (0-16%) on the matrices and showed that the degree of compaction of the matrix and UTS increased with increasing strain (Balestrini, Billiar 2009).

Other studies have also shown that mechanical stimulation promotes secretion of TGFβ-1 from the cells (Ng, Hinz et al. 2005, Kessler, Dethlefsen et al. 2001, Webb, Hitchcock et al. 2006) and may contribute towards the increase in collagen synthesis in the matrices. Mechanical stimulation has also been shown to cause alignment of the fibres in the matrices in the direction of the applied force (Henshaw, Attia et al. 2006, Ng, Hinz et al. 2005, Ng, Swartz 2003, Girton, Barocas et al. 2002) and promote the secretion of MMPs which aid the remodelling of the extracellular matrix (Le, Rattner et al. 2002, Prajapati, Chavally-Mis et al. 2000a, Berry, Shelton et al. 2003).

2.7.2.2. The Effect of Mechanical Stimulation Parameters on Cellular Responses

The cell responses have been shown to be dependent on a number of parameters that control the mechanical stimulation regime. These include the type, magnitude, frequency and duration of the mechanical stimulation as well as the total study period over which the stimulation was applied and is discussed below.

2.7.2.3. Type of Stimulation

The importance of selection of the type of mechanical stimulus used to elicit cellular responses has been demonstrated in a study of bone marrow derived mesenchymal stem cells (BMSCs) and smooth muscle cells (SMCs) in a PGA/PLLA scaffold (Engelmayr, Rabkin et al. 2005). The application of cyclic flexure for 3 weeks resulted in the 42% and 63% increase in collagen synthesis for the BMSC and SMC construct respectively, compared to the control. However, application of cyclic flexure and shear flow resulted in no increase in collagen synthesis by the SMCs but a 75% increase when using BMSCs (Engelmayr, Rabkin et al. 2005).

2.7.2.4. Magnitude

The magnitude of the mechanical force is also important as it needs to be sufficient to cause a cellular response (Eastwood, Porter et al. 1996, Syedain, Weinberg et al. 2008), but not to high to cause undesired responses such as cell apoptosis (Kearney, Prendergast et al. 2008), undesired cell phenotype changes (Ng, Hinz et al. 2005, Syedain, Weinberg et al. 2008, Arora, Narani et al. 1999, Tomasek, Gabbiani et al. 2002, Grinnell 2000), rapid degradation of the matrix (Seliktar, Nerem et al. 2003, Seliktar, Nerem et al. 2001) and tearing of the matrix (Syedain, Weinberg et al. 2008).

The use of incremental strain, where the magnitude of the strain was increased over study duration has been shown to increase in collagen synthesis and mechanical properties compared to using a constant strain over the study duration (Syedain, Weinberg et al. 2008, Isenberg, Tranquillo 2003). The use of incremental strain from 5% to 15% resulted in a 36% increase in mechanical properties and 84% increase collagen content compared to using constant strain. This was supported by a study of HDF seeded fibrin matrices subjected to equibiaxial strain which also showed that collagen deposition correlated with increasing strains from 2%-16% (Balestrini, Billiar 2009).

2.7.2.5. Frequency

It has been shown that the application of cyclic mechanical stimulation is beneficial for collagen synthesis compared to application of continuous mechanical stimulation (Balestrini, Billiar 2009). The frequency and duration of the cycle control the time that the cells are stimulated and are at rest. Studies have shown that longer relaxation times in between stimulation of SMC and HDF seeded fibrin gels increased mechanical properties and collagen content (Balestrini, Billiar 2009, Isenberg, Tranquillo 2003).

2.7.2.6. Total Duration of Application

Finally, the majority of studies investigating the effects of mechanical stimulation on tissue-engineered constructs only compare the properties of tissue-engineered constructs at the start and end points of the study. Fewer studies have monitored the collagen content and mechanical properties at several time points during the culture period. These studies demonstrated that prolonged mechanical stimulation could also have a detrimental effect on the construct properties. For example, a 20-week study of SMCs in a PGA matrix, showed an increase in mechanical properties of the construct up to 10 weeks but a decrease in subsequent weeks (Kim, Nikolovski et al. 1999). Comparison of the mechanical properties at the start and end points only would have shown that mechanical stimulation caused an increase in mechanical properties but would not have shown the peak in mechanical properties that occurred after 10 weeks. Separate studies of SMCs and HDFs in a collagen matrices showed similar results where an increase in mechanical properties was observed after 4 days followed by

deterioration over the following 4 days, although they remained higher than the properties of static controls (Seliktar, Nerem et al. 2003).

2.7.3. Mechanotransduction

On a molecular level, many studies have identified the mechanisms by which cells detect and respond to mechanical stimulation (Figure 5) and this process of mechanotransduction has been recently review by Chiquet, Gelman et al. 2009, Wang, Tytell et al. 2009 and Ingber 2006. Mechanical stimulation activates mechanoreceptors such as integrins, G proteins, receptor tyrosine kinases and stretch activation channels on the cell membrane. These cause changes in the structure of the cytoskeleton and activate signalling pathways which lead to the activation of transcription factors, gene transcription and subsequent cellular responses such as protein synthesis, cell division and apoptosis (Iqbal, Zaidi 2005, Coppolino, Dedhar 2000, Ingber 2003a, Ingber 2003b, Eckes, Zigrino et al. 2000).

In particular, integrins $\alpha1\beta1$ and $\alpha2\beta1$ have been shown to be responsible for the binding of fibroblasts to collagen in the extracellular matrix, in response to tension and the transmission of mechanical stimuli between cells and ECM (Ng, Hinz et al. 2005, Langholz, Roeckel et al. 1997, Heino 2000). Integrin $\alpha1\beta1$ has been shown to regulate collagen synthesis and be necessary for cell and matrix alignment in matrices subjected to mechanical stimulation (Ng, Hinz et al. 2005, Langholz, Roeckel et al. 1997, Heino 2000). Integrin $\alpha2\beta1$ has been shown to be responsible for fibroblast spreading and adhesion to collagen fibres, matrix contraction, cell migration, regulation of MMP-1, and the up-regulation of collagen synthesis and fibril formation, when fibroblasts are subjected to mechanical stimulation (Ng, Hinz et al. 2005, Eckes, Zigrino et al. 2000, Eckes, Zweers et al. 2006). Other studies have shown that application of tensile force to fibroblasts up-regulates secretion of TGF-$\beta1$ which is required for the activation of the Smad signalling pathways and subsequently leads to the transcription of procollagen $\alpha1$(I) gene expression (Lindahl, Chambers et al. 2002, Verrecchia, Mauviel 2002).

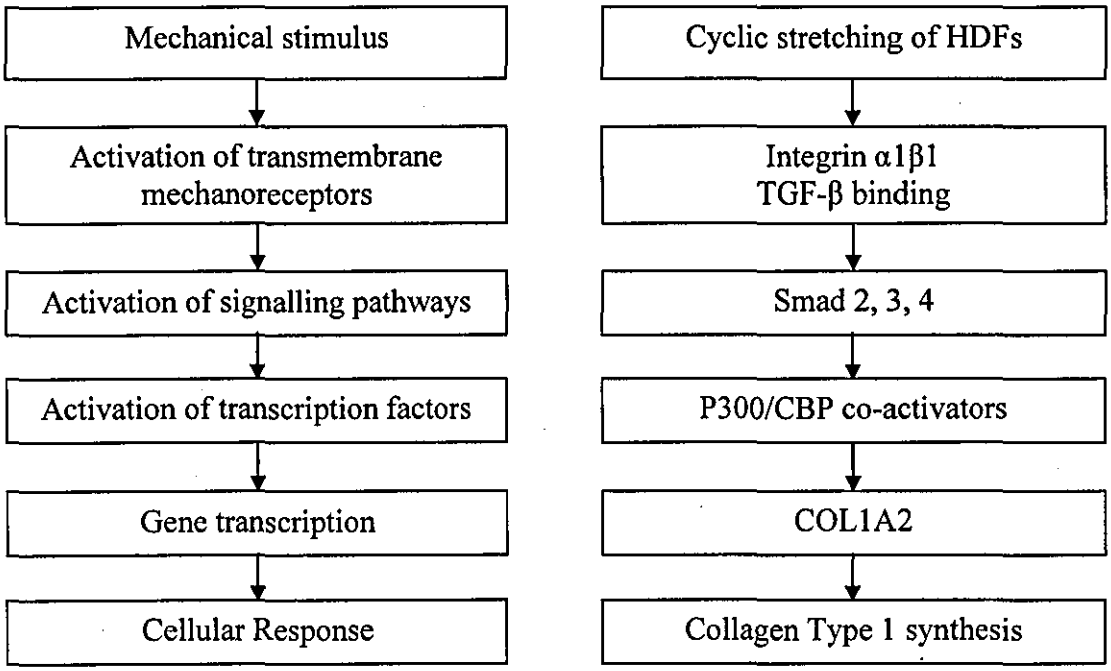

Figure 5 Left: Simplified overview of the mechanotransduction process. Right: Potential signalling pathway involved in collagen type 1 synthesis

Cell type	Scaffold	Mechanical Stimulus	Collagen I increase	UTS	E	Reference
Rat Smooth muscle cell	Type 1 collagen sponge	7% Cyclic strain, 1 Hz for 20 wks	~67%	600% ↑	1700% ↑	(Kim, Nikolovski et al. 1999)
Myofibroblast	Non-woven PGA	Laminar flow for 2 wks	52%	-	-	(Jockenhoevel, Zund et al. 2002)
Myofibroblast	Non-woven PGA/P4HB	9% Cyclic uniaxial strain, for 3 wks	71±23%	-	-	(Mol, Bouten et al. 2003)
Tendon Fibroblasts	Human tendon fascicles	5% Cyclic uniaxial strain, 1 Hz for 24 hrs	25.1%	-	-	(Screen, Shelton et al. 2005)
Chrondocytes	2% agarose hydrogel	10% Dynamic compression 1Hz for 21 days	37%	-	300%↑	(Mauck, Soltz et al. 2000)
SMC	PGA/ PLLA	Cyclic flexure, 1 Hz for 3 wks	63%	-	78%↑	(Engelmayr, Rabkin et al. 2005)
BMSC	PGA/ PLLA	Cyclic flexure 1 Hz	42%	-	187%↑	(Engelmayr, Sales et al. 2006)
		Flow induced shear stress,1 dyne/cm^2	16%	-	159%↑	
		Flexure and flow, for 3 wks	75%	-	166%↑	
SMC	PGA/ PLLA	Flexure and flow, for 3 wks	0%	-	78%↑	
SMC	Collagen gel	Cyclic distension, 5 wks	0%	80%	80%	(Isenberg, Tranquillo 2003)
SMC	Collagen gel	Cyclic distension, 8 days	-	240%	108%	(Seliktar, Black et al. 2000)
Human nucleus pulpous	Type 1collagen gel	Hydrostatic pressure,1Hz, 0.25MPa for 24hrs	~30%	-	-	(Neidlinger-Wilke, Wurtz et al. 2005)
HDF	Fibrin gel	0-16% Equibiaxial strain @0.2Hz for 8 days	15%	10%↑	0%	(Balestrini, Billiar 2006)
HDF	Collagen gel	10% Uniaxial Strain@1Hz for 24 hrs Pre-loading 2mN and 10mN	11% (2mN) 0% (10mN)	17%↓ 28%↓	25%↑ 30%↑	(Berry, Shelton et al. 2003)

Table 4 The effect of mechanical stimulation on collagen type I content and mechanical properties of cell-seeded matrices compared to static controls

2.8. The Effect of Ultrasound on Biological Responses

2.8.1. Diagnostic, Therapeutic and Disruptive Ultrasound

Ultrasound is defined as acoustic or mechanical waves of frequencies above 20 kHz (Kinsler, Frey et al. 2000). Ultrasound is produced by a piezoelectric transducer which transforms electrical energy into mechanical energy and delivers acoustic waves through the transducer (Kinsler, Frey et al. 2000). The ultrasound frequency, intensity, duty cycle and duration have been shown to affect the propagation of acoustic waves through tissues and the subsequent cellular responses. The acoustic conditions determine whether the ultrasound application has a therapeutic, disruptive or diagnostic use through thermal and/or biological effects (Ziskin 1987, Baker, Robertson et al. 2001).

Typically, diagnostic ultrasound uses microsecond pulses at frequencies in the kilohertz range and therapeutic ultrasound millisecond to second pulses at frequencies of 1 to 20MHz. Disruptive ultrasound typically uses frequencies is in the upper region of the therapeutic range. The most common use of diagnostic ultrasound is for imaging developing foetuses and it has more recently been applied to cardiac and ophthalmic diagnosis (Barnett, Ter Haar et al. 2000). Disruptive ultrasound uses high intensity ultrasound to cause targeted cavitation in tissues. It is routinely used to as a non-invasive technique to break up kidney stones and more recently to target and treat tumours (Miller 2007, ter Haar 2007). Ultrasound in the therapeutic range has become increasingly used to elicit positive responses in a number of biological applications and is reviewed in the following sections.

2.8.2. Ultrasound and Wound Healing In-Vivo

In-vivo, therapeutic ultrasound has been used in physiotherapy to accelerate healing of soft tissue injuries, accelerate the bone healing through the promotion of new bone formation, enhance drug uptake through the skin and more recently to transfer genes into diseased tissue (ter Haar 2007, Chang, Sun et al. 2002). Several studies have shown that ultrasound aids wound healing of rat tendon through an increase in collagen deposition, UTS and stiffness (DA Cunha, Parizotto et al. 2001, Ng, Ng et al. 2004, Ng, Wong 2008, Yeung, Guo et al. 2006).

Application of ultrasound to rat skin wounds has also been reported to have beneficial effects during the first 14 days of wound healing (Mendonça, Ferreira et al. 2006). In this study pulsed ultrasound was applied at a frequency of 1.5MHz, duty cycle of 20% and intensity of 0.3W/cm^2 for 10 minutes on alternate days for 14 days. After 3 days less fibrin and more young collagen was observed in histology sections of the ultrasound stimulated group compared to the non-stimulated group. After 7 days, more regularly distributed collagen was observed in the ultrasound group and a small but statistically significant increase of 0.37% in collagen types I and III was reported compared to the control groups. By day 14, more developed collagen, the development of dermal papillae and partially repaired sebaceous glands and pilary follicles were observed in the ultrasound group. Accelerated re-epithelisation was also reported in the ultrasound group and the formation of a thicker epidermis after 14 days.

This study is supported by a study which applied ultrasound to wounded pigs and observed increased collagen deposition in the wound compared to the non-stimulated control pigs (Baker, Robertson et al. 2001, Byl, McKenzie et al. 1992). However, a study of the healing rates of cockerel tendon showed that ultrasound did not accelerate wound healing (Ramirez, Schwane et al. 1997, Turner, Powell et al. 1989). The difference in response of healing rates to the ultrasound may have been due to the driving frequency of ultrasound used. In the study of cockerel tendon healing, a 3MHz frequency was used compared to 1-1.5MHz frequency used in the other studies of skin and rat tendon healing (Table 7).

2.8.3. The Effect of Ultrasound on Cellular Responses In-Vitro

In-vitro application of ultrasound to cell monolayers and tissue-engineered constructs has been shown to affect cellular responses such as, cell proliferation and synthesis of collagen, proteoglycans, GAGs and growth factors. The application of ultrasound has been shown to increase cell proliferation in monolayers of chrondocytes, fibroblasts and human mesenchymal stem cells (Doan, Reher et al. 1999, Webster, Pond et al. 1978, Zhou, Schmelz et al. 2004) and in cellular tissue-engineered constructs (Hsu, Kuo et al. 2006, Takeuchi, Ryo et al. 2008, Noriega, Mamedov et al. 2007). However, other studies have reported no increase in cell proliferation of osteoblast, chrondocyte and hMSC cells (Takeuchi, Ryo et al. 2008, Ebisawa, Hata et al. 2004, Harle, Salih et al. 2001, Nishikori, Ochi et al. 2002, Parvizi, Parpura et al. 2002).

There are also contrasting reports on the effects of ultrasound on collagen, proteoglycan and GAG synthesis (Table 5). Monolayers of chrondocytes, fibroblasts osteoblasts and human mesenchymal stem cells (hMSCs) have been reported to increase collagen, proteoglycan and GAG synthesis when stimulated by ultrasound (Ebisawa, Hata et al. 2004, Tsai, Pang et al. 2006, Yang, Lin et al. 2005). In addition, ultrasound was shown to increase collagen synthesis from cultures of fibroblasts which had been treated with collagenase to simulate injury (Ramirez, Schwane et al. 1997, Doan, Reher et al. 1999). In these studies, it was shown that collagen synthesis was increased by up to 40% after collagenase treatment and application of ultrasound compared to the controls. However, it was also shown that ultrasound decreased collagen synthesis from fibroblast monolayers not treated with collagenase and ultrasound (Ramirez, Schwane et al. 1997, Doan, Reher et al. 1999).

Similarly, there are contrasting reports of the effect of ultrasound on collagen, GAG and proteoglycan secretion from cells in tissue-engineered constructs (Table 6). Increased collagen and ECM synthesis has been reported from chrondocytes seeded in a range of matrices for cartilage regeneration and nucleus pulpous and annulus fibrous cells seeded in alginate beads for intervertebral disc regeneration (Hsu, Kuo et al. 2006, Noriega, Mamedov et al. 2007, Cui, Park et al. 2006, Iwashina, Mochida et al. 2006, Miyamoto, An et al. 2005). However, decreases in mechanical properties and collagen synthesis have also been reported in a chrondocyte seeded fibrin matrix (Duda, Kliche

et al. 2004). Comparison of the differences in the response of the cells seeded in matrices is problematic due to the wide range of acoustic conditions used to stimulate the constructs and experimental arrangements as discussed in section 2.8.5.

Intercytex have investigated the effect of ultrasound on collagen synthesis and mechanical properties of ICX-SKN constructs (Johnson, Marshall et al. 2006). Ultrasound was applied to the ICX-SKN constructs through a transducer secured to the base of the culture dish. A 1MHz frequency and ultrasound pulse of 10 seconds on and 180 second off was applied for 21 days. However, the results were inconclusive as an increase in mechanical properties and collagen content was only observed in one of six constructs tested (Personal communication Dr.P.Johnson, Research Director Intercytex, 2007). The experimental set-up and 21 day stimulation duration is likely to have caused heating in the constructs due to the build up of standing waves (section 2.8.5). This may have affected the cellular responses and variation in the results.

Few studies have investigated the affect of different acoustic conditions on cellular responses. The frequency and intensity of the ultrasound has been shown to affect cell viability and collagen synthesis. One study showed that collagen synthesis from chrondocytes seeded in a chitosan scaffold was increased with increasing the frequency from 1.5MHz to 5MHz over a range of intensities and duty cycles (Noriega, Mamedov et al. 2007). Other studies have shown that a lower ultrasound intensity of $0.002W/cm^2$ promotes collagen synthesis from chrondocyte monolayers at 1.5Hz frequency and 20% duty cycle compared to a higher intensity of $0.03W/cm^2$ (Zhang, Huckle et al. 2003). In addition, it has been reported that intensities above $0.4W/cm^2$ at 1MHz frequency and 20% duty cycle can cause fibroblast lysis and detachment from the surrounding matrix (Doan, Reher et al. 1999).

The role of TGF-β in the up-regulation of collagen synthesis has been discussed previously (section 2.7.1). Ultrasound stimulation has been shown to increase TGF- β from monolayers of fibroblast and osteoblast cells (Tsai, Pang et al. 2006, Harle, Mayia et al. 2005) which has also been reported for other forms of mechanical stimulation of tissue-engineered constructs (Ng, Hinz et al. 2005, Kessler, Dethlefsen et al. 2001, Webb, Hitchcock et al. 2006). In addition, supplements of TGF-β to culture media have

also been shown to up-regulate proteoglycan synthesis from hMSCs stimulated by ultrasound (Ebisawa, Hata et al. 2004).

2.8.4. Mechanisms that Cause Cellular Responses

The propagation of ultrasound waves through tissue-engineered constructs cause cellular responses through thermal and non-thermal effects (Baker, Robertson et al. 2001). The exact mechanisms by which ultrasound elicits cellular responses are not currently fully understood. However, it is believed that mechanical stimulation of the cells and thermal effect are caused by particle oscillation, cavitation and acoustic streaming as it propagates through the construct (Williams 1983) and are discussed below.

When ultrasound waves propagate through a material several phenomena may occur to cause particle movement (Challis, Povey et al. 2005). Firstly, propagating waves will pass through solid and liquid components of a material to cause particle movement. The speed of the wave propagation is dependent on the compressibility and elastic modulus of the components in the tissue. For instance, the wave propagation velocity through collagen has been shown to be greater than that through water (Duck 1990). Secondly, the propagating wave causes local compression and expansion of liquid and solid particles as the wave energy is stored elastically and subsequently released as kinetic energy. The release of kinetic energy can cause particle movement and heating of the material as the energy is deposited in the surrounding material.

Cavitation is defined as the formation and life of bubbles in liquids (Suslick, Nyborg 1990). Bubbles resting near a boundary oscillate when ultrasound is applied, causing fluid flow and shear stress at the boundary (Miller 2007, Challis, Povey et al. 2005). Bubbles formed away from boundaries travel towards the boundary before collapsing. Three possible effects of collapsing bubbles have been reported (Mitragotri, Kost 2004). Firstly, the bubble can collapse near the boundary causing pressure waves on the surface of the boundary. Secondly the collapse of the bubble at the boundary can cause pressure waves which resonate through the boundary.

Finally, the bubble can cause disruption of the boundary. The formation, movement and collapse of the bubbles may impart shear and compressive forces on cell membranes and the extracellular matrix. The magnitude of shear force that is required to cause a cellular response has not been reported. However, studies have shown that cellular responses to local shear stresses on cells in suspension is dependent on the cell density (Miller 2007) and that a shear stress of 100-160Pa is required for detachment of adherent cells in culture (Ohl, Wolfrum 2003).

Acoustic streaming can be categorised as bulk streaming and micro-streaming. Bulk streaming is caused by propagation of the ultrasound through a liquid and movement of the fluid in a single direction. Micro-streaming causes eddies to flow adjacent to an oscillating source and is associated with cavitation (Baker, Robertson et al. 2001, Starritt, Duck et al. 1991). Micro-streaming is more mechanically powerful than bulk streaming ((Mitragotri, Kost 2004, Ogura, Paliwal et al. 2008, Kushner IV, Kim et al. 2007) and has been shown to alter cell membrane permeability as a result of the streaming disturbing concentration gradients at the cell membrane interface (Starritt, Duck et al. 1989, Starritt, Hoad et al. 2000, Pohl, Antonenko et al. 1993).

Other studies have shown that ultrasound stimulation increases cell permeability by demonstrating the increased uptake of fluorescent dyes into the cells (Yang, Shirakata et al. 2005, Husseini, Diaz de la Rosa, et al. 2005), increased uptake of insulin and calcium ions into fibroblasts (Parvizi, Parpura et al. 2002, Mitragotri, Kost 2004) and the recent use of ultrasound for enhanced drug uptake reviewed by (ter Haar 2007). However, cell apoptosis, damage to intercellular organelles such as lysosomes and mitochondria (Baker, Robertson et al. 2001), and cytoplasm leakage have also been associated with cavitation and acoustic streaming (Hallow, Mahajan et al. 2006, Lai, Wu et al. 2006).

Finally, the molecular mechanisms by which ultrasound stimulation is converted into biochemical signals have been shown to be via integrin transmembrane mechanotransducers and formation of focal adhesion in cells stimulated by ultrasound (Zhou, Schmelz et al. 2004, Yang, Lin et al. 2005, Tang, Lu et al. 2007). Specific molecules in signalling pathways associated with collagen synthesis and cell proliferation have also been shown to be up-regulated by ultrasound (Zhou, Schmelz et

al. 2004). For example, ultrasound stimulation (1.5 MHz, 200μs pulse modulated at 1 kHz) of human dermal fibroblast monolayers, resulted in increased cell proliferation via the integrin β1 receptor and the Rho/Rock/Src/ERK signalling pathway. These reports are comparable to reports of tissue-engineered constructs mechanically stimulated by tensile, compressive and shear forces (Billiar, Throm et al. 2005, Paez, Jose et al. 2000).

2.8.5. Experimental Apparatus for In-Vitro Ultrasound Stimulation

A number of different experimental set-ups have been used to apply ultrasound to tissue-engineered constructs and cell monolayers. The simplest set-up attaches an ultrasound transducer to the base of a culture dish via a coupling gel or in the media above the cells (Zhou, Schmelz et al. 2004, Nishikori, Ochi et al. 2002, Tsai, Pang et al. 2006). However, ultrasound stimulation of the cells in this set-up is in the near field of the ultrasound beam where there are large variations in acoustic pressure (Humphrey, Duck 1998). This can cause inhomogeneous stimulation of the cells. In addition, the cells are prone to heating as standing waves are likely to develop in the cultures.

Other apparatus have been used to stimulate cells and tissue engineered constructs in the far field of the ultrasound beam where the acoustic pressure is the most homogeneous. Typically, the culture dish is placed in a water bath so that the base of the dish is in contact with the water. The water bath is adapted so that an ultrasound transducer can be attached to the base and the ultrasound propagates through the water bath to the cells (Hsu, Kuo et al. 2006, Siu, Jackson et al. 2007, Warden, Favaloro et al. 2001). However, this experimental arrangement is still prone to the build-up of standing waves and heating of the cells. Addition of a liquid path for the ultrasound to propagate through after it has passed through the cells would minimise the build up of standing waves. This experimental arrangement has been used for cells cultured in flasks and an ultrasound absorbing material was also used to reduce the reflection of the ultrasound back into the constructs (Harle, Salih et al. 2001).

Monolayer Cell Type	Frequency (MHz)	Intensity (W/cm^2)	Duty Cycle (%)	Delivery Regime	Study Duration	Main outcome	Reference
Chrondocyte	1.0	0.33-1.0	20 & 50	10min/day	6 days	Cell no. ↑ @0.67W/cm², 20%	(Hsu, Kuo et al. 2006)
Chrondocyte	1.5	0.002-0.03	20	20min/day	7 days	Cell no. ↑@day 3 only Collagen II ↑ @0.002W/cm²	(Zhang, Huckle et al. 2003)
Osteoblast	3	0.13-0.18	100	10min/day	1 day	TGFβ↑ with intensity Cell no. ↔	(Harle, Mayia et al. 2005)
Osteoblast	1.0	0.06- 0.2	-	10min/day	-	Collagen I ↑ @0.1W/cm² Integrin expression ↑	(Yang, Lin et al. 2005)
Fibroblast	1.5	0.03	20-100	6-11mins	1 day	Cell no ↑ Formation of focal adhesions	(Zhou, Schmelz et al. 2004)
Fibroblast	1.0	0.1-0.4	20	5mins	9 days	Cell no ↑ 50% Collagen ↓	(Doan, Reher et al. 1999)
Fibroblast	1.0	0.4	20 and 100	3min/day	-	Collagen ↔ Collagen ↑ when cells treated with collagenase	(Ramirez, Schwane et al. 1997)97.
hMSC	1.0	0.015-0.12	20	20min/day	-	Cell no. ↔ Proteoglycan↑ and Aggrecan↑ with TGFβ in media only	(Ebisawa, Hata et al. 2004)
Tendon cells	1.0	0.1-1.0	20	5min	1 day	Collagen I and III ↑ TGFβ ↑ with intensity	(Tsai, Pang et al. 2006)
Leukaemia Cells	1.0	0.1-2.0	100	10min	-	Cell apoptosis↑ with intensity	(Feril, Kondon 2004)

Table 5 The acoustic conditions used to elicit cellular responses from cell monolayers. ↑= increase, ↓=decrease, ↔ = no significant difference

Tissue-engineered construct	Frequency (MHz)	Intensity (W/cm^2)	Duty Cycle (%)	Delivery Regime	Study Duration	Main Outcomes	Reference
Chrondocytes in polyester scaffold	1.0	0.03-0.1	20	10min/day	7 wks	Cell no.↑ GAG ↑ Collagen ↑	(Hsu, Kuo et al. 2006)
Chrondocytes in collagen sponge	1.5	0.03	20	20min/day	3-14 days	UTS ↑ Collagen I ↑ Collagen II ↔ Cell no. ↑	(Takeuchi, Ryo et al. 2008)
Chrondocytes in chitosan scaffold	1.5 & 5	1.5 5 8.5	161sec on 51 sec on 24 sec on	Twice a day	10 days	Cell no. ↑ Collagen ↑ @ 5MHz Collagen↔ @ 1.5MHz	(Noriega, Mamedov et al. 2007)
Chrondocytes in Atelocollagen gel	1.5	0.03	20	20mins/day	3 wks	Proteoglycan 52%↑ Cell no↔ Stiffness↔	(Nishikori, Ochi et al. 2002)
Chrondocytes in fibrin glue	1.5	0.03	-	20min/day	1-12 wks	Collagen II ↓ E ↓	(Duda, Kliche et al. 2004)
Fibroblasts in collagen gel	2.0	8	-	60secons	-	Cell permeability ↑	(Yang, Shirakata et al. 2005)
Nucleus pulpous & annulus fibrous in alginate beads	-	0.03	-	20min/day	20 days	Proteoglycan 24% ↑ Collagen II 16%↑	(Miyamoto, An et al. 2005)
Nucleus pulpous & annulus fibrous in alginate beads	1.0	0.075-0.12	20	20min/day	12 days	Proteoglycan ↑	(Iwashina, Mochida et al. 2006)
hMSC in PGA mesh	0.8	0.2	-	10mins/day	4 wks	Cell no↔ Compressive strength ↑ GAG more distributed	(Cui, Park et al. 2006)

Table 6 The acoustic conditions used to elicit cellular responses from tissue-engineered constructs. ↑= increase, ↓=decrease, ↔ = no significant difference

In-vivo wound healing	Frequency (MHz)	Intensity (W/cm^2)	Duty Cycle (%)	Delivery Regime	Study Duration	Main Outcomes	Reference
Rat Achilles tendon	1.0	1.0 & 2.0	100	4mins for 6days/wk	25 days	UTS@1W/cm^2↑15% UTS@2W/cm^2↑40%	(Ng, Ng et al. 2004)
	-	0.5	20	5mins	-	UTS ↑ E ↑ Collagen ↑	(Yeung, Guo et al. 2006)
	1.0	0.5	20-100	5mins	14days	Collagen bundle organisation ↑	(DA Cunha, Parizotto et al. 2001)
Cockerel tendon	3.0	0.2	-	-	-	Collagen ↔	(Turner, Powell et al. 1989)
Skin (rat)	1.5	0.03	20	10mins alternate days	14days	Accelerated healing	(Mendonça, Ferreira et al. 2006)
Skin (pig)	1.0	0.1-0.3	-	-	-	Collagen↑	(Byl, McKenzie et al. 1992)
Skin permeability	0.2-0.4	1-3MHz	-	-	-	Insulin uptake ↑@1MHz	(Mitragotri, Kost 2004)

Table 7 The acoustic conditions used in-vivo to accelerate wound healing. ↑= increase, ↓=decrease, ↔ = no significant difference

2.9. Conclusion

The processes that occur in cell seeded fibrin constructs to produce a collagen matrix for tissue-engineering applications have been widely reported. Human dermal fibroblast (HDF) cells seeded in a fibrin matrix have been used to develop tissue-engineered constructs for dermal regeneration applications and to investigate the wound healing remodelling process in-vitro. The major processes that occur in HDF seeded fibrin matrices are cell proliferation, matrix compaction, fibrin degradation and collagen synthesis. These processes were also observed in fibrin matrices seeded with smooth muscle cells (SMC) for cardiovascular applications.

The Intercytex dermal substitute, ICX-SKN, is currently produced by seeding HDF cells in a fibrin matrix and culturing the constructs for 49 days. Increases in the mechanical properties and collagen content of a HDF seeded fibrin matrix over this duration have been reported by one study which compared the properties after 21 days and 51 days in culture (Neidert, Lee et al. 2002). However, more frequent measurements would provide a better understanding of the rate of change and trends in the property evolution during this period. A 5-week study of SMCs in a fibrin matrix monitored the changes in mechanical properties, fibrin degradation, collagen synthesis and cell proliferation at weekly time points (Ross, Tranquillo 2003). A similar method could be adopted to provide a better understanding of the interactions between the changes in biochemical, physical and mechanical properties of ICX-SKN over the 49 day manufacturing process.

It is well established that the compaction of restrained cell seeded matrices results in a decrease in the thickness of the constructs (Grinnell 2003). However, few studies have analysed the homogeneity of the matrix structure through the thickness of the construct after the compaction. The efficacy of ICX-SKN is hypothesised to be dependent on the degradation rate of the collagen as discussed in section 2.4.3. Therefore, further investigation into the homogeneity of the matrix would be of value to provide further understanding of the degradation rate in different areas of the construct. In addition, reports of the thickness of the tissue-engineered constructs have been based on single point measurements (Tuan, Song et al. 1996). Analysis of the thickness of the whole

constructs would be beneficial for ICX-SKN as it also aims to provide structural support when applied to a wound.

A number of techniques to qualify and quantify the changes in the physical, biochemical and mechanical properties of tissue-engineered constructs have been reported. The quantity of collagen deposited in cell seeded fibrin gels and the mechanical properties of the final matrices are suggested to be the key parameters for improving the efficacy of tissue-engineered constructs in-vivo. Hydroxyproline based assays are most commonly used to measure the quantity of collagen deposited in cell seeded fibrin gels. However, studies by Intercytex have shown that the hydroxyproline assay produces positive reading when applied to control fibrin matrices and may provide misleading data (Marshall 2005). Further development of the hydroxyproline assay to eliminate the fibrin content before testing or use of alternative assays such as ELISA is required for measurement of collagen in ICX-SKN.

Repeatable measurement of the mechanical properties of cell seeded fibrin matrices has also been shown to be problematic due to their gel-like properties (Billiar, Throm et al. 2005). Inflation techniques that apply biaxial strain and rheology applying shear strain have been shown to the most repeatable techniques for determining the UTS and viscoelastic properties of gel-like planar tissue-engineered constructs. In addition, it has been shown that careful preparation of tissue-engineered constructs for observation by electron microscopy is required to minimise damage to the structure of the matrix. High pressure freezing and resin embedded sections for analysis of the surface and cross-sections of the constructs have been shown to be suitable techniques but are expensive and time consuming.

Many of the characterisation techniques described in the literature were destructive and therefore require a large number of samples to be produced when monitoring the changes in properties of tissue-engineered constructs over time. Manual production of large batches of constructs are susceptible to variation and contamination due to lapses in aseptic technique due to operator fatigue. The development of non-destructive tests to analyse the biochemical and physical properties of tissue-engineered construct would allow for a reduction in operator related batch variation and more cost effective research.

A current challenge for tissue-engineered constructs is to achieve biochemical functionality and mechanical properties suitable for application in-vivo. Many studies have reported the use of biochemical and mechanical stimulation to increase the collagen content and improve the mechanical properties of tissue-engineered constructs.

The use of culture media supplemented with EGF and TGF-β1 in combination with plasmin and insulin has been shown to increase collagen synthesis and mechanical properties in for HDF seeded fibrin matrices by up to 4-fold. In addition, increasing the frequency that the media and growth factors were replenished from once a week to 3 times a week showed a further increase in collagen synthesis and mechanical properties. Intercytex have developed a media formulation, Total Media, for the culture of ICX-SKN which contains EGF and TGF-β1, plasmin and insulin. The frequency of the media change in the current process is 3 times per week and therefore, further investigation into increasing collagen synthesis and mechanical properties of ICX-SKN will be focused on using mechanical stimulation.

Application of mechanical stimulation to cell seeded matrices has been shown to increase collagen synthesis and mechanical properties of a range of tissue-engineered constructs. The type of stimulation (tensile, compressive or shear), magnitude, frequency and total duration of stimulation has been shown to affect the degree of collagen synthesis from the cells. For HDF seeded fibrin gels, it has been shown that collagen synthesis and mechanical properties increase with increasing cyclic equibiaxial strain form 0% to 16% (Balestrini, Billiar 2009). In addition, it was shown that application of intermittent strain (6 hours on, 18 hours off) increased collagen synthesis compared to continuous strain (24hours on) over an eight day study duration (Balestrini, Billiar 2009).

However, many of the apparatus used to apply the mechanical stimulation required physical coupling to the constructs. This would be problematic for the ICX-SKN constructs as they initially have gel-like properties which are prone to tearing. Ultrasound has been identified as a practical method of applying mechanical stimulation to gel-like constructs without the need for physical coupling. The use of ultrasound in the therapeutic range has also been shown to increase collagen synthesis and mechanical properties in a number of cell seeded scaffolds for tissue-engineering applications.

Most commonly, ultrasound stimulation has been used to promote collagen synthesis from chrondocyte seeded matrices for cartilage regeneration (Hsu, Kuo et al. 2006, Takeuchi, Ryo et al. 2008) and nucleus pulpous seeded matrices for intervertebral disc regeneration (Iwashina, Mochida et al. 2006). In-vivo, ultrasound has also been shown to increase the rate of wound healing in bone and soft tissue (Yeung, Guo et al. 2006, Mendonça, Ferreira et al. 2006, Perry, Parry et al. 2009,Kaufman, Luo et al. 2008). Intercytex have previously investigated the use of ultrasound on collagen synthesis in ICX-SKN. However, the experimental arrangement used was prone to inhomogeneous stimulation of the constructs and undesired heating effect which may have caused the inconclusive results. Other studies investigating the effect of ultrasound on HDF seeded fibrin gels has not been reported in the literature.

Ultrasound has also been shown to decrease collagen synthesis and mechanical properties when applied to cell seeded constructs. However, the reasons for the differences in cell response are difficult to establish due to the large range of experimental arrangements and acoustic parameters used in independent studies. A few studies have shown that the magnitude of the ultrasound intensity and frequency can affect collagen synthesis. However, investigation into the affect of the combinations of intensity, frequency and duration of stimulation has not been reported.

Chapter 3 Characterisation of SKN Construct Properties

3.0. Introduction

ICX-SKN constructs are currently manufactured by casting human dermal fibroblasts (HDF) in a fibrin matrix and feeding the constructs with a specific media formulation for 49 days (section 2.4.1). The construct is then freeze dried for storage and sterilised by gamma-irradiation. Prior to application in a wound site in-vivo, the constructs are repopulated with HDF cells (Flasza, Kemp et al. 2007). The characterisation studies in this thesis are focused on the first 49 days of the manufacturing process where it has been shown that the fibroblasts breakdown the fibrin matrix and secrete collagen to form the final ICX-SKN product (Boyd, Flasza et al. 2007).

The following characterisation study aims to improve the qualitative model of the processes that occur during manufacturing as described in section 2.4.3 and by Boyd, et al 2007. The constructs used in the following studies were produced using the same process as described for the manufacture of ICX-SKN (Flasza, Kemp et al. 2007) but substituted the human fibrinogen, with bovine fibrinogen to allow for cost-effective research. These constructs are referred to as SKN constructs in this thesis. The methodologies developed for SKN constructs have been shown to be transferable to ICX-SKN constructs (personal communication with P.Johnson, Director of Research, Intercytex, 2007). Other research groups have previously reported changes in biochemical and mechanical properties of similar cellular fibrin gels over time (Ahlfors, Billiar 2007, Neidert, Lee et al. 2002). However, no study has characterised the physical, structural, biochemical and mechanical properties over a 49 day study period.

The materials and methods used to produce the SKN constructs is described in sections 3.1 to 3.2. The materials and methods to characterise the physical, structural, biochemical and mechanical properties of the SKN constructs during manufacturing are described in sections 3.3 to 3.5. The results of the characterisation studies are described in sections 3.6 to 3.9. The improved four phase SKN construct manufacturing process model is described in section 3.10. Further areas of research to improve the cost-effectiveness of the process and build upon the process model developed in this study are summarised in section 3.11 and expanded in Chapter 7.

3.1. Materials and Methods

The materials and methods used for the production of SKN constructs and characterisation of the physical, structural and mechanical properties and biochemical composition of SKN constructs during manufacturing are described in the following sections. A separate batch of SKN constructs was cast for each characterisation technique described unless otherwise stated. The time points during manufacturing at which the constructs were characterised for each technique is summarised in Table 8. Section 3.2.1 describes the semi-automated production of master and working human dermal fibroblast cells banks using the CompacT SelectT (The Automation Partnership, UK) and the method for casting SKN constructs.

Section 3.3 describes the materials and methods used to model the physical changes in the SKN constructs using precision surface profiling and observe changes in the structure and composition of the matrix by light and electron microscopy. SKN constructs were prepared for histology, immunohistochemistry (IHC) and confocal laser fluorescent scanning microscopy (CLFM) at the Advanced Microscopy Unit (AMU), Nottingham University, UK. Standard preparation techniques used for tissue samples were optimised by Dr.S.Anderson, M.Smith and D.Christie, for imaging of the SKN constructs. Cross-sections of the SKN constructs were analysed for changes in the composition of fibrin, collagen, proteoglycans and elastin using histology and the type of collagen using IHC. CLFM was used to analyse the orientation and spatial distribution of the cells and collagen structure viewed from the top and bottom surfaces of the SKN constructs.

Scanning electron microscopy (SEM) was used to investigate the morphology of the SKN construct matrix and interactions with the cells at higher magnifications. Since the constructs were comprised of over 50% water, conventional sample preparation techniques were modified to minimise the shrinkage of the construct and damage to the native structure. Development of the sample preparation methodology for the SKN constructs and imaging by SEM was carried out by Dr.A.Brain, Chief Technical Officer at the Centre of Ultrastructural Imaging (CUI), King's College London. Transmission electron microscopy (TEM) was used to investigate the internal structure of the fibroblast cells to give an insight into cell activity in the SKN constructs. Preparation of

resin embedded TEM sections and imaging was also carried out at the AMU, Nottingham University, UK.

Section 3.4 describes quantitative assays to measure the changes in the biochemical composition of the SKN constructs during manufacturing. The number of human dermal fibroblast cells in the construct was determined using trypan blue and the percentage of live, apoptotic and dead cells determined by flow cytometry. The time taken to digest the SKN constructs in collagenase B was used as an indication of the degree of cross-linking in the constructs. The SKN constructs were dehydrated to evaluate the change in the percentage of water and insoluble extracellular matrix during manufacturing. The quantity of collagen type I was analysed using an enzyme –linked immunosorbent assay (ELISA). Finally, the use of Raman spectroscopy was investigated as a non-contact, non-destructive technique to identify the structure and biochemical composition of the SKN constructs in collaboration with Dr.I.Notingher, Nottingham University School of Physics, UK.

Section 3.5 describes the rheological analysis of the viscoelastic properties of SKN constructs during manufacturing to provide quantitative data to support the qualitative physical and structural observations and changes in biochemical composition. The rheological protocol was developed with assistance from Dr.L.Hamilton, Nottingham University School of Pharmacy and Mr.S.Goodyear, Anton Paar, UK.

Statistical differences between the averages of results of each time point during the manufacturing period was analysed using a 2 sample T-tests in Minitab® 14 Statistical Software. A statistically significant difference was represented by a p-value of less than 0.05.

Characterisation Technique	Property Characterised	D-2	D0	D7	D14	D21	D28	D35	D42	D49	Batch
Surface Profiling	Surface Profile Thickness Volume										1,2,AC
Histology	Fibrin Structure Collagen Structure										3
IHC	Collagen Type I Collagen Type III										3
CLFM	Cell Orientation Collagen Type I Structure			D6							4
SEM	Matrix Structure Cell Distribution		D3								5
FEGSEM	Matrix Structure Cell Distribution										6
TEM	Cell Ultrastucture and Activity			D5				D33			7
Digestion	Collagen/Fibrin cross-linking										8
Flow Cytometry	Live, apoptotic, dead cells										8
Dehydration	Wet weight Dry weight of ECM										9,10,AC2
ELISA	Collagen Type I										11
Raman Spectroscopy	Collagen/Fibrin Composition									D63	9, AC3
Rheology	Shear storage modulus Shear loss modulus										10,AC4,CD

Table 8 Summary of the techniques used to characterise the SKN constructs and the time points at which measurements were taken during manufacturing (shaded). Far right column: The batch of constructs used for each characterisation technique where AC=acellular constructs. CD=cadaver dermis

3.2. Production of SKN Constructs

3.2.1. Cell Culture

A master cell bank for use in SKN constructs was created by culturing passage 0 (P0) neonatal human dermal fibroblast (HDF) cells (TCS Cellworks, UK) to P3 using the CompacT SelecT robotic automated cell culture system manufactured by TAP (The Automation Partnership, UK). The CompacT SelecT comprises of a robotic arm, which manipulates tissue culture flasks, and an integrated incubator and cell counting system (CEDEX, Innovartis, Germany). Automated programs for the seeding, culturing, harvesting and counting of the HDF cells were developed from the standard operating procedures for manual culture of HDF cells (see Appendix I for automated programs and manual protocols).

Briefly, DMEM-10 culture media comprising of Dulbecco's Modified Eagle's Medium (BE12604, Lonza, UK), supplemented with gamma irradiated fetal bovine serum (10%, SAFC Biosciences, UK) and L-Glutamine (5%, Sigma-Aldrich, UK) was prepared and loaded on the CompacT SelecT. P0 HDF cells were manually recovered from cryostorage according to Experimental Operating Procedure, EOP008 (Appendix I). The HDF cells were resuspended in DMEM-10 media and the cell suspension (30mL) was seeded in a bar-coded T175 tissue culture flask (BD Biosciences, UK) at a density of 5000 cells/cm^2. The flask was imported into the CompacT SelecT and stored in the humidified incubator at 37°C and 5% CO_2. The CompacT SelecT was programmed to retrieve the flask from the incubator after 3 days, dispose of the spent media, dispense fresh DMEM-10 media (30mL) and replace the flask back in the incubator for further cell proliferation.

After 7 days, the cells were near confluence under these growth conditions. The CompacT SelecT was programmed to dispose of the spent media, dispense 0.25% trypsin/EDTA (6mL, Sigma-Aldrich, UK) into the flask and replace the flask in the incubator for 6 minutes to allow enzymatic detachment of cells from the growing surface. The flask was then retrieved from the incubator and DMEM-10 media (10mL) was added to inactivate the trypsin. The flask now containing the P1 cells was exported from the CompacT SelecT and the cells pelleted by centrifugation at 500g for 5

minutes. The supernatant was aspirated and the cell pellet manually resuspended in DMEM-10 media (30mL). The cell suspension was placed in a new bar-coded flask which was then imported into the CompacT SelecT. The cell concentration was determined using the integrated CEDEX automated cell counter and the required volume of DMEM-10 media was added to obtain a final cell suspension of $8.75x10^5$ cells/mL. The number of flasks that could be seeded from this cell suspension at a density of 5000cells/cm^2 was calculated. DMEM-10 media (29mL) and 1mL of the cell suspension from the imported flask was dispensed into the calculated number of new flasks in the CompacT SelecT before placing in the incubator. The DMEM-10 media in these flasks was changed after 3 days and the cells trypsinised after 7 days as described previously. The resulting P2 cells were pooled in a single flask before exporting and centrifuging as described previously.

This was repeated until P3 when the cells were resuspended in DMEM-10 supplemented with DMSO (10% Sigma-Aldrich, UK) at a density of $1.5x10^7$ cells/mL. 1mL of the cell suspension was place in a cryovial and the cryovials placed in a "Mr Frosty" cell freezing container stored at 4°C (Nalgene Labware, NY, USA) with 250mL of isopropanol (Sigma-Aldrich, UK) as per the manufacturer's instructions. The "Mr. Frosty" was placed in a -80°C freezer for 24 hours after which the cryovials were transferred to liquid nitrogen to store the master cell bank. One vial of P3 HDF cells was taken from the master cell bank after 24 hours, recovered from cryopreservation and cultured to P7 using the CompacT SelecT procedures described above. The P7 cells were cryopreserved as described above to create a working cell bank. This was repeated for subsequent vials of P3 HDF cells to replenish the working cell bank when necessary. The P7 cells were recovered from cryopreservation immediately prior to use in the SKN constructs and resuspended at a density of $3x10^6$cells/mL in DMEM-10.

3.2.2. Casting of SKN Constructs

SKN constructs were produced by adding 2.6mL of 5mg/mL bovine fibrinogen (Sigma-Aldrich, UK) in phosphate buffered saline (PBS minus Mg^{2+} and Ca^{2+}, Lonza, Switzerland), 0.63mL of the HDF cell suspension and 0.63mL of 25IU/mL thrombin (Baxter Healthcare, UK) in PBS, to a 15mL Falcon tube. Immediately after addition of the thrombin solution, 3.4mL of the mixture was drawn into a 5mL micropipette and cast into a rectangular 28mm x 38mm well in a culture dish (Nunc, NY, USA). The constructs were allowed to gel for 10 minutes at room temperature before DMEM-10 media (4mL) was placed on the top of the constructs to break the surface tension. This media was aspirated and 2mL of fresh DMEM-10 media was placed on each construct. The casting day was denoted D-2. After 48 hours Total Media (TM) was used to feed the SKN constructs every Monday, Wednesday and Friday for the total manufacturing period of 49 days The first feeding of the constructs with Total Media (TM), two days post-casting, was denoted day 0 (D0). Total Media was produced immediately prior to use by adding the supplements specified in Table 10 to Matrix Producing Media (MPM) specified in Table 9, which was prepared in advance. This process is equivalent to the ICX-SKN manufacturing process except for the substitution of bovine fibrinogen for human fibrinogen.

Matrix Producing Media (MPM)				
Component	Supplier	Dissolving Solution	Component Concentration	Volume (mL)
Dulbecco's Modified Eagle's Medium (DMEM)	Lonza	-	N/A	646
Hams F12	Lonza	-	N/A	216
Fetal Bovine Serum	SAFC Biosciences	-	N/A	100
L-Glutamine	Lonza	ddH_2O	200mM	10
Hydrocortisone	Sigma	5mg/mL ethanol and ddH_2O	200µg/mL	2
Ethanolamine + O-Phosphoryl-ethanolamine	Sigma	ddH_2O	50mM + 50mM	2
Triiodo-l-thyronine + Transferrin	Sigma + Millipore	1M HCl	2.5mg/mL + 10µM/mL	2
Selenious acid	Molekula	ddH_2O	3.39µg/mL	2
Ascorbate	Molekula	ddH_2O	25µg/mL	2
L-Proline	Molekula	ddH_2O	100µg/mL	2
Glycine	Molekula	ddH_2O	50µg/mL	2
Polyethyleneglycol MW 3,400-3,700	Sigma	PBS	10%(w/v)	5
Amphotericin B	Invitrogen	ddH_2O	250µg/mL	1
Gentamycin	Molekula	ddH_2O	50mg/mL	1

Table 9 Composition of Matrix Producing Media (MPM)

MPM Supplement	Supplier	Dissolving Solution	Supplement Concentration	Volume/mL of MPM
rhTGF-β	R&D Systems	1mg/mL Bovine Serum Albumin (Serologicals) in 4mM HCL	10µg/mL	5µl
rhEGF	R&D Systems	1mg/mL Bovine Serum Albumin in PBS -	10µg/mL	6.25µl
Plasmin	Calbiochem	PBS	1U/mL	10µl
Insulin	Serologicals	PBS	2.5µg/mL	2µl

Table 10 Supplements added to MPM to produce Total Media

3.3. Physical and Structural Properties

3.3.1. Precision Surface Profiling

The surface profile of SKN constructs was mapped using a Talysurf300 Precision 3D Surface Profiler with 3mm white light CLA gauge (Taylor-Hobson Precision, UK). The SKN constructs in the culture dishes were removed from the 37°C and 5% CO_2 incubator, the media was aspirated and the constructs were placed in the surface profiler (Figure 6 top). 100 data points on the surface of the SKN construct were taken at 2.6mm and 3mm intervals, over a 26 x 36mm area, in the x and y axis respectively to produce a 3D meshed image. A 4mm slip-gauge was used as a z-axis reference point and to ensure that the maximum height of the SKN construct was within the 3mm working range of the machine gauge (Figure 6, bottom). It was not possible to obtain data from the outer 2mm perimeter of the SKN constructs due to the deflection of the white light by the edge of the culture dish, away from the receiver.

The volume of the SKN construct was calculated by multiplying the average area in the y-axis (calculated by the TalySurfGold software) by 26 (the width of the construct) and adding the rectangular volume of the construct below the slip gauge. The thickness, t, of the constructs was calculated by adding the distance between the top of the construct at the centre and the top of the slip gauge, to the distance between the base of the culture dish and the top of the slip gauge (Figure 6, bottom). After measurement, 2mL of fresh media was placed on the constructs and the culture dish replaced in the incubator. Three SKN constructs were cast as a batch and the surface profile, volume and thickness of these constructs was measured on days D-2, D0, D2, D5, D7 and then every 7 days until D49. This was repeated for a separate batch of SKN constructs (n=3) and acellular constructs (n=3).

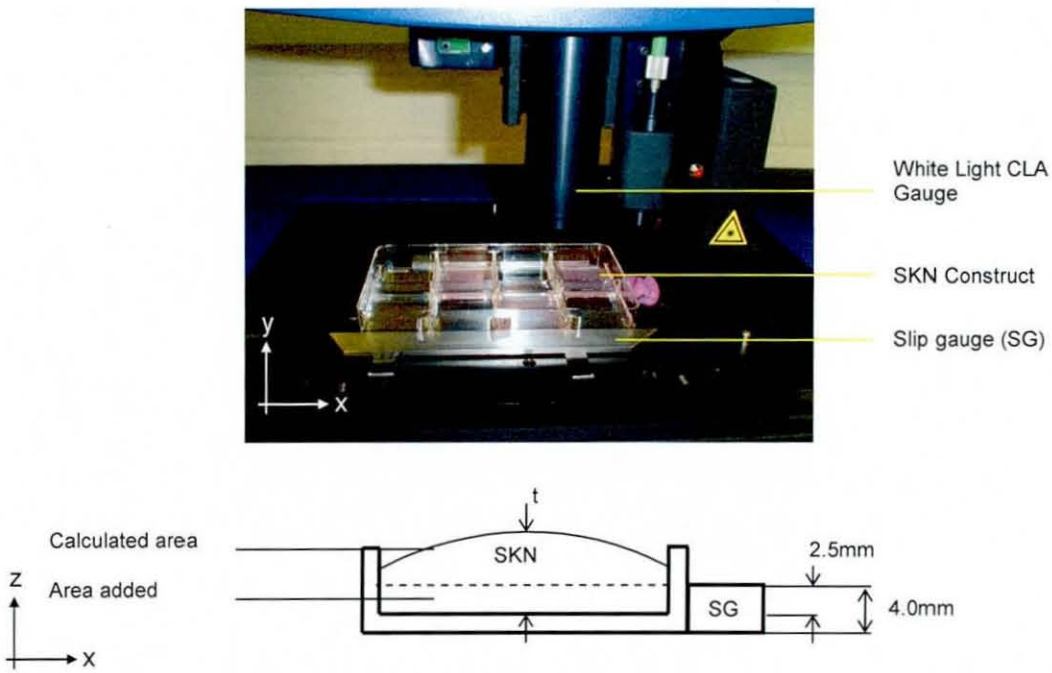

Figure 6 Top: Experimental Set-up of SKN Construct in the Precision 3D Surface Profiler. Bottom: Schematic of cross-section where t=thickness and SG = slip gauge

3.3.2. Histology

On D0, D21 and D49 a section (approximately 3mm x 10mm) was cut from the centre of the SKN construct using a scalpel and fixed in 10% neutral buffered formalin (Sigma-Aldrich, UK) for 24 hours. The section was processed through a series of increasing ethanol concentrations (70%, 80%, 96% and 100%), xylene and molten wax over 17 hours using a Leica TP 1020 automatic tissue processor (Appendix II for full tissue processor timings). The samples were then embedded in wax using a Leica EG1150c tissue embedding station and 8μm cross-sections were cut using a Leica RM2135 rotary microtome. The samples were stained with Masson's Trichrome (MT) for detection of fibrin and collagen and viewed under a light microscope. This was repeated using Alcian Blue (AB) stain for detection of proteoglycans and Elastic Van Gieson's (EVG) stain for detection of elastin (Appendix II for full staining protocols). Samples of human liver, skin and intestine were used as controls for the respective stains.

3.3.3. Immunohistochemistry

The wax embedded samples prepared for histological analysis were also used for immunohistochemical analysis as follows. After cutting the 8μm sections on the rotary microtome, the IHC sections were placed in xylene for 30 minutes to remove the wax, then in decreasing grades of ethanol for 10 seconds (100% three times, 90%, 70% and 50%) followed by distilled water for 10 seconds to rehydrate the sample. The sections were placed in 1:100 Antigen Unmasking Solution (Vector, CA, US) in ultra-pure water and heated in a 950W microwave three times for 7 minutes at 60% power setting. The sections were cooled at room temperature for 20 minutes and then washed in PBS. The sections were washed twice in Buffer at room temperate for 5 minutes and then placed in Buffer supplemented with normal goat serum (2%, NGS) for 10 minutes. The Buffer comprised of PBS supplemented with bovine serum albumin (1%, Invitrogen, UK) and Tween 20 (0.2%, Sigma-Aldrich, UK).

Primary antibodies for collagen type I (ab292 Abcam, UK) and type III (ab6310, Abcam, UK) were used for immunohistochemical determination of these two collagens in the SKN construct. Secondary antibodies conjugated to FITC (#111-095-003 Jackson-Immuno, US) and TRITC (#115-025-003 Jackson-Immuno, US) were used to detect anti-collagen type I and anti-collagen type III antibodies respectively. Working solutions of the primary and secondary antibodies were prepared in Buffer at 1:200 dilutions. Collagen type I primary antibody (250μL) was placed on each section for 20 hours at 4°C and then washed twice in buffer for 5 minutes. FITC secondary antibody (250μL) was placed on each sample for 3 hours at room temperature, in the dark and then washed twice in buffer for 5 minutes. This was repeated for the collagen III primary and TRITC secondary antibodies. The sections were mounted on a glass slide with DABCO fluorescent mounting medium and analysed using a Leica Leitz DMRB fluorescent microscope. This was repeated for a D49 SKN construct without the addition of the primary collagen type I and III antibodies, to determine the level of background fluorescence of the FITC and TRITC antibodies.

3.3.4. Confocal Laser Fluorescent Microscopy (CLFM)

On D-2, D6 and D49, sections (approximately 5mm x 5mm) were cut from the corner of a SKN construct and placed in a 24-well tissue culture plate. The samples were fixed in 5mL of 4% paraformaldehyde in 0.1M sodium cacodylate for 30 minutes. The samples were washed in PBS for 30 minutes followed by two 5 minute washes in Buffer (described in section 3.3.3) and a 10 minute wash in Buffer supplemented with 2% NGS.

Primary antibody for collagen type I (ab292 Abcam, UK) and secondary antibody conjugated to FITC (#111-095-003 Jackson-Immuno, US) were used to detect collagen type I in the SKN constructs. Alexa Flour® 647 phalloidin (A22287, Invitrogen, UK) was used to detect the cell actin filaments and DAPI (D1306, Invitrogen, UK) to detect the cell nuclei. Working solutions of each antibody were prepared according to the manufacturer's guidelines for CLFM prior to use. Briefly, 1:100 dilutions of collagen type I and FITC antibodies were prepared with Buffer. The Alexa Flour® 647 phalloidin was dissolved in methanol to yield a stock solution of 200unit/mL from which a 1:50 working solution was prepared with PBS. A 5mg/mL working solution of DAPI was prepared with PBS.

Collagen type I antibody (200μL) was placed on the sample for 20 hours at 4°C in the dark and the samples were then washed twice in Buffer for 5 minutes. This was repeated for FITC and conjugated phalloidin. DAPI (200μL) was then placed on the sample for 30 minutes at room temperature, in the dark to stain the cell nuclei. The samples were washed twice in Buffer for 5 minutes and mounted in a glass bottomed 6 well-plate for imaging on a Leica SP2 confocal laser fluorescent microscopy with Leica DM1RE2 inverted fluorescent microscope. Images were taken using sequential acquisition at intervals of 1μm from the top surface of the SKN construct to a depth of 40μm and repeated from the bottom surface by turning the samples over. A x20 magnification glycerol immersion lens was used unless otherwise stated. This was repeated on a D49 SKN construct without the addition of the primary collagen type I antibody, to determine the level of background fluorescence of the FITC antibody.

3.3.5. Scanning Electron Microscopy

On D0, D3, D14, and then every 7 days until D49 sections (approximately 5mm x 10mm) were cut from the centre of SKN constructs and fixed in 3% glutaraldehyde in 0.1M sodium cacodylate buffer (5mL) for 2 hours. The samples were washed twice in 0.1M sodium cacodylate buffer (5mL) for 20 minutes and then placed in 2.3M sucrose (5mL) for 24 hours at 4°C. Smaller sections (approximately 5mm x 2mm) were cut from the samples which were then rapidly frozen in slush liquid nitrogen. The samples were transferred onto an aluminium plate in the liquid nitrogen where they were fractured with a hammer and razor blade. The fractured pieces were washed twice in distilled water for 15 minutes and then placed in increasing concentrations of acetone (30%, 50%, 70%, 90% and 100%) three times at each concentration for 15 minutes. The samples were placed in microporous critical point drying sample holders (Agar Scientific, UK) filled with 100% acetone and dried in a Polaron E3000 critical point dryer with 3 flushes of liquid carbon dioxide over a 90-minute soaking period. The dried samples were mounted on stubs with adhesive carbon pads and splutter coated with gold for 2 minutes in a Polaron E5100 sputter coater. The samples were imaged using a Leica StereoScan360 SEM on D3, D14, D21, D28 and D35. Higher resolution images were taken using an FEI Quanta 200F Field Emission Scanning Electron Microscope (FEGSEM) operated at 5kV in high vacuum mode on D0, D14 and D49 using SKN constructs from a different batch.

3.3.6. Transmission Electron Microscopy

On D5, D21, D33 and D49 sections (approximately 5mm x 10mm) were cut from the centre of the SKN constructs and fixed in 3% glutaraldehyde in 0.1M sodium cacodylate Buffer (5mL) for 24 hours. The samples were washed, post-fixed in 1% osmium tetroxide in 0.1M sodium cacodylate buffer (5mL) and then rinsed 5 times in distilled water for 1 minute. The samples were dehydrated using increasing concentrations of ethanol (30%, 50%, 70%, 90% and 100%) and gradually infiltrated with resin over 24 hours using a 3:1 acetone:resin mixture, followed by 1:1 acetone:resin mixture. The samples were then incubated in three changes of pure resin, embedded in BEEM® capsules and polymerised at 60°C for 48hrs. Semi-thin resin cross-sections (0.5µm) were cut using a glass knife on a Reichert-Jung ultra-cut ultramicrotome and placed on glass microscope slides for staining with 2% toluidine blue. The sections were examined using a Leica DM4000B light microscope to ensure that sections contained the sample. The block face was trimmed to a trapezoidal shape and ultra-thin (90nm) sections were cut using a diatome diamond knife and collected on hexagonal 100 mesh copper grids (Agar Scientific, UK). The sections were contrasted using methanolic uranyl acetate and lead citrate and viewed in an FEI Tecnai BioTwin TEM operated at 100kV.

3.4. Biochemical Composition

3.4.1. Collagenase Digestion and Flow Cytometry

On D-2, D7 and weekly intervals until D49, three SKN constructs were placed in separate bijou tubes containing 0.28U/mL collagenase B (Roche, Switzerland) in PBS (2mL). The bijou tubes were placed in a water bath at 37°C until the HDF cells were released from the constructs and the constructs were fully digested with no solid matrix visible. The digested solution (1mL) was placed in the CEDEX automated cell counting machine and the total cell number recorded. The remaining solution was used for flow cytometry analysis as described below.

Flow cytometry using Vybrant® Apoptosis Assay Kit #2 (Molecular Probes, UK) was used to determine the percentage of live, apoptotic and dead cells in the SKN constructs. The apoptotic assay kit used Annexin V, which has a high affinity for phosphatidyl serine present on the outer surface of the cell membrane during apoptosis, and propidium iodide (PI) which binds to nucleic acids in dead cells (Koopman, Reutelingsperger et al. 1994). The cell digest and working solutions were prepared for flow cytometry according to the manufacturer's instructions. Briefly, the cell digest was centrifuged at 500g for 5 minutes, washed in cold PBS (4°C) and suspended in 1X Annexin V–binding buffer at $2x10^6$ cells/mL. 100μL aliquots of the cell suspension were placed in five micro-centrifuge tubes.

A positive control was prepared by adding 70% ethanol (100μL) into one of the aliquots for 3 minutes to induce apoptosis. This aliquot was centrifuged, washed in PBS and suspended in 1X Annexin V-binding buffer. Conjugated Alexa Fluor 488 Annexin V (5μL) and 1mg/mL propidium iodide (1μL) working solution was added to three of the aliquots. The remaining aliquot was used as a negative control without the addition of PI and Alexa Fluor to determine the autoflourecence from the cells and binding buffer. All of the five aliquots were incubated for 15 minutes at room temperature and then 1X Annexin-binding buffer (400μL) was added to each aliquot. The aliquots were stored at 4°C until flow cytometry analysis at fluorescence emissions of 530nm and 575nm.

3.4.2. Chemical Dehydration

On D-2, D0, D7 and weekly intervals until D49, three constructs were carefully removed from the culture dish using tweezers and a spatula. Excess surface water was removed by sliding the top and bottom surfaces of the construct over the edge of the dish. Each construct was placed in a weighing boat and weighed using a Denver Instrument APX-100 balance. The samples were chemically dehydrated by placing in formalin (20mL, Sigma-Aldrich, UK) for 45 minutes followed by increasing concentrations of ethanol (20mL of 10%, 20%, 70%, 100%) for 45 minutes, two changes of 99% absolute ethanol (20mL) for 45 minutes, hexamethyldistalazane (20mL, Sigma-Aldrich, UK) for 45 minutes and finally fresh hexamethyldistalazane (20mL) until the liquid had completely evaporated. The dried constructs were weighed on a Denver Instrument APX-100 balance. This was repeated for a separate batch of SKN constructs (n=5) and a batch of acellular fibrin constructs (n=3).

3.4.3. Collagen Type I Enzyme-Linked Immunosorbant Assay (ELISA)

On D-2, D7 and weekly time-points until D49, three SKN constructs were digested in 5mg/mL of pepsin in 0.5M acetic acid (2mL, Sigma-Aldrich, UK). The constructs were agitated on a shaker for 2 days at 4°C and then stored at -80°C until processing. All of the samples were processed as a batch for ELISA analysis.

The samples were thawed at room temperature and 1mL of each sample was freeze dried for 24 hours. Human Type I Collagen ELISA kit (Chondrex Inc, DC, USA) was used according to the manufacturer's instructions. Briefly, capture antibody solution (100μL) was added to each well of the 96 well-plate and incubated at 4°C overnight. The freeze dried samples were resuspended in ELISA buffer (300μL) and standards were prepared by adding the stock solution to the dilution buffer as detailed in Table 11. The ELISA plate was washed six times with 1X wash buffer and each standard and sample (100μL) was added to the plate in duplicates. The plate was incubated at room temperature for 2 hours and then washed in 1X wash buffer. Detection antibody (100μL) was added to each well and incubated at room temperature for 2 hours. The plate was washed three times with 1X wash buffer and Streptavidin Peroxidase (100μL) was added to each well. The plate was incubated at room temperature for 1 hour and then washed three times in 1X wash buffer. OPD-Urea H_2O_2 (100μL) was added to each well and the reaction was stopped after 15 minutes with stop solution (50μL). The plate was read using a Molecular Devices SpectraMax 190 plate reader, at 490nm.

Standards (μg/mL)	Stock Solution (μL)	Dilution Buffer (μL)
10 (A)	50	450
5 (B)	250 (A)	250
2.5 (C)	250 (B)	250
1.25 (D)	250 (C)	250
0.625 (E)	250 (D)	250
0.313 (F)	250 (E)	250
0.156 (G)	250 (F)	250
0 (H)	0	250

Table 11 Volume of stock solution and dilution buffer for preparation of collagen type I standards for ELISA

3.4.4. Raman Spectroscopy

A Micro-Raman Spectrometer, custom built for analysis of biological materials by Dr.I.Notingher, Nottingham University, UK (Jell, Notingher et al. 2008) , was used to investigate the changes in biochemical composition of the SKN constructs during manufacturing (Figure 7). The D0, D7 and D49 SKN constructs dried by chemical dehydration as described in section 3.4.2 were analysed as follows. A dried sample was placed on a magnesium fluoride cover slip and then on the inverted microscope stage. A 785nm diode laser was energized, sent through the microscope and focused into the sample via a x50 microscope objective lens. Scattered light from the construct was passed back through the microscope objective and a notch filter. The Raman scattered light was focused into the entrance of the spectrometer for detection using a charge-coupled detector (CCD) camera and conversion into Raman Spectra and. The Raman spectra were acquired using an acquisition time of 10s. This was repeated for each dried sample, a hydrated acellular fibrin gel, a D63 hydrated SKN construct and DMEM-10 media as a control.

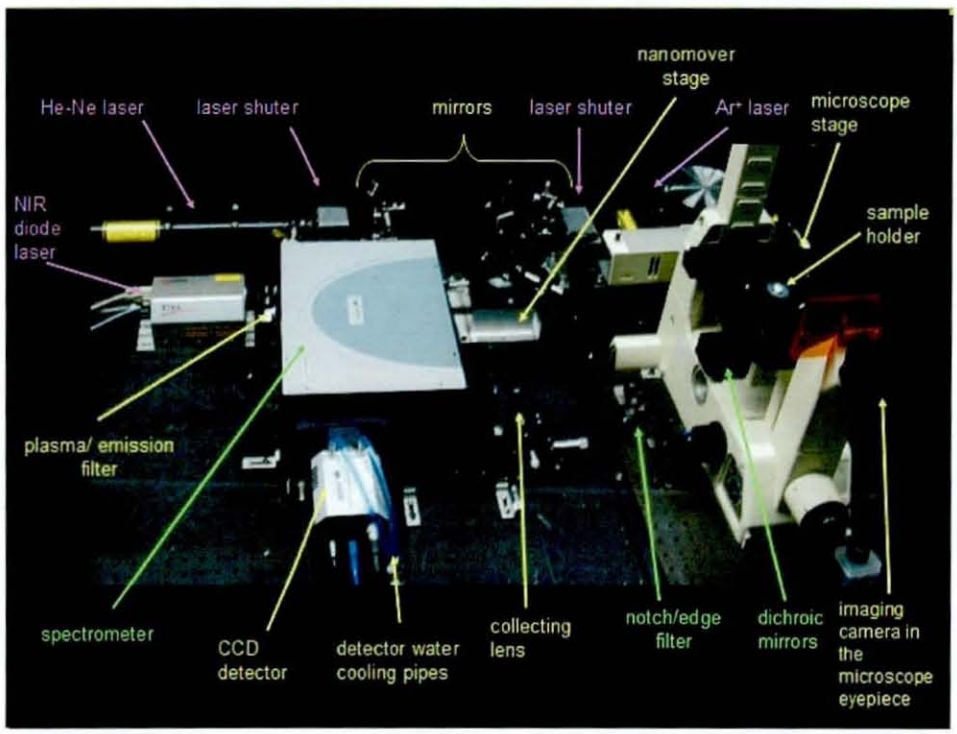

Figure 7 Micro-Raman experimental set-up. Reproduced with permission from Dr.I.Notingher, Nottingham University, UK

3.5. Mechanical Properties

3.5.1. Rheology

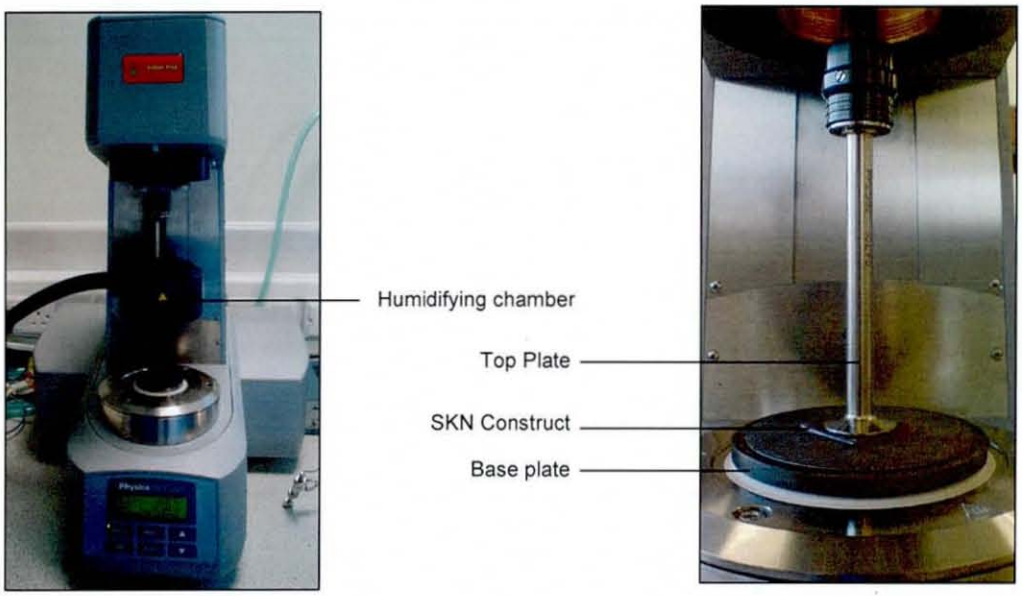

Figure 8 Experimental set-up of rheometer using parallel plates. Left: Rheometer. Right: SKN construct between parallel plates

On D0, D7 and at weekly intervals until D49, the viscoelastic properties of three SKN constructs were measured. An Anton Parr Physica MCR301 Rheometer with parallel plate attachments was used to measure the shear storage modulus (G') and shear loss modulus (G") of the SKN constructs (Figure 8). A 25mm diameter serrated top plate and 100mm serrated base plate were attached to the rheometer. A motor adjustment was run to calibrate the rheometer on each testing day. The temperature of the base plate was set to 37°C and a humidifying chamber was used to minimise evaporation during testing. A SKN construct was carefully removed from the 8-well plate using tweezers and a spatula and excess surface water was removed by sliding the top and bottom surfaces of the construct over the edge of the dish.

The construct was placed on the base plate of the rheometer ensuring that there were no bubbles under the construct to reduce the variation in measurements. The top plate was lowered onto the construct until 0.1N of normal force was applied. This allowed for repeatable, homogeneous loading of each construct and accounted for any variations in thickness. A frequency sweep was carried out at 1.2% strain between 0.001 and 16Hz to observe the construct response to strain rate. This was followed by a strain sweep carried out between 0.01% - 100% at 1Hz to observe the response of the SKN constructs to increasing shear deformation. In addition, a strain sweep was carried out on acellular gels on D0 (n=3) to determine the contribution of the cells to the viscoelastic properties, and on cadaver dermis (n=5), donated by NHSBT, Liverpool, UK, to provide a reference point for the SKN constructs.

3.6. Results and Discussion

The quantitative results are summarised in Table 13 and qualitative results in Table 14.

3.7. Physical and Structural Properties

3.7.1. Surface Profiling

The 3D-meshed images of the surface profile of the SKN constructs showed that the constructs had a convex surface after casting which changed to a concave surface during manufacturing. These results correlated with decreases in the construct volume and thickness (Figure 9). On D-2, the constructs had a convex surface with a centre point thickness of 2.97mm and volume of 2812mm^3 (Figure 10). The volume of the 1mm wide perimeter of the SKN constructs, which could not be measured by this method, was estimated to account for approximately 358mm^3 of the volume of the SKN constructs on D-2 assuming that the thickness was 2.8mm (the average thickness of the outer edge measured) in this area. 3.4mL of the SKN construct casting mixture was used to produce each construct which suggested that the volume of the construct reduced by approximately 229mm^3 between the time of casting and the time of the measurement, 4 hours after casting.

By D0, there appeared to be a decrease in the radius of curvature of the convex surface and the constructs were 70% of the original thickness and 96% of the original volume. The SKN constructs had a concave surface profile by D2 and the radius of curvature appeared to increase until D14. Between D14 and D49 the surface profile did not change, and the thickness and volume of the constructs were 47% and 53% of the original constructs respectively. The thickness of the constructs was greater at the edge compared to the central regions after D2 (Figure 11). Visual inspection of the interface between the constructs and the culture dish showed that the edges of the SKN constructs were anchored to the sides of the culture dish throughout the manufacturing process.

In comparison, the surface profile, thickness and volume of the acellular control constructs remained constant until D35. This showed that the changes in surface profile of the SKN constructs were caused by the HDF cells and was supported the findings of other studies which reported that HDF cells remodelled loosely arranged fibrin fibrils into closely packed organised fibres and in turn caused construct compaction (Tuan, Song et al. 1996). The decrease in thickness and reduction in the radius of curvature of the convex surface of cellular constructs over time has been reported previously (Neidert, Lee et al. 2002, Tuan, Song et al. 1996, Tuan, Song et al. 1996). However, in these studies the observations of the change in surface profile were qualitative and measurement of the thickness of these constructs was limited to a single point measured by focussing a microscope on the top and the base of the constructs. The novel application of surface profiling demonstrated in this study provided a method to quantify the changes of the whole surface profile of the SKN constructs over time and more accurate measurements of the volume and thickness of the constructs.

Precision surface profiling provides a useful tool for non-contact, non-destructive monitoring of the changes in surface profile of tissue-engineered constructs. This may prove useful for future design of restraints and culture dishes which has been shown to control the shape of the constructs (Robinson, Johnson et al. 2008, Sander, Johnson et al. 2008, Isenberg, Williams et al. 2006). In addition, surface profiling may be used to quantify the size and shape of tissue-engineered constructs and determine whether a product is within specification.

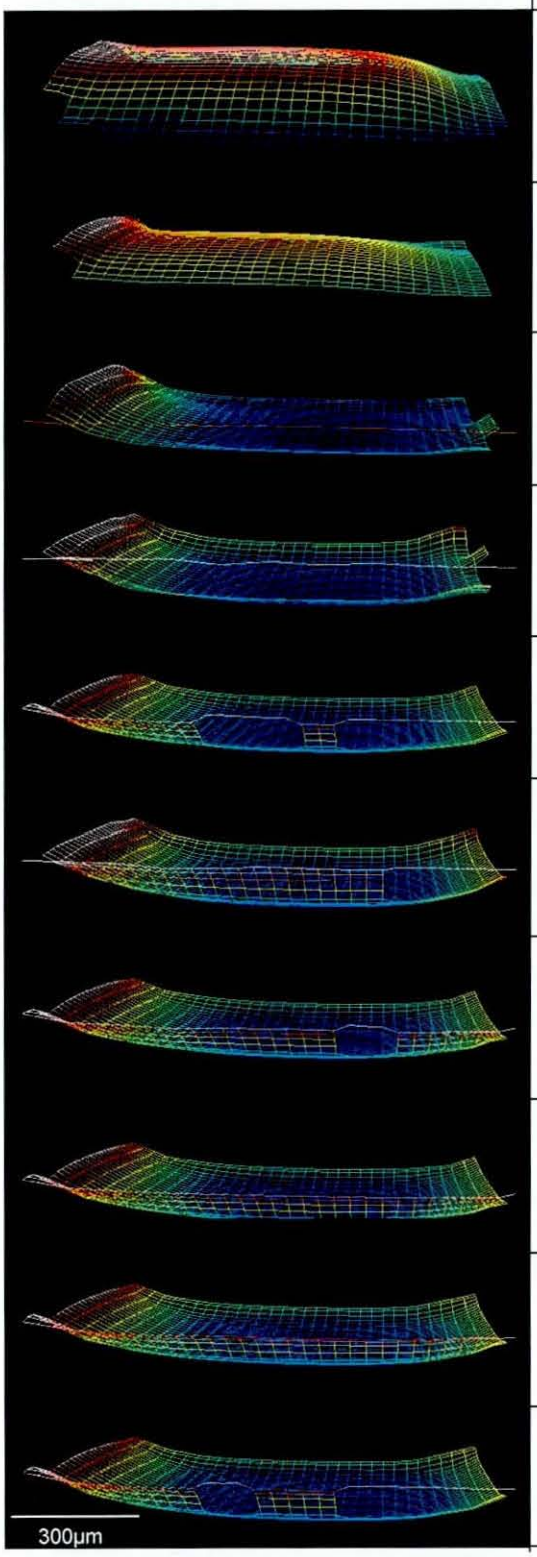

Day	Volume (mm^3)	Thickness (mm)
D-2	2812	2.97
D0	2690	2.07
D2	1935	1.75
D7	1560	1.66
D14	1494	1.57
D21	1495	1.57
D28	1495	1.57
D35	1497	1.57
D42	1494	1.57
D49	1496	1.57

Figure 9 Example of the surface profile of a SKN constructs during manufacturing and the average volume and thickness of the constructs (n=8)

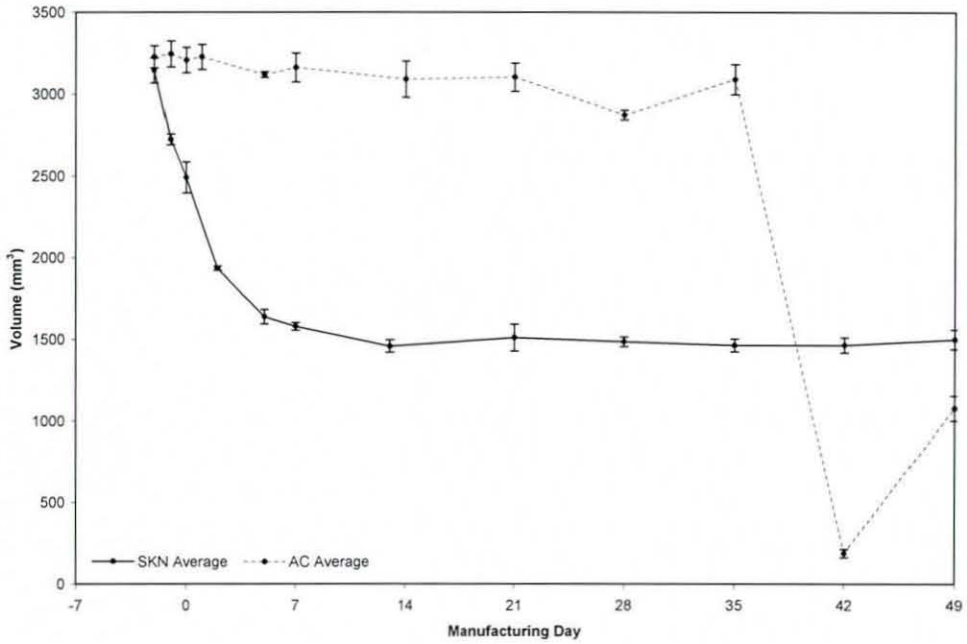

Figure 10 The average volume of two batches of SKN constructs (n=8) and acellular constructs (AC, n=3) during manufacturing. Error bars represent one standard error

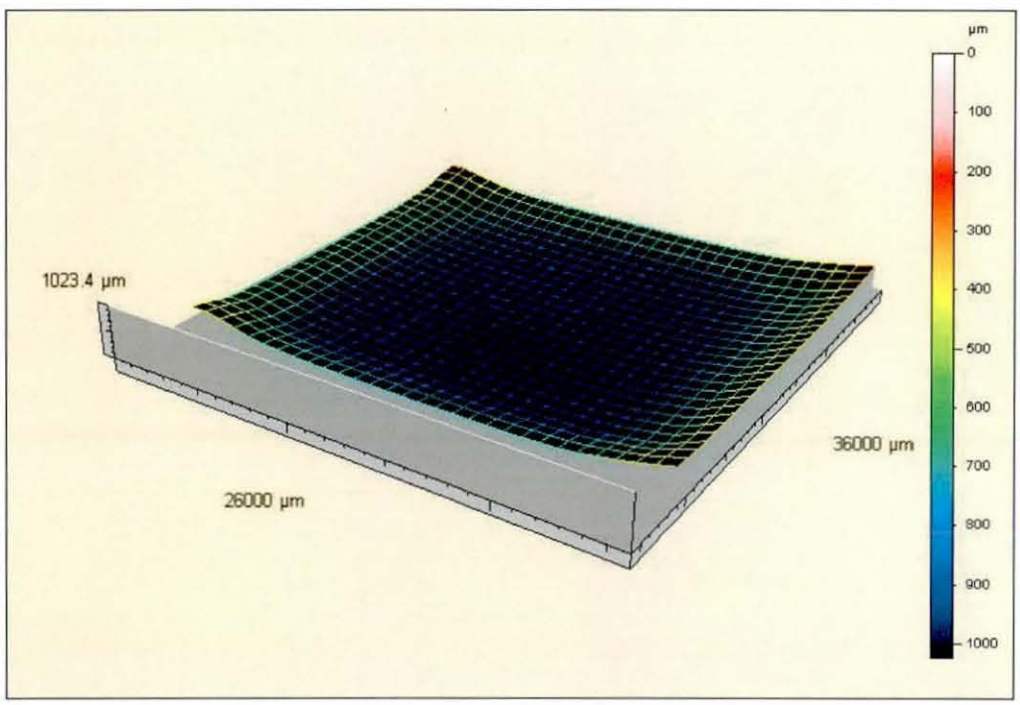

Figure 11 Surface profile image showing the variation in thickness over the whole surface of a D49 SKN construct. Scale bar represents distance from the top of the slip gauge at 1023.4µm to the surface of the construct

3.7.2. Histology

Masson's Trichrome stained the fibrin fibres purple/red, collagen fibres blue and cell nuclei dark blue/black (Figure 12 and Appendix II for control). The results showed that the composition of the SKN construct matrix changed during the manufacturing period from a fibrin matrix to a predominantly collagen matrix. On D0 the matrix was comprised of fibrin and the cell nuclei were evenly distributed throughout the thickness of the construct. On D21, the majority of the matrix was composed of collagen but some areas of fibrin were also evident. The cell density appeared to be greater compared to D0 and a layer of cells had formed at the construct-media interface.

On D49 there was a dense collagen matrix with more intense collagen staining around the cell nuclei. Higher magnification images of the D49 construct showed that there were thin collagen fibrils spanning between the cells. These results supported the findings of other studies that showed a change in matrix composition from fibrin to collagen in tissue-engineered cellular fibrin scaffolds for cardiovascular applications over time (Neidert, Lee et al. 2002, Mol, van Lieshout et al. 2005). In addition, these results confirmed the qualitative model proposed for the ICX-SKN manufacturing process described in section 2.4.3 and showed that fibrin was still present in the SKN constructs on D21.

In contrast, there was no evidence of proteoglycans or elastin in the SKN constructs (Figure 13 and Appendix II for control sample) at any time in the manufacturing process. These results were unexpected as other authors have reported the presence of both proteoglycans and elastin in fibroblast seeded fibrin matrices (Ahlfors, Billiar 2007). It was possible that a low concentration of proteoglycans and elastin was present in the SKN constructs but was not detectable using this histology methodology. Further studies are required to confirm these findings and alternative assays such as Blyscan™ for quantitative analysis of sulfated proteoglycans and glycosaminoglycans could be used (Ahlfors, Billiar 2007).

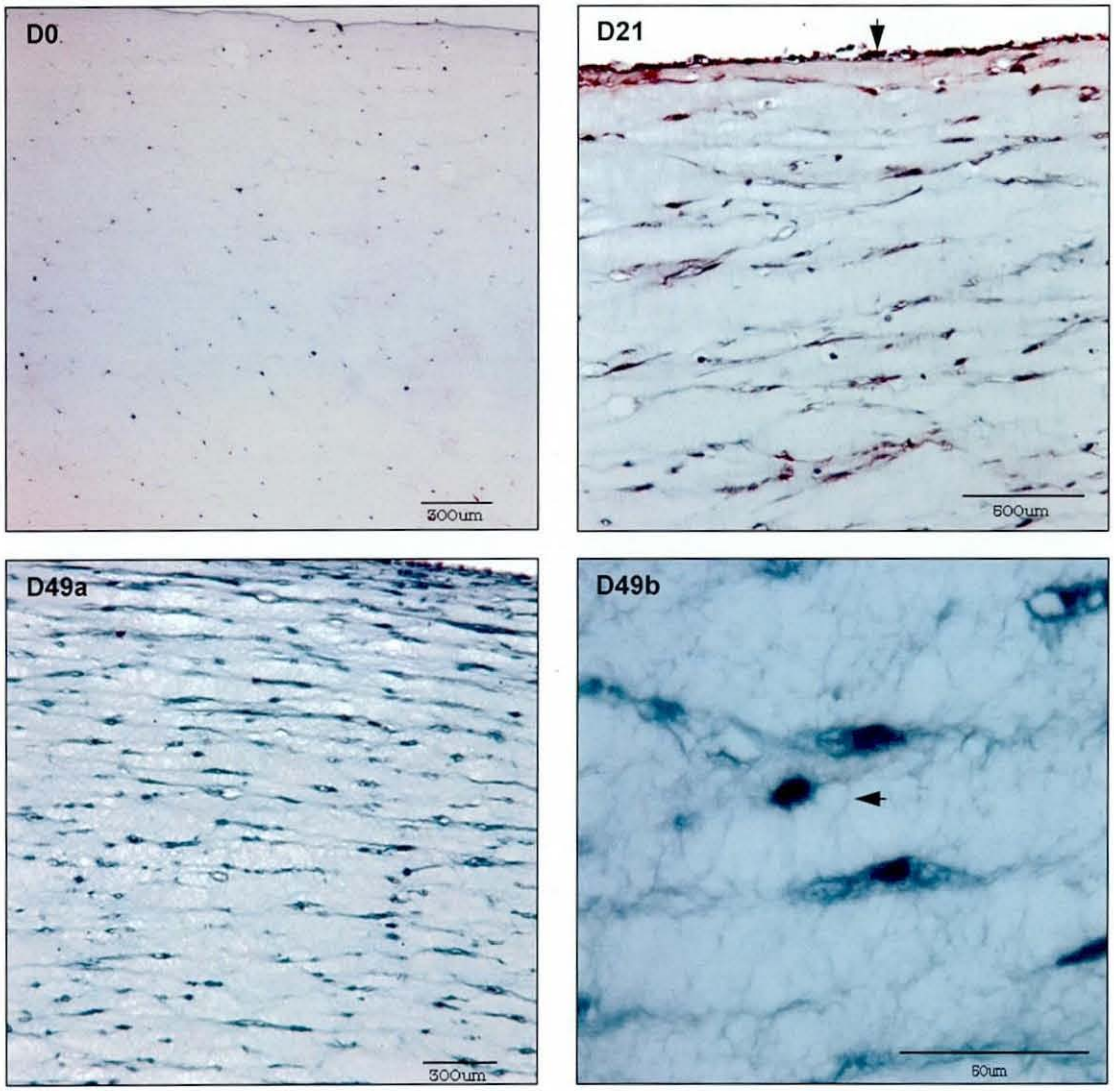

Figure 12 Masson's Trichrome stained cross-sections of SKN construct. D0: Cells (blue/black) evenly distributed in fibrin matrix (purple/red). D21: Collagen (blue) and fibrin in matrix and layer of cells (arrow head) on surface. D49a: Dense collagen matrix with more intense collagen staining around cell nuclei D49b: Thin collagen fibrils (arrow head) spanning between cells

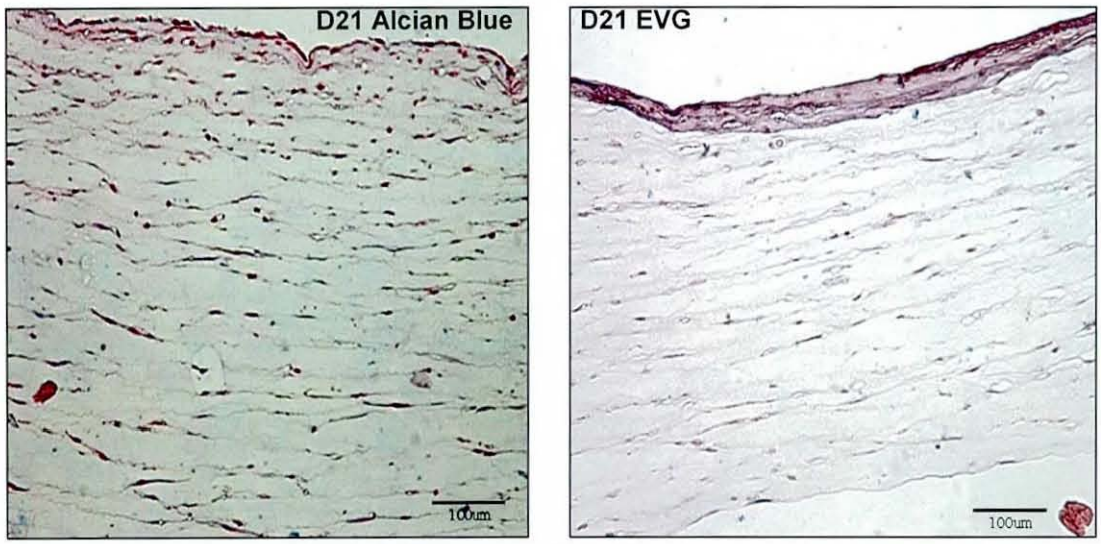

Figure 13 Cross-sections of D21 SKN construct. Left: Cytoplasmic regions (red) but no evidence of proteoglycans (blue). Right: Collagen fibres (dark red) but no evidence of elastin (black)

3.7.3. Immunohistochemistry

The IHC sections stained collagen type I green, collagen type III red and the cell nuclei blue. The negative controls showed low levels of background fluorescence for FITC and TRITC secondary antibodies (Appendix II) The results showed that both collagen type I and collagen type III were present in the SKN construct during the early stages of manufacturing but only collagen type I was present in the final SKN construct on D49. On D0 collagen type I and collagen type III were not present in the constructs (Figure 14 top row) which confirmed the Masson's Trichrome staining that only fibrin was present in the matrix as reported previously. On D21, both collagen type I and III were present in the SKN constructs (Figure 14 middle row). The collagen fibrils were concentrated around the cell membrane but there was little evidence of inter-cellular collagen deposition. In contrast, by D49 only collagen type I was detectable and many thin collagen fibrils were observed between the cells.

The processes that occur during manufacturing of the SKN constructs are similar to that of wound healing in-vivo where HDF cells breakdown the fibrin matrix and secrete collagen types I and III (section 2.2). A study of acute wound healing in humans (Robins, Milne et al. 2003) supported the immunohistolochemical observations reported in this study. In-vivo, equal quantities of collagen type I and III were present in the wound after 21 days but the percentage of collagen type III decreased over time with significant decreases observed at time point after 12 weeks (Robins, Milne et al. 2003). The ratio of collagen type III to collagen type I in SKN constructs showed a similar trend to this in-vivo study but the degradation of collagen type III was more rapid as almost no collagen type III was observed after 7 weeks.

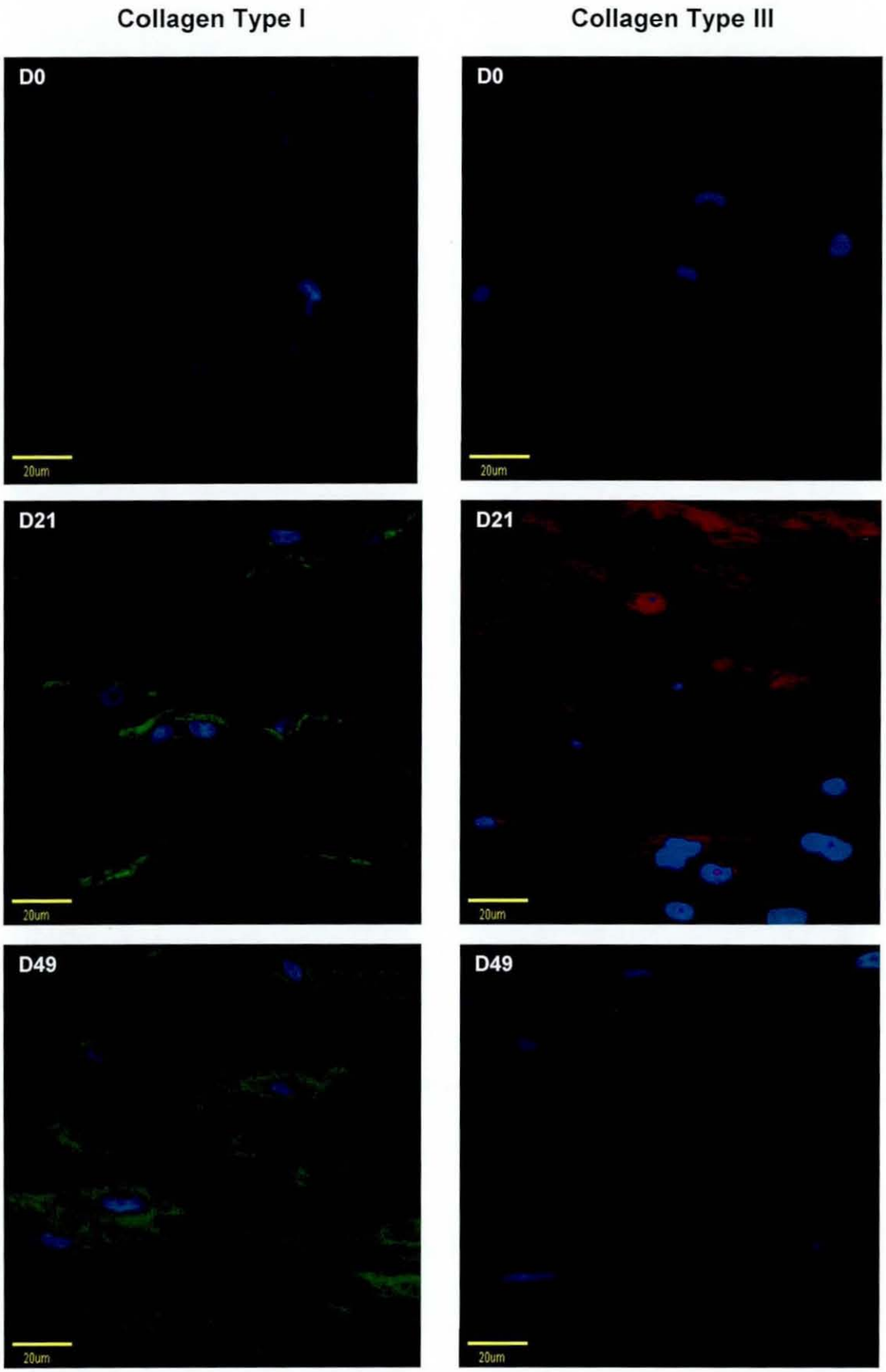

Figure 14 IHC cross-sections of SKN constructs. D0: No collagen type I (green) or III (red). D21: Collagen type I and III present around cell membranes. D49: Collagen type I present around cell membranes with thin fibrils spanning between cells. No collagen III detectable. Cell nuclei (blue)

3.7.4. Confocal Microscopy

The CLFM images stained the cell nuclei blue, cell actin filaments red and collagen type I fibres green. The negative control showed low levels of background fluorescence from the secondary antibody (Appendix II). Images of the individual layers of the SKN constructs viewed from the top of the construct (Figure 15) and the bottom of the construct (Figure 16) showed that the morphology of the cells was bipolar and Y shaped. In addition, the density of cells was greater towards the top at the construct-media interface compared to areas nearer the construct- tissue culture plastic interface. The cells did not show any preferred orientation apart from those on the top surface at the edge of the constructs. The cells in this area were orientated towards the centre (Figure 15).

Between D-2 and D49, stacked images of the central region of the top 40μm of the SKN constructs showed an increase in cell density and collagen type I (Figure 17). The D-2 SKN construct showed that there was no collagen in the matrix and that there was no cross-reactivity between the fibrin matrix and collagen type I antibody. There was an increase in cell density between D-2 and D6, and there was intense staining of collagen around the cell membranes on D6. A further increase in the number of cells and collagen was observed in the D49 construct with evidence of inter-cellular collagen deposition. These results supported the histological and immunohistochemical findings which also showed an increase in the number of cells and quantity of collagen during manufacturing.

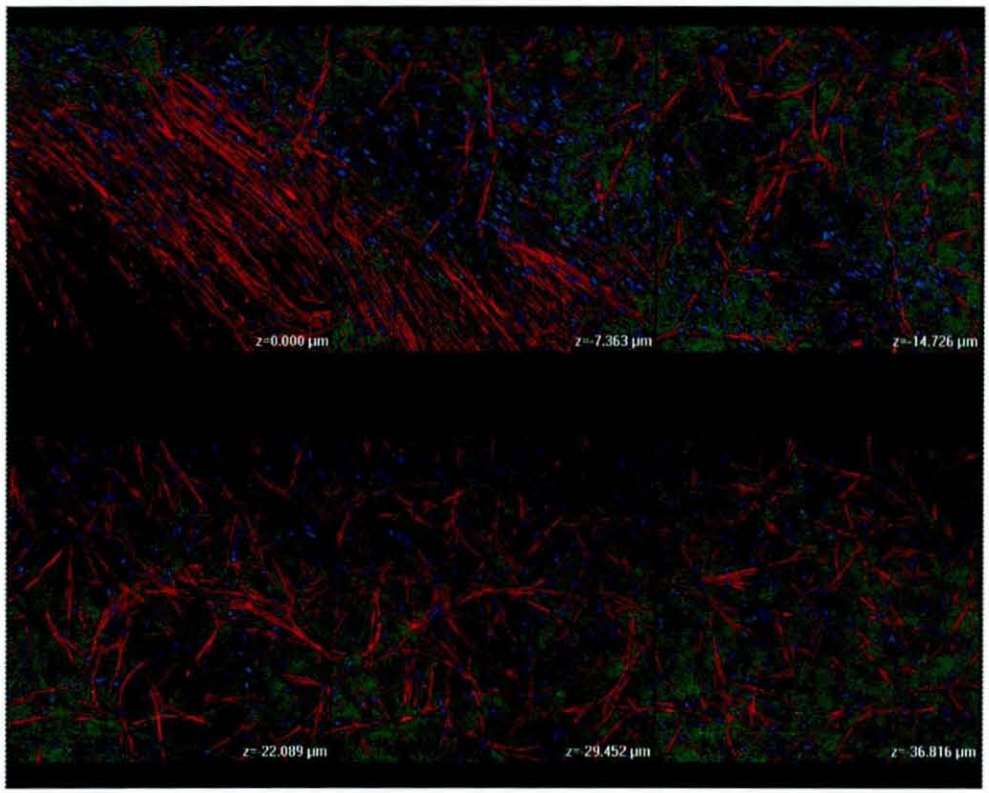

Figure 15 Representative 1µm CLFM layers of a D49 SKN construct through the depth of the SKN construct, view from the top surface. HDF cells preferentially orientated on top surface (z=0µm) at edge but no preferential orientation below 14µm. Magnification x20

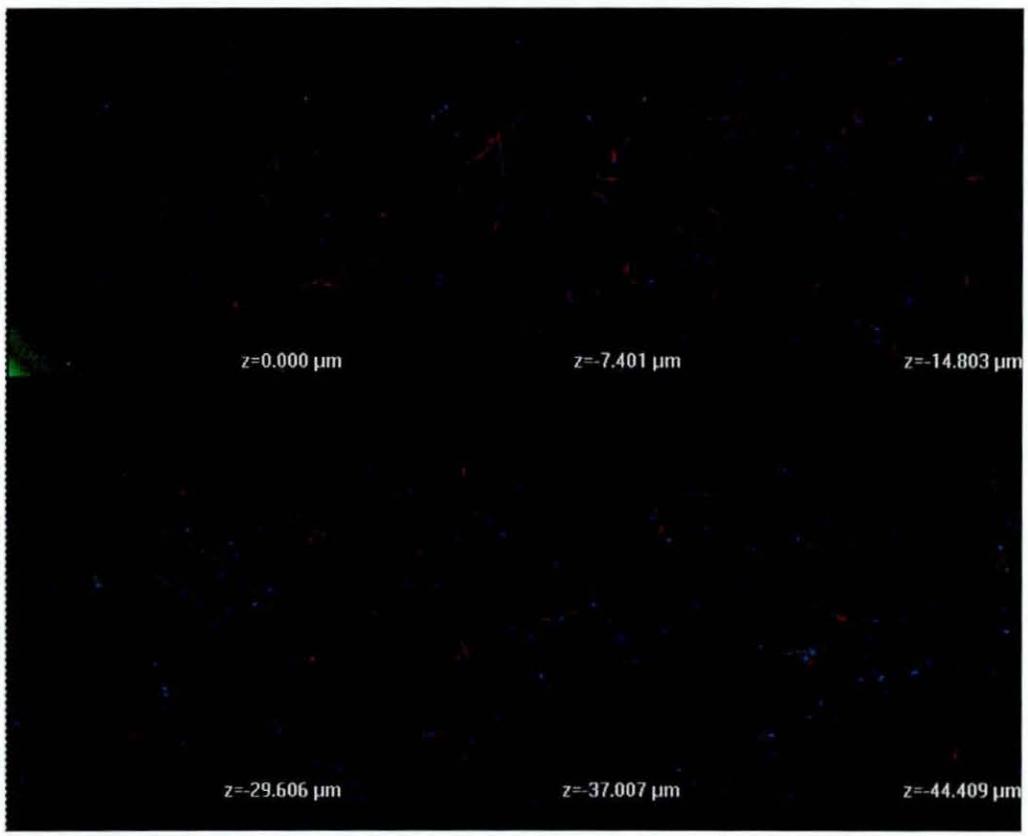

Figure 16 Representative 1µm CLFM layers of a D49 SKN construct through the depth of the SKN construct, view from the bottom surface. (z=0µm). Fewer cells compared to top of construct and no cell orientation. Magnification x20

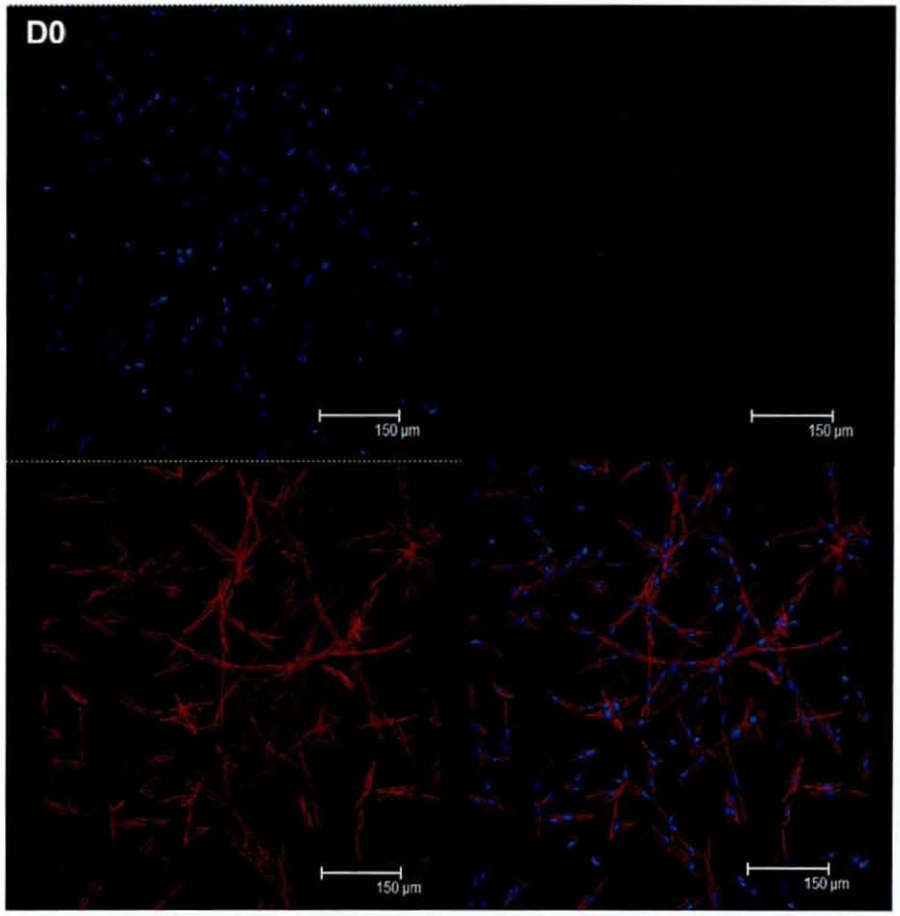

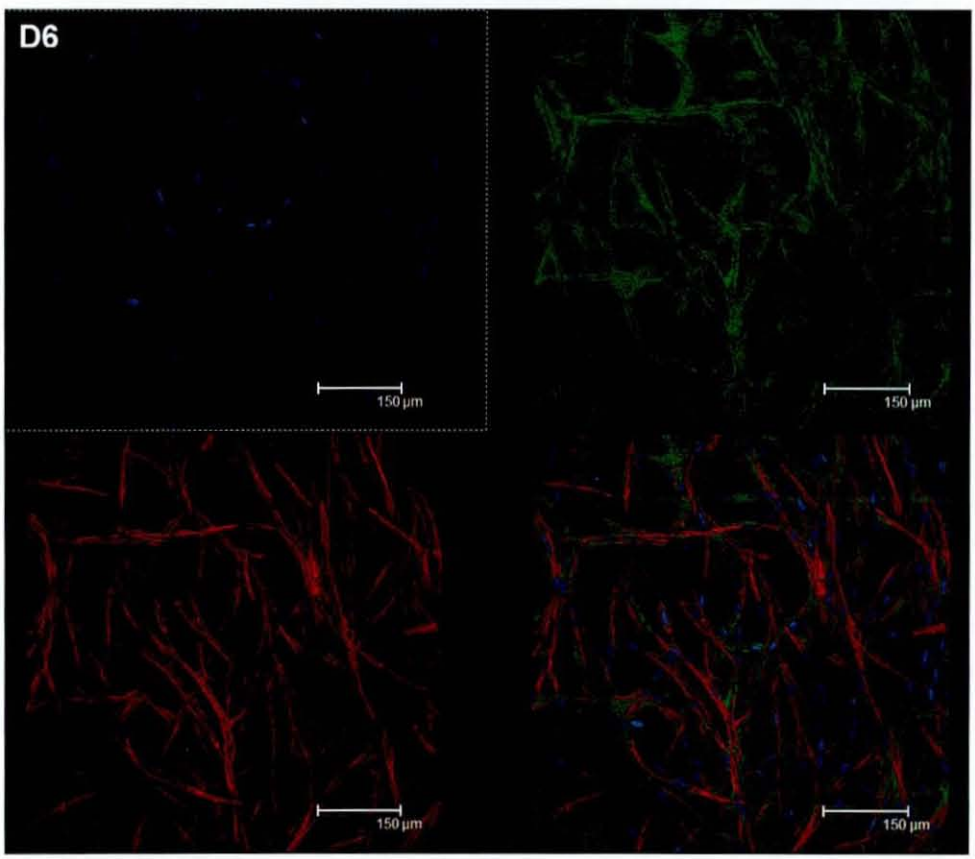

(Caption on next page)

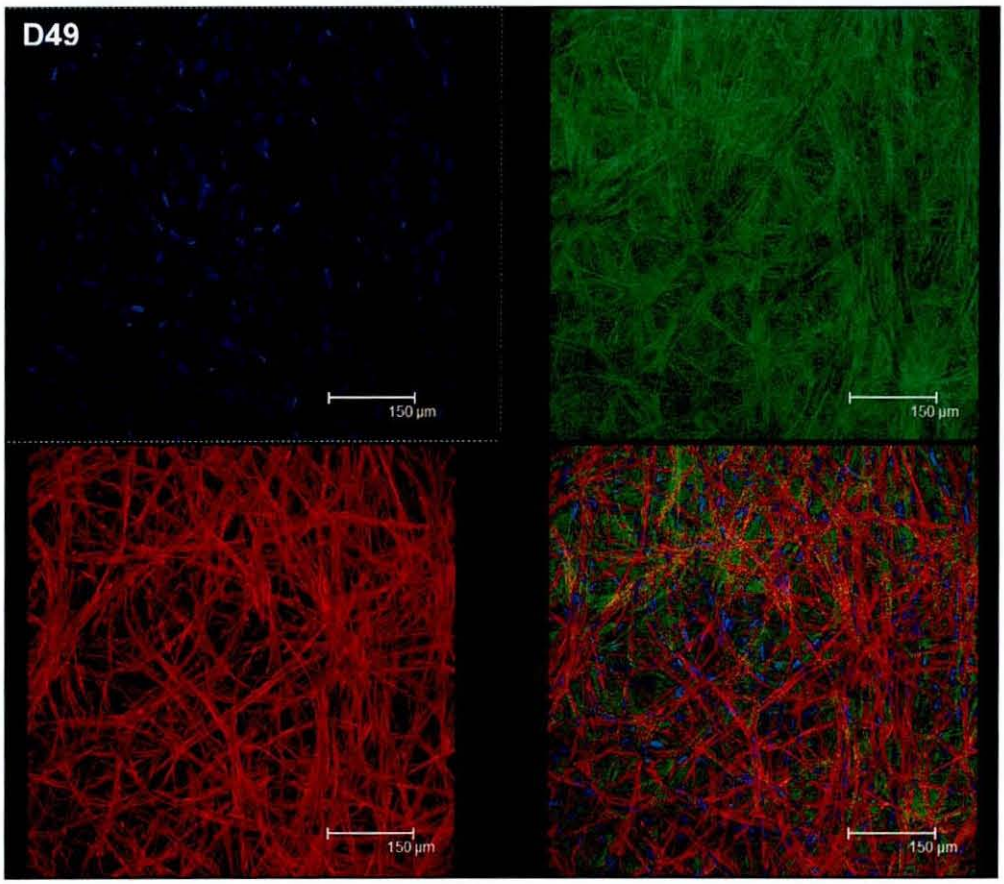

Figure 17 Stacked CLFM image of the top 40µm of SKN constructs. Top Left Quarter: Cell nuclei. Top Right Quarter: Collagen type I. Bottom Left Quarter: Cell Actin filaments. Bottom Right Quarter: Complied image. D-2 (previous page): Bipolar cells but no collagen type I in matrix. D6: More cells than D-2 and staining of collagen type I around the cell membranes. D49 (previous page): High cell density, intense staining of collagen type 1 around the cell membranes and inter-cellular collagen deposition

3.7.5. Scanning Electron Microscopy (SEM)

Analysis of the morphology of the SKN constructs at higher magnifications using SEM showed that the fibroblasts cells were embedded in a highly cross-linked, porous matrix. The density of the matrix and degree of cross-linking appeared to decrease between D3 and D14. However, the matrix density appeared to increase between D14 and D35 (Figure 18).

Higher resolution, low magnification images of the D0, D14 and D49 SKN constructs using FEGSEM showed that the thickness of the constructs decreased between D0 and D14 but was similar between D14 and D49 (Figure 19 left column). This supported the surface profiling results reported in section 3.7.1. However, the thickness of the construct on D0 was measured as 2.07mm using surface profiling but only 1.38mm when measured from the FEGSEM image. Similarly, on D14 the thickness of the construct was 1.57mm using surface profiling compared to 1.18mm measured by the SEM images. This suggested that the sample preparation of SKN constructs for SEM resulted in approximately 30% shrinkage on D0 and approximately 25% shrinkage in the constructs after D14.

In addition, these images showed that the cells were evenly distributed through the matrix on D0 but on D14 and D49, the cell density appeared to be greater at the top of the constructs (Figure 19 left column). Images of the surface of the constructs at the construct-media interface showed that there were no cells on the surface of the construct on D0 but a layer of cells on the surface on D14 (Figure 19 right column) and D49 (data not shown). In contrast, only a few cells were observed on the bottom surface of the constructs at the construct-tissue culture plastic interface at these time points (Figure 19 right column). These observations supported the CLFM findings which also showed a greater cell density towards the top of the construct.

Further analysis of the cross-section of the D49 construct at 2500x magnification showed that the matrix pores were elliptical towards the top of the construct compared to approximately circular pores towards the bottom of the construct (Figure 20, left column). This may have been caused by the compaction of the construct reported in section 3.7.1. In addition, a cell layer with fibrils between the cells was observed at the construct-surface interface and supported the histological results. In contrast, only a few cells protruding through the matrix at the construct-tissue culture plastic interface (Figure 20, right column).

Analysis of the SKN constructs at 10 000x magnification showed that the D0 fibrin matrix shown by histological analysis was comprised of thin fibres that formed aggregates on D0 (Figure 21 top). In contrast, the D49 collagen matrix appeared to be denser and have a highly interconnected network of individual collagen fibrils. Thicker fibres, which appeared to be collagen fibril bundles around the cell membrane, were also observed (Figure 21 bottom). The diameters of these matrix structures ranged between 62.5nm and 125nm, which are typical of collagen fibrils and fibril bundles (Kadler, Holmes et al. 1996). The D14 matrix appeared to have a combination of collagen fibril and aggregates of fibrin fibres (Figure 21 middle) which supported the Masson's Trichrome stained sections which showed that both collagen and fibrin were present on D21.

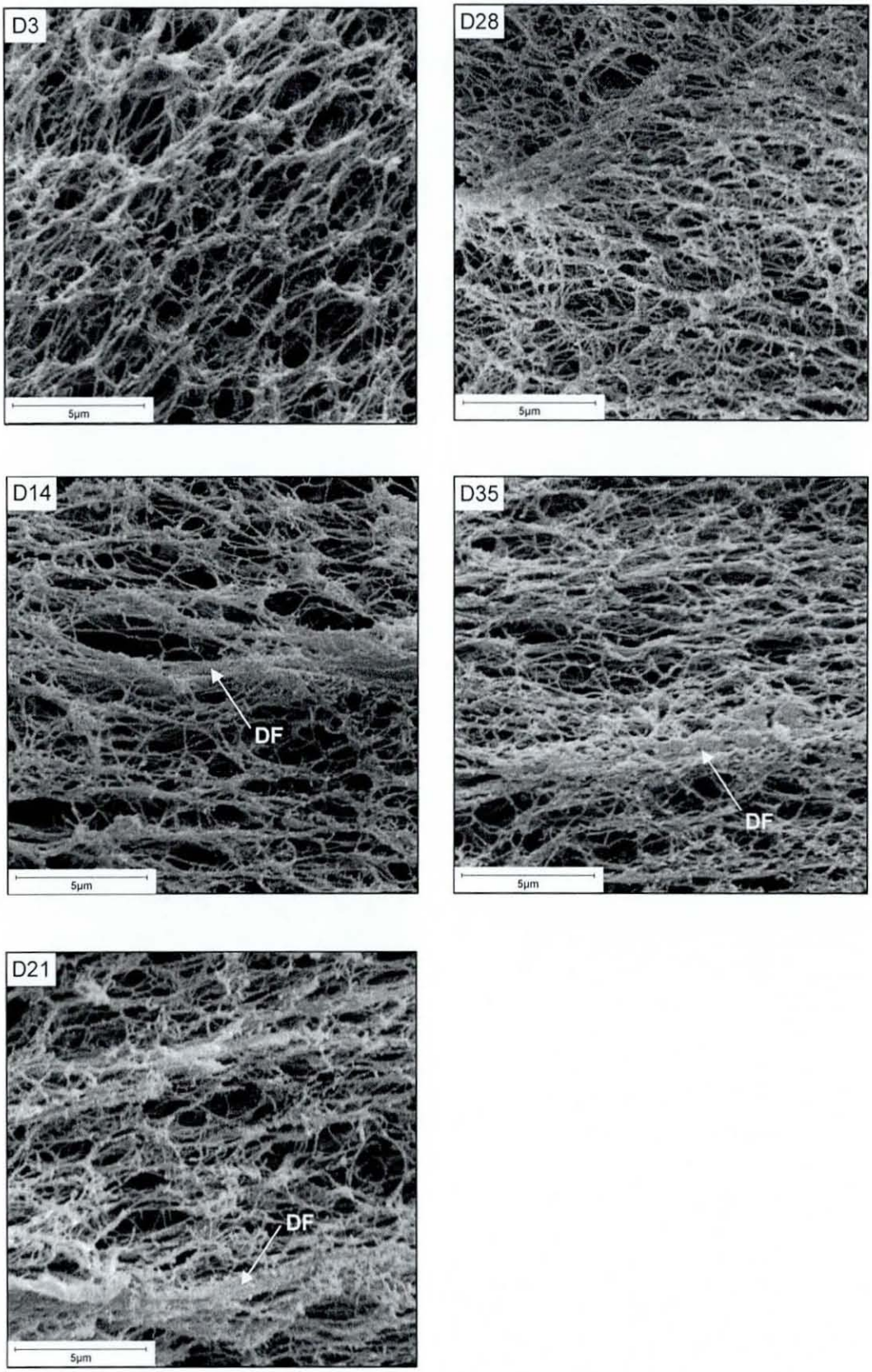

Figure 18 SEM cross-section of SKN constructs during manufacturing. D3: Thick fibres and large pores. D14 to D35 more structured matrix with increasing matrix density. DF = human dermal fibroblast

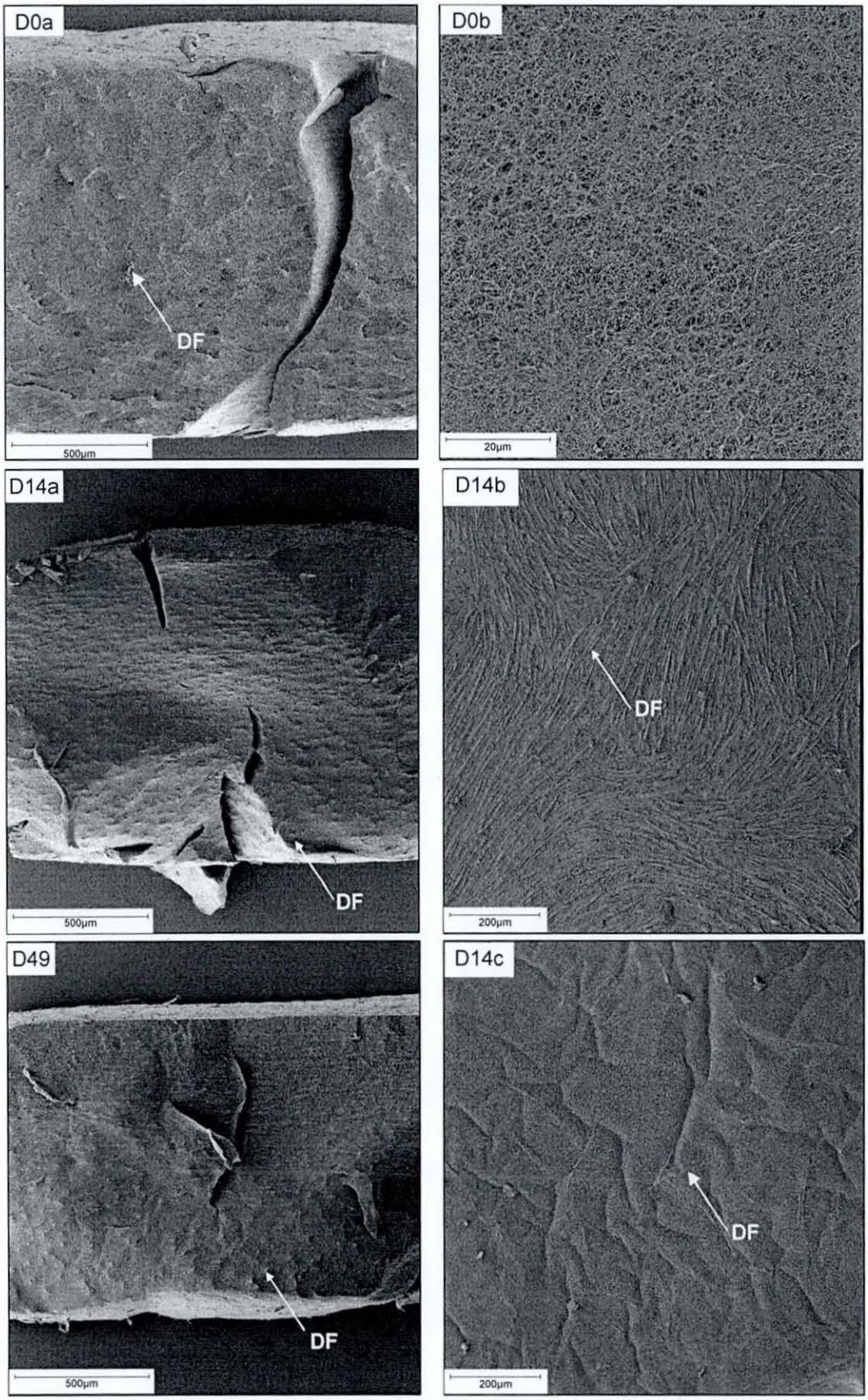

Figure 19 Left column: SEM cross-sections of SKN constructs during manufacturing. D0a Evenly distributed cells in construct. D14a and D49: Higher cell density at top of construct. Right column: Surface view of SKN constructs. D0b: Top surface with no cells. D14b: Layer of dermal fibroblasts (DF) on top surface. D14c: Few cells on bottom surface of SKN construct

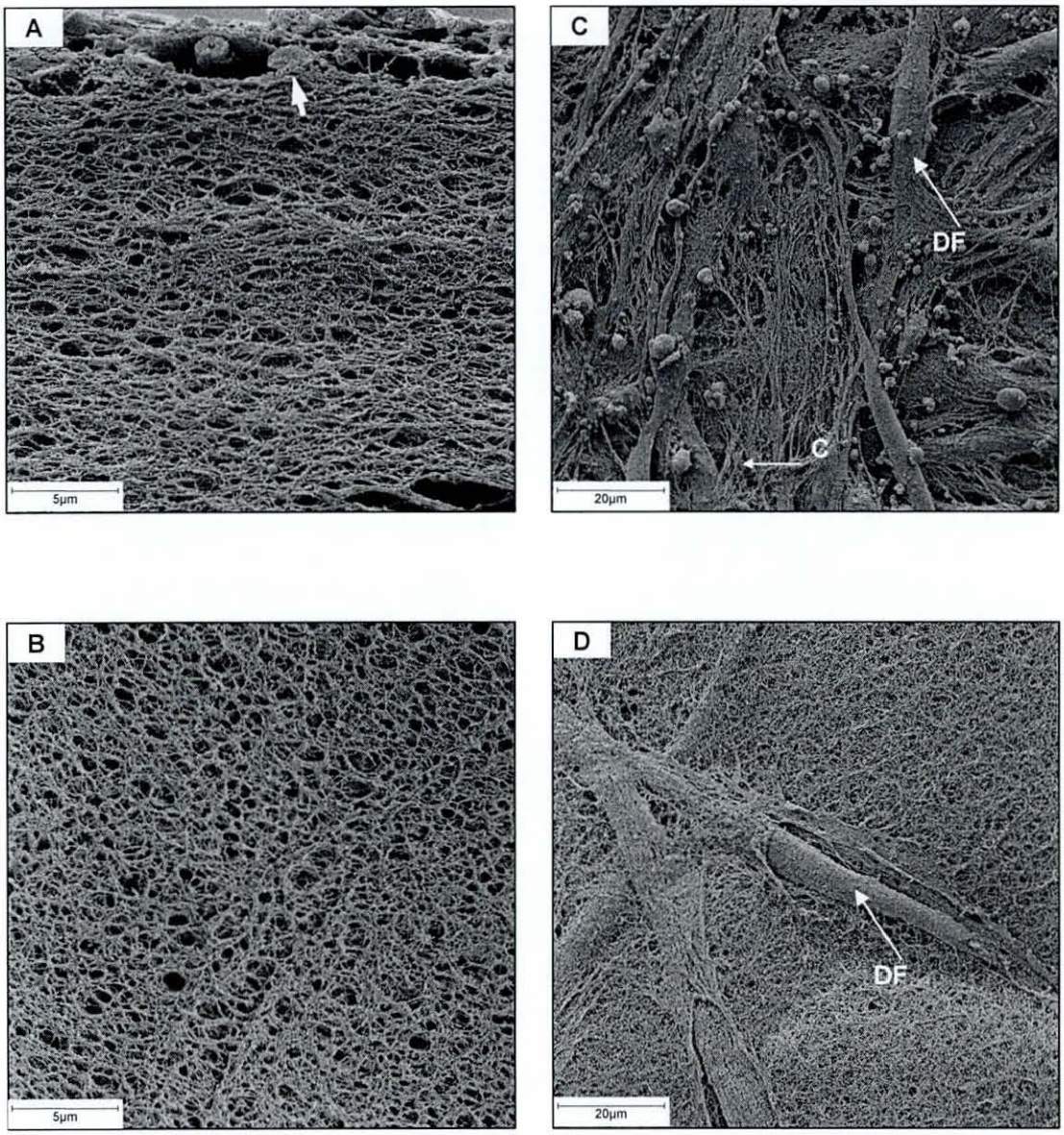

Figure 20 D49 SKN construct at 2500x magnification. A: Cross-section of top of SKN construct with elliptical pores and cell layer at construct-media interface (arrow). B: Cross-section of bottom surface of SKN construct with circular pores. C: Top surface view of dermal fibroblast (DF) with collagen (C) between the cells. D: Bottom surface view of cell protruding through the collagen matrix

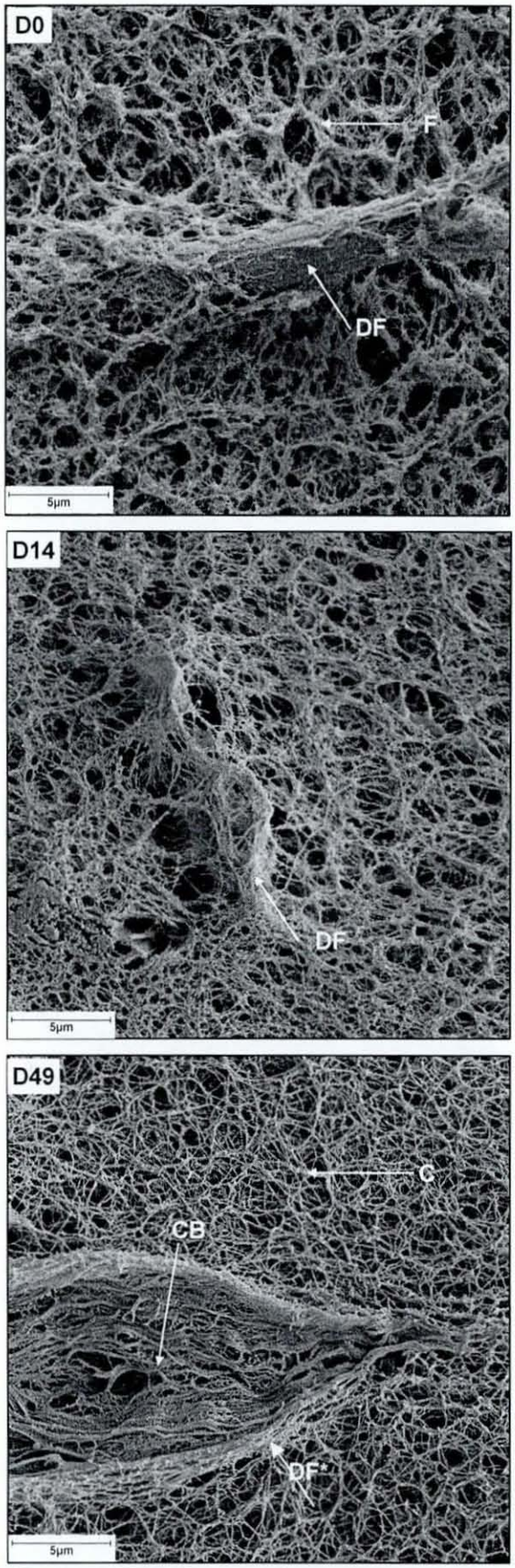

Figure 21 10000x magnification SEM Cross-sections of SKN constructs. D0: Fibrin fibril aggregates (F). D14: Fibrin and collagen matrix. D49: Structured collagen matrix (C) with collagen fibril bundles (CB). DF=dermal fibroblast. *fibroblast fallen out on fracture

3.7.6. Transmission Electron Microscopy (TEM)

The ultrastructure of the fibroblast cells and the matrix in the SKN constructs changed during manufacturing. The individual cells shown in Figure 22 were representative of the majority of the population of fibroblast cells in the SKN constructs at each time point. On D5 the fibroblasts had a very convoluted cell membrane and nucleus (Figure 22, D5a). There were many secretory vesicles, mitochondria, endoplasmic reticulum and Golgi apparatus (Figure 22, D5b). There also appeared to be an abundance of procollagen in the top right end of the cell (Figure 22, D5c). These features suggested that the cell was actively secreting collagen as it is known that procollagen molecule chains are assembled in the endoplasmic reticulum and packaged into vesicles in the Golgi apparatus which then move to the plasma membrane where the contents is discharged (Ghosh 2002, Fawcett 1994). In addition, the long mitochondria function to provide usable chemical energy for processes such as protein synthesis (Sadava 1993).

On D21 the cell membrane was less convoluted and there was a high density of collagen fibrils surrounding the cell membrane. The matrix also appeared more structured and collagen fibrils orientated parallel to the cells were observed. By D33 numerous lysosomes were present in many of the cells and the matrix surrounding the cells was denser than the matrix on D21. Lysosomes contain digestive enzymes and one of their functions is to breakdown injured or ageing cell organelles (Fawcett 1994) which suggested that some of the cells were beginning to undergo apoptosis by D33.

On D49 the cells were beginning to detach from the surrounding matrix and also contained many lysosomes and some lipids (Figure 22, D49a). Detachment from the matrix caused by cell shrinkage is also associated with cell apoptosis (Bortner, Cidlowski 1998, Barry, Behnke et al. 1990, Bride, Viennet et al. 2004). A dense matrix surrounded the cells and higher magnification images showed that the matrix fibres had the typical collagen banding pattern (Figure 22, D49b).

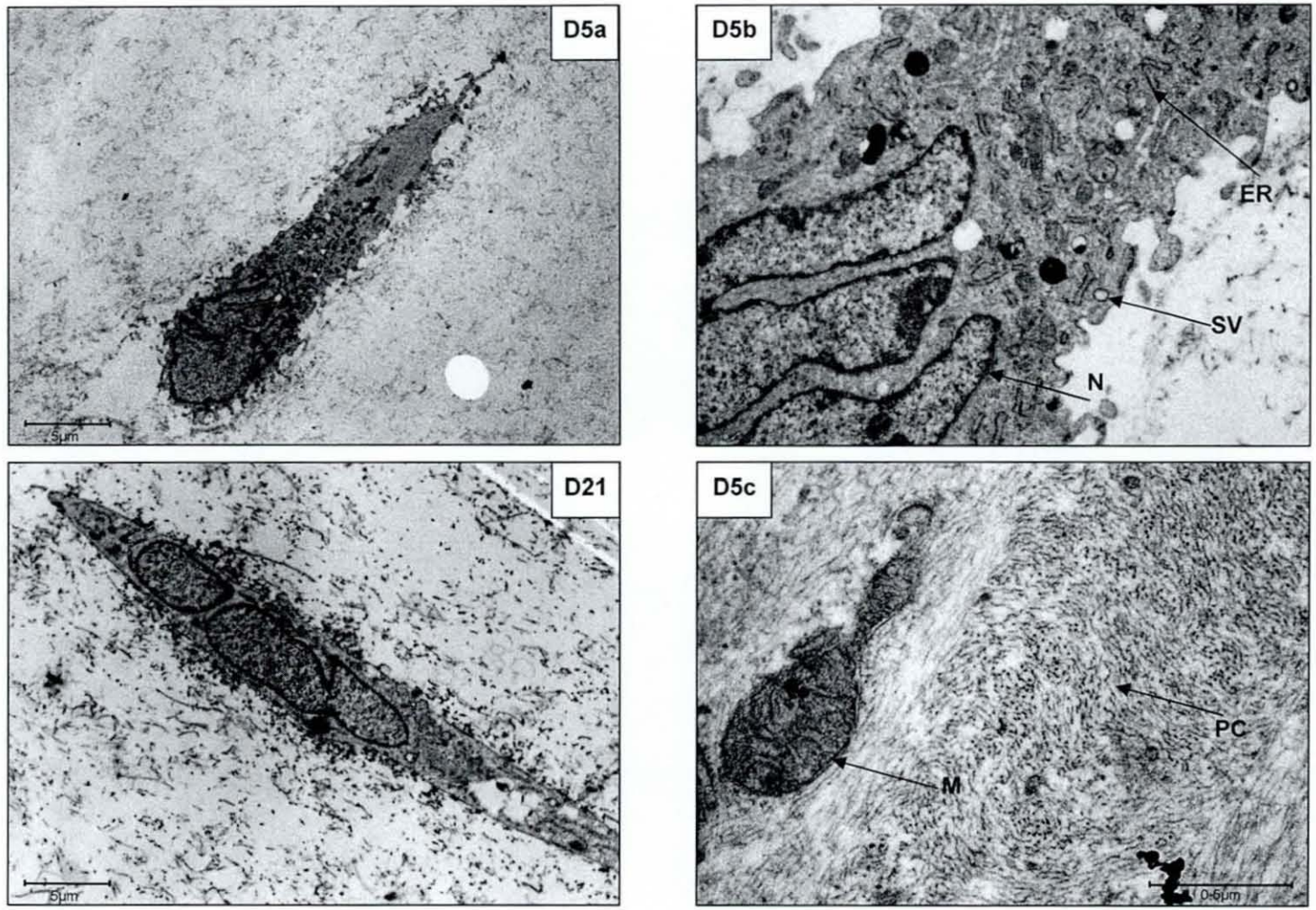

(Caption on next page)

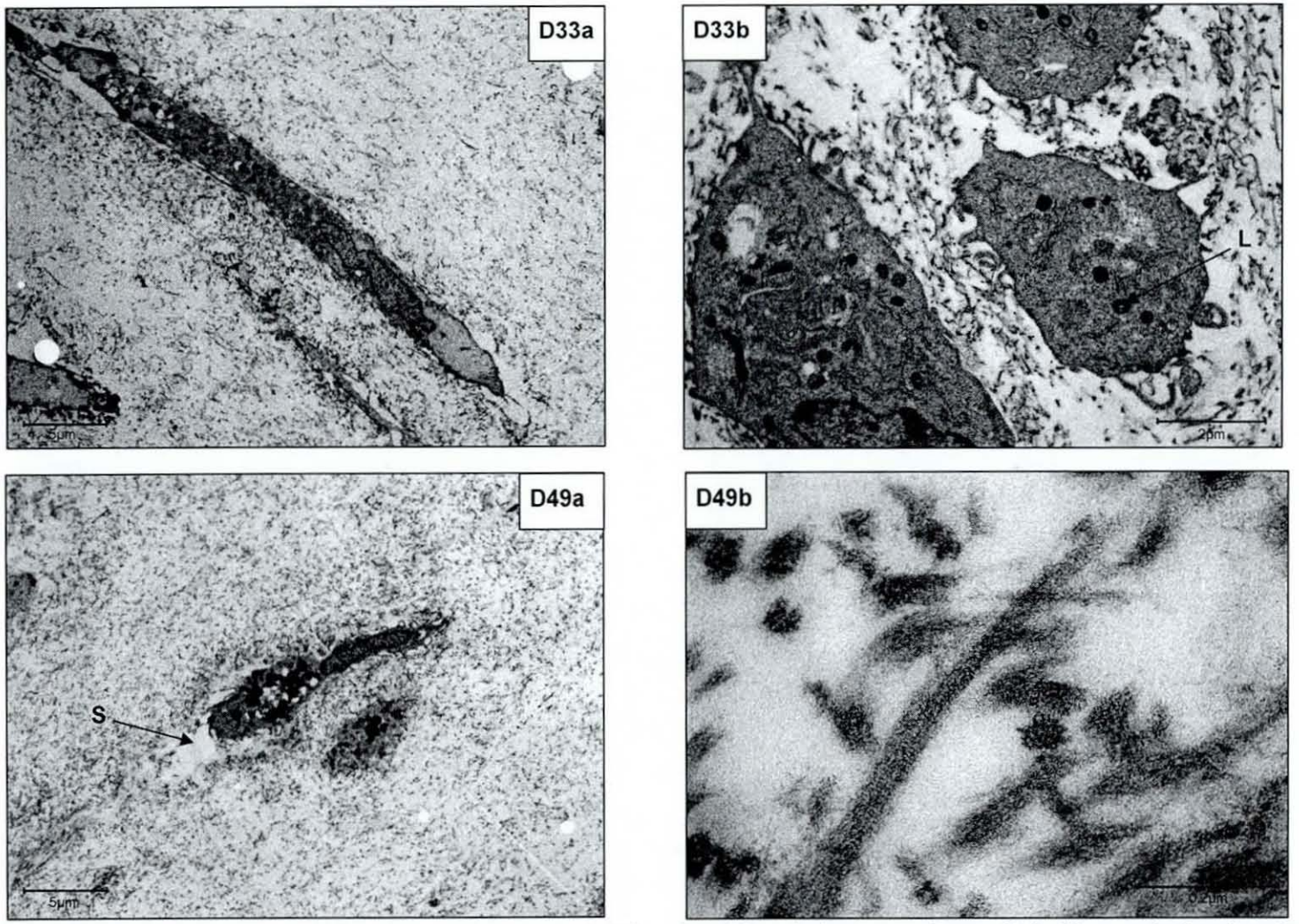

Figure 22 TEM cross sections of SKN constructs. D5a: Active cell with convoluted nucleus (N) and plasma membrane. D5b: Many endoplasmic reticulum (ER) and secretory vesicles (SV). D5c: Procollagen (PC) and mitochondria (M). D21 Collagen fibrils around cell membrane. D33a and b: Increasing presence of lysosomes (L) and collagen between the cells. D49a: Cell shrinkage away from matrix (S). D49b: Collagen banding on fibril

3.8. Biochemical Composition

3.8.1. Collagenase Digestion and Flow Cytometry

The number of live, apoptotic and dead HDF cells in the SKN constructs during manufacturing is shown in Figure 23. The average total number of cells (n=3) in the construct 3 hours after casting was $1.35x10^6$ (σ= $4.73x10^4$) with 4% (σ= 0.33) apoptotic cells and 8 % (σ= 4.4) dead cells. On D7 the average total number of cells had significantly increased to $6.72x10^6$ (σ= $6.53x10^5$, p= 0.005) cells. Between D7 and D42, the average total number of cells fluctuated between $6.72x10^6$ and $7.93x10^6$. However, the number of live cells remained relatively constant at an average of $5.41x10^6$ (σ= $2.90x10^5$). The percentage of apoptotic cells was 13.5% (σ= 2.5) and dead cells was 9% (σ= 2) between D7 and D35 but increased to 17% (σ= 1) apoptotic and 18.5% (σ= 0.5%) dead cells after D35. On D49 the average total number of cells significantly decreased to $6.08x10^6$ cells (σ= $4.88x10^6$, p= 0.016) and the average number of live cells decreased by 26% compared to D42. These findings supported the increase in the number of cells observed in the light and electron microscopy sections during manufacturing and the apparent increase in the percentage of apoptotic cells after D33 observed by TEM (sections 3.7.2 to 3.7.6).

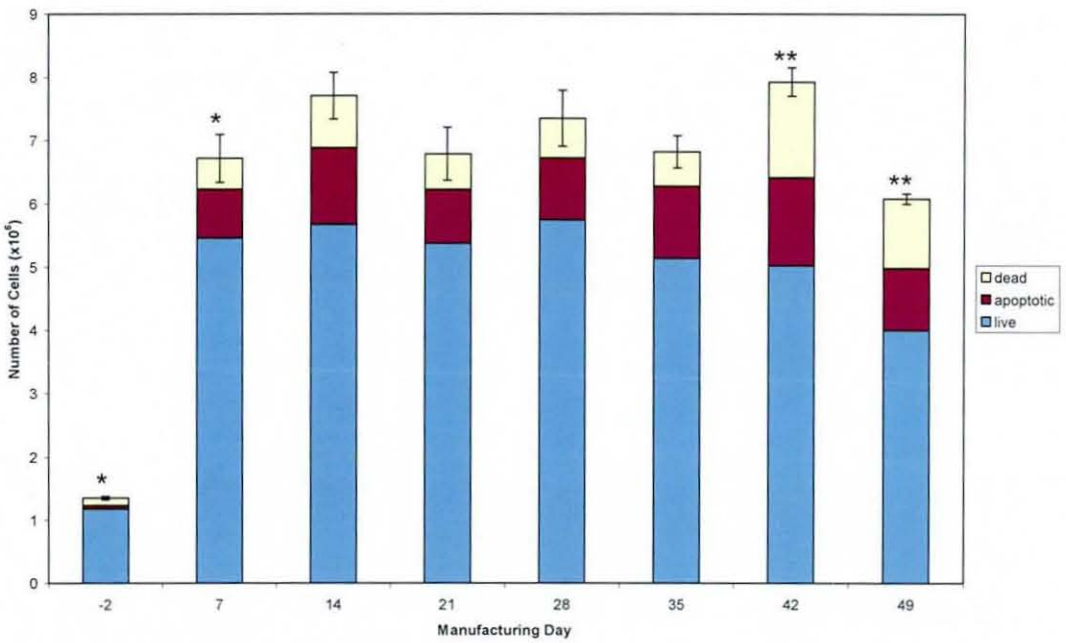

Figure 23 Average number of live, apoptotic and dead cells in SKN constructs during manufacturing (n=3). Error bars represent one standard error of the total number of cells. * p=0.005. **p=0.016

3.8.2. Digestion Time

The average digestion time (n=3) was relatively constant between D-2 and D28 but significantly increase by 48% (p=0.002) between D28 and D42 (Figure 24). This suggested that the degree of cross-linking in the SKN constructs increased between D28 and D42 of the manufacturing period. A 12% decrease in the average digestion time occurred between D42 and D49 but there was no statistical difference between the results at these time points. The plateau in the digestion time between D42 and D49 suggested that collagen synthesis had ceased or that the matrix was being remodelled. However, further measurement of the digestion time after D49 are required to confirm this.

The method used for determining the digestion time was reliant on operator judgement as to when the SKN construct had fully digested. However, judgment of this point was problematic as some small areas of the constructs did not fully breakdown in some of the constructs. Measurement of the digestion rate by recoding the change in weight of the constructs over time may improve the accuracy of this measurement and provide an increased understanding of the development of the cross-links in the constructs during manufacturing. Further work is required to develop a more repeatable method for determining the quantity of cross-linking in the constructs.

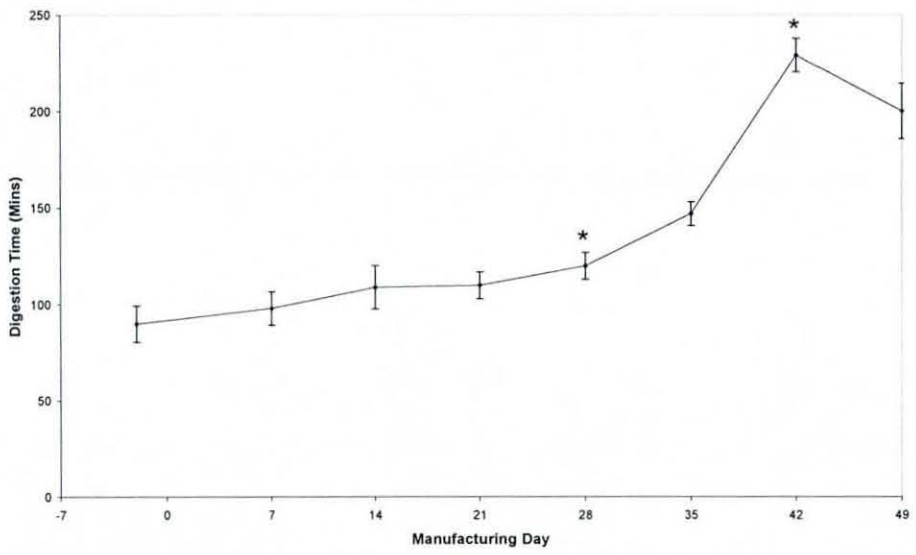

Figure 24 Average time taken to digest SKN constructs in collagenase solution during manufacturing (n=3). Error bars represent one standard error. * p=0.002

3.8.3. Dehydration

A 50% decrease in the wet weight of the SKN constructs was measured between D-2 and D7 (p=0), followed by a relatively stable wet weight between D7 and D49 for two separate batches of SKN constructs (Figure 25). However, the wet weight of the acellular constructs did not significantly differ during the manufacturing period which showed that the cells were responsible for the decrease in wet weight. In addition, the change in the wet weight of the SKN constructs correlated with the compaction of the matrix reported in section 3.7.1 which suggested that water was squeezed out from the constructs due to the compaction by the HDF cells.

The dry weight of the SKN constructs decreased by 30% between D-2 and D-1 and then remained relatively constant between D-1 and D28 (Figure 26). This suggested that the degradation of the fibrin matrix began soon after casting of the SKN constructs and that collagen deposition in the matrix occurred after D-1 to balance the decrease in dry weight due to the fibrin degradation. The dry weight significantly increased by 16% (p=0.002) on D35 and 28% (p=0.000) on D49 compared to D-1 which suggested that the changes in the extracellular matrix were dominated by collagen deposition rather than fibrin degradation after D28. Analysis of the results using the Two Sample T-Test showed that the increase in dry weight between D-1 and D49 was between 3.0mg and 5.5mg using 95% confidence intervals. In comparison, the acellular dry weight decreased between D0 and D21 and then increase between D21 and D49. However, the reasons for the changes in the acellular dry weight are not known.

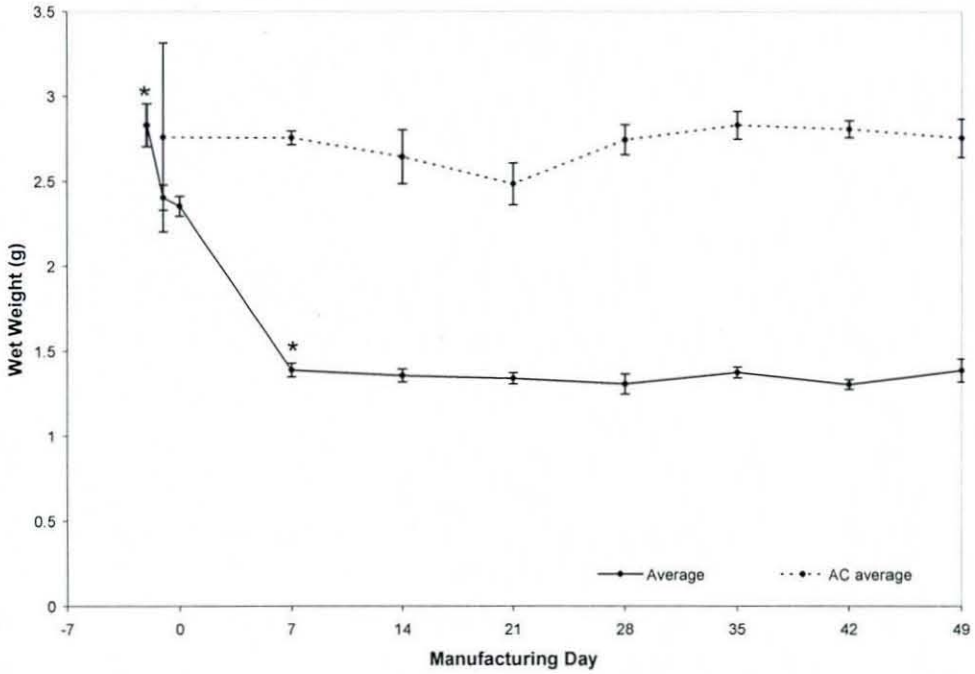

Figure 25 Average wet weight of two batches of SKN constructs (n=6) and one batch of acellular constructs (AC, n=3) during manufacturing. Error bars represent one standard error. * p=0.000

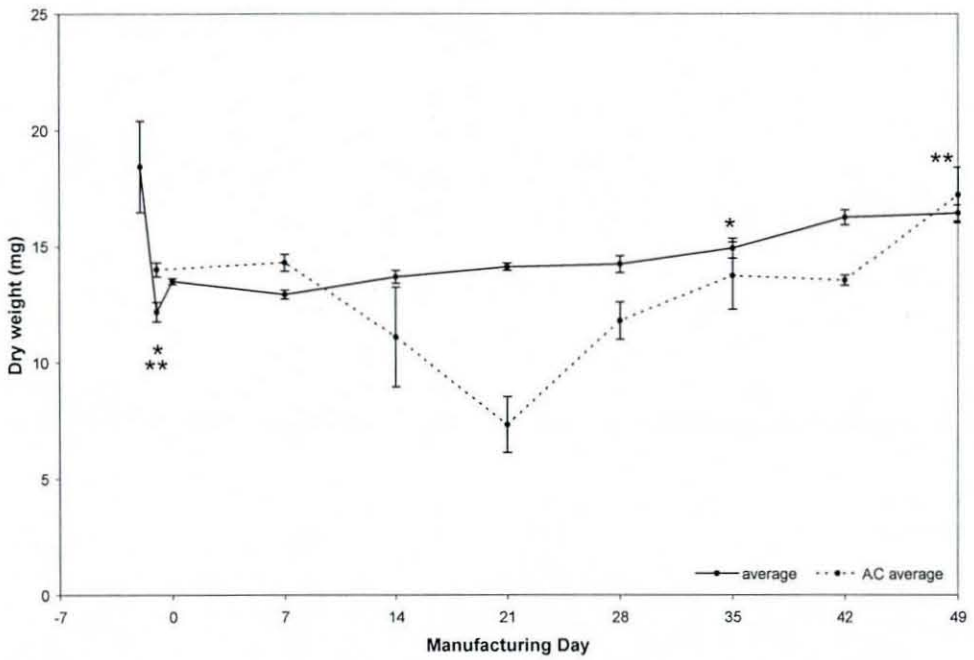

Figure 26 Average dry weight of two batches of SKN constructs (n=6) and one batch of acellular constructs (AC, n=3) during manufacturing. Error bars represent one standard error. * p= 0002. **p= 0.000

3.8.4. Collagen Type I Enzyme-Linked Immunosorbant Assay (ELISA)

The collagen type I ELISA aimed to provide quantitative data on the concentration of collagen type I in the SKN constructs. However, the method used in this study proved to be unsuitable for SKN constructs and development of a quantitative collagen assay is still required. The results showed that the collagen concentration in the SKN constructs increased between D-2 and D21, decreased between D21 and D42 and then increased between D42 and D49 (Figure 28). However, the data between D-2 and D42 was not reliable as the absorbance signal from the samples was very low and the associated collagen concentration had to be extrapolated beyond the first data point the standard curve, 0.149μg/mL, (Figure 27). In addition, calculation of the total quantity of collagen type I in the D49 construct using the ELISA results showed that the average weight of collagen type I was 0.724μg. This was significantly below the dry weight of 16.4mg measured on D49 (section 3.8.3) and it was expected that collagen type I would account for the majority of the total dry weight of the construct as suggested by the D49 histological sections.

The low absorbance signal from the SKN constructs using this methodology may be due to a number of factors which include poor extraction of the collagen from the SKN construct or poor binding of the antibodies to the epitotes of the extracted collagen. Further investigation is required to improve the extraction of collagen from the SKN constructs or use of an alternative assay such as Chloramine T which has been demonstrated by other authors for detection of collagen (Ahlfors, Billiar 2007, Ibusuki, Fujii et al. 2003, Balestrini, Billiar 2006, Boccafoschi, Habermehl et al. 2005).

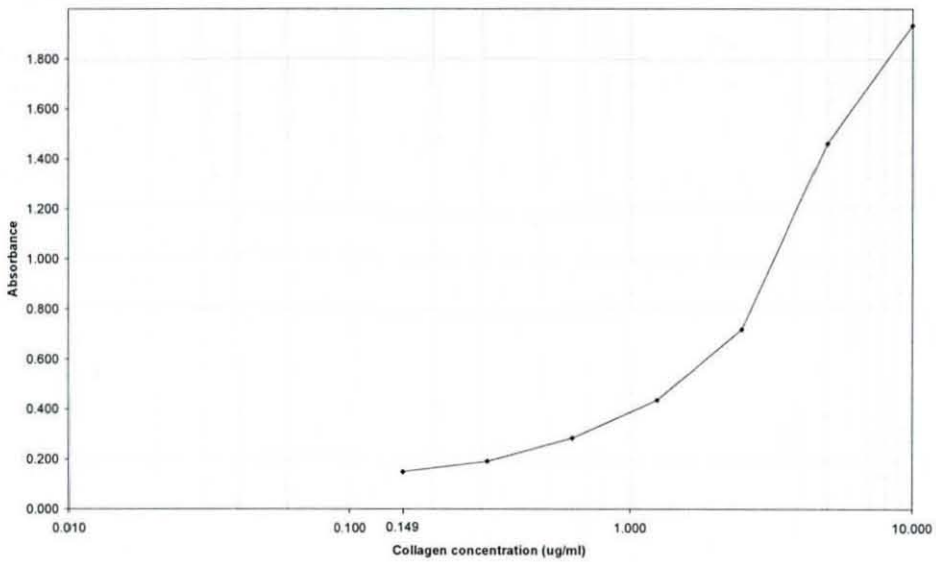

Figure 27 Standard curve for human collagen type I ELISA

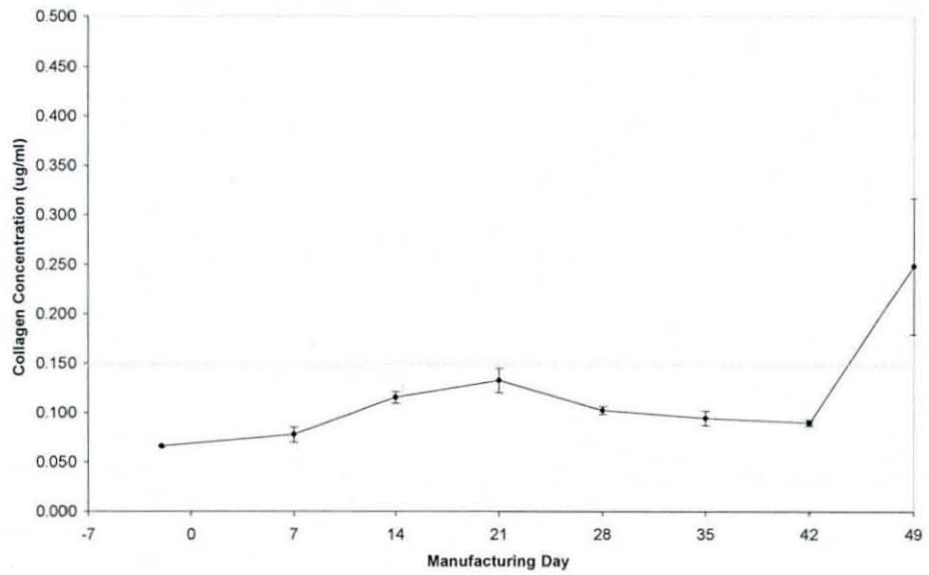

Figure 28 The average concentration of collagen in SKN constructs over the manufacturing period (n=3). Error bar represent one standard error. Extrapolated results below dashed line

3.8.5. Raman Spectroscopy

Analysis of dehydrated SKN constructs and SKN constructs in their native state showed that there was potential to identify the biochemical changes that occurred in the constructs during manufacturing using Raman spectroscopy. The Raman spectra for the dried SKN constructs showed common peaks at D0, D7 and D49 indicating their similarity in biochemical composition (Figure 29). In particular, common peaks at 1248cm^{-1}, 1451cm^{-1} and 1670cm^{-1} were similar to those found in Raman spectra for collagen type I and human dermis (Caspers, Lucassen et al. 1998, Fendel, Schrader 1998, Azrad, Zahor et al. 2006, Nijssen, Schut et al. 2002). In addition, peaks at 856cm^{-1} and 938 cm^{-1} were identified and represented the vibrating of C-C bonds in the collagen backbone and the amino acid proline ring respectively and are found in high concentration in collagen (Caspers, Lucassen et al. 1998). The wavelengths of the prominent peaks in the Raman spectra and the associated molecular components are summarised in Table 12.

The D0 Raman spectra showed additional peaks at 520cm^{-1}, 665cm^{-1} and 784cm^{-1} not observed in the other constructs. This suggested that the peaks were associated with fibrin as previous analysis of the SKN constructs using light microscopy showed that the matrix was only composed of fibrin on D0. The peaks that were associated with collagen in the D0 Raman spectra were unexpected as collagen was not detectable by light microscopy at this time point. These peaks may have been detected from collagen that had not yet formed into fibrils and were not visible by light microscopy. Other studies have shown that collagen is biochemically detectable in fibroblast seeded fibrin gels after 2 days in culture (D0 of this study) but only detectable by TEM after 9 days in culture (Tuan, Song et al. 1996).

In addition, the peaks associated with fibrin in the D0 spectra were not present in the D7 spectra although the histology images showed that fibrin was present in the constructs for at least 21 days after casting. This may be due to rapid degradation of the fibrin matrix by the cells between D0 and D7 reducing the fibrin signal in the Raman spectra. Other studies have shown that the rate of fibrin degradation by myofibroblasts is the greatest in the first 5 days post-casting after which the degradation rate decreased (Grassl, Oegema et al. 2002).

Initial experiments to analyse the composition of the SKN constructs in their native sate showed that the Raman spectra of an acellular fibrin construct and a D63 SKN construct was dominated by the composition of the DMEM-10 media (Figure 30). However, peaks at 520cm^{-1}, 665cm^{-1} and 784cm^{-1} were identified in the Raman spectra of the acellular fibrin construct and correlated with the peaks identified in the D0 dried sample. In addition, a peak at 856cm^{-1} which is associated with the proline ring found in collagen was identified in the D63 SKN construct.

The results suggested that there was potential for use of Raman spectroscopy as a non-contact, non-destructive tool to determine the composition of SKN constructs in their native state. However, improvements in the Raman system are required to improve the acquisition of the signal and resolution of the peaks in the spectra especially from the hydrated constructs. For the ICX-SKN constructs, Raman spectroscopy could also be used as a non-destructive technique to identify the biochemical composition of ICX-SKN constructs after the freeze-drying stage of the manufacturing process.

Wavelength (cm^{-1})	Component	Reference
622 and 1006	Phenylalanine	(Frushour, Koenig 1975)
856	ν(C-C) proline ring	(Caspers, Lucassen et al. 1998, Fendel, Schrader 1998, Azrad, Zahor et al. 2006, Nijssen, Schut et al. 2002)
938	ν(C-C) of protein backbone	
1248	Amide III group	(Fendel, Schrader 1998, Azrad, Zahor et al. 2006)
1451	δ(CH3, CH2)	(Azrad, Zahor et al. 2006, Frushour, Koenig 1975)
1670	Amide I group	(Azrad, Zahor et al. 2006, Frushour, Koenig 1975)

Table 12 Components represented by the prominent peaks in the Raman spectra of dehydrated constructs and also identified in human dermis

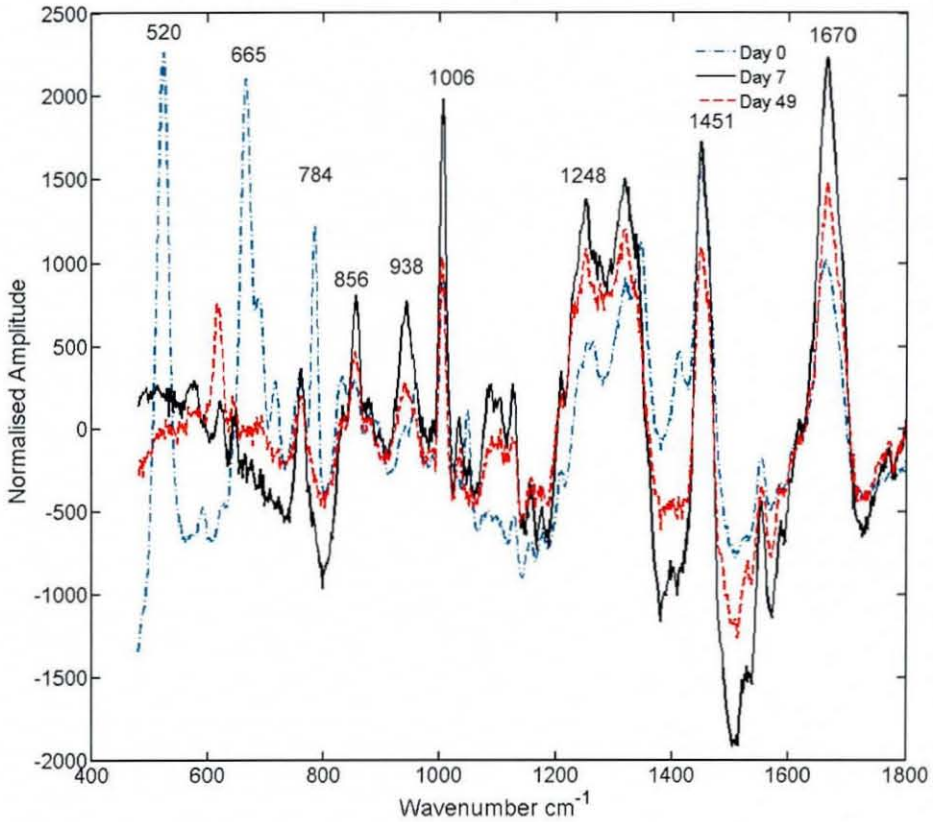

Figure 29 Raman spectra of dehydrated SKN constructs on D0, D7 and D49

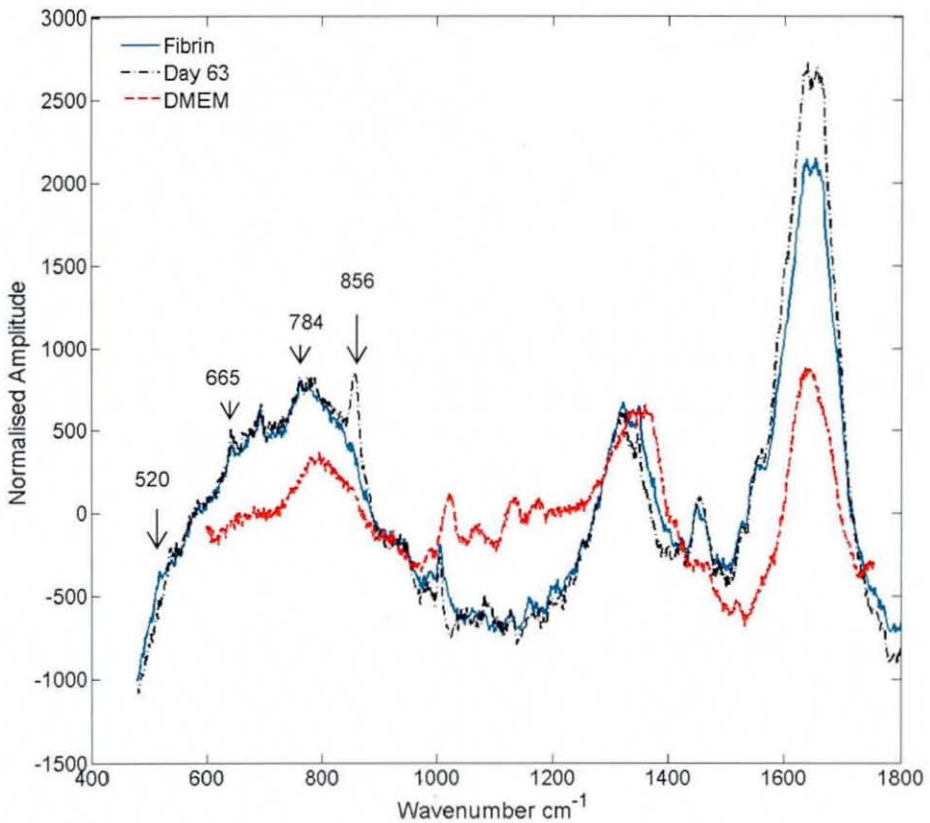

Figure 30 Raman spectra of hydrated, acellular fibrin gel, D63 SKN constructs and DMEM-10 media

3.9. Mechanical Properties

3.9.1. Rheology

The shear storage modulus (G') represented the elastic properties of the SKN construct and the shear loss modulus (G") represented the viscous properties. The frequency sweep results showed that the viscoelastic behaviour of the SKN constructs was independent of frequency below 3Hz at constant strain of 1%. G' was greater than G" for frequencies below 3Hz for each time point measured during the manufacturing process (Figure 31). This showed that the SKN constructs behaved more like an elastic solid and the deformations of the construct were essentially elastic and recoverable (Rao 2007). Deformation of the constructs above 3Hz resulted in a decrease in G' and an increase in G". Above 10Hz, G" was greater than G', which showed that the behaviour of the SKN constructs was more liquid-like and the energy used to deform the construct was viscously dissipated (Rao 2007).

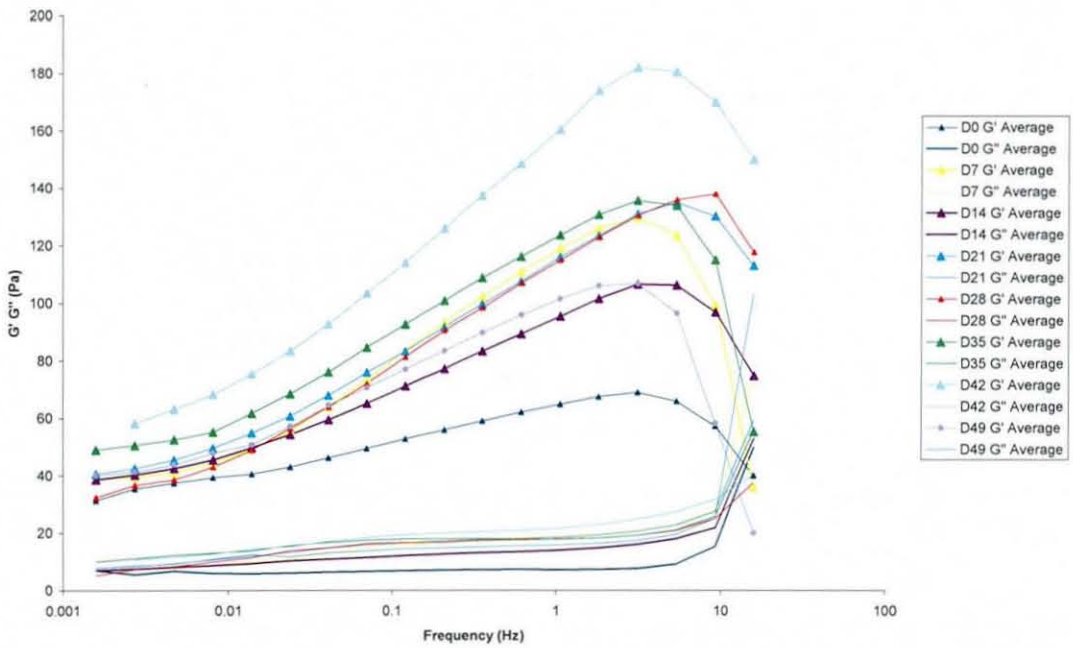

Figure 31 Viscoelastic properties of the SKN constructs over the manufacturing period in response to frequency and 1% strain (n=3). Standard error for each data point ranged between 1.2Pa and 6.3Pa. Error bars not shown for clarity

In the SKN constructs the elastic properties are related to the straightening and relaxation of the matrix fibres such as fibrin and collagen. The viscous properties are related to the flow of the fluid in the constructs which may be affected by numerous factors such as the viscosity of the fluid, concentration of proteoglycans which bind water to collagen fibrils (Silver, Seehra et al. 2002) and the structure of the matrix. The cross-over of G' and G" at high frequencies may have been due to the decreasing ability of the fibres to straighten and relax as the rate of loading increased and therefore, caused an increase in the dissipation of the deformation energy by the viscous components.

The strain sweep was carried out at 1Hz so that analysis of the response of the SKN constructs to strain was independent of frequency and to minimise the testing time. The strain sweep showed that there was a linear viscoelastic region (LVR) where the SKN constructs were independent of strain (Figure 32). The constructs behaved more like an elastic solid in this region as G' was greater than G". After the LVR, G' decreased and G" increased resulting in G" being greater than G' for the D0 and D7 constructs. Visual extrapolation of the curves for the D14 to D49 constructs indicated that G" would be greater than G' at strains above 100%. A greater G" than G' indicated that the SKN constructs had more liquid-like behaviour in this region of strain (Rao 2007). The transition from predominantly elastic properties to predominantly liquid properties due to shear deformation may have been due to disruption of the cross-links or a decrease in entanglements in the SKN matrix.

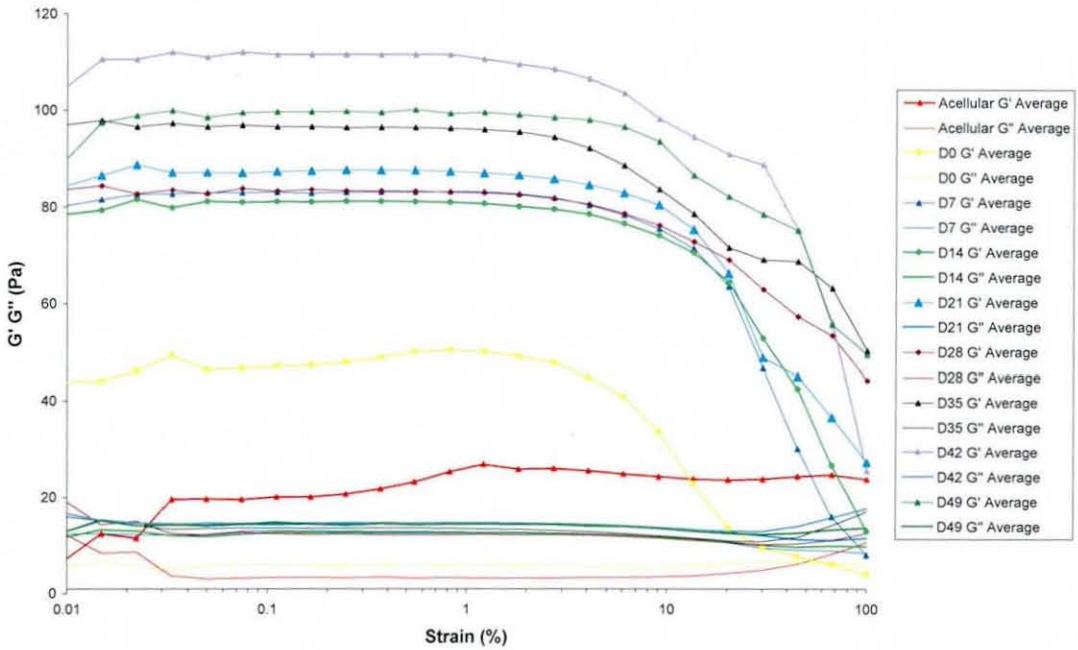

Figure 32 Viscoelastic properties of the SKN constructs over the manufacturing period in response to strain at 1Hz frequency (n=3). Standard error for each data point ranged between 1.7Pa and 6.5Pa. Error bars not shown for clarity

Comparison of the viscoelastic properties of the acellular and D0 SKN constructs showed that G' and G" were 128% and 78% greater for the D0 construct, respectively (Figure 33). This suggested that the fibroblast cells contributed towards the viscoelastic properties of the construct. In addition, G' began to decrease after approximately 3% strain for the D0 SKN construct compared to approximately 90% strain for the acellular constructs. This was unexpected as the fibrin matrices used for both constructs were cast from the same working solution of fibrinogen and thrombin. However, a possible explanation for this result is that the decrease in elastic properties of the D0 SKN construct was caused by detachment of the HDF cells from the matrix (Figure 33).

The HDF cells in the construct also appeared to affect the structure of the fibrin matrix. Extrapolation of the G' and G" curves above 100% strain for the acellular SKN constructs and the cellular D0 constructs showed that the cross-over point of G' and G" occurred at a greater strain for the acellular constructs (Figure 33). The transition of the properties of the D0 SKN construct from predominantly elastic solid to predominantly viscous liquid at a lower strain compared to the acellular construct suggested that the

fibrin matrix in the D0 construct had less cross-links or less entanglements assuming that the majority of the cells were detached from the matrix at this strain.

In comparison to the D0 construct, the cross-over point of the D7 to D49 SKN constructs occurred at greater strain and the viscoelastic properties in the LVR were greater. In this study, it has been shown that the number of cells, collagen deposition and cross-linking increased between D0 and D7 (section 3.7). These increases may have caused the increase in G' and G" in the LVR and the increased strain at which G' and G" crossed over (Figure 33). This would support the findings of other studies which showed that G' and G" increased with increasing collagen content and cross-linking (Sheu, Huang et al. 2001, Sosnik, Sefton 2005, Vanderhooft, Alcoutlabi et al. 2008).

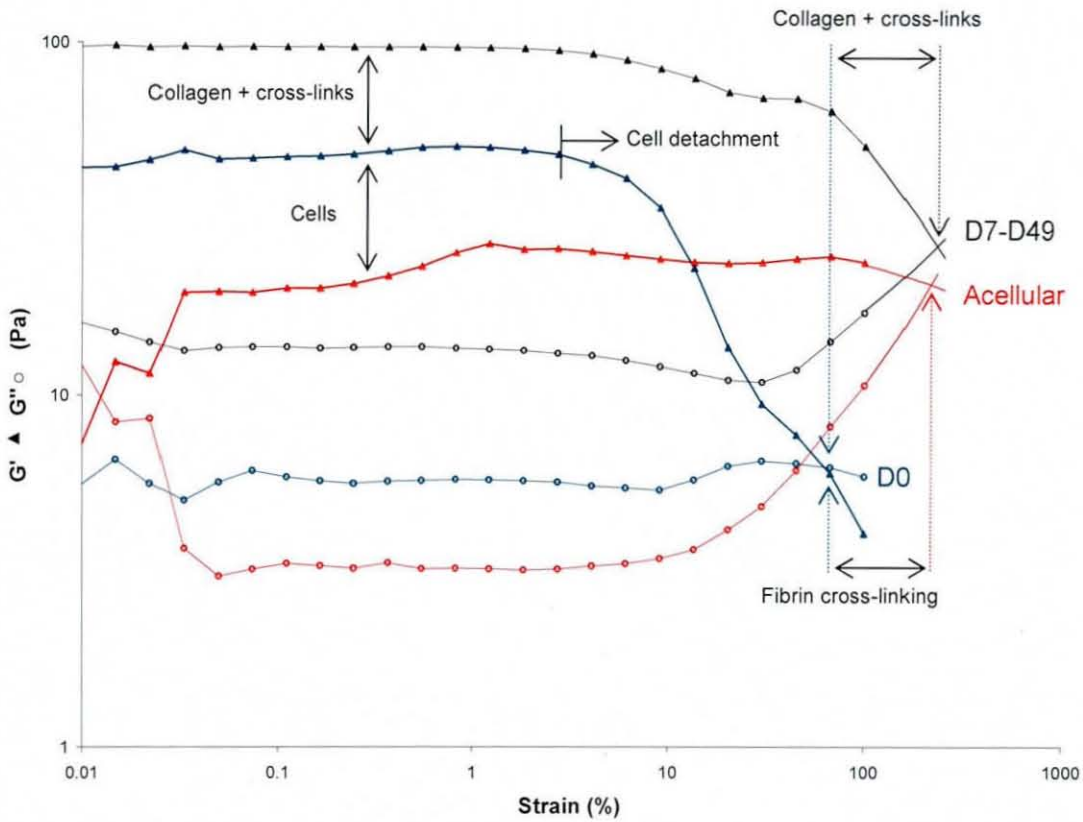

Figure 33 Proposed relationships between the SKN matrix composition and viscoelastic properties. Acellular construct (red lines). D0 construct (blue lines). G' and G" representative of D7-D49 construct (black lines). Data extrapolated above 100% strain

The viscoelastic properties of the SKN construct also correlated with the changes in the biochemical composition and structure of the matrix describe in previous sections. The cell proliferation and matrix compaction between D-2 and D7 correlated with a 70% increase in G'. After D7, it has been shown that construct compaction ceased and the number of viable cells in the construct remained constant (sections 3.7.1 and 3.8.1). Therefore, the elastic properties of the SKN constructs during this part of the manufacturing process were of primary interest as they represented the changes in the quantity and degree of cross-linking in the matrix. The changes in G' in the linear viscoelastic region during manufacturing is shown in Figure 34. Between D7 and D28, G' remained relatively constant at 84±3Pa. G' then increased to 96.5Pa (not significant) on D35 and 112Pa (p=0.006) on D42 compared to D7 before reaching a plateau between D42 and D49. These results correlated with the measurements of dry weight and digestion time (sections 3.8.2 and 3.8.3) and qualitative observations of increasing matrix density and collagen in the SKN constructs (section 3.7.2 to 3.7.6).

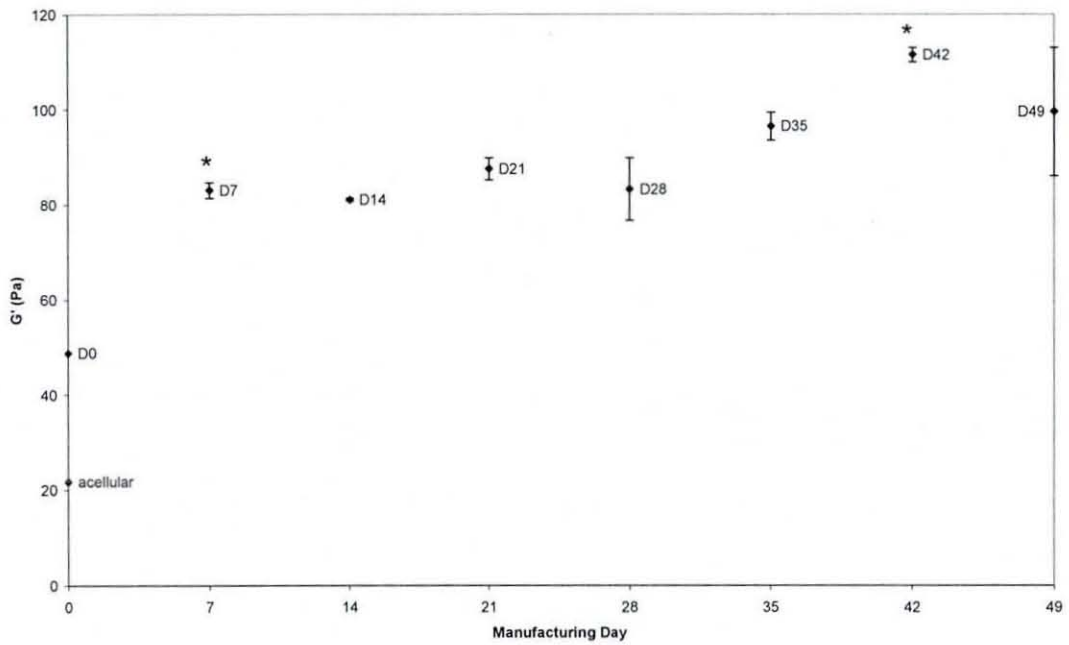

Figure 34 Shear storage modulus (G') of the SKN constructs in the linear viscoelastic region over the manufacturing period (n=3). Error bars represent one standard error. * p=0.006

Finally, comparison of the SKN constructs with cadaver dermis showed that the viscoelastic properties were approximately ten times greater for the dermis which had a G' of 1000Pa and G" of 200Pa in the linear viscoelastic region. This was supported by the SEM images of the dermis which showed a denser collagen matrix with large fibre bundles (Figure 36). The linear viscoelastic region for the dermis was also greater, between 0% and 8%, after which G' decreased. The viscous properties represented by G" also began to decrease after 30% strain and G' did not cross G' in contrast to the SKN constructs. The magnitude of the viscoelastic properties of the SKN construct relative to the native dermis that are required to improve the efficacy of the constructs in-vivo are not known. However, the preliminary data of the efficacy of ICX-SKN in the Phase I clinical trials suggested that the constructs did not have to be of similar magnitude in terms of viscoelastic properties for successful integration into a wound site as suggested by other authors (Hilborn, Bjursten 2007).

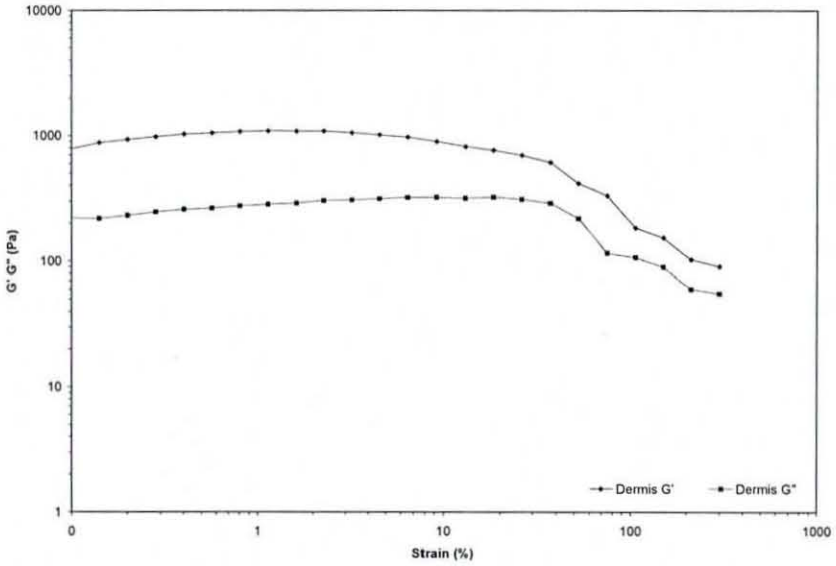

Figure 35 Viscoelastic properties of cadaver dermis (n=1) in response to increasing strain at 1Hz frequency

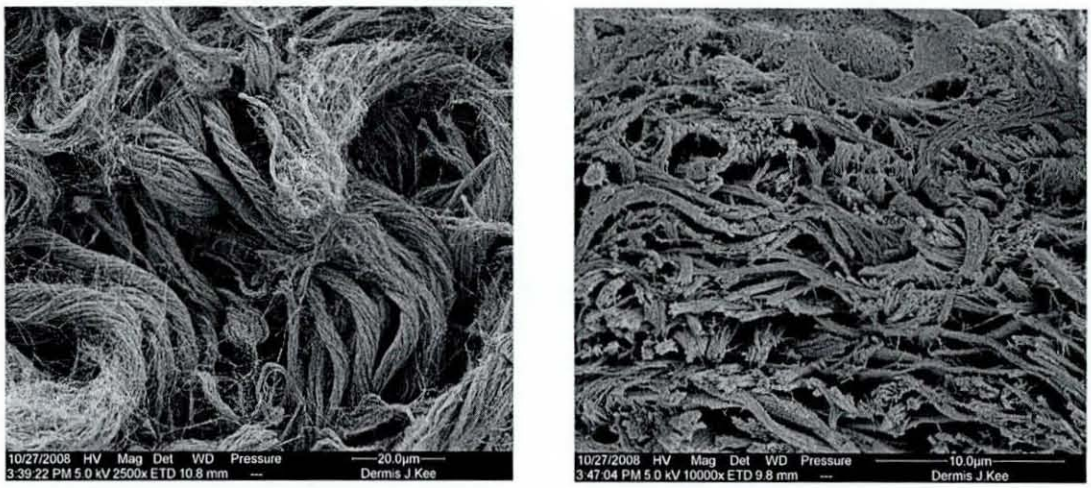

Figure 36 SEM cross-section of human dermis (donated by NHSBT, Liverpool) Left: Collagen fibrils forming collagen bundles (x2500 mag). Right: Cross-section of fibre bundle made up of many fibril bundles (x10000 mag)

	n	D-2	D0	D7	D14	D21	D28	D35	D42	D49
Surface profile		Convex	Convex	Concave	Concave	Concave	Concave	Concave	Concave	Concave
Thickness (mm)	8	2.97	2.07	1.66	1.57	1.57	1.57	1.57	1.57	1.57
% decrease		*	*30*	*44*	*47*	*47*	*47*	*47*	*47*	*47*
Volume (mm^3)	8	2690	1560	1494	1494	1495	1495	1497	1494	1496
% decrease		*	*42*	*44*	*44*	*44*	*44*	*44*	*44*	*44*
Viable cell number	3	1.35E+06	~	6.72E+06	5.82E+06	6.41E+06	6.23E+06	5.82E+06	5.99E+06	4.79E+06
% increase		*	~	*397*	*331*	*374*	*361*	*331*	*343*	*254*
% Apoptotic cells	3	3.95%	~	11.43%	15.70%	12.61%	13.30%	16.67%	17.53%	16.22%
% Dead cells	3	8.38%	~	7.23%	10.67%	8.21%	8.48%	7.94%	19.08%	18.04%
Digestion time (min)	3	90	~	98	109	110	120	147	229	200
% increase		*	~	*9*	*21*	*22*	*33*	*63*	*154*	*122*
Wet weight (g)	6	2.83	2.35	1.39	1.36	1.34	1.31	1.37	1.30	1.39
% decrease		*	*17*	*51*	*52*	*53*	*54*	*51*	*54*	*51*
Dry weight (mg)	6	18.43	13.50	12.93	13.69	14.11	14.23	14.92	16.24	16.43
% increase		*	*27*	*30*	*26*	*23*	*23*	*19*	*12*	*11*
G' (Pa)	3	~	48.80	83.07	81.07	87.50	83.25	96.45	111.50	99.50
% increase		~	*	*70*	*66*	*79*	*71*	*98*	*128*	*104*
G" (Pa)	3	~	5.68	12.87	12.57	14.50	12.15	13.65	14.67	14.47
% increase		~	*	*127*	*121*	*155*	*114*	*140*	*158*	*155*

Table 13 Summary of characterisation results during manufacturing. Percentage change calculated relative to D-2 or D0 as indicated by*

	D-2	D0	D7	D14	D21	D35	D49
TEM			Active cells with many organelles, secretory vesicles and procollagen		Active cells with collagen fibrils parallel to cell membrane	Increased presence of lysosomes in cells. Denser matrix	Cell shrinkage and increased presence of lysosomes. Collagen banding on fibrils
SEM		Clumps of fibres + evenly distributed cells		More structured matrix+ higher cell density at surface	Increased matrix density	Increased matrix density	More defined matrix, individual fibrils, collagen fibril bundles
Histology MT		Fibrin + evenly distributed cells			Fibrin and collagen matrix + cell layer at surface		Collagen matrix + cell layer at surface
Histology Alcian Blue		No proteoglycans			No proteoglycans		No proteoglycans
Histology EVG		No elastin			No elastin		No elastin
IHC		No collagen I or III			50:50 collagen I : III matrix		Collagen I only with fibrils spanning between cells
CLFM	No collagen I		Collagen I matrix+ orientated cells on surface at edge				Increased collagen I

Table 14 Summary of structural analysis of SKN constructs during manufacturing

3.10. Characterisation Conclusion

Characterisation of the SKN constructs has provided an improved understanding of the changes in physical, biochemical and mechanical properties that occur during the 49-day manufacturing process. This study also confirmed that the human dermal fibroblast cells were the processing units responsible for the majority of these changes. The HDF cells functioned to compact the SKN construct, degrade the fibrin matrix and synthesise collagen. It is suggested that biochemical and mechanical signalling from the changing composition and mechanical properties of the SKN construct stimulated the cells responses. Four phases of cellular activity were identified in the SKN manufacturing process and are discussed below and illustrated in Figure 37.

In addition, the shear storage modulus (G') and shear loss modulus (G"), measures of the elastic and viscous properties respectively, were shown to be related to the changes in the biochemical composition and physical properties of the SKN construct. In particular, the elastic properties were related to the quantity and degree of cross-linking in the SKN construct matrix, and the adhesion of the cells to the matrix whereas the viscous properties were related to the ability of the fluid to flow within the constructs in response to shear deformation. The relationship between the change in physical, biochemical and mechanical properties and the shear storage modulus is also illustrated in Figure 37.

3.10.1. Phase 1: D-2 to D7 Cell Proliferation and Matrix Compaction

Between D-2 and D7, the manufacturing process was dominated by cell proliferation and compaction of the matrix by the cells suggested to be through the reorganisation of the fibrin fibres (Tuan, Song et al. 1996). The number of viable cells in the SKN construct increased by 397% and the volume fraction of cells in the construct increased from 1% to approximately 14% (Figure 38 and Appendix III for assumptions used for calculation of cell volume fraction). The construct was compacted to 47% of the original thickness and 53% of the original volume. This correlated with a 70% increase in the shear storage modulus and 127% increase in the shear loss modulus. The stimulus for cell proliferation may have been from biochemical and mechanical signalling from the fibrin matrix as other studies have shown that the fibrinogen and thrombin formulation used to produce the fibrin matrix affects the degree of cell proliferation

(Cox, Cole et al. 2004, Duong, Wu et al. 2009). In addition, Total Media, which contained TGF-β1 and insulin, may have also stimulated cell proliferation as observed in other studies of cell seeded fibrin matrices (Ross, Tranquillo 2003).

Mapping of the surface profile of the SKN constructs showed that cellular construct compaction caused the initial convex surface to become concave in profile and that compaction ceased by D14. The decrease in wet weight of the construct over the same period suggested that water was squeezed out from the constructs due to the compaction and resulted in a decrease in volume fraction of water from approximately 98% on D-2 to 88% after D7 (Figure 38). In addition, confocal microscopy images showed that the cells around the edge of the top surface of the construct were preferentially aligned towards the centre of the construct. Other studies have shown that tension is generated in cellular matrices in response to matrix compaction (Grinnell 2003, Georges, Janmey 2005) and that cells orientate in a preferential direction in response to directional mechanical stress (De, Zemel et al. 2007, Mudera, Pleass et al. 2000, Eastwood, Mudera et al. 1998). The aligned cells observed in this study suggested that tension generated by compaction was greater on the surface of the construct between the edge of the SKN constructs and the culture dish. Mechanical signalling from the tension generated in the matrix may have been responsible for the cease in matrix compaction by the HDF cells after D14.

Histological analysis using Masson's Trichrome staining showed that the matrix comprised of fibrin on D0 with cells evenly distributed thought the matrix. However, the 27% decrease in dry weight between D-2 and D0 suggested that degradation of the fibrin matrix by the cells occurred rapidly after casting the constructs. Collagen type I deposition by the cells was detected by D6 in the CLFM images. However, analysis of the biochemical composition using Raman spectroscopy suggested that collagen was present as early as D0. This supported the findings of other studies which showed that collagen is biochemically detectable in fibroblast seeded fibrin gels after 2 days in culture (D0 of this study) but only detectable by TEM after 9 days in culture (Tuan, Song et al. 1996). In addition, highly active cells containing many cellular organelles and secretory vesicles, characteristic of cell protein synthesis, were observed by TEM on D5.

3.10.2. Phase 2: D7 to D28 Fibrin Degradation and Collagen Synthesis

Between D7 and D28, the total number of viable cells was relatively constant ($5.41x10^6$, $\sigma=5.8x10^5$) and matrix compaction had ceased. No significant differences in dry weight (13.9±1mg), digestion time (110±10minutes) and shear storage modulus (72.5±6.5Pa) during this period suggested that the manufacturing process was dominated by fibrin degradation and collagen synthesis. The Masson's Trichrome stained histological sections showed that on D21, the majority of the matrix was composed of collagen but some areas of fibrin matrix were still present. The IHC sections showed that both collagen type I and type III were present on D21 which is consistent with the composition of acute wound healing sites in humans after 3 weeks (Robins, Milne et al. 2003). Other studies have shown that fibrin stimulates collagen secretion from HDF cells (Grassl, Oegema et al. 2002, Grassl, Oegema et al. 2003) and this may have provided part of the stimulus for collagen synthesis by the HDF cells during this period.

In addition, after D7 the cell density appeared to be greater towards the top of the construct and a layer of cells had formed on the construct-media interface. This cell layer was not present on the D0 construct which suggested that the cells migrated to the surface of the construct. The reason for the migration is not known but may be due to the greater availability of nutrients from the media on the surface. It is also possible that there was also a higher concentration of nutrients towards the top of the construct resulting in cell migration or greater cell proliferation observed in this area by CLFM and SEM. However, the difference in cell density may have also been caused by compaction of the constructs.

Further investigation into the cause of the inhomogeneous cell density in the SKN constructs may lead to process and product improvement and is discussed in section 3.11.

3.10.3. Phase 3: D28 to D35 Collagen Synthesis

Between D28 and D35, there were significant increases in dry weight by 16%, ($p=0.002$), digestion time by 48% ($p=0.002$) and shear storage modulus by 33% ($p=0.006$). This was supported by the SEM cross-sections which showed an increasing

matrix density and the formation of collagen fibril bundles during this period. These results suggested that fibrin degradation had ceased between D21 and D28 and the manufacturing process was dominated by collagen deposition during this period. This was supported by other studies which used fluorescent labelling of fibrinogen to show that the degradation of a fibrin matrix by myofibroblasts occurred over a period of approximately 20 days (Grassl, Oegema et al. 2002, Ye, Zünd et al. 2000).

3.10.4. Phase 4: D42 to D49 Remodelling

Between D42 and D49, no significant difference in dry weight, digestion time and shear storage modulus was observed but the number of viable cells decreased by approximately 26%. Histological and immunohistochemical analysis showed that the matrix was composed of collagen type I but there was no evidence of any collagen type III, proteoglycan or elastin deposition reported by other studies of cellular fibrin matrices (Ahlfors, Billiar 2007). These events are similar to those that occur during the remodelling stage of wound healing in-vivo when collagen type III is broken down and cell apoptosis increases (section 2.2). However, in-vivo, further remodelling occurs through lysis of old collagen and secretion of new collagen over several years until the wound has regained approximately 80% of the strength of the native tissue (Li, Chen et al. 2007). It has been suggested that biomechanical signalling across the wound and movement from joints provides the stimulus responsible for these events (Li, Chen et al. 2007, Clark 1996). However, such mechanical stimuli are not present in-vitro and between D42 and D49 the biochemical composition and mechanical properties of the SKN construct may have become suitable for the function of sustaining the cells in the culture dish. Further secretion of collagen to increase the mechanical properties of the SKN construct is likely to require an external mechanical stimulus and is investigated through use of ultrasound stimulation in Chapters 4 and 5.

In summary, the 4-Phase model of the SKN manufacturing process has provided an increased understanding of the changes and interactions between the biochemical, physical and mechanical properties of the SKN constructs and the time scales over which the changes in properties occur. It is the first study to the author's knowledge that has monitored the changes and interaction of these properties of a cellular fibrin matrix

over a 49 day study period. This study showed that after 21 days (the typical study period reported by other authors), the fibrin matrix continues to degrade and further collagen is synthesised by the cells until D42 when collagen synthesis reaches a plateau.

The time scales over which these events occur are likely to be dependent on a number of factors. These include the structure and biochemical composition of the initial fibrin matrix, the total number of viable cells supported by the matrix during manufacturing and the composition and availability of the media to the cells in the matrices. a greater understanding of the interaction and affects of these factors on collagen synthesis and the mechanical properties of the constructs will allow for further process and product improvement of the tissue-engineered constructs.

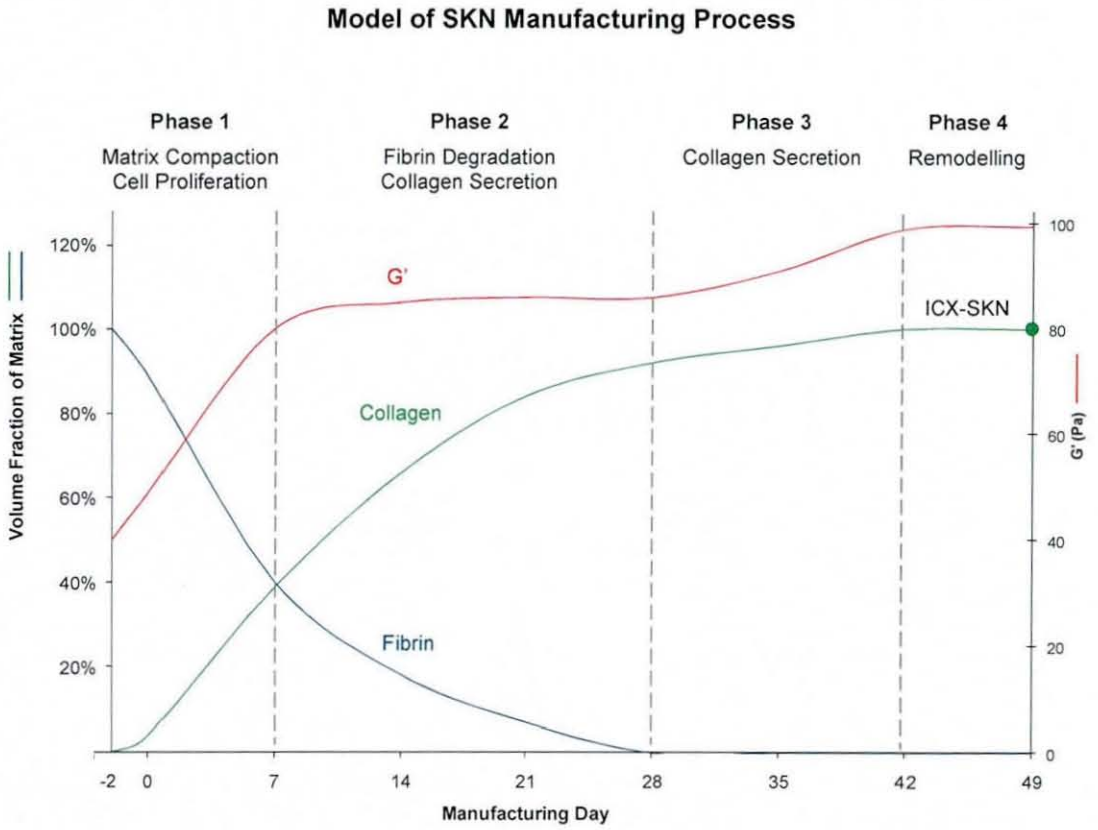

Figure 37 Improved model of the fibrin degradation (blue), collagen deposition (green) and elastic properties (red) of SKN during manufacturing

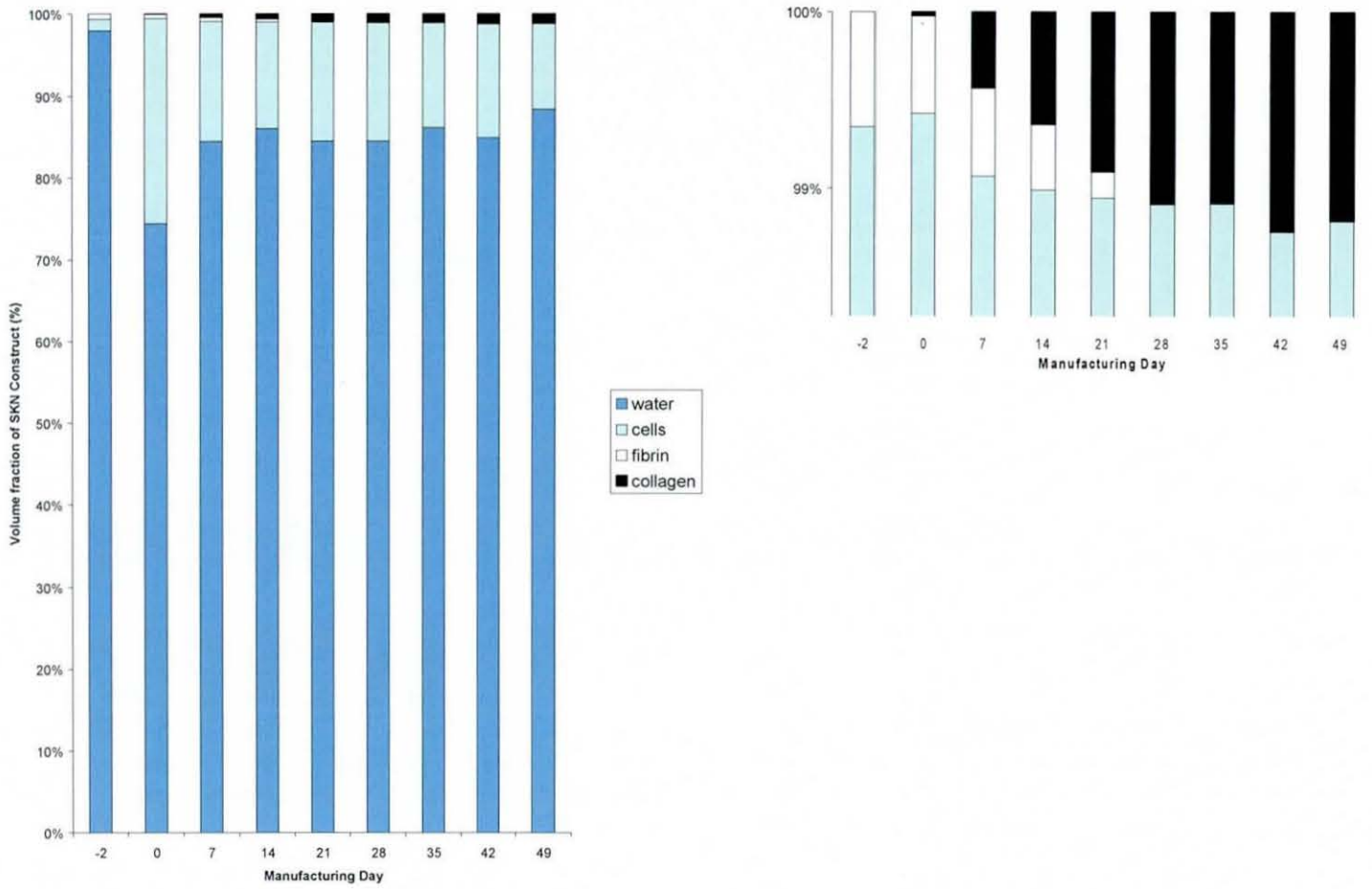

Figure 38 Estimated volume fraction of cells, water, fibrin and collagen in the SKN constructs (left). Enlarged chart of volume fraction between 99% and 100%

3.11. Further Work

Characterisation of the SKN constructs confirmed that the HDF cells were responsible for the changes in physical, biochemical and mechanical properties during the 49-day manufacturing process. Further research to investigate the effect of increasing the total number of cells in the SKN constructs through optimisation of the fibrin matrix formulation and supply of culture media is described in Chapter 7. It is hypothesised that increasing the number of cells in the construct will increase the rate of fibrin degradation and collagen synthesis and in turn improve the cost-effectiveness of the manufacturing process through a reduction in manufacturing time.

This study also provided an increased understanding showing the key phases of the manufacturing process and produced a semi-quantitative process model. Further improvements to this model can be achieved through development of assays to quantify collagen concentration, digestion rate and fibrin degradation rate in the SKN constructs and are discussed in Chapter 7. These areas of further work are important in the commercialisation of tissue-engineered products as firstly, cost-effective manufacture is required for profitable reimbursement of products. Secondly, quantification of key processing parameters allows measurement of the magnitude of improvement from process changes for cost-benefit analysis, measurement of the product properties for development of product specification and an improved understanding of the mechanisms of action of iterations of the product in-vivo.

Chapter 4 Ultrasound Stimulation of SKN Constructs

4.0. Introduction

This chapter investigates the use of ultrasound stimulation in the therapeutic range to improve the biochemical and mechanical properties of the SKN construct. In vitro, therapeutic ultrasound stimulation of tissue-engineered constructs for applications such as cartilage repair (Ebisawa, Hata et al. 2004) and intervertebral disc regeneration (O'Halloran, Pandit 2007) have been shown to increase collagen synthesis from cells and improve mechanical properties of the constructs. In-vivo, therapeutic ultrasound also been used to accelerate wound healing in bone (ter Haar 2007, Chang, Sun et al. 2002) and skin (Mendonça, Ferreira et al. 2006). However, the effect of ultrasound stimulation on tissue-engineered skin constructs or human dermal fibroblast cells seeded in a fibrin matrix has not been reported in the public domain.

The use of ultrasound as a form of mechanical stimulation has several key advantages compared to other forms of mechanical stimulation. These include firstly, the ability to couple the ultrasound transducer to the cellular constructs through liquid paths, such as the culture media. This is beneficial as other stimulation devices require physical coupling to the constructs which is problematic for SKN constructs as their gel-like properties make them susceptible to tearing at the physical point of application. Secondly, the wide availability of different sizes and shapes of ultrasound transducers and the ability to focus the ultrasound beam can provide homogeneous stimulation over the whole SKN construct. The ability to control the ultrasound output and potential for non-contact application provides a means of mechanical stimulation which is suitable for scale-up.

However, the optimum ultrasonic parameters required to elicit a positive biological response is not clear as it has also been reported that ultrasound does not accelerate wound healing in-vivo or promote collagen synthesis in-vitro (Duda, Kliche et al. 2004, Turner, Powell et al. 1989). There are numerous combinations of ultrasound parameters such as intensity, duty cycle and duration of stimulation that can be used for stimulation. It is likely that the ultrasound parameters required to promote desired

cellular responses are dependent on the type of tissue or cellular construct that is stimulated.

This chapter demonstrates the use of a screening design of experiments (DOE) methodology to investigate the effect of different combinations of ultrasound intensity, duty cycle and stimulation time on the collagen synthesis and the mechanical properties of SKN constructs. The use of ultrasound stimulation in the SKN manufacturing process to improve the properties of the SKN construct, based on the DOE results is discussed in Chapter 5.

4.1. Experimental Set-Up

Ultrasound stimulation in the therapeutic range was provided through a Sonoplus490 physiotherapy ultrasound unit (Enraf Nonius, Netherlands) which allowed control of the ultrasound intensity (I), duty cycle (DC), and stimulation duration (t). The ultrasound unit was calibrated at each duty cycle, over the full range of the transducer output power, using a radiation force balance (Farmery, Whittingham 1978) to determine the actual acoustic intensity at the transducer face (Appendix IV for calibration curve).

A custom-built ultrasound stimulation device was designed in collaboration with Dr.M.Mather, remedi Nottingham University and Mr.S.Hall, Biomedical Science Workshop, Nottingham University to couple the SKN constructs and ultrasound transducer for repeatable and reproducible stimulation of the constructs (Figure 39). The device comprised of a Teflon water column, stainless steel cradle with central cut-out and water tank lined with an ultrasound absorbing material (Aptflex F28, Precision Acoustics, UK). A clamp was designed to securely fix the transducer to the top of the water column. The ultrasound was coupled to the SKN constructs through a 0.6μm Teflon acoustic window at the base of the water column which was in turn coupled media above the constructs. The acoustic window was set at a distance of 100mm from the transducer face so that the SKN constructs were stimulated in the far field of the ultrasound beam where the pressure was the most homogeneous but least divergent (see Appendix IV for calculations).

The location pins on the water tank ensured that the culture dish, cradle and water column were centrally aligned to enable repeatable and reproducible ultrasound stimulation. The central cut-out in the cradle allowed the culture dish to contact the water in the water tank. This allowed propagation of the ultrasound away from the constructs and minimised the affects from undesired heating in the constructs. The ultrasound absorbing lining prevented the formation of standing waves between the water tank and SKN constructs which may have caused uncontrolled ultrasound stimulation.

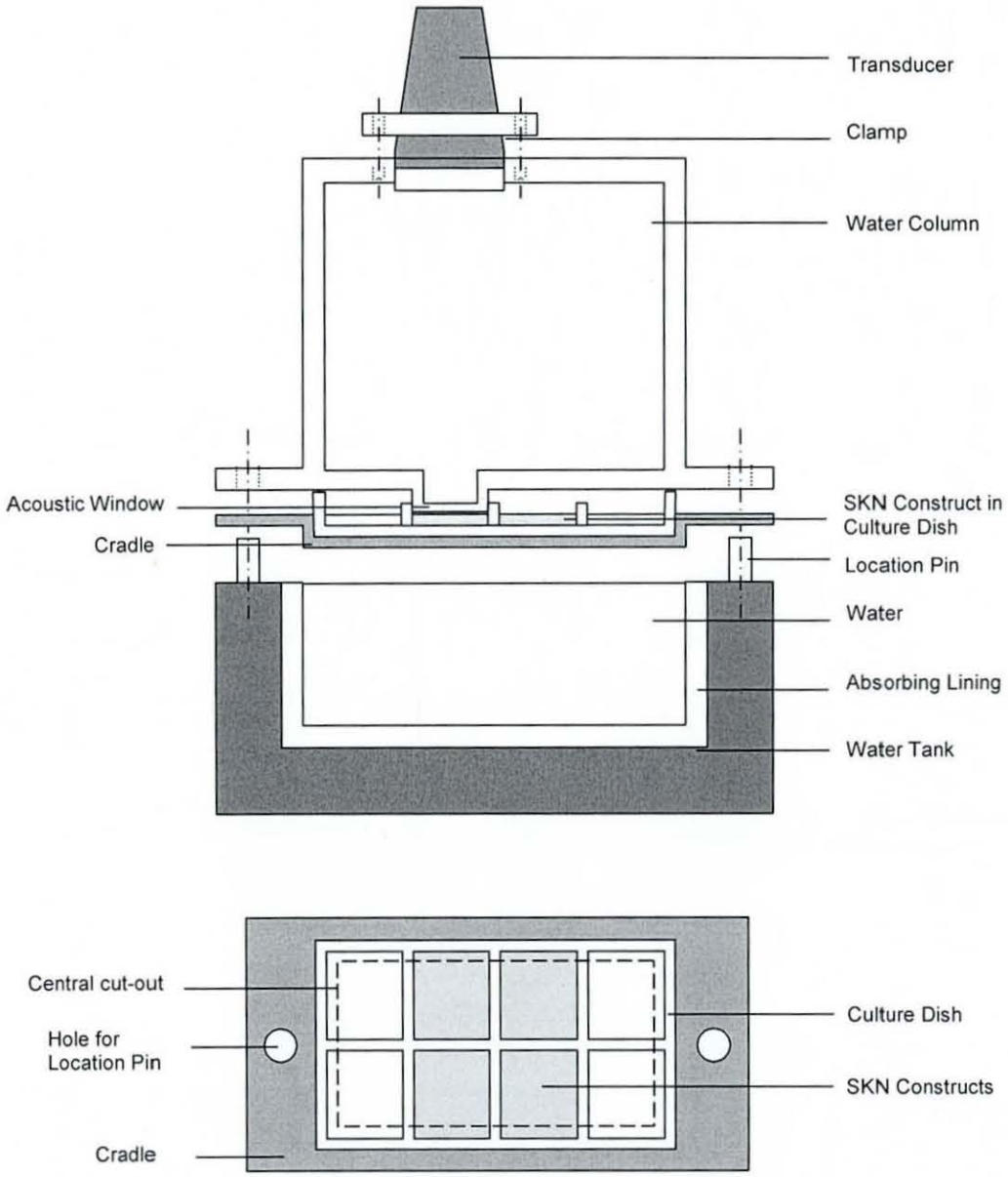

Figure 39 Top: Schematic of custom-built ultrasound stimulation device for SKN constructs Bottom: Plan view of cradle with cut-out (dashed lines) housing SKN constructs (grey) in central wells of culture dish

4.2. The Effect of Ultrasound on SKN Construct Properties

4.2.1. Screening Design of Experiment

Mintitab® 14 Statistical Software was used to generate a design of experiments (DOE) with 3 factors (ultrasound intensity, duty cycle and stimulation duration), 2 levels (maximum and minimum settings for each factor available on the ultrasound unit), one centre point (midpoint setting for each factor) and three replicates (n=3 SKN constructs). The minimum and maximum settings for the Sonoplus490 ultrasound unit were 0.5W/cm^2 and 2.5W/cm^2 intensity, 5% and 80% duty cycle, and 5 minutes and 30 minutes duration. The midpoint settings generated by the DOE were 1.5W/cm^2 intensity, 42.5% duty cycle and 17.5 minutes duration. However, 50% duty cycle and 18 minutes duration were used in this study as these were the closest settings available on the ultrasound unit. The ultrasound unit frequency of 1MHz was used in the experiments. The complete DOE with random run order is shown in Appendix IV and summarised in Table 15. Three SKN constructs were not stimulated by ultrasound and used as controls.

Sample I.D.			Intensity (W/cm^2)	Duty cycle (%)	Duration (mins)
2	6	25	2.5	5	30
13	17	18	2.5	5	5
3	8	10	2.5	80	5
1	14	16	2.5	80	30
5	9	21	0.5	5	5
7	19	23	0.5	5	30
4	15	22	0.5	80	5
12	20	24	0.5	80	30
11	-	-	1.5	50	18
26	27	28	0.0	0	18

Table 15 Summary of the DOE ultrasound parameters

4.2.2. Method

28 SKN constructs were cast in the central four wells of seven culture dishes (Figure 39). The water column and water tank were filled with sterile water 24 hours before each ultrasound stimulation session to allow the water to de-gas. A culture dish was placed in the cradle which was then placed on the water tank location pins so that the base of the culture dish was in contact with the water below. The transducer was clamped to the water column which was then placed on the water tank location pins so that the acoustic window was in contact with the media above the constructs. Care was taken to ensure that no bubbles formed between the base of the culture dish and the water in the water tank and between the acoustic window and the culture media to ensure homogeneous propagation of the ultrasound through the SKN constructs. The ultrasound parameters were set on the SonoPlus490 unit to stimulate the constructs. This was repeated for each construct in each culture dish and the control constructs for 18 minutes (the midpoint duration) with no stimulation.

Ultrasound stimulation was applied to the SKN constructs two days post casting and then prior to the media change every Monday, Wednesday and Friday to coincide with the current media feeding regime described in section 3.2.2. The media was changed after ultrasound stimulation was applied to each of the constructs in the culture dish. This was repeated for 21 days and the constructs were harvested two days after the last ultrasound stimulation on day 23 post casting.

4.2.3. Characterisation of the SKN Constructs

On day 23 (D23) a 10mm x 28mm section was cut from one end of the construct to form a $28mm^2$ square construct. Two 5mm x 5mm samples were then cut from the 10mm x 28mm section in a location that avoided edge effects from the culture dish. These samples were prepared for analysis by histology and SEM as described previously in sections 3.3.2 and 3.3.5 respectively. The shear storage modulus (G') and shear loss modulus (G") of the square constructs were analysed using a rheological strain sweep as described in section 3.5.1. The number of cells were counted using CEDEX after the rheological testing as described in section 3.4.1. Finally, statistical analysis of the combinations of ultrasound parameters that cause a significant effect on G' was carried out using the Pareto Chart of Standardised Effects in MiniTab® 14.

4.2.4. Results and Discussion

SKN construct samples 1-4 and 21-25 were removed from the study on day 18 due to the occurrence of bacterial contamination. At least one construct from each ultrasound group was not affected which allowed analysis of the DOE results to proceed (Table 16).

4.2.4.1. Cell Number

The total number of cells in the ultrasound stimulated constructs ranged between $3.4x10^6$ and $4.5x10^6$ cells compared to the control which had an average of $4.0x10^6$ (σ= $4x10^5$). The cell viability ranged between 93% and 96% for the ultrasound stimulated constructs compared to 97% in the control (Figure 40). No statistically significant differences in cell number were observed between the ultrasound groups (with n>1) and the control. These results suggested that ultrasound stimulation did not affect the total number of HDF cells in the SKN constructs which is supported by similar findings in other studies (Ebisawa, Hata et al. 2004, Nishikori, Ochi et al. 2002, Cui, Park et al. 2006). In addition, there was no correlation between the shear storage modulus (section 4.2.4.2) and the number of cells.

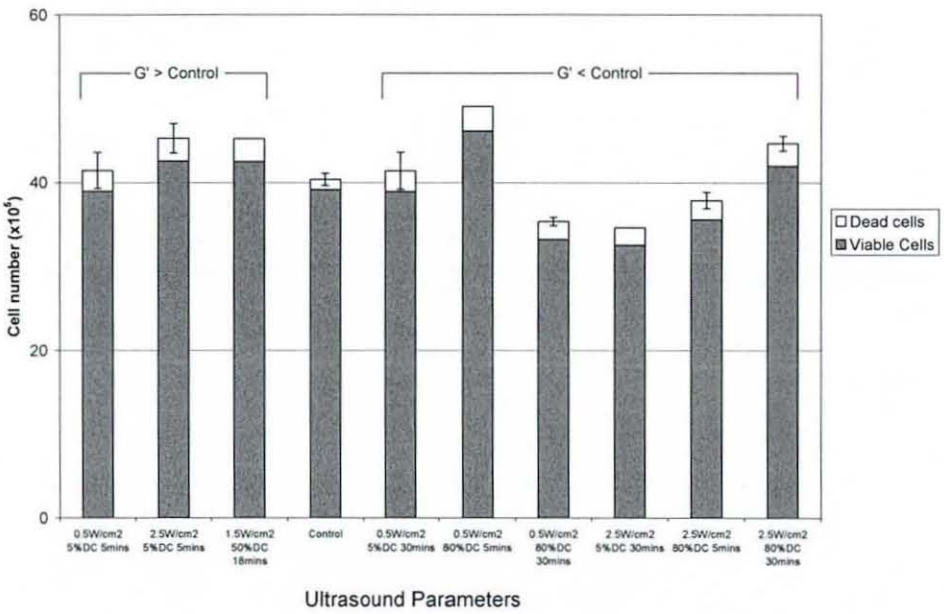

Figure 40 The average number of viable and dead cells in each group of ultrasound stimulated constructs compared to the control. Error bars represent 1 standard error of the total number of cells where n>1

4.2.4.2. Microstructure and Mechanical Properties

The Masson's Trichrome stained histological sections showed that the D23 control and ultrasound stimulated constructs were comprised of a collagen matrix (Figure 41). Intense collagen staining was observed around the cell membranes and thin inter-cellular collagen fibrils were present. The ultrasound combinations of 1.5W/cm^2 intensity, 50% duty cycle and 18 minute duration and the combinations of 5% duty cycle and 5 minute duration for both 0.5W/cm^2 and 2.5W/cm^2 intensity caused an increase in overall collagen staining and deposition of inter-cellular collagen fibrils (Figure 41 top). Higher magnification SEM images showed that these construct also had a denser matrix compared to the control (Figure 42 top). These observations were supported by measurement of the shear storage modulus (G') and the shear loss modulus (G") which were greater than the control by up to 139% and 165% respectively (Table 16).

In comparison, the other combinations of ultrasound parameters caused a decrease in collagen staining in the histological sections (Figure 41 bottom) and a decrease in matrix density shown in the SEM images (Figure 42 bottom). G' and G" for these constructs was up to 64% and 50% less than the control respectively (Table 16). However, the linear viscoelastic region was greater (0%-5% strain) for the constructs with a G' less than the control compared to the constructs with a G' greater than the control (0%-3% strain, Figure 43). This suggested that the combination of ultrasound parameters may have affected the attachment of the cells to the matrix, as describe in section 3.9.1, and that the ability of the HDF cells to adhere to the ultrasound stimulated constructs when subjected to shear deformation was less for the constructs with a greater G' than the control.

Sample			I (W/cm^2)	DC (%)	t (min)	Average G' (Pa)	Change G' (%)	Average G'' (Pa)	Change G'' (%)
11	~	~	1.5	50	18	251	139	34	165
5	9	21*	0.5	5	5	230	119	31	146
13	17	18	2.5	5	5	223	112	30	134
Control			**0**	**0**	**0**	**105**	**0**	**13**	**0**
12	20	24*	0.5	80	30	80	-23	12	-5
4	15*	22*	0.5	80	5	62	-41	9	-29
2	6*	25*	2.5	5	30	37	-64	6	-50
1*	14	16	2.5	80	30	72	-31	8	-36
7	19	23*	0.5	5	30	81	-23	8	-36
3*	8	10	2.5	80	5	75	-28	12	-7

Table 16 Average G' and G'' in the linear viscoelastic region and percentage change compared to the control for each combination of ultrasound parameters. Shaded area: matrix density greater than control. *removed from study on day 18 days due to occurrence of contamination.

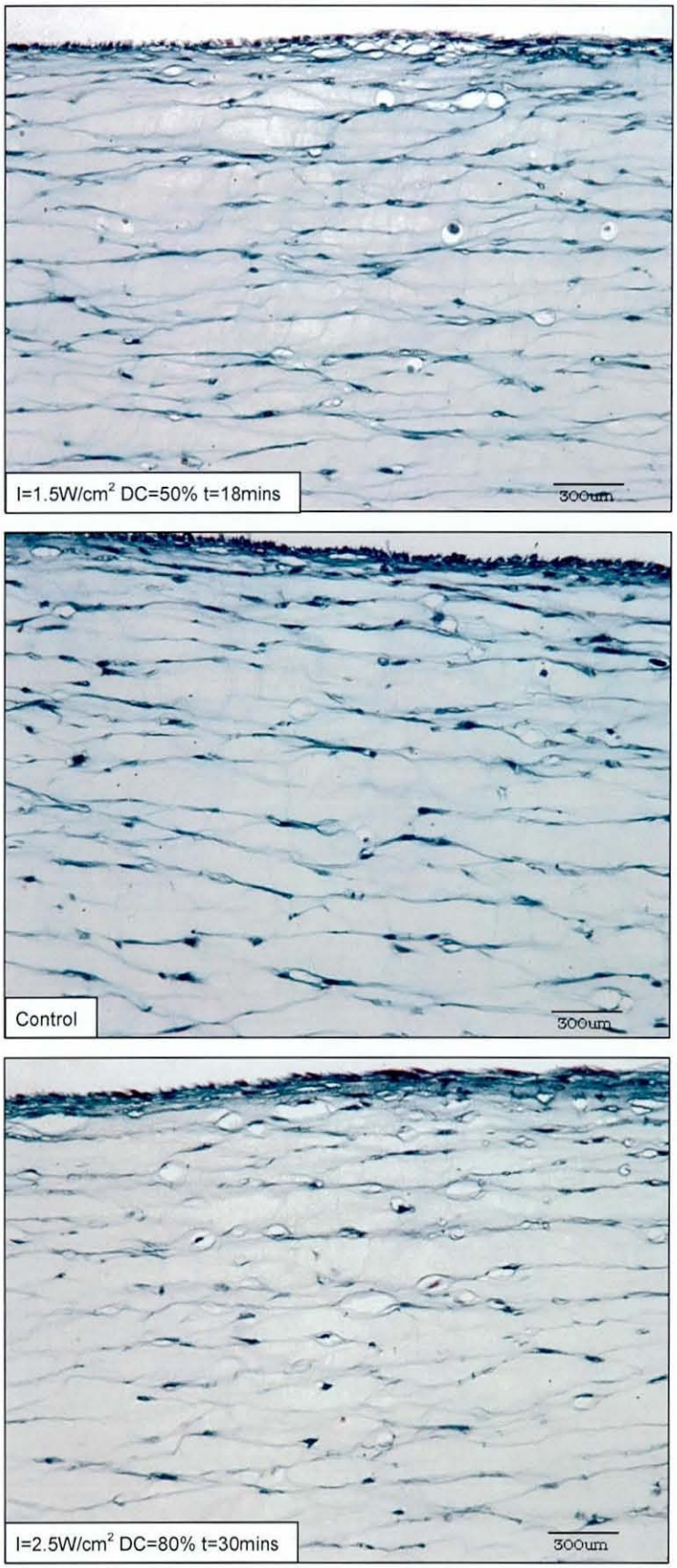

Figure 41 Examples of MT stained cross-section of SKN constructs with increased (top) and decreased (bottom) matrix density and concentration of inter-cellular fibrils compared to the control (middle). Collagen (blue), cell nuclei (dark blue). Ultrasound parameters on individual images

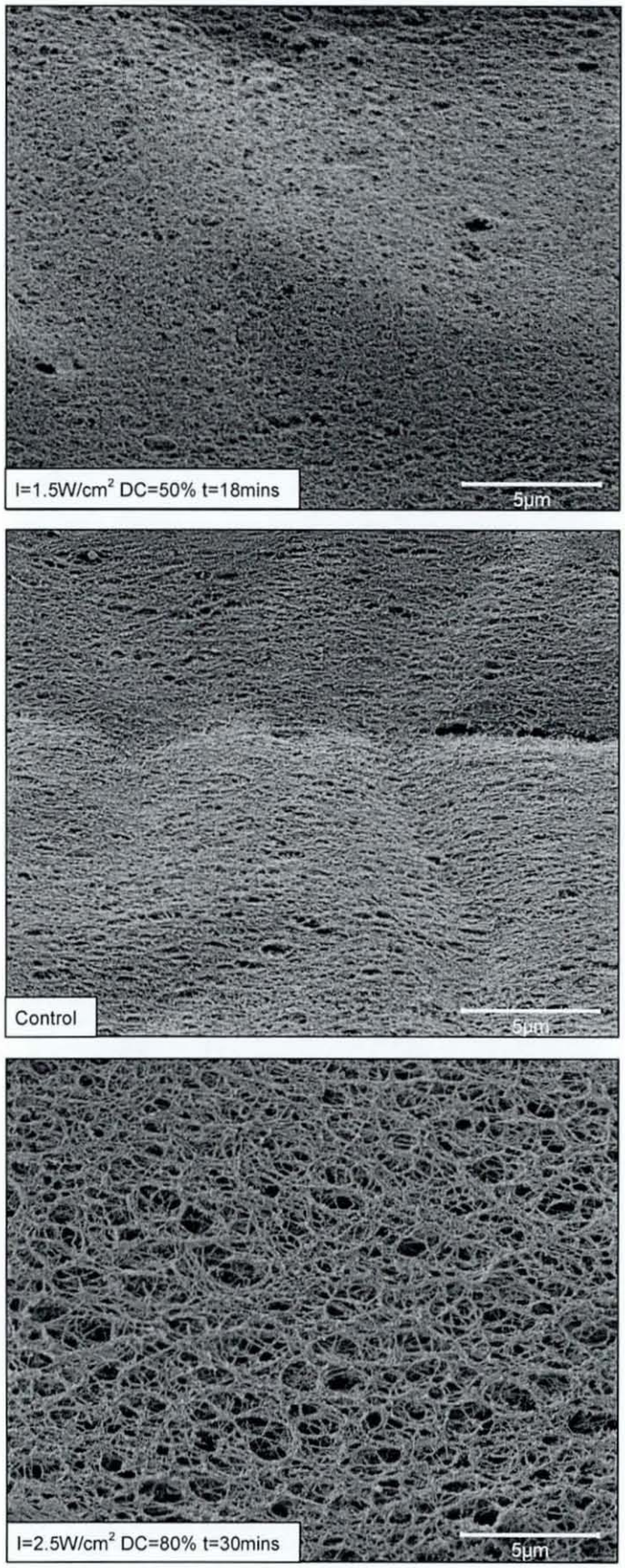

Figure 42 Examples of SEM Cross section of SKN constructs at 10000x magnification. Increased (top) and decreased (bottom) matrix density compared to control (middle). Ultrasound parameters on individual images

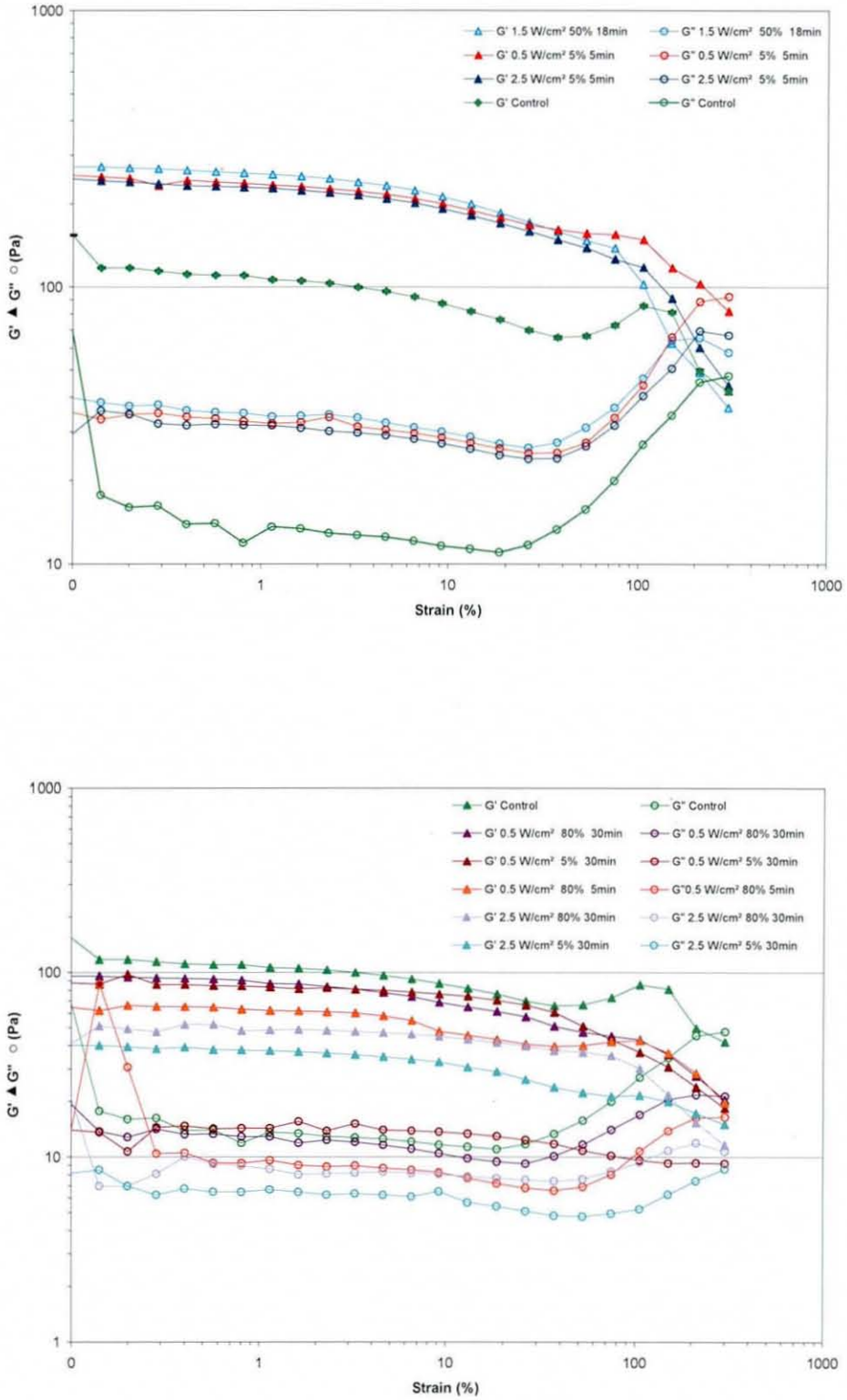

Figure 43 Average G' (▲) and G" (○) for each combination of ultrasound parameters greater (top) and less than (bottom) than the control (green line) with increasing strain

4.2.4.3. Effect of Ultrasound Intensity, Duty Cycle and Duration on G'

The Pareto Chart of Standardised Effects was used to determine the ultrasound parameters that had a significant effect on the shear storage modulus (G') through analysis of the results from each ultrasound group. The analysis showed that the combination of duty cycle and duration caused a statistically significant effect ($p<0.05$) on G' (Figure 44). However, individual factors and other combinations of intensity, duty cycle and duration did not have a significant effect.

The duty cycle controlled the time that the ultrasound was on and off in one ultrasound cycle and hence, the time that the HDF cells were stimulated and at rest. The duration controlled the total number of cycles that the HDF cells in the construct experienced. The ultrasound combinations using 5% duty cycle and 5 minute duration, and 50% duty cycle and 18 minute duration were previously shown to improve the biochemical and mechanical properties of the SKN constructs. The Sonoplus490 ultrasound unit produced a cycle length of 10ms (Enraf Nonius, Sonoplus490 User Manual) and therefore, application of caused the HDF cells in these construct to be subjected to a 0.5ms on, 9.5ms off cycle for $3x10^4$ cycles and 5ms on, 5ms off cycle for $10.8x10^4$ cycles for the respective combinations of duty cycle and duration (Figure 45).

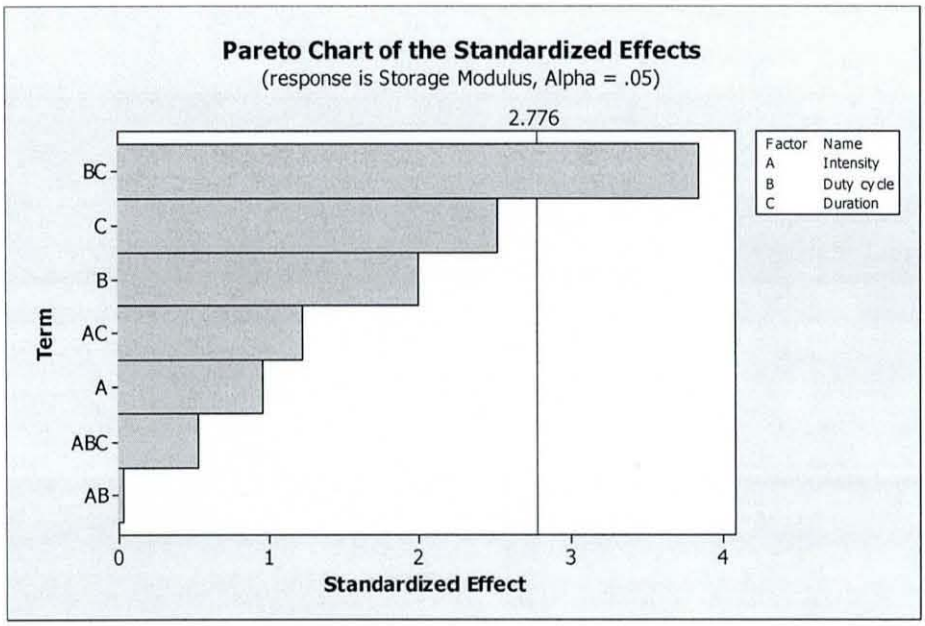

Figure 44 Combinations of ultrasound parameters with a significant effect on the shear storage modulus of SKN constructs

			Cycle Time (ms)		
Duty Cycle (%)	Duration (min)	Total no. cycles (x10^4)	On	Off	Total time (s)
5*	5*	3.0	0.5	9.5	15
5	30	18.0	0.5	9.5	90
80	5	3.0	8.0	2.0	240
50*	18*	10.8	5.0	5.0	540
80	30	18.0	8.0	2.0	1440

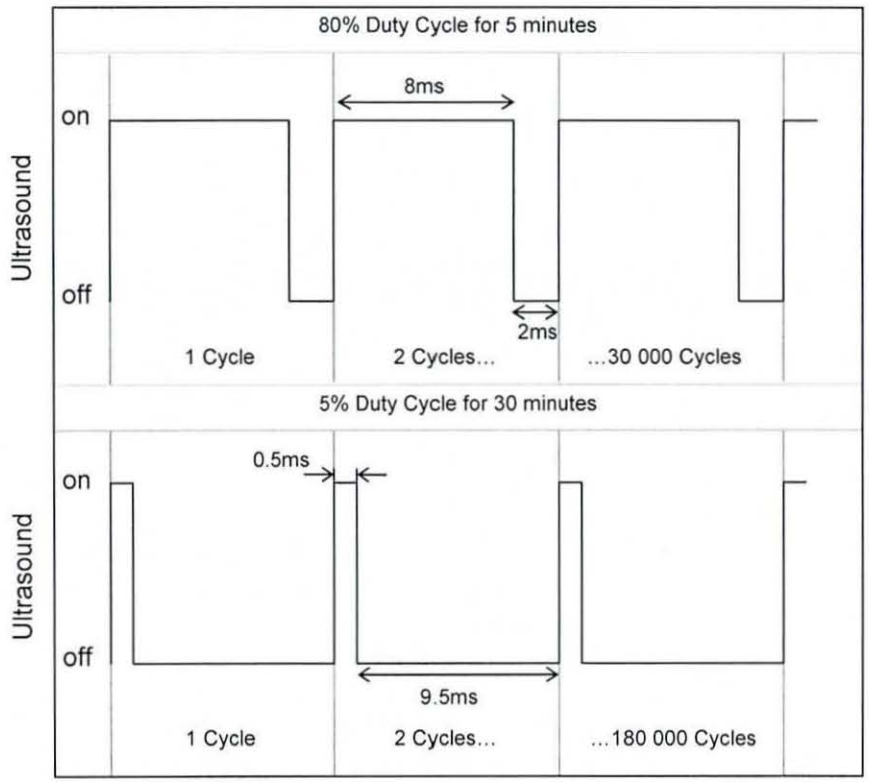

Figure 45 Top: Relationship between the combination of duty cycle and duration and the ultrasound stimulation (on) and rest (off) cycle and number of cycles experienced by the HDF cells in the SKN construct. Bottom: Schematic of the ultrasound pulse for two combinations of duty cycle and duration

In addition The SKN constructs subjected to 80% duty cycle (8ms on and 2ms off) resulted in a lower G' than the control regardless of the total number of pulses. Similarly, subjecting the cells to a total of $18x10^4$ pulses (30 minute duration) regardless of the duty cycle caused a G' less than the control. In contrast, the SKN constructs subjected to 5% duty cycle (0.5ms on, 9.5ms off) for 5 minutes ($3x10^4$ pulses) and the midpoint settings of 50% duty cycle (5ms on, 5ms off) for 18 minutes ($10.8x10^4$ pulses) resulted in a greater G' than the control (Figure 46). These results suggested that combinations of duty cycles between 5% and 50% and the stimulation durations between 5 minutes and 18 minutes could increase the properties of the SKN constructs. In comparison, duty cycles and durations greater than 80% and 30 minutes respectively caused a decrease in the properties of the SKN constructs.

Since the SonoPlus490 ultrasound unit used in this study has a limited selection of duty cycles (5%, 10%, 20%, 50%, 80% and 100%), further investigation into improvements in the SKN construct properties is limited to combinations of duty cycle between 5% and 50% (Figure 46). A custom-built ultrasonic system would be required to investigate the affect of combinations of duty cycle between 50% and 80% (Figure 46).

Significantly, the total time that the ultrasound was stimulating the constructs (calculated by multiplying the time the ultrasound was "on" by the total number of pulses) did not correlate with changes in the shear storage modulus (Figure 45). The total stimulating time for the constructs with a G' greater than the control ranged between 15 seconds and 540 seconds but ranged from 90 seconds to 1440 seconds for constructs with a G' less than the control. This showed that the stimulation and rest cycle and number of cycles rather than the total stimulation time was responsible for causing a significant cellular response.

Finally, the application of different combinations of stretching and relaxation cycles on the ultimate tensile strength (UTS) of myofibroblast seeded fibrin gels subjected to cyclic distension (Isenberg, Tranquillo 2003) also supported the results in this study. In particular, duty cycles of less than 12% improved the ultimate tensile strength (UTS) and collagen synthesis compared to duty cycles greater than 40% which decreased the UTS compared to the non-stimulated control. However, this study did not investigate the effect of the combinations of duty cycle and duration which have been shown to be significant in this study.

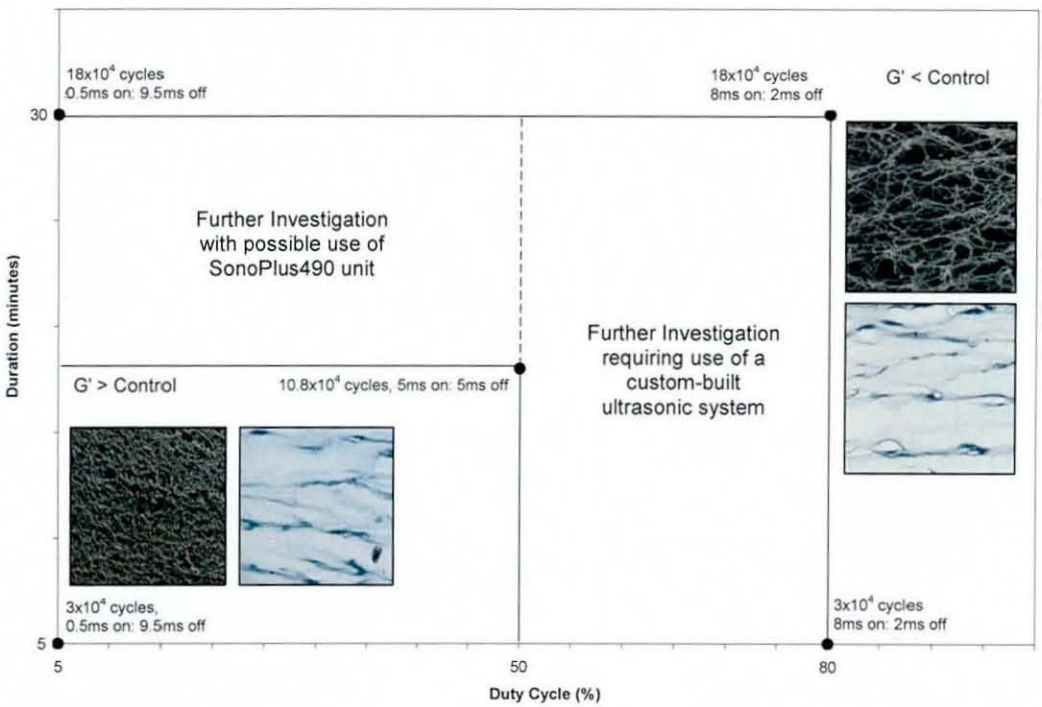

Figure 46 Summary of results and combinations of duty cycle and duration for further investigation for maximising the improvement of SKN construct properties. Inserts: SEM and histology cross-sections of SKN construct for G'>control and G'< control

4.2.5. DOE Conclusion

This study demonstrated the use of a Design of Experiments (DOE) methodology to investigate the effect of ultrasound stimulation on the biochemical and mechanical properties of the SKN constructs. The DOE methodology enabled efficient investigation of the effect of the combinations and range of ultrasound parameters compared to the affect of single parameters which is commonly reported.

This study showed that ultrasound stimulation can be used to influence the microstructure of the SKN constructs by stimulating or inhibiting the quantity of collagen synthesised from cells and degree of inter-cellular collagen deposition. The changes in the microstructure were supported by measurements of the shear storage (G') and shear loss (G") modulus. Significant changes in G' were caused by the combination of duty cycle and duration which were related to the ultrasound stimulation-rest cycle and number of cycles to which the cells were subjected. Ultrasound stimulation did not affect the total number of cells in the construct which suggested that the changes in the microstructure and viscoelastic properties were primarily a result of the quantity of collagen secreted by each cell. The DOE results identified the range in which the different combinations of ultrasound parameters could be used to improve the properties of the SKN construct and are further investigated in Chapter 5.

Chapter 5 Ultrasound Stimulation for Improvement of SKN Construct Properties

5.0. Introduction

This chapter describes the use of ultrasound stimulation to further improve the properties of the SKN constructs. The design of experiments study identified the range and combinations of ultrasound parameters that increased the shear storage modulus (G') of the SKN constructs. The equation for calculation of G' was derived using the response optimiser function in MiniTab® 14 and is:

$$G' = 275 + 0.13 \text{ (Duty Cycle * Duration)}$$

The ultrasound parameters of 1.5W/cm^2 intensity, 42.5% duty cycle and 17.5 minute duration were calculated to maximise G'. A duty cycle of 50% instead of 42.5% was used in the following experiments as it was the closest available setting on the ultrasound unit. The duration used was decreased to 14 minutes to account for the change in the duty cycle. Non-stimulated control constructs were characterised on day 0 (D0), day 23 (D23) and day 49 (D49) of the manufacturing period and ultrasound stimulated constructs on D23. The effect of ultrasound on the SKN construct properties was compared between D0 and D23. The D23 ultrasound stimulated constructs were compared with the D49 control constructs produced by the current manufacturing process to assess the use of ultrasound for improvement of the biochemical and mechanical properties.

5.1. Method

24 SKN constructs were cast as a batch in the centre four wells of six culture dishes. 18 constructs were randomly chosen as controls and six of these constructs were harvested for characterisation on D0, D23 and D49 respectfully. The remaining six constructs were stimulated by ultrasound, using the parameters stated in section 5.0, for 21 days and harvested on D23, as described in section 4.2.2. Three sections (approximately 5mm x 10mm) were cut from the centre of one SKN construct from each of the ultrasound stimulated and control groups. The cut samples were prepared for SEM, TEM (D23 construct only), histology staining with Masson's Trichrome (MT) and Alcian blue, and IHC for detection of collagen type I and III (Figure 47) as described in sections 3.3.2 to 3.3.6.

The viscoelastic properties (G' and G") of the remaining constructs from each group (n=5) were measured using the rheological strain sweep as described in section 3.5.1. Following rheological testing the constructs were placed in 2mL of 0.28U/mL of collagenase B, for measurement of the digestion time and the total number of cells as described in section 3.4.1. The dry weight of the constructs was then determined by freeze drying the collagenase digest for 96 hours and the digestion rate calculated by dividing the digestion time by the dry weight. This was repeated for 2 batches of SKN constructs labelled 2005 and 2010 (batch reference number).

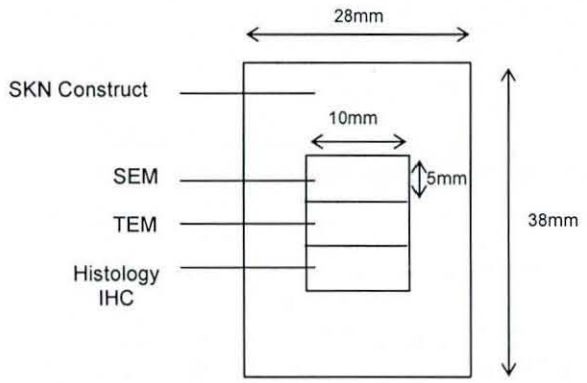

Figure 47 Schematic of sections cut from SKN construct for characterisation by light and electron microscopy

5.2. Results

The quantitative results for the D0, D23, D49 control constructs and the D23 ultrasound stimulated constructs are summarised in Table 17 and discussed in the following sections.

	D0 (n=10)	D23 Batch 2005 (n=5)		D23 Batch 2010 (n=5)		D49 (n=10)	D23 DOE Midpoint Settings (n=1)
	Control	Control	Ultrasound	Control	Ultrasound	Control	Ultrasound
Average G' (Pa)	65	117	202	118	185	137	239
Average G'' (Pa)	7	19	33	19	30	21	34
Total number of cells ($x10^6$)	1.54	6.68	7.26	5.78	7.54	3.70	4.52
Average Dry Weight (g)	0.17	0.31	0.32	0.30	0.33	0.44	No data
Average Digestion rate (mg/min)	1.46	1.60	1.47	1.43	1.42	3.29	No data

Table 17 Summary of ultrasound improvement experimental results compared to the DOE midpoint setting results

5.2.1. D0 Control Construct

The D0 SKN constructs for both the 2005 and 2010 batches were similar in composition and structure. The quantitative data reported for the D0 constructs is the combination of the data from both batches (n=10). Masson's Trichrome staining of the D0 SKN construct confirmed that the matrix was comprised of fibrin (Figure 48 left). Higher magnification SEM images showed that the D0 construct was comprised of a highly cross-linked matrix of fibrils surrounding the cells (Figure 48 right). The G' and G" of the D0 construct was 65Pa (σ= 8) and 7 Pa (σ= 1) respectively which was similar to the values reported for D0 constructs in section 3.9.1. The cell viability (Figure 49) was 95% and total number of viable cells in the construct was $1.54x10^6$ (σ= $9.7x10^4$). The average dry weight of the construct was 0.17g (σ= 0.02) and average digestion rate was 1.46mg/min (σ= 0.12) as shown in Figure 56.

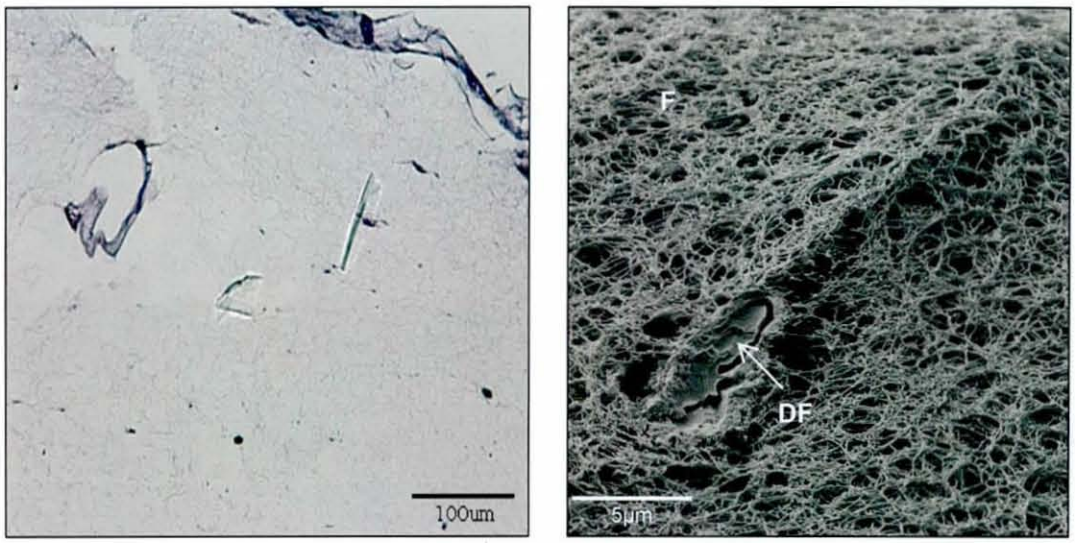

Figure 48 Cross-section of D0 SKN construct. Left: MT stained section with fibrin matrix (purple) and cell nuclei (dark purple). Right: 10 000x magnification SEM image with human dermal fibroblast cells (DF) embedded in a highly cross-linked fibrin matrix (F)

5.2.2. D23 Control and Ultrasound Stimulated SKN Constructs

5.2.2.1. Cell Number and Viability

The viability for both the ultrasound stimulated and control SKN constructs ranged between 91% and 95%. The total number of viable cells in the D23 ultrasound stimulated constructs was $7.2x10^6$ (σ= $7.8x10^5$) and $7.5x10^6$ (σ= $6.9x10^5$) cells for the 2005 and 2010 batches respectively compared to 6.6 $x10^6$ (σ= $3.5x10^5$) and 5.7 $x10^6$ (σ= $4.7x10^5$) cells in the respective control samples (Figure 49). However, there was no statistically significant difference between the total number of cells in the control and ultrasound stimulated constructs which supported the DOE findings (section 4.2.4.1).

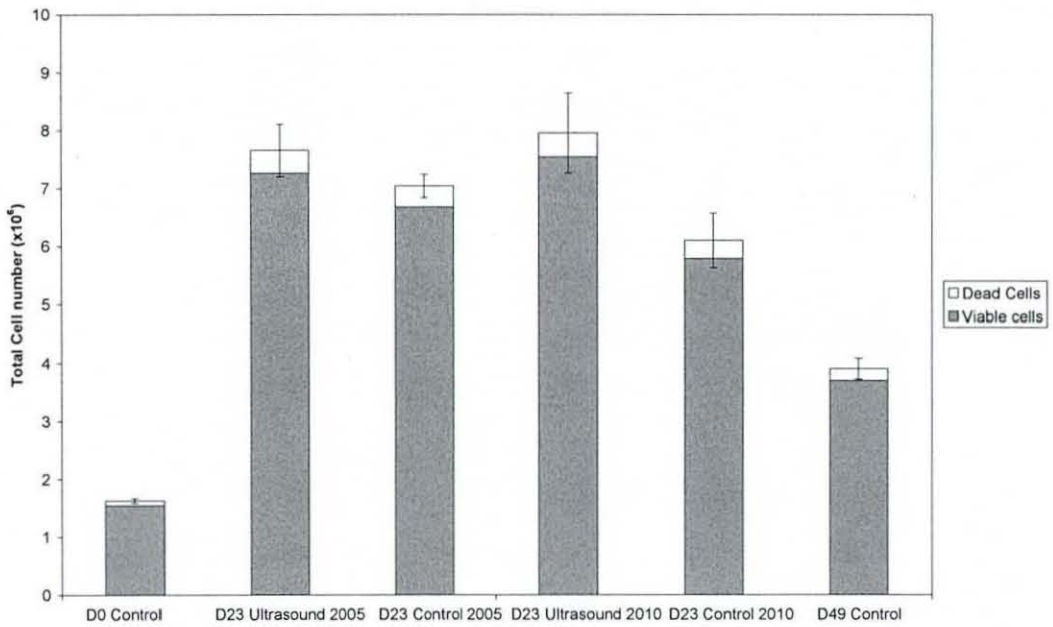

Figure 49 Comparison of the number of viable and dead cells in the D0 (n=10), D23 (n=5), D49 (n=10) control and D23 (n=5) ultrasound stimulated constructs for the 2005 and 2010 batches. Error bars represent 1 standard error of the total number of cells

5.2.2.2. Microstructure and Mechanical Properties

The Masson's Trichrome stained histology sections showed that the ultrasound stimulated and control constructs were comprised of both collagen and fibrin on D23 (Figure 50) in comparison to the D0 construct which was comprised of fibrin only. The ultrasound stimulated constructs had more staining for collagen and in particular, more inter-cellular collagen fibrils compared to the control (Figure 50). More intense collagen staining was observed around the cell membranes for both constructs. However, more voids inside of these areas of denser staining were observed in the ultrasound stimulated constructs. Fibrin which stained purple was predominantly observed at the top of both the control and ultrasound stimulated constructs.

The IHC sections showed that only collagen type I was present in both the ultrasound stimulated and control constructs on D23 and that more collagen type I was present in the ultrasound stimulated constructs (Figure 52). Collagen type III was not observed in the control or ultrasound stimulated constructs. This is in contrast to the previous observations on D21 discussed in section 3.7.3 where both collagen type I and type III were present. The histology sections stained with Alcian Blue showed that proteoglycans were present in the ultrasound stimulated constructs but not in the control (Figure 51) which supported the findings of other authors that ultrasound stimulated cells to secrete proteoglycans (Hsu, Kuo et al. 2006, Miyamoto, An et al. 2005, Iwashina, Mochida et al. 2006).

Higher magnification SEM images showed that a layer of cells had formed at the construct-media interface of the ultrasound stimulated and control constructs (Figure 53 top row). The matrix density was greater around the membranes of the cells which supported the histological observations (Figure 53 middle row). The ultrasound stimulated constructs appeared to have a denser matrix than the control constructs and areas of thicker fibres which, may have been formation of collagen fibril bundles (Figure 53 bottom row).

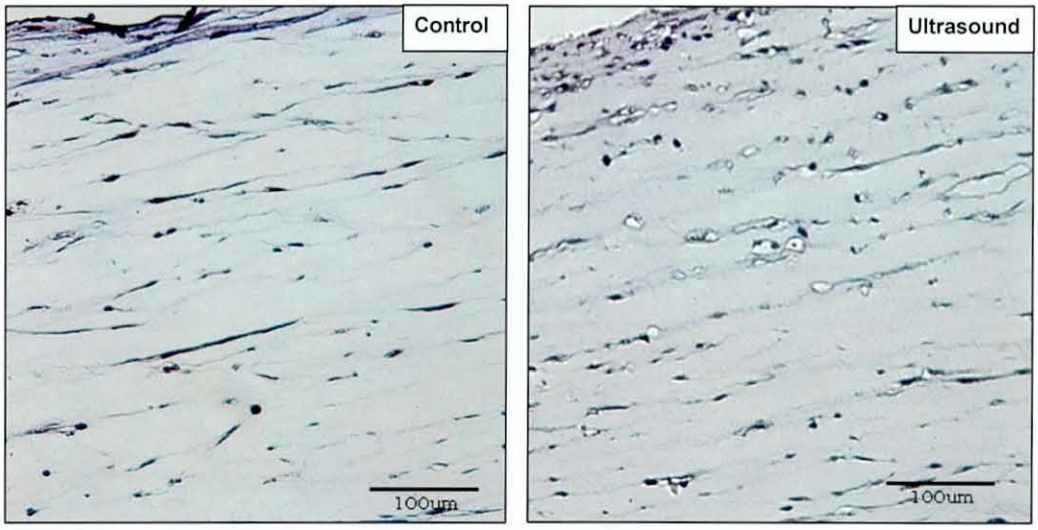

Figure 50 MT stained cross-sections of D23 control (left) and ultrasound stimulated (right) SKN constructs. Collagen (blue), fibrin (purple) and cell nuclei (dark purple)

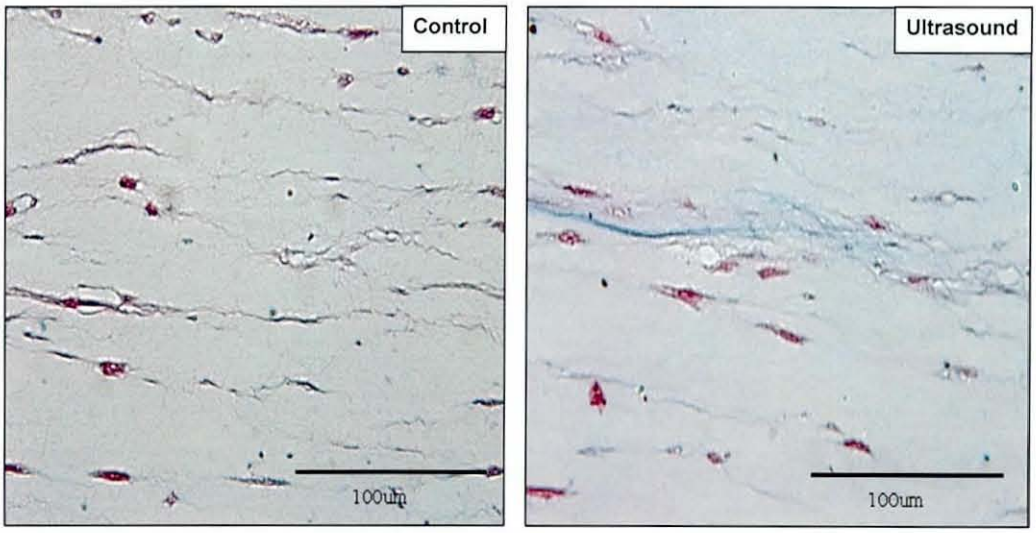

Figure 51 Alcian blue stained cross-sections of D23 control (left) and ultrasound stimulated (right) SKN constructs. Proteoglycans (blue), other cytoplasmic areas (purple) and cell nuclei (red)

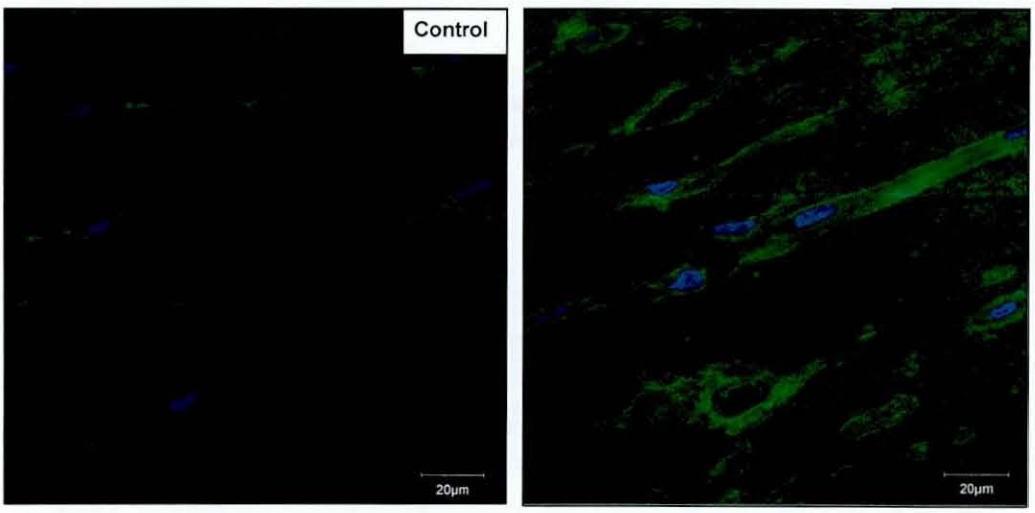

Figure 52 Immunohistochemistry cross-sections of D23 control (left) and ultrasound stimulated (right) SKN constructs. Collagen type I (green), cell nuclei (blue)

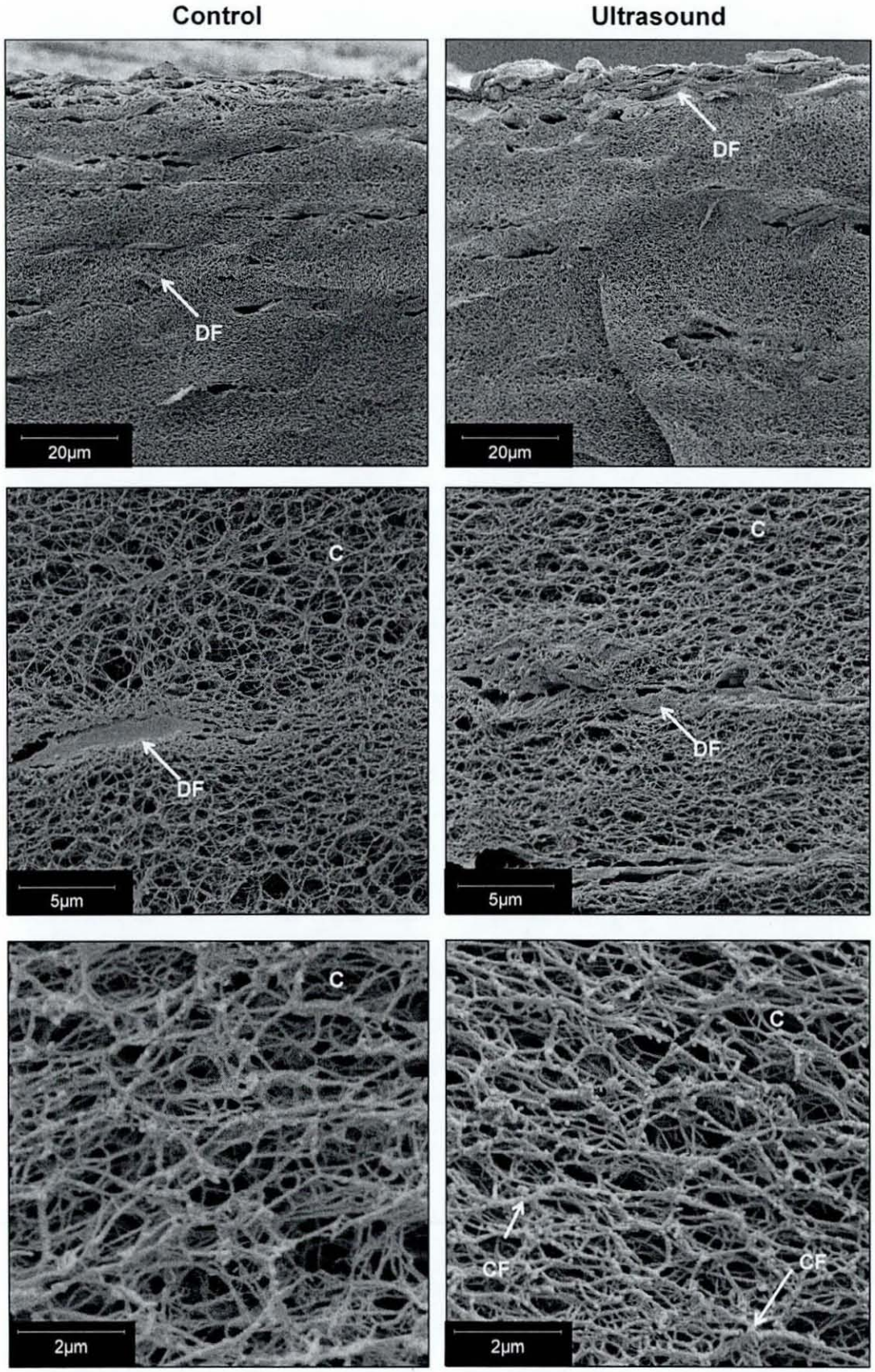

Figure 53 SEM cross-sections of D23 control (left column) and D23 ultrasound stimulated (right column) SKN constructs. Top: x2500. Middle: x10000. Bottom: x30000. CF=collagen fibril bundle, DF = Dermal fibroblast and C= collagen matrix

Measurement of the shear storage modulus (G') and shear loss modulus (G") supported the structural observations. Comparison of the D0 control construct and D23 control and ultrasound stimulated constructs showed that G' increased by approximately 81% for the control constructs but by 211% (2005 batch) and 185% (2010 batch) for the ultrasound stimulated constructs (Figure 55).

Comparison of the D23 control and ultrasound stimulated construct strain sweep showed that for both the 2005 and 2010 batches, the linear viscoelastic region for the shear storage modulus (G') and shear loss modulus (G") was between approximately 0% and 20% (Figure 54). G' and G" in the ultrasound stimulated constructs were greater than the control constructs up to 90% strain for both the 2005 and 2010 batches and the cross-cover point of G' and G" was similar at approximately 120% strain (Figure 54). The contribution of the cells to the viscoelastic properties and the effect on cell detachment from the matrix on G' has been discussed previously (section 3.9.1). These results suggested that this combination of ultrasound parameters did not affect the strain at which the cells detached from the matrix but did increase the degree of cross-linking and/or quantity of collagen in the constructs. These findings are supported by other studies which have also shown that ultrasound stimulation increased collagen secretion from and cells and correlated with an increase in the mechanical properties of chrondocyte seeded in a collagen sponge in-vitro and rat Achilles tendon in-vivo (Takeuchi, Ryo et al. 2008, Yeung, Guo et al. 2006).

In the linear viscoelastic region, the G' of the ultrasound stimulated constructs was 202Pa compared to the control of 117Pa and equated to a 72% ($p=0.013$) increase for the 2005 batch. The control construct in the 2010 batch had a similar G' of 118Pa and this increased by 56% ($p=0.02$) to 185Pa with ultrasound stimulation (Figure 55). Similarly, G" increased by 73% ($p=0.01$) and 59% ($p=0.02$) for the 2005 and 2010 batches respectively. For both batches of constructs, the G' and G" of the ultrasound stimulated constructs had a greater standard deviation (σ= 42Pa for G' and σ= 6.3Pa for G") compared to the control (σ= 8Pa for G' and σ= 1.6Pa for G") which suggested that the ultrasound stimulation process introduced variation into the SKN manufacturing process.

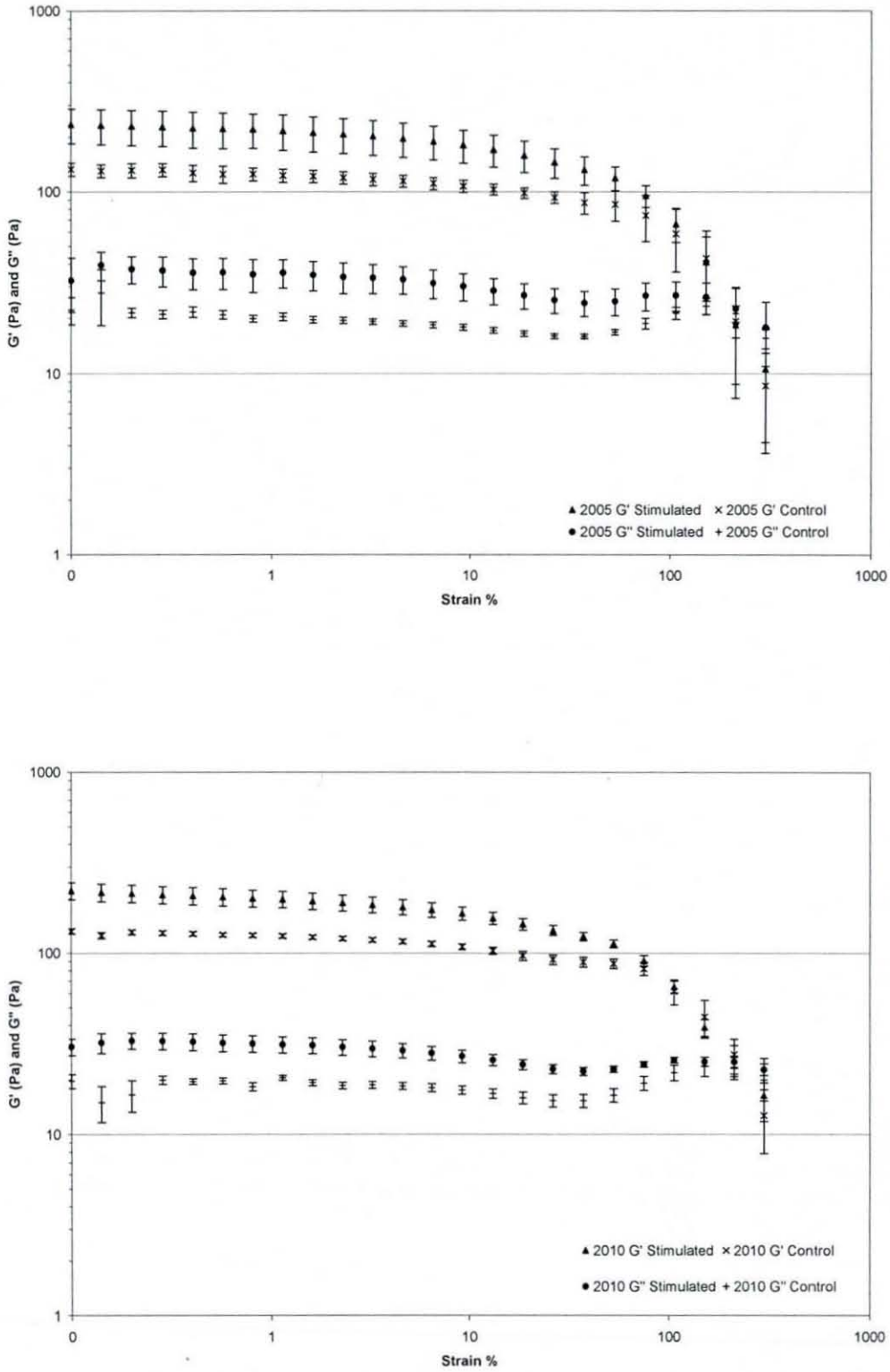

Figure 54 Viscoelastic properties G' and G" of control and ultrasound stimulated SKN constructs with increasing strain for batch 2005 (top) and batch 2010 (bottom). Error bars represent 1 standard error (n=5)

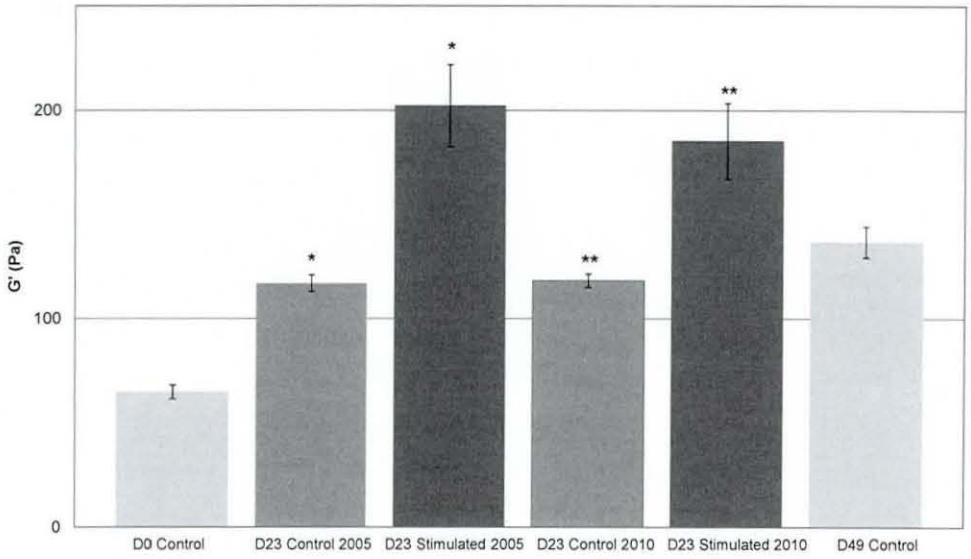

Figure 55 Comparison of G' in the linear viscoelastic region of D0 (n=10), D23 (n=5) and D49 (n=10) control SKN constructs and D23 (n=5) ultrasound stimulated constructs for the 2005 and 2010 batches. Error bars represent 1 standard error. * p=0.013, **p=0.02

5.2.2.3. Dry Weight and Digestion Rate

The average dry weight of the D23 control and ultrasound stimulated constructs increased between D0 and D23. For the control constructs the dry weight increased by 84% (2005 batch) and 78% (2010 batch). For the ultrasound stimulated constructs the dry weight increased by 89% (2005 batch) and 100% (2010 batch). However, comparison of the dry weight of the D23 control and ultrasound stimulated constructs was not conclusive. The average dry weight of the ultrasound stimulated constructs was greater than the control for both batches (Figure 56 top) but only significantly different by 3% ($p=0.04$) for the 2005 batch.

No significant difference in digestion rate between D0 and D23 control and ultrasound constructs was observed and supported the findings of the characterisation study (section 3.8.1). This suggested that ultrasound stimulation did not significantly increase the rate of fibrin degradation or collagen synthesis to alter the degree of cross-linking in the constructs during this period. Comparison of the D23 control and ultrasound stimulated constructs showed that the average digestion rate of the ultrasound stimulated constructs was slightly lower than the control (Figure 56 bottom). However, these results were not statistically different for either batch. These results did not support the observations of increased collagen synthesis and cross-linking discussed previously (section 5.2.2.2). However, the digestion assay may not have sufficient resolution to detect changes in the degree of cross-linking between the control and ultrasound SKN constructs on D23 as it is reliant on operator judgement as discussed in section 7.2.

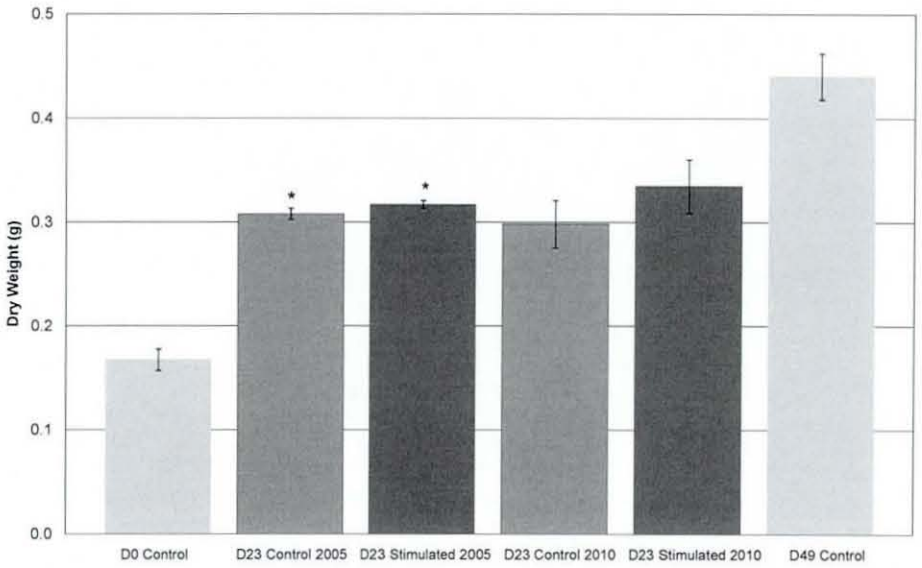

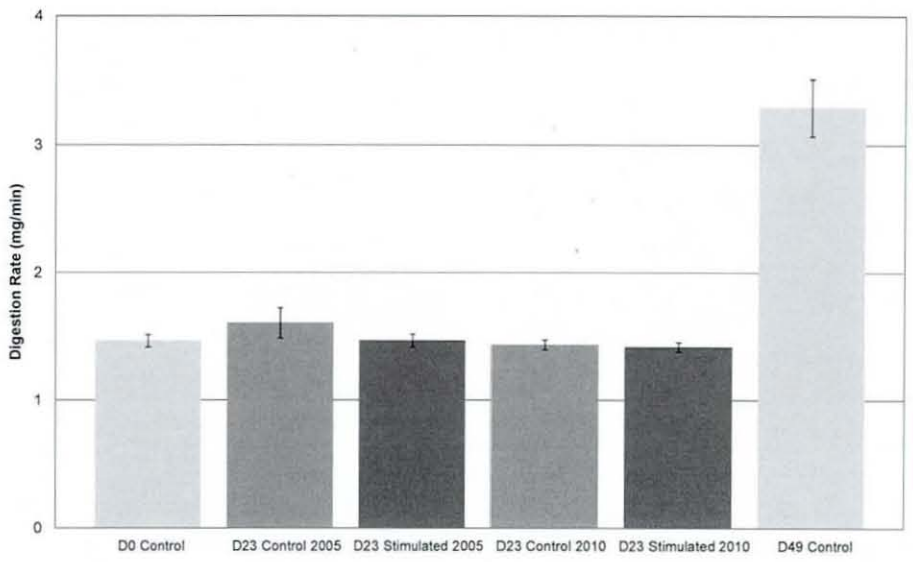

Figure 56 Comparison of D0 (n=10), D23 (n=5) and D49 control (n=10) and D23 ultrasound stimulated (n=5) SKN constructs. Top: Dry weight. Bottom: Digestion rate. Error bars represent one standard error. * p=0.04

5.2.3. Comparison of D23 Ultrasound Stimulated Constructs and D49 Controls

The D49 SKN constructs for both the 2005 and 2010 batches were similar in composition and structure. The quantitative data reported for the D0 constructs is the combination of the data from both batches (n=10). The D23 ultrasound stimulated constructs appeared to have more inter-cellular collagen fibrils (Figure 57) and a denser matrix (Figure 58) compared to the D49 constructs. This was supported by a 123% (p=0.000) and 131% (p=0.000) increase in the digestion rate of the D49 construct compared to the 2010 and 2005 ultrasound stimulated constructs respectively (Figure 56 bottom). This suggested that ultrasound stimulation caused an increase in cross-linking in the constructs.

These results also correlated with a 35% (p=0.047) and 48% (p=0.027) increase in G' for the 2010 and 2005 ultrasound stimulated batches respectively (Figure 55). However, the dry weight of the D49 constructs was 38% (p=0.02) and 33% (p=0.01) greater than the D23 ultrasound stimulated constructs (Figure 56). This suggested that ultrasound stimulation of SKN constructs for 21 days resulted in increased cross-linking in the D23 constructs but did not increase the quantity of collagen synthesis by the cells compared to the D49 control. These results are in contrast to the SEM and histology images and the greater G' of the ultrasound stimulated constructs compared to the D49 control. The reason for the contrasting results is unknown but a possible explanation may be that the total number of viable cells in the D49 constructs decreased by approximately 40% compared to the D23 constructs. This may have resulted in a greater volume fraction of the D49 construct to be occupied by a less dense collagen matrix compared to the D23 ultrasound stimulated constructs.

It was suggested that by D49 the biochemical composition and mechanical properties of the construct were sufficient for supporting the cells in the culture dish and less cells were required to maintain the construct matrix (section 3.10). Application of ultrasound stimulation to the SKN constructs for 49 days would demonstrate the effect of sustained mechanical signalling on cell proliferation as well as collagen deposition compared to the D49 SKN constructs produced by the current manufacturing process.

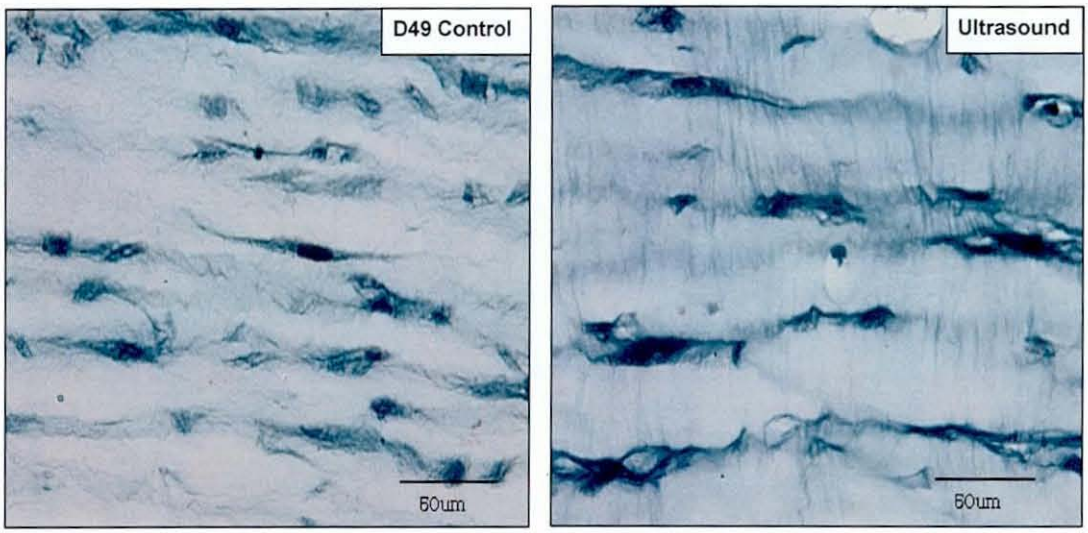

Figure 57 MT stained cross-sections of SKN constructs with collagen (blue) and cell nuclei (dark blue) Left: D49 Control. Right: D23 Ultrasound stimulated

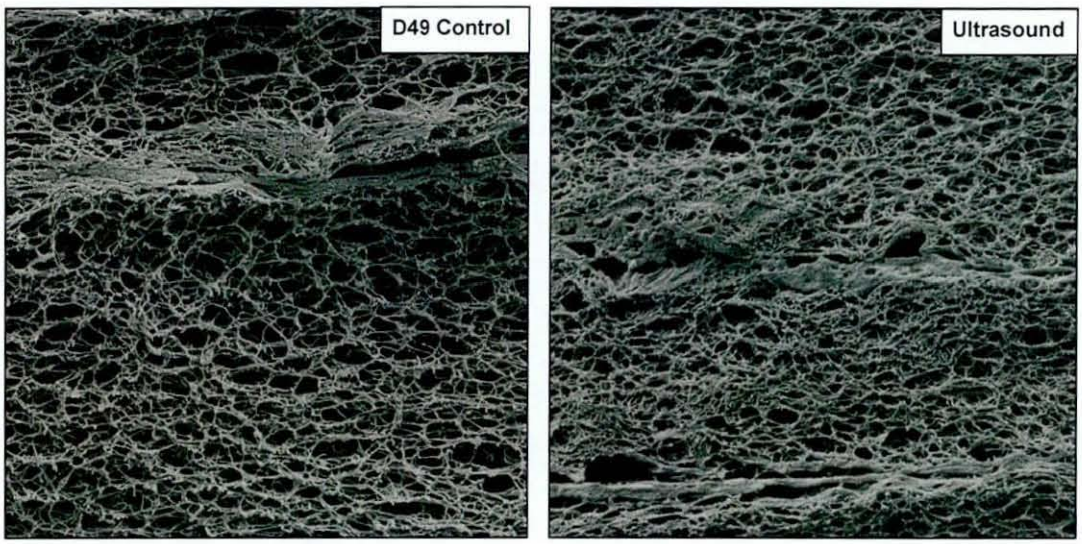

Figure 58 Comparison of SEM cross-section of D49 control (left) construct and D23 ultrasound stimulated (right) SKN construct

5.2.3.1. Fibroblast Ultrastructure

The TEM images showed that the live fibroblast cells in the D23 control construct had a smooth plasma membrane, extensive endoplasmic reticulum, long mitochondria and several secretory vesicles (Figure 59a). These features suggested that the cell was actively secreting collagen. It is known that procollagen molecule chains are assembled in the endoplasmic reticulum and packaged into vesicles in the Golgi apparatus. These vesicles then move to the plasma membrane where the content is discharged (Ghosh 2002, Fawcett 1994). In addition, the long mitochondria function to provide usable chemical energy for processes such as protein synthesis (Sadava 1993).

In comparison, the fibroblast cells in the ultrasound stimulated constructs had many blebs on the cell membrane (protrusions from the cell membrane), dilated endoplasmic reticulum, many vacuoles and secondary lysosomes (Figure 59b). The dilated endoplasmic reticulum and vacuoles have previously been observed in fibroblasts stimulated with hormones that up-regulated collagen synthesis (Lupulescu 1974). Also, similar differences in the morphology of the plasma membrane have been shown to be caused by mechanical stimulation in fibroblast seeded collagen constructs (Lee, Lin et al. 1993). However, the presence of numerous secondary lysosomes is characteristic of apoptosis (Formigli, Papucci et al. 2000, Kulkarni 1994). This suggested that the cells had been mechanically stimulated by ultrasound but may also be undergoing apoptosis by D23.

In the control and ultrasound stimulated constructs cell shrinkage away from the surrounding matrix, a characteristic feature of cell apoptosis (Formigli, Papucci et al. 2000, Kulkarni 1994), was also observed in some cells (Figure 59c and d). In the ultrasound constructs, cell necrosis was also observed (Figure 59d) which is characterised by an electron-translucent nucleus, disruption of the plasma membrane and cytoplasmic discharge (Formigli, Papucci et al. 2000, Kulkarni 1994, Tinari, Giammarioli et al. 2008). These results showed that the ultrasound parameters used in this experiment caused premature cell death as well as stimulating collagen synthesis from the cells.

The presence of dead cells in the SKN constructs is not a major concern as the SKN constructs are freeze dried for storage in subsequent steps of the manufacturing process. However, premature cell death by necrosis may reduce the that rate of collagen synthesis in the SKN constructs as there will be a smaller population of viable cells that can secrete collagen.

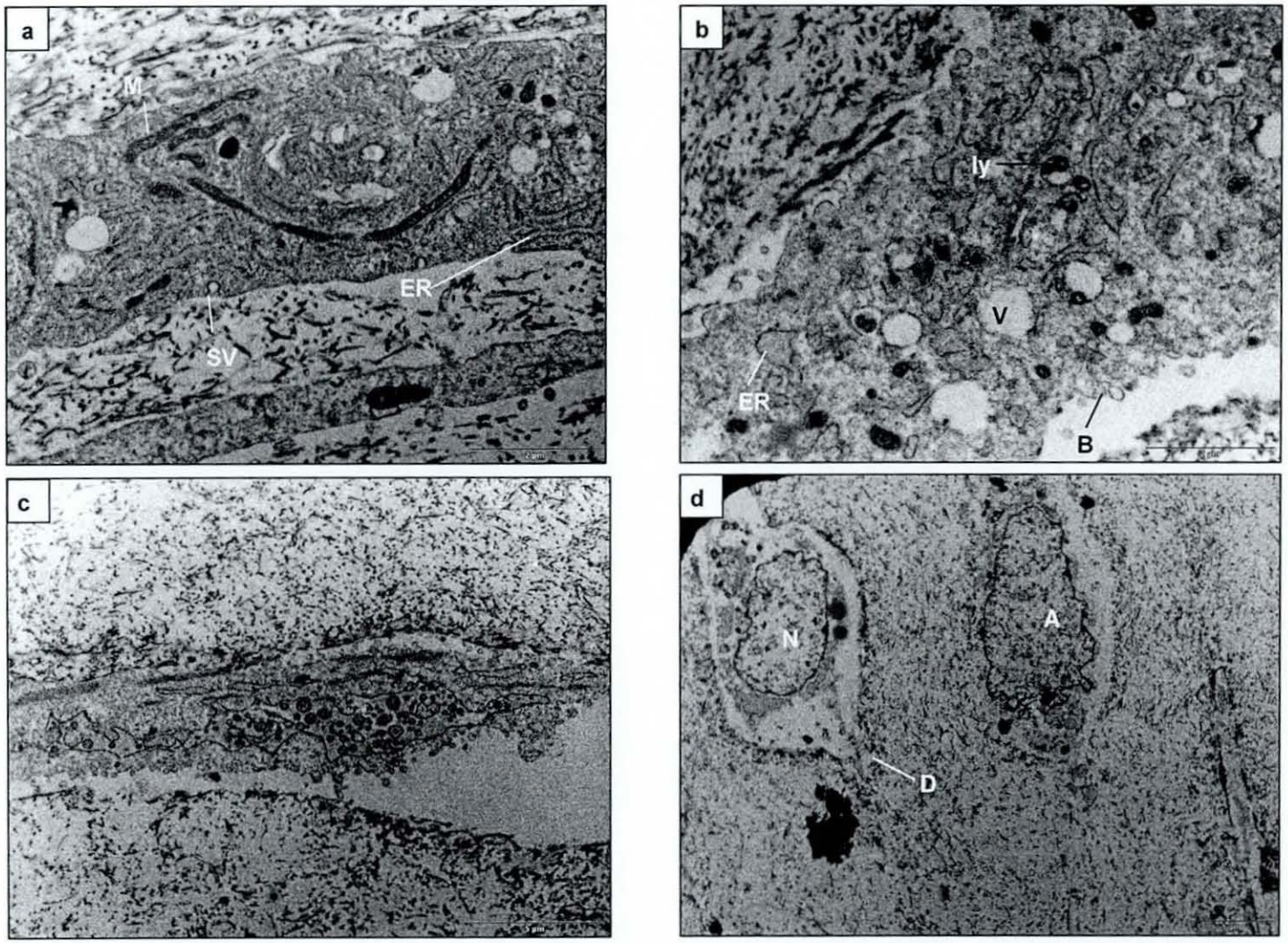

Figure 59 TEM Cross-sections SKN constructs. a: Live cell in control construct with a smooth plasma membrane, extensive endoplasmic reticulum (ER), long mitochondria (M) and secretory vesicles (SV). B: Live cell in ultrasound stimulated construct with many blebs (B) on the plasma membrane, dilated endoplasmic reticulum (ER) many vacuoles (V) and secondary lysosomes (ly). c: Apoptotic cell in control construct shrinking away from the matrix. d: Apoptotic (A) and necrotic cell (N) with cytoplasmic discharge (D) in ultrasound stimulated construct

5.3. Conclusion

Ultrasound stimulation of the SKN constructs for 21 days at 1.5W/cm^2 intensity, 50% duty cycle and 14 minute duration caused a significant increase in the shear storage modulus (G') and in shear loss modulus (G") compared to the non-stimulated D23 control constructs. A 72% (p=0.013) and 56% (p=0.02) increase in G' and 73% (p=0.01) and 59% (p=0.02) increase G" was observed for the 2005 and 2010 batches respectively. Qualitative observations of the histological and SEM images suggested that the increase in viscoelastic properties was due to an increase in collagen and inter-cellular fibril deposition. However, comparison of the number of cells, dry weight and digestion rate showed that there was no significant difference between the ultrasound stimulated and control constructs apart from a 3% (p= 0.04) increase in the dry weight of the 2005 batch. There was also no significant difference between the number of cells in the construct. This suggested that ultrasound stimulation did not promote cell proliferation and that the increases in G' and G" were not associated with the number of cells in the constructs.

Comparison of the D23 ultrasound stimulated and D49 control constructs showed that ultrasound stimulation could be used to improve G' and G" of the SKN constructs through an increase in collagen cross-linking in the matrix. This was demonstrated by the significant increase of 123% (p=0.00) and 131% (p=0.00) in digestion rate of the D49 constructs compared to the 2005 and 2010 batches respectively of the D23 ultrasound stimulated constructs. However, ultrasound stimulation for 21 days did not increase the quantity of collagen in the matrix compared to the D49 construct as the dry weight of the D49 construct was 38% (p=0.02) and 33% (p=0.01) greater than the D23 ultrasound stimulated constructs for the 2005 and 2010 batches respectively.

It was also shown that the ultrasound parameters used for product improvement (1.5W/cm^2 intensity, 50% duty cycle for 14 minutes) caused premature cell death by necrosis. Further understanding of the mechanisms by which ultrasound causes necrosis would improve the selection of the ultrasound parameters so that cell viability can be maintained during the manufacturing period. A reduction in cell necrosis may lead to an increase in total collagen synthesis or the rate of collagen synthesis.

Further experiments are required to monitor the effect of ultrasound on viscoelastic properties, quantity of extracellular matrix and cross-linking over the 49 day manufacturing period. This would firstly provide an insight into the magnitude of improvement in SKN construct properties that could be achieved using ultrasound stimulation. Secondly, ultrasound was applied 3 times/week for 3 weeks in this study. Further work is required to determine the frequency of each ultrasound session and the duration of the manufacturing period over which ultrasound would maximise improvement in SKN construct properties. This may in turn lead to improvement of the efficiency of the manufacturing process through a reduction in manufacturing time.

5.3.1. Variation Caused by the Ultrasound Stimulation Process

Ultrasound stimulation of the SKN constructs improved the mechanical properties of the constructs but also increased the variation in the mechanical properties compared to the control. The design of the ultrasound stimulation device was such that the alignment of the ultrasound transducer and the SKN constructs was repeatable for every ultrasound session. The most probable cause of the variation was the output from the ultrasound transducer itself and the homogeneity of the propagation of ultrasound through the SKN constructs due to localised variations in the cell density and extracellular matrix. Further work to reduce the variation in the ultrasound stimulation process, through improvements to the ultrasound stimulation system and mapping of ultrasound propagation through the SKN constructs, is discussed in section 7.4.

5.3.2. Improvement of Ultrasound Parameters

This experiment used ultrasound parameters of 1.5W/cm^2 intensity and 50% duty cycle for 14 minutes and caused an increase in G' of up 72%. In comparison, the midpoint settings used in the DOE of 1.5W/cm^2 intensity and 50% duty cycle for 18 minutes resulted in an 165% increase in G' (Table 17). The 50% duty cycle used in both experiments related to an ultrasound stimulation-rest cycle of 5ms on and 5ms off. However, the extra 4 minute duration used in the DOE increased the number of cycles the cells were subjected to by 29%. This suggested that for a 50% duty cycle, and increase in G' through an increase in collagen secretion and cross-linking could be achieved by increasing the number of ultrasound cycles to which the constructs were subjected.

However, comparison of the SEM images from the DOE and improvement studies showed that the matrix of the control construct from the DOE study was denser than the control matrix in the improvement study (sections 4.2.4.2 and 5.2.2.2 respectfully). The differences between these batches may have also affected the cellular responses caused by the ultrasound. Therefore, further work to investigate the source of the batch-to-batch variation in the current process and procedures to minimise the variation is first required, and is discussed in section 7.3.

In summary, ultrasound stimulation can be used to improve the shear storage and shear loss modulus of the SKN constructs through an increase in collagen cross-linking. The ultrasound stimulation caused increased variation in the viscoelastic properties of the construct which is likely to be caused by fluctuations in the transducer output. The ultrasound stimulation regime can be further improved to increase the biochemical and mechanical properties of the SKN constructs but batch-to-batch variation in the current manufacturing process must first be controlled.

Chapter 6 Conclusion

6.0. Integration of Biological Science and Process Engineering

The regenerative medicine industry is redirecting its focus from scientific research to translation of the research into commercially viable products (Mason 2007). There are many commercial issues which need to be met such as, regulatory, financial and supply chain, as well as building upon the 25 years of scientific research in this field (Mason 2007, Kemp 2006). A key challenge is the development of cost-effective manufacturing processes that allows sufficient income from reimbursement and implementation of good manufacturing practice (GMP) standards to satisfy regulatory requirements of repeatable product manufacture to predetermined specifications. Continuous product improvement to exceed customer and stakeholder expectations is also necessary for the realisation of routine use of regenerative medicine products in patients.

In this thesis, the value of the integration of biological research with manufacturing and process engineering principles in the development of ICX-SKN constructs was demonstrated. ICX-SKN is a dermal skin substitute for the treatment of acute wounds currently being developed by healthcare company Intercytex. ICX-SKN aims to provide an alternative to the current gold standard treatment of skin grafting, eliminate the need of a donor graft site and reduce surgical time and cost. Phase I clinical trials demonstrated the safety of ICX-SKN and provided preliminary evidence of efficacy in-vivo (Boyd, Flasza et al. 2007). However, further understanding of the processes that occur during manufacture of ICX-SKN was required to identify areas of process and product improvement. In this thesis, the constructs were produced using bovine fibrinogen instead of human fibrinogen for cost-effective research and were denoted SKN constructs.

The first part of this thesis provided an increased understanding of 49 day manufacturing process through characterisation of the changes in the biochemical, mechanical and physical properties of the SKN construct and lead to identification of areas for process improvement. The second part of this thesis demonstrated the use of ultrasound stimulation in the manufacturing process to make a step-change in the properties of the SKN constructs for product improvement.

6.1. Improved SKN Manufacturing Process Model

The characterisation study in this thesis identified four phases in the SKN manufacturing process. Between D-2 and D7, the manufacturing process was dominated by HDF cell proliferation (397%) and matrix compaction (50%), and there was evidence of fibrin degradation and collagen synthesis. Between D7 and D28, cell proliferation and matrix compaction ceased and the main processes were fibrin degradation and collagen synthesis shown by relatively constant measurements of dry weight (13.9±1mg), digestion time (110±10minutes) and shear storage modulus (72.5±6.5Pa). Between D28 and D42, fibrin degradation ceased and collagen synthesis continued which was shown by significant increases in dry weight (16%, $p=0.002$), digestion time (48% $p=0.002$) and shear storage modulus (33%, $p=0.006$), and observations of increased matrix density in the light and electron microscopy sections. Finally, between D42 and D49, the dry weight, digestion time and shear storage modulus appeared to reach a plateau suggesting that remodelling of the matrix had begun or that the biochemical composition and mechanical properties of the matrix were sufficient to support the cells in the culture dish. Changes in the physical, biochemical and mechanical properties of cellular fibrin gels have not been previously reported over a 49 day week period.

6.2. Development of Characterisation Techniques for Tissue-Engineered Constructs

The characterisation of tissue-engineered products with gel-like properties is problematic as they are generally fragile to handle and are composed of more than 50% water and less extracellular matrix when compared to tissue. Characterisation techniques and methodologies were developed for such constructs in this thesis and demonstrated using SKN constructs. The methodologies developed for the preparation of the SKN constructs for structural characterisation by light and electron microscopy enabled observation of the constructs with minimal damage to the native structure. The shear storage modulus (G') and shear loss modulus (G") provided quantitative data to support the observed, qualitative structural changes and also reflected the physical and biochemical changes that occurred during manufacturing. In particular, G', representative of the elastic properties of the SKN constructs, correlated with the quantity of extracellular matrix and degree of cross-linking in the matrix as well as the degree of construct compaction.

In addition, the novel application of automated, real-time, non-contact, non-destructive measurement systems was also demonstrated in this thesis. Precision surface profiling was shown to provide models for the compaction of cellular constructs over the whole surface compared to single point measurements previously reported (Robinson, Johnson et al. 2008). The potential use of Raman spectroscopy to determine the changes in biochemical composition of the SKN constructs during manufacturing was also demonstrated and has not been used for this application for tissue-engineered constructs previously.

Further development of such non-contact, non-destructive techniques would be beneficial in the development and commercialisation of tissue-engineered products. The key benefits include the ability to monitor the properties of a large sample of each batch of products during manufacturing. This would provide an increased understanding of the batch-to-batch and within batch process variation, identify areas for process improvement and minimise the production of out of specification product. In addition, the cost-effectiveness of research and product testing would be improved through a reduction in samples required for destructive testing.

6.3. Batch-to-Batch Variation

In the current SKN manufacturing process, greater batch-to-batch variation was observed in the structure, shear storage modulus and total number of HDF cells of the non-stimulated SKN constructs compared to within batch variation (section 5.3.1). This suggested that there was variation in the process inputs and in particular, variation in the activity of the cell population, components of the culture media and structure of the fibrin matrix. Further work to control the pre-processing of the raw material inputs and development of robust measurement systems to test the materials prior to use in the manufacturing process and is discussed further in sections 7.2 and 7.3. This work is important as it may lead to a reduction in the variation manufacturing process and final product and aid compliance with GMP standard of repeatable manufacture of product to predetermined specifications.

6.4. DOE Methodology to Determine Cellular Responses to Ultrasound Stimulation

The use of ultrasound stimulation in-vivo to accelerate wound healing and in-vitro to improve the properties and functionality of tissue-engineered constructs has been shown to produce both positive and negative results (Mendonça, Ferreira et al. 2006, Tsai, Pang et al. 2006, Takeuchi, Ryo et al. 2008, Noriega, Mamedov et al. 2007, Turner, Powell et al. 1989). Comparison of the contrasting results was problematic due to the large range of ultrasonic parameters used and the variations in response associated with the type of cells, matrix composition and tissues stimulated. This thesis demonstrated the use of a design of experiments (DOE) methodology to efficiently determine the range of each ultrasound parameter and the significant combinations of parameters which elicited desired biological responses from the HDF cells in the SKN constructs. The use of such a methodology minimised the need for iterative experiments and reduced the labour time and costs which would be beneficial in an industrial setting.

The DOE results showed that the combination and magnitude of the ultrasound parameters affected the total quantity of collagen and deposition of inter-cellular collagen fibrils in the SKN constructs but did not affect the total number of cells. In comparison to the non-stimulated controls, the shear storage modulus was increased by up to 139% and decreased by up to 64% using different combinations of ultrasound parameters within the range of the physiotherapy ultrasound unit used in this study. This suggested that therapeutic ultrasound could be used to promote or inhibit the amount of collagen secreted by each HDF cell in the SKN construct.

In addition, the combination of the ultrasound duty cycle and duration was shown to cause a significant effect on the shear storage modulus. These parameters controlled the cell stimulation and rest time within each ultrasound cycle and the number of cycles to which the cells were subjected. In comparison, the magnitude of the ultrasound intensity and other combinations of intensity, duty cycle and duration were shown to not have a significant effect. The use of an 80% duty cycle resulted in a decrease in the mechanical properties of the SKN constructs regardless of the duration. Similarly, the use of a 30 minute duration resulted in a decrease in the mechanical properties regardless of the duty cycle. Combinations of duty cycle between 5% and 50% and durations between 5 minutes and 18 minutes were shown to increase the mechanical properties of the SKN constructs.

6.5. Product Improvement using Ultrasound

Following the ICX-SKN Phase I study, it was hypothesised that the mechanism of action of the ICX-SKN constructs in-vivo was related to the biochemical composition and structure of the matrix (Boyd, Flasza et al. 2007). The ultrasound parameters of 1.5W/cm^2 intensity, 50% duty cycle and 14 minute duration were shown to improve the SKN constructs by increasing the viscoelastic properties and collagen deposition in the D23 SKN constructs after 21 days of stimulation. The shear storage modulus of two separated batches of SKN constructs was increased by 56% ($p=0.02$) and 73% ($p=0.01$) respectively in comparison with the D23 non-stimulated control. These results were supported by qualitative observations of increased collagen deposition, matrix density and cross-linking in light and electron microscopy images. However, a significant

difference in dry weight and digestion rate was only observed for the dry weight of the 2005 batch which was 3% (p=0.04).

The D23 ultrasound stimulated constructs were also shown to have an improved shear storage modulus through an increase in cross-linking compared to the non-stimulated D49 SKN constructs produced by the current manufacturing process. The shear storage modulus was increased by 35% (p=0.047) and 48% (p=0.027) for the 2010 and 2005 batches respectfully and the digestion rate decreased by 123% (p=0.000) and 131% (p=0.000) respectfully. These results show that introduction of ultrasound into the SKN manufacturing process also has potential for reducing the total manufacturing time. Further studies using ultrasound stimulation over the 49 day manufacturing process would identify the period over which collagen deposition and viscoelastic properties were maximised.

6.6. Scale-up and Improvement of Ultrasound System

The proof-of-principle, custom-built ultrasound stimulation device used in this study allowed repeatable and reproducible coupling of the ultrasound transducer to the SKN constructs in the optimum region of the ultrasound beam. This device demonstrated that ultrasound could be used to stimulate cellular responses in tissue-engineered constructs by coupling of the ultrasound through a liquid path. The elimination of the need for physical coupling to the constructs provides a system that is suitable for scale-up.

However, ultrasound stimulation also increased the variation in the shear storage modulus of the SKN constructs compared to the controls. It is likely that the source of the variation was from fluctuations in the output from the ultrasound transducer. Replacement of the ultrasound unit with a higher specification, custom built ultrasonic system would provide a more stable output and is discussed further in section 7.4.1.

Chapter 7 Further Work

7.0. Introduction

This chapter describes key areas of further work with both an industrial focus to improve the SKN manufacturing process and an academic focus to further understand the relationship between cell responses to the surrounding extracellular matrix and external mechanical stimulation.

This study provided an improved model of the SKN manufacturing process and identified areas for process improvement (Chapter 3). Section 7.1 describes further understanding of the interactions between the properties of the fibrin matrix, diffusion patterns of the culture media and cell responses required to enable process improvements. Research to improve the cost-effectiveness of the manufacturing process, build on the process model developed in this study and minimise the process variation are described in sections 7.1 to 7.3.

Ultrasound stimulation of the SKN constructs was shown to cause a step-change in improvement of the biochemical and mechanical properties of SKN constructs. However, the use of ultrasound stimulation also increased variation in the properties compared to the control (Chapters 4 and 5). Section 7.4 describes further research to identify and minimise the sources of variation. In addition, further research to increase understanding of the homogeneity of ultrasound propagation though the SKN construct and the resultant effect on cellular responses is discussed. Sections 7.5 and 7.6 describe further areas of research to improve the understanding of the physical and molecular mechanisms by which ultrasound is detected by the cells to elicit cellular responses.

7.1. Improvement of the SKN Construct Manufacturing Process

The human dermal fibroblast (HDF) cells are responsible for the breakdown of the fibrin matrix and secretion of the collagen matrix. It is hypothesised that increasing the total number of cells in the SKN constructs will increase the rate of fibrin degradation and collagen synthesis and in turn reduce the manufacturing time and associated material and labour costs. Two key areas of further research required to enable an increase the number of HDF cells in the SKN constructs have been identified and are discussed below. These are firstly, understanding of the properties of the fibrin matrix that influence cell proliferation. Secondly, understanding of the diffusion patterns of the nutrients in the culture media through the SKN constructs.

7.1.1. Relationship between the Fibrin Matrix and Cell Proliferation

Other studies have shown that different formulations of fibrinogen and thrombin concentrations used to form the fibrin matrix influence the rate of cell proliferation and the total number of cells in the fibrin matrix (Cox, Cole et al. 2004). In particular, 30% more HDF cells were reported using concentrations of 5mg/mL fibrinogen and 1U/mL thrombin and 17.3mg/mL fibrinogen and 167U/mL thrombin after 7 days (Cox, Cole et al. 2004) compared to the number of cells in the SKN construct which used 5mg/mL fibrinogen and 25U/mL thrombin formulation. The cell seeding density has also been shown to influence the rate of cell proliferation and the total number of cells in a fibroblast seeded fibrin matrix after 21 days (Duong, Wu et al. 2009).

The porosity and stiffness of the fibrin matrices formed by different formulations have been suggested to influence cell proliferation (Duong, Wu et al. 2009, Collet, Park et al. 2000). The porosity of the matrix affects the diffusion of nutrient from the media through the matrix which in turn affects cellular processes such as proliferation (Collet, Park et al. 2000). Fibrin matrices with low porosity have also been shown to inhibit cell spreading and rounding which has been suggested to be necessary for cell proliferation (Duong, Wu et al. 2009). The stiffness of the matrix has been shown to affect the locomotion of the cells and rate of proliferation (Yeung, Georges et al. 2005, Lo, Wang et al. 2000). The porosity and mechanical properties of the fibrin matrices can be changed using different formulations of fibrinogen and thrombin (Duong, Wu et al. 2009, Mooney, Costales et al. 2008, Wolberg 2007). However, the mechanisms by

which these factors affect cell proliferation are not fully understood. Further understanding of the biochemical and mechanical signalling of the cells from the fibrin matrices associated with cell proliferation would allow optimisation of the fibrin matrix for cell seeded fibrin constructs.

7.1.2. Relationship between the Distribution of Media in the SKN Constructs and Cell Proliferation

Secondly, analysis of the cell distribution through the thickness of the SKN constructs showed that the cells were evenly distributed in the fibrin matrix after casting. However, 7 days post casting, the cell density towards the top of the constructs was greater compared to the bottom. In addition, it was shown that the cells migrated to the surface of the construct to form a cell layer at the construct-media interface (section 3.7.5). There are a number of factors that may have caused the inhomogeneous cell distribution.

Firstly, passive diffusion of the culture media may have resulted in a greater concentration of nutrients towards the top of the constructs which stimulated the HDF cells either to migrate or proliferate more in this region. Secondly, the volume of media (2mL) supplied to the constructs 3 times/week may not have been sufficient for the requirements of all of the cells in the construct. The cells present at the top of the constructs may have used the majority of nutrients in the media before it could diffuse to the bottom. Finally, the compaction of the top of the SKN constructs described in section 3.7.1 may have also contributed to the increased cell density.

Further understanding of the contribution of each of these factors to the increased cell density at the top of the constructs would allow for process improvements to increase the number of cells that could be supported at the bottom of the constructs. Mathematical and experimental models to assess the diffusion of the media through matrices with different porosity and structure could be used to improve understanding of the distribution of the media through the thickness of the constructs. The use of an automated, continuous feeding device such as those described for other tissue-engineered constructs (Pörtner, Nagel-Heyer et al. 2005, Schulz, Wustneck et al. 2008)

would provide understanding of whether the supply of media was the limiting factor for cell proliferation and collagen synthesis.

Finally, other studies have used apparatus to physically compress HDF seeded collagen matrices (Brown, Wiseman et al. 2005). Controlled compression of the cell seeded matrices using such apparatus would provide further understanding of the affect of compaction on cell distribution.

7.2. Improvement of the SKN Construct Model

This study provided a semi-quantitative model of the current SKN manufacturing process and increased the understanding of interactions between the physical, biochemical and structural changes. However, this model can be improved further through development of quantitative assays to support the qualitative changes observed in the composition and structure of the matrix and in turn provide further understanding of the changes in the shear storage modulus reported in this study. In particular, the development of an assay to quantify the concentration of collagen and fibrin and improvement of the repeatability and reproducibility of the digestion assay is required and candidate approaches are discussed below.

7.2.1. Development of a Quantitative Collagen Assay

In this study, the collagen type I ELISA used to quantify changes in collagen in the SKN constructs was not conclusive as the absorbance signal from the constructs was very low and outside of the standard curve. Further work into the extraction of collagen from the SKN constructs and suitability of the antibodies used for detection of the collagen may improve the absorbance signal. Alternatively, other studies have reported the use of hydroxyproline based assays, such as Chloramine T, for detection of collagen secreted by cells in fibrin matrices (Ross, Tranquillo 2003, Grassl, Oegema et al. 2003) and could be assessed for suitability of use in SKN constructs. Although it was shown that fibrin matrices caused positive readings using this type of assay (Marshall 2005), further work to identify methods of removing the fibrin before testing maybe an option.

7.2.2. Development of a Repeatable and Reproducible Assay for Quantification of Cross-linking

The digestion assay used in this thesis was reliant on operator judgement to determine the point at which the SKN the construct was fully digested in the collagenase B solution. A methodology and measurement system to remove the need for operator judgement would increase the resolution of the assay and achieve more reproducible and repeatable results. In addition, the digestion solution should be developed to incorporate other enzymes present in wound sites, such as MMPs (Gilliver, Ruckshanthi et al. 2007), as this may provide a more realistic measure of the rate of degradation of SKN constructs in-vivo.

7.2.3. Quantification of the Fibrin Degradation Rate

The development of an assay to quantify the rate of fibrin degradation in the SKN constructs may improve the understanding of the influence of biochemical signalling from the fibrin matrix on collagen synthesis by the cells. This study showed by histological analysis that fibrin was still present in the matrix after 21 days. However, it could only be inferred from the increases in dry weight, digestion rate and shear storage modulus that the fibrin matrix was fully degraded between D21 and D28 of the manufacturing period. Other studies have shown that fibrin stimulates collagen synthesis from cells (Grassl, Oegema et al. 2002, Neidert, Lee et al. 2002, Tuan, Song et al. 1996, Ng CP, Swartz MA 2006). Further understanding of the volume fraction of fibrin in the SKN construct matrix required to stimulate collagen synthesis would enable optimisation of the digestion rate of the fibrin matrix. Measurement of the fibrin digestion rate in SKN constructs could be achieved through measurement of the intensity of fluorescently labelled fibrinogen as described by Grassl, E.D. 2002.

7.3. Reduction in Batch-to-Batch Variation

7.3.1. Control of Human Dermal Fibroblast Cell Population

The human dermal fibroblast (HDF) cells were confirmed to be responsible for the processes that occurred in the SKN manufacturing process to produce the final product. In this study, a semi-automated process was used to produce master and working HDF

cell banks to reduce the variation in the cell culture process and cell population used in the manufacture of SKN constructs when compared to manual cell culture. The use of a fully automated cell culturing process would be beneficial to further reducing process variation and variation in the cell population (Liu, Chandra et al. 2008).

Development of a fully automated protocol using the CompacT SelecT requires changes to the manual trypsinisation process. In the manual cell culture process, trypsin is used to enzymatically detach cells from the culture flask for passaging of the cells but is then removed from the cell suspension by centrifugation and aspiration to minimise damage to the cells through prolonged exposure to the trypsin. However, the current automated cell culturing system (CompacT SelecT, TAP, UK) does not have the facility to centrifuge the cell suspension and remove trypsin. A fully automated cell culture process where trypsin enzymatically detaches cells from the culture flask but minimises damage to the cells is required. This could be achieved through investigation of the volume of media required to reduce the concentration and activity of trypsin once the cells were detached from the flask. The concentration and incubation time of the trypsin on the cells required for enzymatic digestion could also be investigated.

In addition, cell damage and therefore variation in the cell population, is most likely to be caused by cryopreservation and recovery of the cells from cryopreservation as well as trypsinisation during cell culture. Optimisation of these processes to minimise cell damage would improve cell viability and potentially improve the suitability of the cells for their function in the SKN manufacturing process. The processes could be optimised using a design of experiments methodology to analyse the interactions between the key parameters of each process as well as individual parameters. For the trypsinisation process, the key parameters include trypsin concentration and temperature, volume of dilution media and incubation time. For the cryopreservation and recovery processes, the key parameters include the cell density and volume, rate of freezing and rate of thawing when recovering cells from cryopreservation.

Finally, development of a measurement system that would improve the understanding of the suitability of the cell population for the SKN manufacturing process would allow for optimisation and selection of cell populations prior to use. The identification of specific cell surface markers that are indicative of the optimum cells for use in SKN

constructs is many years away. However, assays such as Alamar Blue are readily available for analysis of metabolic activity of cell populations. The coupling of cell viability, cell yield and metabolic activity would provide an improved profile of the cells used in the manufacturing process and provide a better understanding of the variation in the manufacturing process that is caused by variations in cell populations.

7.3.2. Control of Culture Media

The culture media is composed of 18 different supplements and is currently used for a maximum of 30 days before disposal. The stability of the components in the media over time and the effectiveness of each of the supplements with respect to maximising collagen synthesis and cell proliferation should be investigated to potentially reduce process variation and cost of goods through the removal of ineffective supplements. It is suggested that the effectiveness of the media supplements is investigated using a design of experiments as described previously for the optimisation of the trypsinisation process.

It is recognised that changes to the media formulation would also cause further expenditure as regulators would require evidence that there was no change in efficacy of the SKN product compared to that used in the Phase I clinical trial. The cost of such a study and magnitude of the potential savings needs to be balanced with the regulatory costs. It is suggested that such a study is conducted in collaboration with an applied manufacturing academic research group to generate preliminary evidence for a business case.

7.3.3. Control of the Fibrin Matrix

The fibrinogen and thrombin used to produce the fibrin matrix for ICX-SKN constructs has inherent variation due to its human source (bovine source for SKN constructs). It is not currently known if this causes variation in the fibrin matrices as the biochemical and mechanical properties of the fibrin matrix are not measured before used in the SKN manufacturing process. The fibrin matrix may be a source of process variation as it has been shown that cell proliferation is affected by the properties of the matrix (Cox, Cole et al. 2004). Development of a measurement system that to test the biochemical and mechanical properties would provide an understanding of the variation and allow development of specifications for the matrix prior to use in the manufacturing process. The rheological method developed in this thesis in a potential candidate system to test the viscoelastic properties of the matrix. Further development of this methodology to assess the repeatability and reproducibility of the measurement system is first required and could be analysed using a nested Gauge R&R study (Mason, Gunst et al. 2003).

7.4. Improvement of Ultrasound Stimulation Process

7.4.1. Reducing Variation in Ultrasound Stimulation Process

The SonoPlus490 ultrasound unit provided a cost-effective, off-the-shelf system for ultrasound stimulation of the SKN constructs. However, assembly of a custom-built ultrasonic system would provide greater control of the ultrasound output and reduce variation in the ultrasound stimulating the HDF cells in the SKN constructs. The main components of an ultrasonic system are the pulser/receiver, transducer and associated communications and application software which provides the user interface for control of the ultrasound parameters (National Instruments Ultrasonic Developer Zone, http://zone.ni.com/). The pulser/receiver generates a high-voltage pulse that vibrates the piezoelectric ceramics in the transducer to generate an ultrasonic wave. The pulser/receiver controls the intensity, and frequency of the voltage as well as the pulse length, damping and band filter pass settings received by the transducer. Use of a pulser/receiver that allows greater control of these settings compared to the SonoPlus490 unit will allow optimal excitation of the transducer and greater output stability. In addition, coupling the pulser/receiver to a transducer with uniform output across the whole face will provide more homogeneous stimulation of the HDF cells in the SKN construct. The cost and suppliers of the components required for such a system is detailed in Appendix V. Such a system could be used to investigate the effect of the ultrasound duty cycle between 50% and 80% which is not possible with the SonoPlus490 unit.

7.4.2. Improvement in Understanding of Ultrasound Output and Propagation

The force balance used to measure the output of the transducer in this study provided an average output power measurement over the whole transducer face. However, further understanding of the homogeneity of the output across the transducer face and the propagation of ultrasound through the construct is required to improve understanding of the cellular responses reported in this study. Spatial mapping of the ultrasound field using a hydrophone (which converts acoustic pressure to a measurable output voltage) would allow measurement of variation in output across the transducer face of the SonoPlus490 or custom-built unit. In addition, a needle hydrophone can used to map the ultrasound output in the SKN constructs. This would provide an understanding of

the homogeneity of the ultrasound propagation through the construct and the effect on cellular responses as the extracellular matrix composition changes during manufacturing.

7.4.3. Improvement of the Ultrasound Stimulation Parameters and Regime

This study identified the range and combinations of ultrasound parameters that could be used to improve the biochemical and mechanical properties of SKN constructs. Further experiments to optimise the ultrasound parameters for maximum collagen synthesis and shear storage modulus are required. This can be achieved using a design of experiments, as described in section 4.2.1, with maximum and minimum duty cycles of 20% and 50%, durations of 5 and 18 minutes and intensities of 0.5W/cm^2 and 1.5W/cm^2 for the current experimental set-up with the SonoPlus490 ultrasound unit. A custom-built ultrasonic system (section 7.4.1) would allow optimisation at duty cycles between 20% and 50% as well as between 50% and 80%.

In addition, increasing the levels of ultrasound stimulation during the manufacturing process could be investigated as this has been reported to increase collagen synthesis from cells in fibrin gels subjected to stepped increases of uniaxial strain compared to the gels stimulated by the same magnitude of strain (Syedain, Weinberg et al. 2008). For instance, using the DOE results in this study, ultrasound parameters of 2.5W/cm^2 intensity, 5% duty cycle and 5 minute duration which increased G' by 112% could be used between D0 and D7. Between D7 and D14, 0.5W/cm^2 intensity, 5% duty cycle and 5 minutes duration which increased G' by 119% could be used and between D14 and D21, 1.5W/cm^2 intensity, 50% duty cycle and 18 minute duration which increased G' by 139% could be used.

Finally, mathematical modelling programs can be used to support optimisation of the ultrasound parameters and stimulation regime. Modelling programs such as Field II (http://server.elektro.dtu.dk/personal/jaj/field/) are commercially available and can be used to simulate the ultrasound output from the transducer and propagation through the SKN constructs in a similar manner that describe for simulation of ultrasound propagation through bone (Kaufman, Luo et al. 2008).

7.5. Ultrasound Induced Mechanisms Affecting Cell Responses

It has been widely reported that ultrasound stimulation increases collagen synthesis from cells and the mechanical properties of cell seeded matrices. These findings were confirmed in this study using human dermal fibroblast seeded fibrin matrices. The phenomena that occur when ultrasound propagates through materials is well established (Challis, Povey et al. 2005). There are also many studies on the safety of ultrasound propagation through tissue when used for imaging of foetuses (Duck 2008). However, the mechanisms by which ultrasound stimulate cell responses, such as collagen synthesis, in-vitro are not fully understood.

There are a number of mechanisms that may cause cell responses when stimulated by ultrasound. Firstly, the propagation of ultrasound may improve the availability of oxygen and nutrients to the cells through physical diffusion of the media through the cell seeded matrices. A system to assess fluid flow through matrices with different matrix densities, with and without ultrasound stimulation, would improve the understanding of the effects of ultrasound on media distribution.

Secondly, the propagation of ultrasound through materials is known to cause physical deformation through compression and expansion of the materials as described in section 2.8.3. Optical techniques such as holography and interferometry can been used to measure sub-micron deformation of materials and observe changes in the morphology of cell surface (Joeris, Frerichs et al. 2002, Neto, Agero et al. 2006, Cuche, Bevilacqua et al. 1999). These techniques could be used to understand the effect of ultrasound on the compression and expansion of cells in monolayers. This would provide further understanding of the relationship between cellular responses, such as cell proliferation and collagen synthesis, and the degree of cell deformation caused by ultrasound.

Thirdly, the velocity of ultrasound propagation differs through the cells, extracellular matrix and fluid in cell seeded matrices. This causes the cells to be subjected to shear forces at the interface between the cell membrane and surrounding extracellular matrix. Studies of the effect of interstitial flow through cell seeded collagen matrices showed that shear forces could stimulate collagen synthesis from the cells (Ng, Hinz et al. 2005). Application of different combinations of ultrasound parameters, measurement of the shear force and cellular responses such as collagen synthesis would provide further understanding of the mechanisms by which ultrasound causes cellular responses. In addition, it has been shown that cells detect ultrasound through integrin receptors on the cell membrane (Zhou, Schmelz et al. 2004). These receptors detect mechanical stimulation and analysis of the activation of the integrin receptors, as described by Zhou et al 2004, could be used to provide further understanding of the contribution of the effect of cell deformation and shear force on cell responses.

Finally, there is currently much debate on the acoustic conditions required for the formation of cavitation bubbles and the effect of cavitation in cell monolayers and cell seeded matrices. In this study, there was evidence of some cell necrosis together with collagen synthesis when the SKN constructs were stimulated with ultrasound. The formation and collapse of cavitation bubbles on the cell membrane has been suggested to cause cell necrosis through penetration of the membrane (Miller 2007). However, it has also been shown that ultrasound improves the permeability of cell membranes for the uptake of drugs (Husseini, Diaz de la Rosa et al. 2005). The degree of cavitation induced by ultrasound in these studies may account for the different cellular responses reported.

Further understanding of the acoustic conditions that cause the formation of cavitation bubbles could be studied through use of time-lapse microscopy. Calculation of the magnitude of the force of impact of bubbles with the cell membrane would provide an understanding of the effect of cavitation on cell responses and would allow for better selection of the ultrasound parameters to elicit desired cell responses.

7.6. Molecular Mechanisms Affecting Cell Responses

The processes of mechanotransduction whereby mechanical stimuli are converted by cells into intracellular chemical signals have been widely reported and have been recently reviewed (Chiquet, Gelman et al. 2009, Wang, Tytell et al. 2009, Ingber 2006). Cells bind to the surrounding extracellular matrix through formation of focal complexes, focal adhesions and fibrillar adhesions (Chiquet, Gelman et al. 2009). These matrix adhesions contain integrin receptors as their main transmembrane proteins. The integrins bind to specific extracellular matrix molecules and to adaptor proteins in the cell which are linked to the cell actin cytoskeleton (Wang, Tytell et al. 2009). The detection of mechanical stimuli by the integrin receptors causes reorganisation of the actin cytoskeleton and in turn activates signalling pathways which lead to cell responses such as collagen synthesis (Chiquet, Gelman et al. 2009). Methods to measure cytoskeletal forces have been demonstrated by a number of studies (Choquet, Felsenfeld et al. 1997, Spudich, Pelham et al. 1999, Schwarz, Balaban et al. 2002, Sniadecki, Anguelouch et al. 2007). However, the degree of cytoskeletal reorganisation caused by mechanical stimulation, to elicit desired cell responses requires further investigation. A study which applied cyclic strain to cardiac fibroblasts showed that the COL1A1 gene associated with synthesis of collagen type I was regulated by a signalling pathway dependent on TGF-β (Lindahl, Chambers et al. 2002). However, it has also been shown that over stimulation of cells causes disassembly of focal adhesions and can lead to undesired cell responses such as apoptosis (Kearney, Prendergast et al. 2008).

The selection of appropriate combinations of ultrasound intensity, duty cycle and duration to elicit desired cell responses requires further research. Firstly, an understanding of the magnitude of mechanical force on the cell caused by ultrasound stimulation required to activate integrin receptors and the associated cytoskeletal force is required. Secondly, understanding of the optimum frequency and duration over which integrin receptors can respond to mechanical stimuli would enable optimisation of mechanical stimulation regimes and aid the choice of the most suitable combinations of ultrasound parameters.

Finally, it has been shown that cells respond to changes in the stiffness of the extracellular matrix through formation and disassembly of focal adhesions (Chiquet, Gelman et al. 2009, Discher, Janmey et al. 2005). An understanding of the whether the matrix stiffness is altered as ultrasound propagates through it would provide an insight in to whether this is also a mechanism by which ultrasound stimulation elicits responses from cells seeded in matrices.

In summary, there are three key areas of further work required to develop manufacturing processes and products that meet business and customer needs for the realisation of the routine use of regenerative medicine products in patients. Firstly, improved understanding of current manufacturing processes and development of repeatable and reliable measurement systems is required to identify areas to improve the cost-effectiveness of the process. Secondly, research into minimising the variation in the process input raw materials is required to reduce the variation in the manufacturing processes and improve product quality. Finally, further understanding of the effect of the type, magnitude, frequency and duration of mechanical stimulation on cell responses will enable a step-change in improvement of product properties through use of mechanical stimulation.

References

AHLFORS, J.-W. and BILLIAR, K.L., 2007. Biomechanical and biochemical characteristics of a human fibroblast-produced and remodelled matrix. *Biomaterials,* **28**(13), pp. 2183-2191.

ARORA, P.D., NARANI, N. and MCCULLOCH, C.A.G., 1999. The Compliance of Collagen Gels Regulates Transforming Growth Factor-ß Induction of {alpha}-Smooth Muscle Actin in Fibroblasts. *American Journal of Pathology,* **154**(3), pp. 871-882.

AUGER, F.A., LACROIX, D. and GERMAIN, L., 2009. Skin substitutes and wound healing. *Skin pharmacology and physiology,* **22**(2), pp. 94-102.

AZRAD, E., ZAHOR, D., VAGO, R., NEVO, Z., DORON, R., ROBINSON, D., GHEBER, L.A., ROSENWAKS, S. and BAR, I., 2006. Probing the effect of an extract of elk velvet antler powder on mesenchymal stem cells using Raman microspectroscopy: enhanced differentiation toward osteogenic fate. *Journal of Raman Spectroscopy,* **37**(4),. .

BAKER, K.G., ROBERTSON, V.J. and DUCK, F.A., 2001. A Review of Therapeutic Ultrasound: Biophysical Effects. *Physical Therapy,* **81**(7), pp. 1351.

BALESTRINI, J.L. and BILLIAR, K.L., 2009. Magnitude and Duration of Stretch Modulate Fibroblast Remodeling. *Journal of Biomechanical Engineering,* **131**, pp. 051005.

BALESTRINI, J.L. and BILLIAR, K.L., 2006. Equibiaxial cyclic stretch stimulates fibroblasts to rapidly remodel fibrin. *Journal of Biomechanics,* **39**(16), pp. 2983-2990.

BARBUCCI, R., ed, 2002. *Integrated biomaterials science.* 1st edn. New York: Kluwer Academic/Plenum.

BARNETT, S.B., TER HAAR, G.R., ZISKIN, M.C., ROTT, H.D., DUCK, F.A. and MAEDA, K., 2000. International recommendations and guidelines for the safe use of diagnostic ultrasound in medicine. *Ultrasound in medicine & biology,* **26**(3), pp. 355-366.

BARRY, M.A., BEHNKE, C.A. and EASTMAN, A., 1990. Activation of programmed cell death (apoptosis) by cisplatin, other anticancer drugs, toxins and hyperthermia. *Biochemical pharmacology,* **40**(10), pp. 2353-2362.

BATH-HEXTALL, F., LEONARDI-BEE, J., SMITH, C., MEAL, A. and HUBBARD, R., 2007. Trends in incidence of skin basal cell carcinoma. Additional evidence from a UK primary care database study. *International Journal of Cancer,* **121**(9), pp. 2105-2108.

BELLO, Y.M. and PHILLIPS, T.J., 2000. Recent advances in wound healing. *Journal of the American Medical Association,* **283**(6), pp. 716-718.

BENKHEROUROU, M., GUMERY, P.Y., TRANQUI, L. and TRACQUI, P., 2000. Quantification and macroscopic modeling of the nonlinearviscoelastic behavior of strained gels with varying fibrinconcentrations. *Biomedical Engineering, IEEE Transactions on,* **47**(11), pp. 1465-1475.

BERRY, C.C., SHELTON, J.C., BADER, D.L. and LEE, D.A., 2003. Influence of external uniaxial cyclic strain on oriented fibroblast-seeded collagen gels. *Tissue Engineering,* **9**(4), pp. 613-624.

BILLIAR, K.L., THROM, A.M. and FREY, M.T., 2005. Biaxial failure properties of planar living tissue equivalents. *Journal of Biomedical Materials Research Part A,* **73**(2), pp. 182-191.

BLUNK, T., SIEMINSKI, A.L., GOOCH, K.J., COURTER, D.L., HOLLANDER, A.P., NAHIR, A.M., LANGER, R., VUNJAK-NOVAKOVIC, G. and FREED, L.E., 2002. Differential effects of growth factors on tissue-engineered cartilage. *Tissue engineering,* **8**(1), pp. 73-84.

BOCCAFOSCHI, F., HABERMEHL, J., VESENTINI, S. and MANTOVANI, D., 2005. Biological performances of collagen-based scaffolds for vascular tissue engineering. *Biomaterials,* **26**(35), pp. 7410-7417.

BORTNER, C.D. and CIDLOWSKI, J.A., 1998. A necessary role for cell shrinkage in apoptosis. *Biochemical pharmacology,* **56**(12), pp. 1549-1559.

BOYD, M., FLASZA, M., JOHNSON, P.A., ROBERTS, J.S.C. and KEMP, P., 2007. Integration and persistence of an investigational human living skin equivalent (ICX-SKN) in human surgical wounds. *Regen.Med.,* **2**(4), pp. 363-370.

BOZZOLA, J.J. and RUSSELL, L.D., 1999. Electron microscopy: principles and techniques for biologists. Jones & Bartlett Publishers.

BROUGHTON, G.I., JANIS, J.E. and ATTINGER, C.E., 2006. The Basic Science of Wound Healing. *Plastic and Reconstructive Surgery,* **117**(7S), pp. 12S.

BROWN, R.A., PRAJAPATI, R., MCGROUTHER, D.A., YANNAS, I.V. and EASTWOOD, M., 1998. Tensional homeostasis in dermal fibroblasts: Mechanical responses to mechanical loading in three-dimensional substrates. *Journal of Cellular Physiology,* **175**(3), pp. 323-332.

BROWN, R.A., WISEMAN, M., CHUO, C.B., CHEEMA, U. and NAZHAT, S.N., 2005. Ultrarapid engineering of biomimetic materials and tissues: fabrication of nano-and microstructures by plastic compression. *Adv Funct Mater,* **15**(11), pp. 1762–1770.

BRIDE, J., VIENNET, C., LUCARZ-BIETRY, A. and HUMBERT, P., 2004. Indication of fibroblast apoptosis during the maturation of disc-shaped mechanically stressed collagen lattices. *Archives of Dermatological Research,* **295**(8-9), pp. 312-317.

BYL, N.N., MCKENZIE, A.L., WEST, J.M., WHITNEY, J.D., HUNT, T.K. and SCHEUENSTUHL, H.A., 1992. Low-dose ultrasound effects on wound healing: a controlled study with Yucatan pigs. *Archives of Physical Medicine and Rehabilitation,* **73**(7), pp. 656-664.

CASPERS, P.J., LUCASSEN, G.W., WOLTHUIS, R., BRUINING, H.A. and PUPPELS, G.J., 1998. In vitro and in vivo Raman spectroscopy of human skin. *Biospectroscopy,* **4**(5 Suppl), pp. S31-9.

CHALLIS, R.E., POVEY, M.J.W., MATHER, M.L. and HOLMES, A.K., 2005. Ultrasound techniques for characterizing colloidal dispersions. *Rep.Prog.Phys,* **68**, pp. 1541–1637.

CHANG, W.H., SUN, J.S., CHANG, S.P. and LIN, J.C., 2002. Study of thermal effects of ultrasound stimulation on fracture healing. *Bioelectromagnetics,* **23**(4), pp. 256-263.

CHEN, J., ALTMAN, G.H., KARAGEORGIOU, V., HORAN, R., COLLETTE, A., VOLLOCH, V., COLABRO, T. and KAPLAN, D.L., 2003. Human bone marrow stromal cell and ligament fibroblast responses on RGD-modified silk fibers. *Journal of Biomedical Materials Research,* (2).

CHENG, L., 2006. Meeting between Leo Cheng, Consultant Maxillofacial Surgeon, Department of Oral and Maxillofacial Surgery at St. Bartholomew's and The London Hospitals. Loughborugh University: Remedi Health Care Engineering Group.

CHIQUET, M., GELMAN, L., LUTZ, R. and MAIER, S., 2009. From mechanotransduction to extracellular matrix gene expression in fibroblasts. *BBA-Molecular Cell Research.*

CHOQUET, D., FELSENFELD, D.P. and SHEETZ, M.P., 1997. Extracellular matrix rigidity causes strengthening of integrin-cytoskeleton linkages. *Cell,* **88**(1), pp. 39-48.

CLARK, R.A.F., ed, 1996. *The Molecular and Cellular Biology of Wound Repair.* 2nd Edition edn. Netherlands: Kluwer Academic Plenum Publishers.

CLARK, R.A.F., GHOSH, K. and TONNESEN, M.G., 2007. Tissue Engineering for Cutaneous Wounds. *Journal of Investigative Dermatology,* **127**(5), pp. 1018-1029.

COLLET, J.P., PARK, D., LESTY, C., SORIA, J., SORIA, C., MONTALESCOT, G. and WEISEL, J.W., 2000. Influence of Fibrin Network Conformation and Fibrin Fiber Diameter on Fibrinolysis Speed Dynamic and Structural Approaches by Confocal Microscopy. *Arteriosclerosis, Thrombosis, and Vascular Biology,* **20**(5), pp. 1354-1361.

COLWELL, A.S., FAUDOA, R., KRUMMEL, T.M., LONGAKER, M.T. and LORENZ, H.P., 2007. Transforming Growth Factor-[beta], Smad, and Collagen Expression Patterns in Fetal and Adult Keratinocytes. *Plastic and Reconstructive Surgery,* **119**(3), pp. 852.

COPPOLINO, M.G. and DEDHAR, S., 2000. Bi-directional signal transduction by integrin receptors. *The International Journal of Biochemistry & Cell Biology,* **32**(2), pp. 171-188.

COX, S., COLE, M. and TAWIL, B., 2004. Behavior of Human Dermal Fibroblasts in Three-Dimensional Fibrin Clots: Dependence on Fibrinogen and Thrombin Concentration. *Tissue Engineering [Tissue Eng.]. Vol.10,* **10**(5-6), pp. 942.

CUCHE, E., BEVILACQUA, F. and DEPEURSINGE, C., 1999. Digital holography for quantitative phase-contrast imaging. *Optics Letters,* **24**(5), pp. 291-293.

CUI, J.H., PARK, K., PARK, S.R. and MIN, B.H., 2006. Effects of Low-Intensity Ultrasound on Chondrogenic Differentiation of Mesenchymal Stem Cells Embedded in Polyglycolic Acid: An in Vivo Study. *Tissue engineering,* **12**(1), pp. 75-82.

DA CUNHA, A., PARIZOTTO, N.A. and DE CAMPOS VIDAL, B., 2001. The effect of therapeutic ultrasound on repair of the achilles tendon(Tendo calcaneus) of the rat. *Ultrasound in medicine & biology,* **27**(12), pp. 1691-1696.

DAMODARAN, G., SYED, M., LEIGH, I., MYERS, S. and NAVSARIA, H., 2008. Clinical application of skin substitutes. *Expert Rev.Dermatol.,* **3**(3), pp. 345-356.
DE, R., ZEMEL, A. and SAFRAN, S.A., 2007. Dynamics of cell orientation. *Nature Physics,* **3**(9), pp. 655-659.

DICKNEITE, G., METZNER, H., PFEIFER, T., KROEZ, M. and WITZKE, G., 2004. A comparison of fibrin sealants in relation to their in vitro and in vivo properties. *Thrombosis Research,* **112**(1-2), pp. 73-82.

DISCHER, D.E., JANMEY, P. and WANG, Y., 2005. Tissue cells feel and respond to the stiffness of their substrate. *Science,* **310**(5751), pp. 1139-1143.

DOAN, N., REHER, P., MEGHJI, S. and HARRIS, M., 1999. In vitro effects of therapeutic ultrasound on cell proliferation, protein synthesis, and cytokine production by human fibroblasts, osteoblasts, and monocytes. *Journal of Oral and Maxillofacial Surgery,* **57**(4), pp. 409-419.

DUCK, F.A., 2008. Hazards, risks and safety of diagnostic ultrasound. *Medical Engineering and Physics,*

DUCK, F.A., 1990. Physical Properties of Tissue, A Comprehensive Reference Book. London: Academic Press Inc.

DUDA, G.N., KLICHE, A., KLEEMANN, R., HOFFMANN, J.E., SITTINGER, M. and HAISCH, A., 2004. Does Low-Intensity Pulsed Ultrasound Stimulate Maturation of Tissue-Engineered Cartilage? *JOURNAL OF BIOMEDICAL MATERIALS RESEARCH PART B,* **68**(1), pp. 21-28.

DUONG, H., WU, B. and TAWIL, B., 2009. Modulation of 3D Fibrin Matrix Stiffness by Intrinsic Fibrinogen–Thrombin Compositions and by Extrinsic Cellular Activity. *Tissue Engineering Part A,* .

EASTWOOD, M., MUDERA, V.C., MCGROUTHER, D.A. and BROWN, R.A., 1998. Effect of precise mechanical loading on fibroblast populated collagen lattices: morphological changes. *Cell Motil Cytoskeleton,* **40**(1), pp. 13-21.

EASTWOOD, M., PORTER, R., KHAN, U., MCGROUTHER, G. and BROWN, R.A., 1996. Quantitative analysis of collagen gel contractile forces generated by dermal fibroblasts and the relationship to cell morphology. *J Cell Physiol,* **166**(1), pp. 33-42.

EBISAWA, K., HATA, K., OKADA, K., KIMATA, K., UEDA, M., TORII, S. and WATANABE, H., 2004. Ultrasound Enhances Transforming Growth Factor β-Mediated Chondrocyte Differentiation of Human Mesenchymal Stem Cells. *Tissue engineering,* **10**(5-6), pp. 921-929.

ECKES, B., ZIGRINO, P., KESSLER, D., HOLTKÖTTER, O., SHEPHARD, P., MAUCH, C. and KRIEG, T., 2000. Fibroblast-matrix interactions in wound healing and fibrosis. *Matrix Biology,* **19**(4), pp. 325-332.

ECKES, B., ZWEERS, M.C., ZHANG, Z.G., HALLINGER, R., MAUCH, C., AUMAILLEY, M. and KRIEG, T., 2006. Mechanical tension and integrin α2β1 regulate fibroblast functions. *Journal of Investigative Dermatology Symposium Proceedings,* **11**(1), pp. 66-72.

EDELMANN, L., 2002. Freeze-dried and resin-embedded biological material is well suited for ultrastructure research. *Journal of microscopy,* **207**(1), pp. 5-26.

ENGELMAYR, J.G.C., RABKIN, E., SUTHERLAND, F.W.H., SCHOEN, F.J., MAYER, J.,JOHN E. and SACKS, M.S., 2005. The independent role of cyclic flexure in the early in vitro development of an engineered heart valve tissue. *Biomaterials,* **26**(2), pp. 175-187.

ENGELMAYR, J.G.C., SALES, V.L., MAYER, J., JOHN E. and SACKS, M.S., 2006. Cyclic flexure and laminar flow synergistically accelerate mesenchymal stem cell-mediated engineered tissue formation: Implications for engineered heart valve tissues. *Biomaterials,* **27**(36), pp. 6083-6095.

EYRICH, D., BRANDL, F., APPEL, B., WIESE, H., MAIER, G., WENZEL, M., STAUDENMAIER, R., GOEPFERICH, A. and BLUNK, T., 2007. Long-term stable fibrin gels for cartilage engineering. *Biomaterials,* **28**(1), pp. 55-65.

FARMERY, M.J. and WHITTINGHAM, T.A., 1978. A portable radiation-force balance for use with diagnostic ultrasonic equipment. *Ultrasound in medicine & biology,* **3**(4), pp. 373-379. FAWCETT, D.W., 1994. Bloom and Fawcett, a textbook of histology. Chapman & Hall New York.

FENDEL, S. and SCHRADER, B., 1998. Investigation of skin and skin lesions by NIR-FT-Raman spectroscopy. *Fresenius'Journal of Analytical Chemistry,* **360**(5), pp. 609-613.

FENG, Z., YAMATO, M., AKUTSU, T., NAKAMURA, T., OKANO, T. and UMEZU, M., 2003. Investigation on the Mechanical Properties of Contracted Collagen Gels as a Scaffold for Tissue Engineering. *Artificial Organs,* **27**(1), pp. 84-91.

FERIL, J., L.B. and KONDON, T., 2004. Biological Effects of Low Intensity Ultrasound: The Mechanism Involved, and its Implications on Therapy and on Biosafety of Ultrasound. *Journal of radiation research,* **45**(4), pp. 479-489.

FLASZA, M., KEMP, P., SHERING, D., QIAO, J., MARSHALL, D., BOKTA, A. and JOHNSON, P.A., 2007. Development and manufacture of an investigational human living dermal equivalent (ICX-SKN). *Regen.Med.,* **2**(6), pp. 903-918.

FORMIGLI, L., PAPUCCI, L., TANI, A., SCHIAVONE, N., TEMPESTINI, A., ORLANDINI, G.E., CAPACCIOLI, S. and ORLANDINI, S.Z., 2000. Aponecrosis: morphological and biochemical exploration of a syncretic process of cell death sharing apoptosis and necrosis. *Apoptosis,* **41**, pp. 49
FRUSHOUR, B.G. and KOENIG, J.L., 1975. Raman scattering of collagen, gelatin, and elastin. *Biopolymers,* **14**(2), pp. 379-391.

GEORGES, P.C. and JANMEY, P.A., 2005. Cell type-specific response to growth on soft materials. *Journal of Applied Physiology,* **98**(4), pp. 1547-1553.

GHOSH, A.K., 2002. Factors Involved in the Regulation of Type I Collagen Gene Expression: Implication in Fibrosis. *Experimental Biology and Medicine,* **227**(5), pp. 301-314.

GILLERY, P., BELLON, P., COUSTRY, F. and BOREL, J.-, 1989. Cultures of fibroblasts in fibrin lattices: Models for the study of metabolic activities of the cells in physiological conditions. *Journal of Cellular Physiology,* **140**(3), pp. 483-490.

GILLIVER, S.C., RUCKSHANTHI, J.P.D., ATKINSON, S.J. and ASHCROFT, G.S., 2007. Androgens influence expression of matrix proteins and proteolytic factors during cutaneous wound healing. *Laboratory Investigation,* **87**(9), pp. 871-881.

GIRTON, T.S., BAROCAS, V.H. and TRANQUILLO, R.T., 2002. Confined compression of a tissue-equivalent: Collagen fibril and cell alignment in response to anisotropic strain. *Journal of Biomechanical Engineering,* **124**(5), pp. 568-575.

GRANDE, J.P., 1997. Role of transforming growth factor-beta in tissue injury and repair. *Proceedings of the Society for Experimental Biology and Medicine.Society for Experimental Biology and Medicine (New York, N.Y.),* **214**(1), pp. 27-40.

GRASSL, E.D., OEGEMA, T.R. and TRANQUILLO, R.T., 2003. A fibrin-based arterial media equivalent. *J Biomed Mater Res A,* **66**(3), pp. 550-61.

GRASSL, E.D., OEGEMA, T.R. and TRANQUILLO, R.T., 2002. Fibrin as an alternative biopolymer to type-I collagen for the fabrication of a media equivalent. *J Biomed Mater Res,* **60**(4), pp. 607-12.

GREEN, K.A., ALMHOLT, K., PLOUG, M., RØNØ, B., CASTELLINO, F.J., JOHNSEN, M., BUGGE, T.H., RØMER, J. and LUND, L.R., 2008. Profibrinolytic Effects of Metalloproteinases during Skin Wound Healing in the Absence of Plasminogen. *Journal of Investigative Dermatology,* **128**(8), pp. 2092-2101.

GRINNELL, F., 2003. Fibroblast biology in three-dimensional collagen matrices. *Trends in Cell Biology,* **13**(5), pp. 264-269.

GRINNELL, F., 2000. Fibroblast-collagen-matrix contraction: growth-factor signalling and mechanical loading. *Trends in Cell Biology,* **10**(9), pp. 362-365.

GROUF, J.L., THROM, A.M., BALESTRINI, J.L., BUSH, K.A. and BILLIAR, K.L., 2007. Differential Effects of EGF and TGF-β1 on Fibroblast Activity in Fibrin-Based Tissue Equivalents. *Tissue engineering,* **13**(4), pp. 799-807.

HALLOW, D.M., MAHAJAN, A.D., MCCUTCHEN, T.E. and PRAUSNITZ, M.R., 2006. Measurement and correlation of acoustic cavitation with cellular bioeffects. *Ultrasound in medicine & biology,* **32**(7), pp. 1111-1122.

HANSEN, U., SCHÜNKE, M., DOMM, C., IOANNIDIS, N., HASSENPFLUG, J., GEHRKE, T. and KURZ, B., 2001. Combination of reduced oxygen tension and intermittent hydrostatic pressure: a useful tool in articular cartilage tissue engineering. *Journal of Biomechanics,* **34**(7), pp. 941-949.

HARLE, J., MAYIA, F., OLSEN, I. and SALIH, V., 2005. EFFECTS OF ULTRASOUND ON TRANSFORMING GROWTH FACTOR-B GENES IN BONE CELLS. *Eur Cell Mater,* **10**, pp. 70–77.
HARLE, J., SALIH, V., MAYIA, F., KNOWLES, J.C. and OLSEN, I., 2001. Effects of ultrasound on the growth and function of bone and periodontal ligament cells in vitro. *Ultrasound in medicine & biology,* **27**(4), pp. 579-586.

HEINO, J., 2000. The collagen receptor integrins have distinct ligand recognition and signaling functions. *Matrix Biology,* **19**(4), pp. 319-323.

HENSHAW, D.R., ATTIA, E., BHARGAVA, M. and HANNAFIN, J.A., 2006. Canine ACL fibroblast integrin expression and cell alignment in response to cyclic tensile strain in three-dimensional collagen gels. *Journal of Orthopaedic Research,* **24**(3), pp. 481-490.

HILBORN, J. and BJURSTEN, L.M., 2007. A new and evolving paradigm for biocompatibility. *Journal of Tissue Engineering and Regenerative Medicine,* **1**(2).

HOERSTRUP, S.P., KADNER, A., MELNITCHOUK, S., TROJAN, A., EID, K., TRACY, J., SODIAN, R., VISJAGER, J.F., KOLB, S.A. and GRUNENFELDER, J., 2002. Tissue Engineering of Functional Trileaflet Heart Valves From Human Marrow Stromal Cells. *Circulation,* **106**(90121), pp. 143-150.

HONG, H.H., UZEL, M.I., DUAN, C., SHEFF, M.C. and TRACKMAN, P.C., 1999. Regulation of lysyl oxidase, collagen, and connective tissue growth factor by TGF-beta1 and detection in human gingiva. *Laboratory investigation; a journal of technical methods and pathology,* **79**(12), pp. 1655-1667.

HSU, S., KUO, C.C., WHU, S.W., LIN, C.H. and TSAI, C.L., 2006. The effect of ultrasound stimulation versus bioreactors on neocartilage formation in tissue engineering scaffolds seeded with human chondrocytes in vitro. *Biomolecular engineering,* **23**(5), pp. 259-264.

HSU, S., WHU, S.W., HSIEH, S.C., TSAI, C.L., CHEN, D.C. and TAN, T.S., 2004. Evaluation of chitosan-alginate-hyaluronate complexes modified by an RGD-containing protein as tissue-engineering scaffolds for cartilage regeneration. *Artificial Organs,* **28**(8), pp. 693-703.

HUMPHREY, V.F. and DUCK, F.A., 1998. ULTRASONIC FIELDS: Structure and Prediction. *Ultrasound in Medicine.*

HUSSEINI, G.A., DIAZ DE LA ROSA, M.A., RICHARDSON, E.S., CHRISTENSEN, D.A. and PITT, W.G., 2005. The role of cavitation in acoustically activated drug delivery. *Journal of Controlled Release,* **107**(2), pp. 253-261.

IBUSUKI, S., FUJII, Y., IWAMOTO, Y. and MATSUDA, T., 2003. Tissue-Engineered Cartilage Using an Injectable and in Situ Gelable Thermoresponsive Gelatin: Fabrication and in Vitro Performance. *Tissue engineering,* **9**(2), pp. 371-384.

INGBER, D.E., 2006. Cellular mechanotransduction: putting all the pieces together again. *The FASEB Journal,* **20**(7), pp. 811.

INGBER, D.E., 2003a. Tensegrity I. Cell structure and hierarchical systems biology. *J Cell Sci,* **116**(Pt), pp. 1157-73.

INGBER, D.E., 2003b. Tensegrity II. How structural networks influence cellular information processing networks. *J Cell Sci,* **116**(Pt), pp. 1397-408.

IQBAL, J. and ZAIDI, M., 2005. Molecular regulation of mechanotransduction. *Biochemical and Biophysical Research Communications,* **328**(3), pp. 751-755.

ISENBERG, B.C. and TRANQUILLO, R.T., 2003. Long-term cyclic distention enhances the mechanical properties of collagen-based media-equivalents. *Annals of Biomedical Engineering,* **31**(8), pp. 937-949.
ISENBERG, B.C., WILLIAMS, C. and TRANQUILLO, R.T., 2006. Small-Diameter Artificial Arteries Engineered In Vitro. *Circulation Research,* **98**(1), pp. 25-35.

IWASHINA, T., MOCHIDA, J., MIYAZAKI, T., WATANABE, T., IWABUCHI, S., ANDO, K., HOTTA, T. and SAKAI, D., 2006. Low-intensity pulsed ultrasound stimulates cell proliferation and proteoglycan production in rabbit intervertebral disc cells cultured in alginate. *Biomaterials,* **27**(3), pp. 354-361.

JELL, G., NOTINGHER, I., TSIGKOU, O., NOTINGHER, P., POLAK, J.M., HENCH, L.L. and STEVENS, M.M., 2008. Bioactive glass-induced osteoblast differentiation: A noninvasive spectroscopic study. *Journal of Biomedical Materials Research Part A,* (1).

JOCKENHOEVEL S, ZUND G, HOERSTRUP SP, SCHNELL A and TURINA M, 2002. Cardiovascular tissue engineering: a new laminar flow chamber for in vitro improvement of mechanical tissue properties. *ASAIO J,* **48**(1), pp. 8-11.

JOERIS, K., FRERICHS, J.G., KONSTANTINOV, K. and SCHEPER, T., 2002. In-situ microscopy: Online process monitoring of mammalian cell cultures. *Cytotechnology,* **38**(1), pp. 129-134.

JOHNSON, P.A., MARSHALL, D. and MARKX, G., 2006. Skin Composition Treatment (withdrawn 10.11.2006). UK: PCT/GB2006/000900.

JONES, I., CURRIE, L. and MARTIN, R., 2002. A guide to biological skin substitutes. *British Journal of Plastic Surgery,* **55**(3), pp. 185-193.

JUNQUEIRA, L.C.U., BIGNOLAS, G. and BRENTANI, R.R., 1979. Picrosirius staining plus polarization microscopy, a specific method for collagen detection in tissue sections. *The Histochemical journal,* **11**(4), pp. 447-455.

KADLER, K.E., HOLMES, D.F., TROTTER, J.A. and CHAPMAN, J.A., 1996. Collagen fibril formation. *Biochemical Journal,* **316**(1), pp. 1-11.

KATO, S., YASUKAWA, H., FUJIP, T., YAMAGUCHI, M., MIYAGI, N., OKAMOTO, K., WADA, Y., MIYAMOTO, T., MORIMATSU, M. and FOX, J.C., 2000. Coordinate regulation of matrix metalloproteinase-1 and tissue inhibitor of metalloproteinase-1 expression in human vascular smooth muscle cells. *Connective tissue research,* **41**(2), pp. 143-153.

KAUFMAN, J.J., LUO, G. and SIFFERT, R.S., 2008. Ultrasound simulation in bone. *IEEE Transactions on Ultrasonics, Ferroelectrics and Frequency Control,* **55**(6), pp. 1205-1218.

KEARNEY, E.M., PRENDERGAST, P.J. and CAMPBELL, V.A., 2008. Mechanisms of Strain-Mediated Mesenchymal Stem Cell Apoptosis. *Journal of Biomechanical Engineering,* **130**, pp. 061004.
KEARNEY, J.N., 2007. Meeting at NHSBT Liverpool, UK.

KEMP, P., 2006. History of regenerative medicine: looking backwards to move forwards. *Regenerative medicine,* **1**(5), pp. 653-669.

KESSLER, D., DETHLEFSEN, S., HAASE, I., PLOMANN, M., HIRCHE, F., KRIEG, T. and ECKES, B., 2001. Fibroblasts in Mechanically Stressed Collagen Lattices Assume a "Synthetic" Phenotype. *Journal of Biological Chemistry,* **276**(39), pp. 36575-36585.

KIM, B.-., NIKOLOVSKI, J., BONADIO, J. and MOONEY, D.J., 1999. Cyclic mechanical strain regulates the development of engineered smooth muscle tissue. *Nature Biotechnology,* **17**(10), pp. 979-983.

KINSLER, L.E., FREY, A.R., COPPENS, A.B. and SANDERS, J.V., 2000. Fundamentals of Acoustics. 4 edn. John Wiley, New York.

KOOPMAN, G., REUTELINGSPERGER, C.P., KUIJTEN, G.A., KEEHNEN, R.M., PALS, S.T. and VAN OERS, M.H., 1994. Annexin V for flow cytometric detection of phosphatidylserine expression on B cells undergoing apoptosis. *Blood,* **84**(5), pp. 1415-1420.

KÖSE, G.T., KENAR, H., HASIRCI, N. and HASIRCI, V., 2003. Macroporous poly (3-hydroxybutyrate-co-3-hydroxyvalerate) matrices for bone tissue engineering. *Biomaterials,* **24**(11), pp. 1949-1958.

KULKARNI, G.V., 1994. Serum deprivation induces apoptotic cell death in a subset of Balb/c 3T3 fibroblasts. *Journal of cell science,* **107**(5), pp. 1169-1179.

KUSHNER IV, J., KIM, D., SO, P.T.C., BLANKSCHTEIN, D. and LANGER, R.S., 2007. Dual-Channel Two-Photon Microscopy Study of Transdermal Transport in Skin Treated with Low-Frequency Ultrasound and a Chemical Enhancer. *Journal of Investigative Dermatology,* **127**, pp. 2832-2846.

LAI, C.Y., WU, C.H., CHEN, C.C. and LI, P.C., 2006. Quantitative relations of acoustic inertial cavitation with sonoporation and cell viability. *Ultrasound in medicine & biology,* **32**(12), pp. 1931-1941.
LAI-CHEONG, J.E. and MCGRATH, J.A., 2009. Structure and function of skin, hair and nails. *Medicine.*

LANGHOLZ, O., ROECKEL, D., PETERSOHN, D., BROERMANN, E., ECKES, B. and KRIEG, T., 1997. Cell-matrix interactions induce tyrosine phosphorylation of MAP kinases ERK1 and ERK2 and PLCγ-1 in two-dimensional and three-dimensional cultures of human fibroblasts. *Experimental Cell Research,* **235**(1), pp. 22-27.

LE, J., RATTNER, A., CHEPDA, T., FREY, J. and CHAMSON, A., 2002. Production of matrix metalloproteinase 2 in fibroblast reaction to mechanical stress in a collagen gel. *Archives of Dermatological Research,* **294**(9), pp. 405-410.

LEE, T.L., LIN, Y.C., MOCHITATE, K. and GRINNELL, F., 1993. Stress-relaxation of fibroblasts in collagen matrices triggers ectocytosis of plasma membrane vesicles containing actin, annexins II and VI, and beta 1 integrin receptors. *Journal of cell science,* **105**(1), pp. 167-177.

LI, J., CHEN, J. and KIRSNER, R., 2007. Pathophysiology of acute wound healing. *Clinics in dermatology,* **25**(1), pp. 9-18.

LINDAHL, G.E., CHAMBERS, R.C., PAPAKRIVOPOULOU, J., DAWSON, S.J., JACOBSEN, M.C., BISHOP, J.E. and LAURENT, G.J., 2002. Activation of fibroblast procollagen alpha 1(I) transcription by mechanical strain is transforming growth factor-beta-dependent and involves increased binding of CCAAT-binding factor (CBF/NF-Y) at the proximal promoter. *J Biol Chem,* **277**(8), pp. 6153-61.

LIU, Y., CHANDRA, A., HOURD, P. and WILLIAMS, D.J., 2008. Human Cell Culture Process Capability: A Comparison of Manual and Automated Production, December 2008.

LO, C.M., WANG, H.B., DEMBO, M. and WANG, Y., 2000. Cell movement is guided by the rigidity of the substrate. *Biophysical journal,* **79**(1), pp. 144-152.

LU, S., SACKS, M.S., CHUNG, S.Y., GLOECKNER, D.C., PRUCHNIC, R., HUARD, J., DE GROAT, W.C. and CHANCELLOR, M.B., 2005. Biaxial mechanical properties of muscle-derived cell seeded small intestinal submucosa for bladder wall reconstitution. *Biomaterials,* **26**(4), pp. 443-449.

LUPULESCU, A., 1974. Effect of calcitonin on fibroblasts and collagen formation in rabbits: An ultrastructural and scanning electron microscopic study Supported in part by NIH General Aid grant and in part by Medical School Institutional Funds. *Journal of Morphology,* **142**(4),.

MACKENNA, D., SUMMEROUR, S.R. and VILLARREAL, F.J., 2000. Role of mechanical factors in modulating cardiac fibroblast function and extracellular matrix synthesis. *Cardiovascular Research,* **46**(2), pp. 257-263.

MACNEIL, S., 2007. Progress and opportunities for tissue-engineered skin. *NATURE-LONDON-,* **445**(7130), pp. 874.

MACNEIL, S., 2006. Examining Strategic Scale-Up, *4th Annual Commercialisation of Tissue Engineering and Cell Therapy Meeting,* 14 December 2006 .

MADISON, K.C., 2003. Barrier function of the skin:"la raison d'etre" of the epidermis. *Journal of Investigative Dermatology,* **121**(2), pp. 231-241.

MARSHALL, D., 2005. *Assessing collagen content of SKN samples using Chloramine-T (Confidential).* R/2005/008. Manchester: Intercytex Ltd.

MASON, R.L., GUNST, R.F. and HESS, J.L., 2003. Statistical design and analysis of experiments: with applications to engineering and science. Wiley-Interscience.

MASON, C., 2007. Regenerative Medicine 2.0. *Regenerative medicine,* **2**(1), pp. 11-18.

MAUCK, R., SOLTZ, M., WANG, C., WONG, D., CHAO, P., VALHMU, W., HUNG, C. and ATESHIAN, G., 2000. Functional tissue engineering of articular cartilage through dynamic loading of chondrocyte-seeded agarose gels. *JOURNAL OF BIOMECHANICAL ENGINEERING-TRANSACTIONS OF THE ASME,* **122**(3), pp. 252-260.

MENDONÇA, A.C., FERREIRA, A.S., BARBIERI, C.H., THOMAZINE, J.A. and MAZZER, N., 2006. Effects of low-power pulsed ultrasound on second-intention healing of total skin injuries in rats. *Acta Ortopédica Brasileira,* **14**, pp. 152-157.

MILLER, D.L., 2007. Overview of experimental studies of biological effects of medical ultrasound caused by gas body activation and inertial cavitation. *Progress in biophysics and molecular biology,* **93**(1-3), pp. 314-330.

MITRAGOTRI, S. and KOST, J., 2004. Low-frequency sonophoresis A review. *Advanced Drug Delivery Reviews,* **56**(5), pp. 589-601.

MIYAMOTO, K., AN, H.S., SAH, R.L., AKEDA, K., OKUMA, M., OTTEN, L., THONAR, E.J.M.A. and MASUDA, K., 2005. Exposure to Pulsed Low Intensity Ultrasound Stimulates Extracellular Matrix Metabolism of Bovine Intervertebral Disc Cells Cultured in Alginate Beads. *Spine,* **30**(21), pp. 2398.
MOL A., BOUTEN C.V., ZÜND G., GÜNTER C.I., VISJAGER J.F., TURINA M.I., BAAIJENS F.P. and HOERSTRUP S.P., 2003. The relevance of large strains in functional tissue engineering of heart valves. *Thorac Cardiovasc Surg,* **51**(2), pp. 78-83.

MOL, A., VAN LIESHOUT, M.I., DAM-DE VEEN, C.G., NEUENSCHWANDER, S., HOERSTRUP, S.P., BAAIJENS, F.P.T. and BOUTEN, C.V.C., 2005. Fibrin as a cell carrier in cardiovascular tissue engineering applications. *Biomaterials,* **26**(16), pp. 3113-3121.

MOLNAR, J.A., DEFRANZO, A.J., HADAEGH, A., MORYKWAS, M.J., SHEN, P. and ARGENTA, L.C., 2004. Acceleration of Integra Incorporation in Complex Tissue Defects with Subatmospheric Pressure. *Plastic and Reconstructive Surgery,* **113**(5), pp. 1339.

MOONEY, R.G., COSTALES, C., GARNER, W., SHAW, M.C., TUAN, T.L., WU, B. and TAWIL, B., 2008. Mechanical Characteristics of Fibroblast–Fibrin Constructs: Effect of Fibrinogen and Thrombin Concentration. *Wound Repair and Regeneration,* **13**(2), pp. A4-A27.

MOONEY, R.G., COSTALES, C.A., FREEMAN, E.G., CURTIN, J.M., CORRIN, A.A., LEE, J.T., REYNOLDS, S., TAWIL, B. and SHAW, M.C., 2006. Indentation micromechanics of three-dimensional fibrin/collagen biomaterial scaffolds. *J Mater Res,* **21**, pp. 2023-2034.

MUDERA, V.C., PLEASS, R., EASTWOOD, M., TARNUZZER, R., SCHULTZ, G., KHAW, P., MCGROUTHER, D.A. and BROWN, R.A., 2000. Molecular responses of human dermal fibroblasts to dual cues: contact guidance and mechanical load. *Cell Motil Cytoskeleton,* **45**(1), pp. 1-9.

MUSCARIELLO, L., ROSSO, F., MARINO, G., GIORDANO, A., BARBARISI, M., CAFIERO, G. and BARBARISI, A., 2005. A Critical Overview of ESEM Applications in the Biological Field. *Journal of cellular physiology,* **205**(3), pp. 328.

NEIDERT, M.R. and TRANQUILLO, R.T., 2006. Tissue-Engineered Valves with Commissural Alignment. *Tissue engineering,* **12**(4), pp. 891-903.

NEIDERT, M.R., LEE, E.S., OEGEMA, T.R. and TRANQUILLO, R.T., 2002. Enhanced fibrin remodeling in vitro with TGF-[beta]1, insulin and plasmin for improved tissue-equivalents. *Biomaterials,* **23**(17), pp. 3717-3731.

NEIDLINGER-WILKE, C., WURTZ, K., LIEDERT, A., SCHMIDT, C., BORM, W., IGNATIUS, A., WILKE, H.J. and CLAES, L., 2005. A three-dimensional collagen matrix as a suitable culture system for the comparison of cyclic strain and hydrostatic pressure effects on intervertebral disc cells. *J Neurosurg Spine,* **2**(4), pp. 457-65.

NETO, J.C., AGERO, U., GAZZINELLI, R.T. and MESQUITA, O.N., 2006. Measuring optical and mechanical properties of a living cell with defocusing microscopy. *Biophysical journal,* **91**(3), pp. 1108-1115.

NG, G.Y.F., NG, C.O.Y. and SEE, E.K.N., 2004. Comparison of therapeutic ultrasound and exercises for augmenting tendon healing in rats. *Ultrasound in medicine & biology,* **30**(11), pp. 1539-1543.
NG, G.Y.F. and WONG, R.Y.F., 2008. Ultrasound Phonophoresis of Panax Notoginseng Improves the Strength of Repairing Ligament: A Rat Model. *Ultrasound in medicine & biology,* **34**(12), pp. 1919-1923.

NG, C.P., HINZ, B. and SWARTZ, M.A., 2005. Interstitial fluid flow induces myofibroblast differentiation and collagen alignment in vitro. *Journal of Cell Science,* **118**(20), pp. 4731-4739.
NG, C.P. and SWARTZ, M.A., 2003. Fibroblast alignment under interstitial fluid flow using a novel 3-D tissue culture model. *American Journal of Physiology - Heart and Circulatory Physiology,* **284**(5 53-5), pp. H1771-H1777.

NIJSSEN, A., SCHUT, T.C.B., HEULE, F., CASPERS, P.J., HAYES, D.P., NEUMANN, M.H.A. and PUPPELS, G.J., 2002. Discriminating basal cell carcinoma from its surrounding tissue by Raman spectroscopy. *Journal of Investigative Dermatology,* **119**(1), pp. 64-69.

NISHIKORI, T., OCHI, M., UCHIO, Y., MANIWA, S., KATAOKA, H., KAWASAKI, K., KATSUBE, K. and KURIWAKA, M., 2002. Effects of low-intensity pulsed ultrasound on proliferation and chondroitin sulfate synthesis of cultured chondrocytes embedded in Atelocollagen gel. *Mater Res,* **59**, pp. 201-206.

NORIEGA, S., MAMEDOV, T., TURNER, J.A. and SUBRAMANIAN, A., 2007. Intermittent Applications of Continuous Ultrasound on the Viability, Proliferation, Morphology, and Matrix Production of Chondrocytes in 3D Matrices. *Tissue engineering,* **13**(3), pp. 611-618.

OGURA, M., PALIWAL, S. and MITRAGOTRI, S., 2008. Low-frequency sonophoresis: Current status and future prospects. *Advanced Drug Delivery Reviews.*

OHL, C.D. and WOLFRUM, B., 2003. Detachment and sonoporation of adherent HeLa-cells by shock wave-induced cavitation. *BBA-General Subjects,* **1624**(1-3), pp. 131-138.

O'HALLORAN, D.M. and PANDIT, A.S., 2007. Tissue-engineering approach to regenerating the intervertebral disc. *Tissue engineering,* **13**(8), pp. 1927-1954.

PAEZ, G., JOSE, M., CARRERA, A., CORDON, A., JORGE-HERRERO, E., ROCHA, A., SALVADOR, J., MENDEZ, J., CASTILLO-OLIVARES, J.L. and MILLAAN, I., 2000. Uniaxial and Biaxial Tensile Strength of Calf Pericardium Used in the Construction of Bioprostheses: Biomaterial Selection Criteria. *Journal of Biomaterials Applications,* **15**(1), pp. 47.

PAGE-MCCAW, A., EWALD, A.J. and WERB, Z., 2007. Matrix metalloproteinases and the regulation of tissue remodelling. *Nature Reviews Molecular Cell Biology,* **8**(3), pp. 221-233.

PARVIZI, J., PARPURA, V., GREENLEAF, J.F. and BOLANDER, M.E., 2002. Calcium signaling is required for ultrasound-stimulated aggrecan synthesis by rat chondrocytes. *Journal of Orthopaedic Research,* **20**(1), pp. 51-57.

PERRY, M.J., PARRY, L.K., BURTON, V.J., GHEDUZZI, S., BERESFORD, J.N., HUMPHREY, V.F. and SKERRY, T.M., 2009. Ultrasound mimics the effect of mechanical loading on bone formation in vivo on rat ulnae. *Medical Engineering and Physics,* **31**(1), pp. 42-47.

POHL, P., ANTONENKO, Y.N. and ROSENFELD, E., 1993. Effect of ultrasound on the pH profiles in the unstirred layers near planar bilayer lipid membranes measured by microelectrodes. *Biochimica et biophysica acta,* **1152**(1), pp. 155-160.

PÖRTNER, R., NAGEL-HEYER, S., GOEPFERT, C., ADAMIETZ, P. and MEENEN, N.M., 2005. Bioreactor design for tissue engineering. *Journal of bioscience and bioengineering,* **100**(3), pp. 235-245.

PRAJAPATI, R.T., CHAVALLY-MIS, B., HERBAGE, D., EASTWOOD, M. and BROWN, R.A., 2000a. Mechanical loading regulates protease production by fibroblasts in three-dimensional collagen substrates. *Wound Repair and Regeneration,* **8**(3), pp. 226-237.

PRAJAPATI, R.T., EASTWOOD, M. and BROWN, R.A., 2000b. Duration and orientation of mechanical loads determine fibroblast cyto- mechanical activation: Monitored by protease release. *Wound Repair and Regeneration,* **8**(3), pp. 238-246.

RAMIREZ, A., SCHWANE, J.A., MCFARLAND, C. and STARCHER, B., 1997. The effect of ultrasound on collagen synthesis and fibroblast proliferationin vitro. *Medicine & Science in Sports & Exercise,* **29**(3), pp. 326.

RAO, M.A., 2007. Rheology of fluid and semisolid foods: principles and applications. Springer Verlag.
ROBINS, S.P., MILNE, G., DUNCAN, A., DAVIES, C., BUTT, R., GREILING, D. and JAMES, I.T., 2003. Increased Skin Collagen Extractability and Proportions of Collagen Type III Are Not Normalized after 6 Months Healing of Human Excisional Wounds. *Journal of Investigative Dermatology,* **121**, pp. 267-272.

ROBINSON, P.S., JOHNSON, S.L., EVANS, M.C., BAROCAS, V.H. and TRANQUILLO, R.T., 2008. Functional Tissue-Engineered Valves from Cell-Remodelled Fibrin with Commissural Alignment of Cell-Produced Collagen. *Tissue Engineering Part A,* **14**(1), pp. 83-95.

RODRIGUEZ, C., MARTINEZ-GONZALEZ, J., RAPOSO, B., ALCUDIA, J.F., GUADALL, A. and BADIMON, L., 2008. Regulation of lysyl oxidase in vascular cells: lysyl oxidase as a new player in cardiovascular diseases. *Cardiovascular research.*

ROSS, J.J. and TRANQUILLO, R.T., 2003. ECM gene expression correlates with in vitro tissue growth and development in fibrin gel remodelled by neonatal smooth muscle cells. *Matrix Biol,* **22**(6), pp. 477-90.

SADAVA, D.E., 1993. Cell biology: organelle structure and function. Jones and Bartlett Publishers.
SALES, V.L., ENGELMAYR JR, G.C., METTLER, B.A., JOHNSON JR, J.A., SACKS, M.S. and MAYER JR, J.E., 2006. Transforming Growth Factor-{beta} 1 Modulates Extracellular Matrix Production, Proliferation, and Apoptosis of Endothelial Progenitor Cells in Tissue-Engineering Scaffolds. *Circulation,* **114**(1_suppl).

SANDER, E.A., JOHNSON, S.L., BAROCAS, V.H. and TRANQUILLO, R.T., 2008. Matrix remodeling in fibroblast-seeded fibrin gels. *Matrix Biology,* **27**(Supplement 1), pp. 28-28.

SCHULZ, R.M., WUSTNECK, N., VAN DONKELAAR, C.C., SHELTON, J.C. and BADER, A., 2008. Development and validation of a novel bioreactor system for load-and perfusion-controlled tissue engineering of chondrocyte-constructs. *Biotechnology and bioengineering,* **101**(4), pp. 714-728.

SCHWARZ, U.S., BALABAN, N.Q., RIVELINE, D., BERSHADSKY, A., GEIGER, B. and SAFRAN, S.A., 2002. Calculation of forces at focal adhesions from elastic substrate data: the effect of localized force and the need for regularization. *Biophysical journal,* **83**(3), pp. 1380-1394.

SCREEN, H.R.C., LEE, D.A., BADER, D.L. and SHELTON, J.C., 2004. An investigation into the effects of the hierarchical structure of tendon fascicles on micromechanical properties. *Proceedings of the Institution of Mechanical Engineers, Part H: Journal of Engineering in Medicine,* **218**(2), pp. 109-119.

SCREEN, H.R.C., SHELTON, J.C., BADER, D.L. and LEE, D.A., 2005. Cyclic tensile strain upregulates collagen synthesis in isolated tendon fascicles. *Biochemical and Biophysical Research Communications,* **336**(2), pp. 424-429.

SELIKTAR D., BLACK RA., VITO R.P. and NEREM RM., 2000. Dynamic mechanical conditioning of collagen-gel blood vessel constructs induces remodelling in vitro. *Ann Biomed Eng,* **28**(4), pp. 351-62.

SELIKTAR, D., NEREM, R.M. and GALIS, Z.S., 2003. Mechanical strain-stimulated remodelling of tissue-engineered blood vessel constructs. *Tissue Engineering,* **9**(4), pp. 657-666.

SELIKTAR, D., NEREM, R.M. and GALIS, Z.S., 2001. The role of matrix metalloproteinase-2 in the remodelling of cell-seeded vascular constructs subjected to cyclic strain. *Annals of Biomedical Engineering,* **29**(11), pp. 923-934.

SILVER, F.H., SEEHRA, G.P., FREEMAN, J.W. and DEVORE, D., 2002. Viscoelastic properties of young and old human dermis: A proposed molecular mechanism for elastic energy storage in collagen and elastin. *Journal of Applied Polymer Science,* **86**(8), pp. 1978-1985.

SILVER, F.H., SIPERKO, L.M. and SEEHRA, G.P., 2003. Mechanobiology of force transduction in dermal tissue. *Skin Research and Technology,* **9**(1), pp. 3-23.

SIU, T., JACKSON, J., BURT, H. and CHIAO, M., 2007. Drug Uptake Enhancement Using Sonodynamic Effects at 4 MHz—A Potential Application for Micro-Ultrasonic-Transducers. *IEEE Transactions on Biomedical Engineering,* **54**(6 Part 2), pp. 1153-1156.

SNIADECKI, N.J., ANGUELOUCH, A., YANG, M.T., LAMB, C.M., LIU, Z., KIRSCHNER, S.B., LIU, Y., REICH, D.H. and CHEN, C.S., 2007. Magnetic microposts as an approach to apply forces to living cells. *Proceedings of the National Academy of Sciences,* **104**(37), pp. 14553.

SPUDICH, J.A., PELHAM, R.J. and WANG, Y., 1999. High resolution detection of mechanical forces exerted by locomoting fibroblasts on the substrate. *Molecular biology of the cell,* **10**(4), pp. 935-945.

STAMENKOVIC, I., 2003. Extracellular matrix remodelling: the role of matrix metalloproteinases. *The Journal of pathology,* **200**(4).

STARBORG, T., LU, Y., MEADOWS, R.S., KADLER, K.E. and HOLMES, D.F., 2008. Electron microscopy in cell-matrix research. *Methods,* **45**(1), pp. 53-64.

STARRITT, H.C., DUCK, F.A. and HUMPHREY, V.F., 1991. Forces acting in the direction of propagation in pulsed ultrasound fields. *Physics in Medicine and Biology,* **36**, pp. 1465-1474.

STARRITT, H.C., DUCK, F.A. and HUMPHREY, V.F., 1989. An experimental investigation of streaming in pulsed diagnostic ultrasound beams. *Ultrasound in medicine & biology,* **15**(4), pp. 363-373.

STARRITT, H.C., HOAD, C.L., DUCK, F.A., NASSIRI, D.K., SUMMERS, I.R. and VENNART, W., 2000. Measurement of acoustic streaming using magnetic resonance. *Ultrasound in medicine & biology,* **26**(2), pp. 321-333.

STEGEMANN, H. and STALDER, K., 1967. Determination of hydroxyproline. *Clinica chimica acta; international journal of clinical chemistry,* **18**(2), pp. 267-273.

SUSLICK, K.S. and NYBORG, W.L., 1990. ULTRASOUND: Its Chemical, Physical and Biological Effects. *The Journal of the Acoustical Society of America,* **87**, pp. 919.

SYEDAIN, Z.H., WEINBERG, J.S. and TRANQUILLO, R.T., 2008. Cyclic distension of fibrin-based tissue constructs: Evidence of adaptation during growth of engineered connective tissue. *Proceedings of the National Academy of Sciences,* **105**(18), pp. 6537.

TAKEUCHI, R., RYO, A., KOMITSU, N., MIKUNI-TAKAGAKI, Y., FUKUI, A., TAKAGI, Y., SHIRAISHI, T., MORISHITA, S., YAMAZAKI, Y. and KUMAGAI, K., 2008. Low-intensity pulsed ultrasound activates the PI3K/Akt pathway and stimulates the growth of chondrocytes in 3D-cultures: a basic science study. *Arthritis Research & Therapy,* **10**(4), pp. R77.

TANG, C.H., LU, D.Y., TAN, T.W., FU, W.M. and YANG, R.S., 2007. Ultrasound Induces Hypoxia-inducible Factor-1 Activation and Inducible Nitric-oxide Synthase Expression through the Integrin/Integrin-linked Kinase/Akt/Mammalian Target of Rapamycin Pathway in Osteoblasts. *Journal of Biological Chemistry,* **282**(35), pp. 25406.

TER HAAR, G., 2007. Therapeutic applications of ultrasound. *Progress in biophysics and molecular biology,* **93**(1-3), pp. 111-129.

THAMPATTY, B.P., LI, H., HEE-JEONG, I. and WANG, J.H.-., 2007. EP4 receptor regulates collagen type-I, MMP-1, and MMP-3 gene expression in human tendon fibroblasts in response to IL-1β treatment. *Gene,* **386**(1-2), pp. 154-161.

TINARI, A., GIAMMARIOLI, A.M., MANGANELLI, V., CIARLO, L. and MALORNI, W., 2008. Analysing Morphological and Ultrastructural Features in Cell Death. *Programmed Cell Death: General Principles for Studying Cell Death,* , pp. 15.

TOMASEK, J.J., GABBIANI, G., HINZ, B., CHAPONNIER, C. and BROWN, R.A., 2002. Myofibroblasts and mechano: Regulation of connective tissue remodelling. *Nature Reviews Molecular Cell Biology,* **3**(5), pp. 349-363.

TSAI, W.C., PANG, J.H., HSU, C.C., CHU, N.K., LIN, M.S. and HU, C.F., 2006. Ultrasound stimulation of types I and III collagen expression of tendon cell and upregulation of transforming growth factor b. *J Orthop Res,* **24**, pp. 1310-1316.

TUAN, T.L., SONG, A., CHANG, S., YOUNAI, S. and NIMNI, M.E., 1996. In VitroFibroplasia: Matrix Contraction, Cell Growth, and Collagen Production of Fibroblasts Cultured in Fibrin Gels. *Experimental Cell Research,* **223**(1), pp. 127-134.

TURNER, S.M., POWELL, E.S. and NG, C.S.S., 1989. The Effect of Ultrasound on the Healing of Repaired Cockerel Tendon: Is Collagen Crosslinkage a Factor? *Journal of Hand Surgery (European Volume),* **14**(4), pp. 428.

VENTRE, M., MOLLICA, F. and NETTI, P.A., 2009. The effect of composition and microstructure on the viscoelastic properties of dermis. *Journal of Biomechanics,* **42**(4), pp. 430-435.

VERRECCHIA F. and MAUVIEL A., 2002. Transforming growth factor-beta signaling through the Smad pathway: role in extracellular matrix gene expression and regulation. *J Invest Dermatol,* **118**(2), pp. 211-5.

WANG, N., TYTELL, J.D. and INGBER, D.E., 2009. Mechanotransduction at a distance: mechanically coupling the extracellular matrix with the nucleus.

WARDEN, S.J., FAVALORO, J.M., BENNELL, K.L., MCMEEKEN, J.M., NG, K.W., ZAJAC, J.D. and WARK, J.D., 2001. Low-intensity pulsed ultrasound stimulates a bone-forming response in UMR-106 cells. *Biochemical and biophysical research communications,* **286**(3), pp. 443-450.

WEBB, K., HITCHCOCK, R.W., SMEAL, R.M., LI, W., GRAY, S.D. and TRESCO, P.A., 2006. Cyclic strain increases fibroblast proliferation, matrix accumulation, and elastic modulus of fibroblast-seeded polyurethane constructs. *Journal of Biomechanics,* **39**(6), pp. 1136-1144.

WEBSTER, D.F., POND, J.B., DYSON, M. and HARVEY, W., 1978. The role of cavitation in the in vitro stimulation of protein synthesis in human fibroblasts by ultrasound. *Ultrasound in medicine & biology,* 4(4), pp. 343-351.

WELCH, H.G., WOLOSHIN, S. and SCHWARTZ, L.M., 2005. Skin biopsy rates and incidence of melanoma: population based ecological study. *British medical journal,* **331**(7515), pp. 481.

WILLIAMS, A.R., 1983. Ultrasound: Biological effects and potential hazards. *ACADEMIC PRESS, LONDON(UK).1983.,* .

WOLBERG, A.S., 2007. Thrombin generation and fibrin clot structure. *Blood reviews,* **21**(3), pp. 131-142.

WRIGHT, E.R., CONTICELLO, V.P. and APKARIAN, R.P., 2003. Morphological characterization of elastin-mimetic block copolymers utilizing cryo-and cryoetch-HRSEM. *Microscopy and Microanalysis,* 9(03), pp. 171-182.

YANG, L., SHIRAKATA, Y., TAMAI, K., DAI, X., HANAKAWA, Y., TOKUMARU, S., YAHATA, Y., TOHYAMA, M., SHIRAISHI, K. and NAGAI, H., 2005. Microbubble-enhanced ultrasound for gene transfer into living skin equivalents. *Journal of dermatological science,* **40**(2), pp. 105-114.

YANG, R.S., LIN, W.L., CHEN, Y.Z., TANG, C.H., HUANG, T.H., LU, B.Y. and FU, W.M., 2005. Regulation by ultrasound treatment on the integrin expression and differentiation of osteoblasts. *Bone,* **36**(2), pp. 276-283.

YEUNG, T., GEORGES, P.C., FLANAGAN, L.A., MARG, B., ORTIZ, M., FUNAKI, M., ZAHIR, N., MING, W., WEAVER, V. and JANMEY, P.A., 2005. Effects of substrate stiffness on cell morphology, cytoskeletal structure, and adhesion. *Cell motility and the cytoskeleton,* **60**(1), pp. 24-34.

YE, Q., ZÜND, G., BENEDIKT, P., JOCKENHOEVEL, S., HOERSTRUP, S.P., SAKYAMA, S., HUBBELL, J.A. and TURINA, M., 2000. Fibrin gel as a three dimensional matrix in cardiovascular tissue engineering. *European Journal of Cardio-Thoracic Surgery,* **17**(5), pp. 587-591.

YEUNG, C.K., GUO, X. and NG, Y.F., 2006. Pulsed ultrasound treatment accelerates the repair of Achilles tendon rupture in rats. *Journal of orthopaedic research : official publication of the Orthopaedic Research Society,* **24**(2), pp. 193-201.

ZHANG, Z.J., HUCKLE, J., FRANCOMANO, C.A. and SPENCER, R.G., 2003. The effects of pulsed low-intensity ultrasound on chondrocyte viability, proliferation, gene expression and matrix production. *Ultrasound in medicine & biology,* **29**(11), pp. 1645-1651.

ZHOU, S., SCHMELZ, A., SEUFFERLEIN, T., LI, Y., ZHAO, J. and BACHEM, M.G., 2004. Molecular Mechanisms of Low Intensity Pulsed Ultrasound in Human Skin Fibroblasts. *Journal of Biological Chemistry,* **279**(52), pp. 54463.

ZISKIN, M.C., 1987. Applications of ultrasound in medicine—comparison with other modalities. *Ultrasound: Medical applications, biological effects, and hazard potential.Plenum Press, New York,* , pp. 49-59.

Appendix I Manual Experimental Operating Procedures and Automated CompacT SelecT Programs for Culture and of Human Dermal Fibroblasts

Experimental Operating Procedure EOP012 Manual Culture of Human Dermal Fibroblasts

1. PURPOSE

This document describes the procedure for the manual culture of human dermal fibroblast cells grown in monolayer in culture vessels.

2. SCOPE

This EOP is intended to describe specific protocol for the manual culture of human dermal fibroblasts grown in monolayer culture for creating a master and working cell bank. It should be read in conjunction with SOP 012 "Manual Culture of Human Osteoblast like cell line" and relevant local SOPs

3. SPECIAL NOTES – HEALTH & SAFETY

3.1. Risk is low when work involves authenticated cell lines derived from pathogen free animals or cell lines which are known to be free of adventitious agents

3.2. HOWEVER, ALL WORK WITH HUMAN CELLS MUST BE CARRIED OUT UNDER THE ASSUMPTION THAT THE SPECIMIN MAY CARRY AN INFECTIOUS AGENT.

3.3. Human-derived cells may be carrying adventitious agents. Treat as potentially hazardous. Inoculation against Hepatitis B may be appropriate.

3.4. Wear lab coat and gloves.

3.5. Work in a Microbiological Safety Cabinet (MSC).

3.6. Most gases used in cell culture (CO_2, O_2, N_2) are not harmful in small amounts but can be dangerous if handled improperly. When a major leak occurs, there is a risk of asphyxiation from CO_2 and N_2, and a fire hazard from O_2. evacuation and ventilation are necessary in each case.

4. REFERENCES

EOP008 Recovery of Human Dermal Fibroblasts from cryopreservation
EOP013 Trypsinisation of Human Dermal Fibroblasts
SOP003 Disposal and Disinfection of Biological Waste
SOP009 Use and Maintenance of BSC-G2000 Vertical Laminar Airflow Cabinet
SOP020 Use and Maintenance of Water Bath
SOP015 Use and maintenance of the BOECO U032R
SOP022 Use and maintenance of Microscope
SOP025 Use and Maintenance of CO2 Incubator
SOP034 Cell Counting and Viability Assessment
School Risk Assessment SAF/MM/1638 Processes of Cell Culture
Biological Risk Assessment BRA/MM/0003 Isolation, culture and cryopreservation of human, neonatal dermal fibroblasts (HDFs)

5. RESPONSIBILITIES

5.1. This process is for use in the Loughborough University Cell Culture laboratory, T208b, and should be used according to the general rules and local SOPs for using T208b and with good laboratory practice.

5.2. It is the responsibility of the person performing the operation and of their supervisor to ensure that adequate training has been received and that this document is followed as written.

6. EQUIPMENT AND MATERIALS

Equipment

- Biological Safety Cabinet
- Centrifuge (capable of centrifuging 15 or 50ml tubes at 500g)
- Water bath
- Aspirator and pump
- Haemocytometer with cover glass
- Microscope inverted
- Culture flasks (size and quantity as required)
- Pipettes (5ml – 50ml)

Materials

- DMEM-10 media (prepared according to EOP Preparation of DMEM-10)

7. PROCEDURE

7.1. Obtain a cell suspension by trypsinisation according to EOP013 Trypsinisation of Cells, or from recovery from cryopreservation according to EOP008 Recovery of Human Dermal Fibroblasts from Cryopreservation.

7.2. Count cells in suspension according to SOP034 Cell Counting and Viability Assessment" to obtain the cell density

7.3. Calculate the volume of cell suspension required for each flask to be plated by multiplying the surface area of the plating flasks (cm^2) by the required cell density (2500-6000cells/cm^2). Then divide the total number of cells required by the concentration of cells in the cell suspension (cells/ml)

7.4. In the BSC, dilute the stock cell suspension with DMEM-10 if necessary so that at least 1ml of cell suspension can be used in each new culture flask to be plated. The new cell suspension volume required can be calculated as follows. Calculate the new concentration of stock required by dividing the total number of cells required for plating (0.45×10^6) by the desired volume of the cell suspension for plating (e.g. 1ml). Then calculate the new volume of stock required by dividing the total number of cells in the original cell suspension, by the new required concentration. Finally, calculate the additional volume of DMEM-10 required by subtracting the new volume required, by the volume of original cell suspension.

7.5. In the BSC, place sufficient DMEM-10 to the culture flasks to be plated, see table 1, and then the appropriate volume of the new cell suspension prepared in step 7.4.

Flask Size	DMEM-10 (mL)	Cell Suspension (mL)	Minimum Seeding Volume (mL)
T25	5-6	1-2	6
T75	15-20	1-2	16
T175	30-40	1-2	31

Table 1 – Guide to the volume of media and cell suspension to use when culturing HDFs

7.6. Incubate the flasks at 37 °C according to SOP025 Use and Maintenance of CO2 Incubator.

7.7. Every 2-3days, transfer the flasks to the BSC and change the DMEM-10 media, by aspirating the media and replacing with new DMEM-10, until cells are confluent as seen under a microscope (according to SOP022 Use and maintenance of Microscope). See Table 2. Dispose of the used media according to SOP003 Disposal and Disinfection of Biological Waste

7.8. When the cells become confluent, transfer the flasks to the BSC and trypsinise the cells (according to EOP013 Trypsinisation of Human Dermal Fibroblasts). Obtain an appropriate cell suspensions for further cell culture by repeating steps 7.1 – 7.7; for casting of SKN constructs (according to EOP014 Casting of SKN Constructs), or for freezing and storage (according to EOP011 Cryopreservation and Storage of Human Dermal Fibroblasts).

8. DOCUMENTATION

All results should be recorded in the Laboratory note book

Experimental Operating Procedure EOP008 Recovery of Human Dermal Fibroblasts

1. PURPOSE

This document describes the procedure for the recovery of viable human dermal fibroblast cells that have been cryopreserved in liquid nitrogen.

2. SCOPE

This EOP is intended to describe specific protocol for recovering human dermal fibroblasts that have been cryopreserved in liquid nitrogen and must be read in conjunction with SOP 0032 "The Resuscitation of Cryopreserved Mammalian Cell Lines" and other relevant local SOPs

3. SPECIAL NOTES – HEALTH & SAFETY

3.7. Human-derived cells may be carrying adventitious agents. Treat as potentially hazardous. Inoculation against Hepatitis B may be appropriate.
3.8. Wear lab coat and gloves.
3.9. Work in a Biological Safety Cabinet (BSC).
3.10. See Safety Issues as detailed in SOP032 "The Resuscitation of Cryopreserved Mammalian Cell Lines" and
3.11. Personnel who use liquid nitrogen are required to be trained, and familiar with SOP013 "Use and Maintenance of Liquid Nitrogen Stores". PPE including thermally insulated gloves (able to withstand temperatures from -160°C to 150°C), lab coat and face shield are required

4. REFERENCES

SOP003 Disposal and Disinfection of Biological Waste
SOP009 Use and Maintenance of BSC-G2000 Vertical Laminar Airflow Cabinet
SOP013 Use and Maintenance of Liquid Nitrogen Stores
SOP020 Use and Maintenance of Water Bath
SOP015 Use and maintenance of the BOECO U032R
SOP025 Use and Maintenance of CO2 Incubator
SOP034 Cell Counting and Viability Assessment
Biological Risk Assessment BRA/MM/0004 Isolation, culture and cryopreservation of human, neonatal dermal fibroblasts (HDFs)

5. RESPONSIBILITIES

5.1. This process is for use in the Loughborough University Cell Culture laboratory, T208b, and should be used according to the general rules and local SOPs for using T208b and with good laboratory practice.
5.2. It is the responsibility of the person performing the operation and of their supervisor to ensure that adequate training has been received and that this document is followed as written.

6. EQUIPMENT AND MATERIALS

Equipment

- Biological Safety Cabinet
- Centrifuge (capable of centrifuging 15 or 50ml tubes at 500g)
- Water bath

- Liquid nitrogen store
- Aspirator and pump
- Haemocytometer with cover glass
- Microscope inverted
- Plastic Serological Pipettes (1-50ml)
- 50ml Falcon tube
- Appropriate culture flasks

Materials

- DMEM-10 prepared according to EOP Preparation of DMEM-10
- Cryovial of Human Dermal Fibroblasts

7. PROCEDURE

7.1. Remove DMEM-10 from the fridge and allow to reach room temperature.

7.2. In the BSC, place 40ml of DMEM-10 into a 50ml falcon tube

7.3. Remove the cryovial containing human dermal fibroblasts from the liquid nitrogen store according to SOP013 Use and Maintenance of Liquid Nitrogen Stores

7.4. Rapidly thaw the cryovial in a 37°C water bath by swirling the cryovial but ensuring that the cryovial cap remains dry (according to SOP020 Use and Maintenance of Water Bath)

7.5. Once fully thawed, transfer the cryovial to the BSC and place the cell suspension into the 40ml of DMEM-10 using a pipette.

7.6. Place 1ml of the DMEM-10 from the falcon tube into the cryovial to recover any cell from the surface and replace the solution back into the falcon tube using a pipette.

7.7. Count the cells according to SOP034 Cell Counting and Viability Assessment and calculate the required volume of DMEM-10 to suspend the cells at the required density for further manual culture (according to EOP012 "Manual Culture of Human dermal Fibroblasts").

7.8. Replace the cap on the falcon tube and centrifuge at 500g for 5mins to obtain a cell pellet according to SOP015 Use and maintenance of the BOECO U032R

7.9. Transfer the tube back to the BSC and aspirate the supernatant and dispose of according to SOP003 Disposal and Disinfection of Biological Waste. Replace cap and flick the bottom of the falcon tube to distribute the cells in the pellet

7.10. Resuspend the pellet in the required volume of DMEM-10 as calculated in step 7.6

7.11. Mix the cell suspension to obtain a homogeneous single cell suspension by drawing up and expelling the suspension with a pipette

7.12. Use the cell suspension to culture the cells according to EOP012 Manual Culture of Human Dermal Fibroblasts

8. DOCUMENTATION

All results should be recorded in the Laboratory note book

Automated CompacT SelecT Program for Cell Seeding and Counting

This program measures the cell concentration of a human dermal fibroblasts suspension in a T175 flask (assigned the name "pool") imported into the CompacT SelecT for passaging. The appropriate volume of media is added to the flask to achieve the desired cell concentration (875000cells/mL) and new flasks are seeded from this cell suspension.

```
<SelecT_Protocol>

 <properties>
  <description> Seeding  </description>
  <flaskingtime units="s">0</flaskingtime>
  <platingtime units="s">0</platingtime>
 </properties>

 <steps>

  <fetch>
  <putdown name = "pool"/>
  <mix     name = "pool"
       volume = "10ml"
       repeat = "2"
       fromheight = "2mm"
       toheight = "50mm"
       mixspeed = "2ml/s"
       finaldispensespeed = "1ml/s"
       newtip = "yes"/>


  <count     name = "pool"
       fromheight = "2mm"
       aspiratespeed = "5ml/s"
       dispensespeed = "5ml/s"/>
  <pickup name = "pool"/>

  <dispense liquid = "DMEM10"
       volume = "0ml"
       cellconc = "875000"
       minvolume = "0ml"
       maxvolume = "10ml"/>
  <putdown name = "pool"/>

  <new repeat = "27"
       flasktypegroup = "Single">
  <dispense liquid = "DMEM10"
       volume = "29ml"/>
  <putdown name = "output"/>
```

```
  <mix    name = "pool"
      volume = "10ml"
      repeat = "2"
      fromheight = "2mm"
      toheight = "2mm"
      mixspeed = "2ml/s"
      finaldispensespeed = "2ml/s"/>
  <pipette    fromname = "pool"
      toname = "output"
      volume = "1.0ml"
      fromheight = "2mm"
      toheight = "50mm"
      aspiratespeed = "1ml/s"
      dispensespeed = "1ml/s"/>
  <pickup name = "output"/>

 <store passage = "yes" robotspeed = "100%"/>
  </new>

  <pickup name = "pool"/>
  <dispose/>

  </fetch>

 </steps>
</SelecT_Protocol>
```

Automated CompacT SelecT Program for Media Change

This program disposes of the culture media in the flasks and adds fresh culture media

```
<SelecT_Protocol>

 <properties>
  <description> Media Change </description>
  <flaskingtime units="s">0</flaskingtime>
  <platingtime units="s">0</platingtime>
 </properties>

 <steps>

  <fetch>
  <dump pause = "2s"/>
  <dispense liquid = "DMEM10"
      volume = "30ml"/>
  <store passage = "no"/>

  </fetch>

 </steps>
</SelecT_Protocol>
```

Automated CompacT SelecT Program for Cell Harvesting

This program detaches adherent cells from the flask using trypsin and combines the cell suspension from individual flasks into a "pool" flask. Nine individual flasks are pooled before export of the pool flask for cryopreservation of further passaging. Two flasks are processed during the trypsin incubation period of another flask (interleave=3)

```
<SelecT_Protocol>
 <properties>
  <description> Pool and Harvest </description>
  <flaskingtime units="s">0</flaskingtime>
  <platingtime units="s">0</platingtime>
 </properties>

 <steps>
  <new flasktypegroup = "Single">
  <putdown name = "pool"/>
  </new>
  <fetch maxrepeat = "9" staggertime = "0s" interleave = "3">

  <dump pause = "2s"/>
  <dispense liquid = "PBS"
      volume = "10ml"/>
  <swirl repeat = "1" speed = "100%" pause = "0s" capped = "no"/>
   <dump pause = "2s" robotspeed = "100%"/>
<dispense liquid = "JASTRYPSIN"
      volume = "6ml"
                          robotspeed = "100%"/>
 <swirl repeat = "1" speed = "100%" pause = "0s" capped = "yes"/>
    <incubate period = "6m"/>
  <shake repeat = "6" speed = "50%" pause = "0s" capped = "yes"/>
  <dispense liquid = "DMEM10"
      volume = "6ml"
      robotspeed = "100%"/>
 <swirl repeat = "1" speed = "100%" pause = "0s" capped = "no"/>
 <pour name = "pool" pause = "4s" robotspeed = "100%"/>

   <dispose robotspeed = "100%"/>
  </fetch>

  <mix    name = "pool"
      volume = "10ml"
      repeat = "6"
      fromheight = "2mm"
      toheight = "2mm"
      mixspeed = "5ml/s"
      finaldispensespeed = "5ml/s"
      newtip = "yes"/>

  <count    name = "pool"
      fromheight = "2mm"
```

```
      newtip = "no"/>
   <pickup name = "pool"/>
   <outfeed passage = "no"/>

  </steps>
</SelecT_Protocol>
```

Appendix II Protocols for the Preparation and Staining of Paraffin Wax Histology Sections

Leica TP 1020 Automatic Tissue Processor reagents and timings for preparation of wax embedded samples for histology and immunohistochemistry

Reagent	Duration (hour)
10% Formal Saline	1
10% Formal Saline	1
70% Ethanol	1.5
80% Ethanol	1.5
96% Ethanol	1.5
100% Ethanol	1
100% Ethanol	1
100% Ethanol	1
Xylene	1.5
Xylene	1.5
Paraffin Wax	2
Paraffin Wax	2

Masson's Trichrome Histological Staining Protocol (reproduced with permission from the Advance Microscopy Unit, Nottingham University)

Method developed for the staining of fibrin, collagen and cell nuclei in SKN constructs:

- Rehydrate cut section in a series of decreasing ethanol concentrations (100% three times, 90%, 70%, 50%) and then in water.
- Stain with 4%Iron Alum for 5 minutes
- Wash in tap water
- Stain with Mayers Haematoxylin for 1 minute
- Wash in tap water until nuclei appear blue
- Stain with Ponceau Acid Fuschin for 5 minutes
- Wash in tap water
- Differentiate in 1% Phosphomolybdic acid, observe under microscope until collagen appears clear
- Stain in 0.2% light green in 0.2% acetic acid for 2 minutes
- Dehydrate, clear and mount

Collagen stains blue/green

Nuclei stain blue/black

Fibrin and cytoplasm stain red

Figure 60 Cross-section of human liver stained with Masson's Trichrome as a control. Collagen fibres (blue), fibrin fibres (purple/red) and cell nuclei (dark blue black)

Alcian Blue Histological Staining Protocol (reproduced with permission from the Advance Microscopy Unit, Nottingham University)

Method developed for the staining of proteoglycans in SKN constructs:

- Rehydrate cut section in a series of decreasing ethanol concentrations (100% three times, 90%, 70%, 50%) and then in water.
- Stain with Alcian Blue pH 2.5 (1g Alcian Blue in 100ml of 3% acetic acid) for 5 minutes
- Wash in tap water
- Counterstain in 0.1% nuclear fast red for 5 minutes
- Dehydrate, clear and mount

Proteoglycans stain bright blue

Nuclei and other cytoplasmic areas stain red

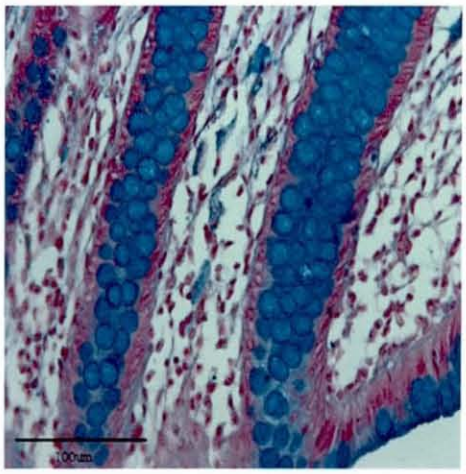

Figure 61 Cross-section of human intestine stained with Alcian blue as a control. Cytoplasmic regions (red) and proteoglycans (blue)

Elastic Van Giesson's Histological Staining Protocol (reproduced with permission from the Advance Microscopy Unit, Nottingham University)

Method developed for the staining of elastin in SKN constructs:

- Rehydrate cut section in a series of decreasing ethanol concentrations (100% three times, 90%, 70%, 50%) and then in water.
- Treat with 0.5% acidified potassium permanganate for 3 minutes
- Wash in tap water
- Bleach sections with 1% oxalic acid to remove brown colouration
- Rinse in Industrial Methylated Spirit (IMS)
- Place sections into Millers elastin for 1 hour
- Wash in tap water
- Differentiate in IMS until the background is colourless
- Wash in tap water
- Stain with Van Gieson solution for 5 minutes
- Blot sections and rinse quickly in IMS
- Clear and mount

Elastin stains blue/black

Collagen stains dark red

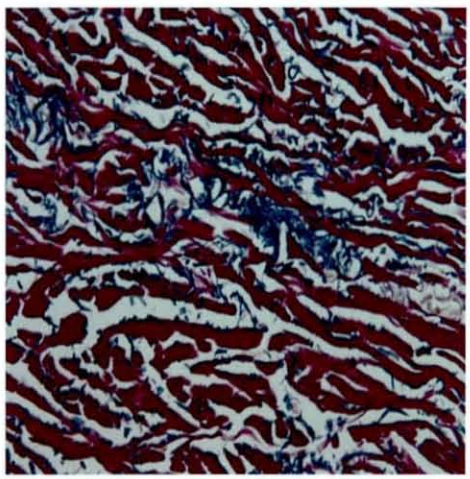

Figure 62 Cross-section of human dermis stained with Elastin Van Gieson's as a control. Collagen fibres (dark red), elastin (black)

Immunohistochemistry and Confocal Laser Fluorescent Microscopy Negative Controls

Negative controls used to assess the fluorescence of the secondary antibody to the in the absence of the primary antibody.

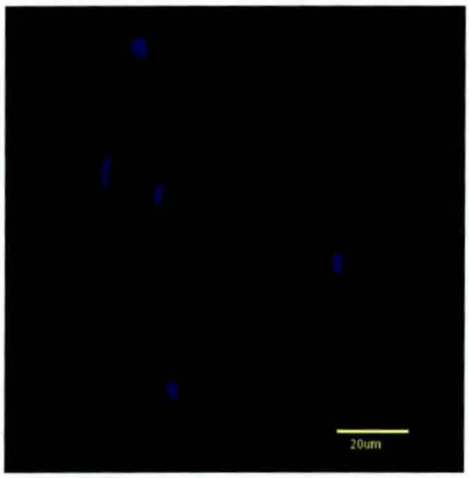

Figure 63 Immunohistochemistry negative control with no primary collagen type I or collagen type III antibody. No cross reactivity between the secondary antibodies and section observed. Cell nuclei stained blue with DAPI

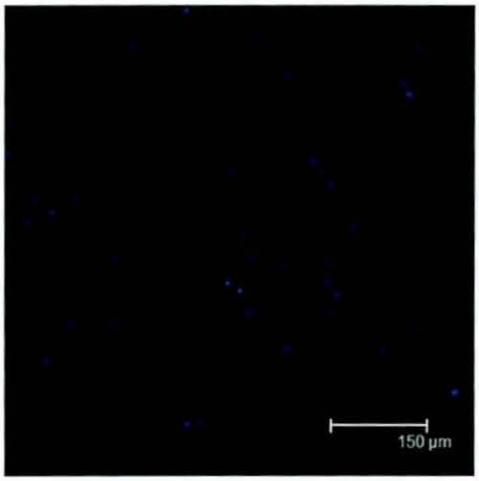

Figure 64 CLFM negative control with no collagen type I primary antibody. No cross reactivity between the secondary antibodies and section observed. Cell nuclei stained blue with DAPI

Appendix III Assumptions for the Calculation of the Volume Fraction of Cells in SKN Constructs

- The volume fraction of the fibroblast cells was approximated by multiplying the volume of the cell by the total number of cells in the construct.
- The volume of the cells was calculated assuming that the cells were cylindrical and using an average length of 150μm and diameter of 8μm measured from the CLFM and SEM images (Figure 65).
- The contribution of the cell membranes to the dry weight was assumed to be negligible and therefore the total cell volume was calculated as a percentage of the volume fraction of water in the constructs.

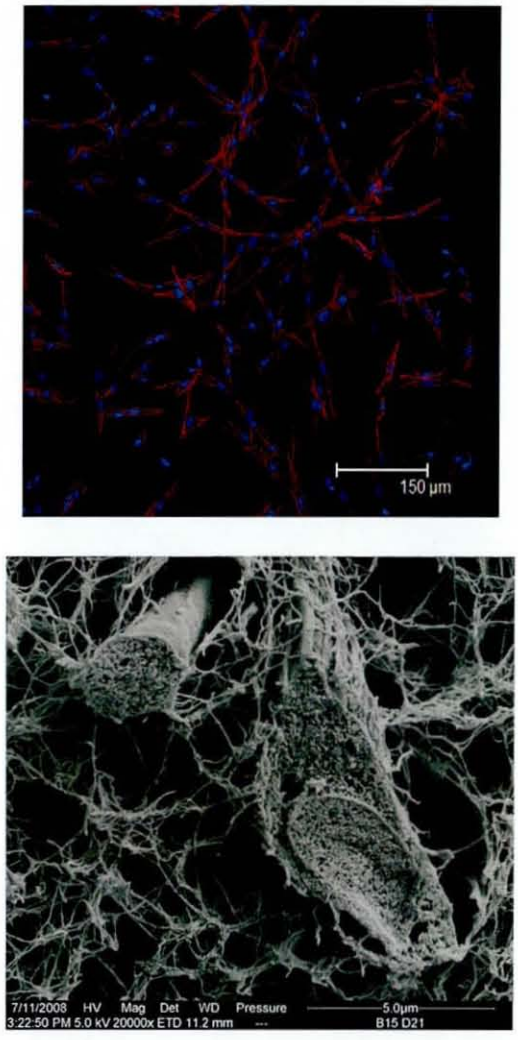

Figure 65 Example of CLFM (top) and SEM (bottom) images from which cell dimensions were measured

Appendix IV Ultrasound Calibration Curve and Experimental Design

Power balance reading for SonoPlus490 Ultrasound Unit at different duty cycles. CW = 100% duty cycle.

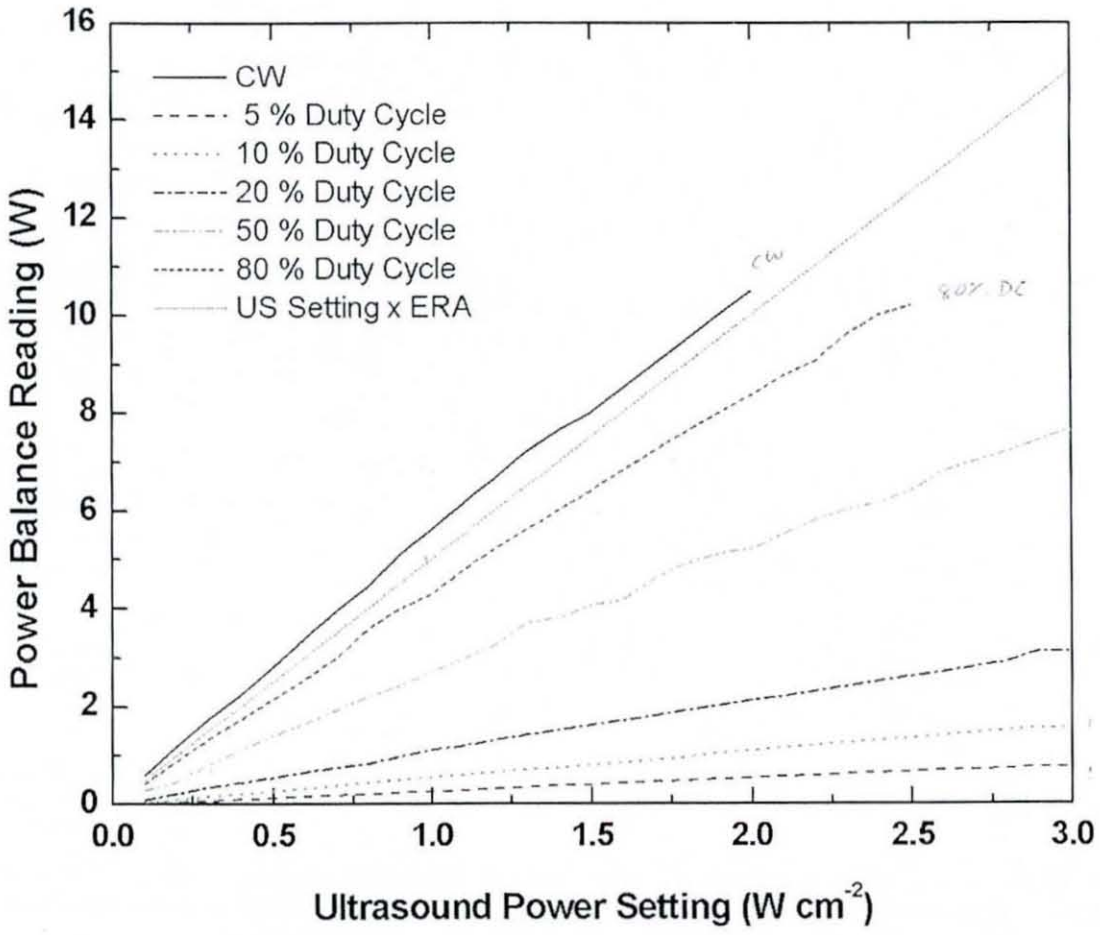

Calculation of the Distance between the Ultrasound Transducer and SKN Construct

The optimum distance between the ultrasound transducer and SKN constructs to enable positioning of the SKN constructs in the most homogeneous but least divergent ultrasound stimulation was calculated as follows:

Optimum distance from transducer face = a^2/λ

Where,

a = radius of transducer face

λ = ultrasonic wavelength

Effective radiating area of Sonoplus490 transducer = $5cm^2$

Radius of transducer = 12.6mm

In soft tissue, λ = 1.50mm (Duck 1990)

Optimum distance from transducer face $= (12.6)^2/1.5$

$= 105.8mm$

In water, λ = 1.48mm

Optimum distance from transducer face $= (12.6)^2/1.48$

$= 107.3mm$

Assuming that the propagation of ultrasonic waves through ICX-SKN constructs is between that of soft tissue and water, the optimum distance from the transducer face is between 105.8mm and 107.3mm.

Reference

DUCK, F.A., 1990. Physical Properties of Tissue, A Comprehensive Reference Book. London: Academic Press Inc.

Design of Experiments (DOE) Run Order for Ultrasound Stimulation Study

The random run order used in the DOE study minimise variation in the results caused by the ultrasound stimulation process such as, time-dependent effects.

Run Order	Sample number	Intensity (W/cm^2)	Duty cycle (%)	Duration (min)
1	2	2.5	5	30
2	21	0.5	5	5
3	4	0.5	80	5
4	13	2.5	5	5
5	23	0.5	5	30
6	7	0.5	5	30
7	8	2.5	80	5
8	1	2.5	80	30
9	24	0.5	80	30
10	3	2.5	80	5
11	22	0.5	80	5
12	10	2.5	80	5
13	11	1.5	42.5	17.5
14	6	2.5	5	30
15	5	0.5	5	5
16	15	0.5	80	5
17	9	0.5	5	5
18	17	2.5	5	5
19	20	0.5	80	30
20	14	2.5	80	30
21	25	2.5	5	30
22	19	0.5	5	30
23	12	0.5	80	30
24	16	2.5	80	30
25	18	2.5	5	5

Appendix V Costing for Custom-built Ultrasonic System

Costing for an upgraded ultrasonic system to deliver a more homogeneous output

Description	Supplier	Manufactured	Cost
Videoscan Contact Transducer	Olympus NDT	UK	£1,500
UT320 Pulser Receiver	Utex Scientific Instruments Inc.	Canada	£5,450
Hydrophone & accessories	Precision Acoustics Ltd	UK	£4,305
Wavesurfer 104XsOscilloscope	LeCroy	Switzerland	£7,013
Software for Oscilloscope	LeCroy	Switzerland	£319
PC			£1,250
		Subtotal for priority items	£19,836
Acoustic Materials (Aptflex tiles, Acoustic Putty)	Precision Acoustics Ltd	UK	£500
Stepper Motor/Scanning Frame			£2,500
Ultrasound transducer array			£10,000
150A100B RF power amplifier	AR Worldwide	USA	£6,520
		Total	**£39,356**

Compiled by Dr.M.Mather, Nottingham University